Minkowski's foundations of spacetime physics and SDSS data motivate reassessment of ΛCDM cosmology

"Failing to grasp the extent of the subversion of academia causes them to try hard to force fit their discoveries into false models."

– Asha Logos

Alexander F. Mayer

SensibleUniverse.net

Abstract

The objective, statistical nature of SDSS astrophysical datasets, which were not driven by any theoretical agenda, reveal false and misleading prior measurements (e.g., redshift-distance) driven by confirmation bias in the context of such agendas. SDSS theta-z, redshift-magnitude (both spectroscopic and photometric pipelines), and galaxy population-density data are shown to conflict with the ΛCDM standard cosmological model. However, all four of those distinct and independent data sets are similarly consistent with a new cosmological model that revives de Sitter's 1917 solution to the field equations, long thought to entail an "empty universe." That new model, which represents a paradigm shift in cosmology, derives from considerations of symmetry and local proper time modeled as a geometric object, motivated by Minkowski (1909). The confrontation of all new predictive equations with corresponding SDSS data sets, using no free parameters, definitively resolves the modern quandary of astrophysical observables interpreted as accelerating cosmic expansion induced by 'dark energy.' The canonical idea of a non-relativistic universal time coordinate (i.e., ~13.7 Gyr of 'Cosmic Time' from initial singularity) is supplanted by a relativistic, strictly-local time coordinate involving no such inscrutable singularity.



The talk on “Space and Time,” which Hermann Minkowski gave at the Convention of German Scientists and Doctors in Cologne, is the last of his ingenious creations. Unfortunately, it was not destined for him *to finish the more detailed development of his audacious concept* of a mechanics in which time is integrated with the three dimensions of space.

– A. Gutzmer

Since my student years Minkowski was my best, most dependable friend who supported me with all the depth and loyalty that was so characteristic of him. …*what death cannot take away is his noble image in our hearts and the knowledge that his spirit in us continues to be active*.

– David Hilbert

You are encouraged to review this fact-finding and independently reproduce all analyses and results. *Due to the unusually disruptive nature of this work, scientific integrity must overrule personal agendas.*

Online self-study slides* including copious text are obviously not intended for audience presentation; this PDF is a digital research report and textbook.

* Internet links are attached to references, names, and graphics in the PDF; cursor typically switches to a hand pointer when hovering over the links. A minority of all available links are highlighted with the link indicator.

Sloan Digital Sky Survey

SDSS.org

Sloan Foundation
2.5-m Telescope
Apache Point, NM



This presentation is
© 2018–2019 A. F. Mayer.

Image credit: Reidar Hahn, *Fermilab Visual Media Services*

Digital Research Report and Instructional Textbook

Table of Contents

PROLOGUE	–	INSTRUMENTS AND TOOLS	7
PART I	–	SDSS THETA-Z DATA	15
PART II	–	SDSS REDSHIFT-MAGNITUDE DATA	57
PART III	–	DE SITTER COSMOLOGY REVISITED	99
PART IV	–	NEW PREDICTIVE EQUATIONS	130
PART V	–	GALAXY SPACE DENSITY	142
PART VI	–	CREDITS AND AFTERWORD	150
PART VII	–	ADDENDUM 1: RELATED COSMOLOGICAL ISSUES	161
PART VIII	–	ADDENDUM 2: RELEVANT HISTORY, ETC.	187

PROLOGUE – INSTRUMENTS AND TOOLS


Apache Point Observatory
Sunspot, New Mexico, USA

SDSS astronomical filters $\lambda_{\rm eff}$ (Å)

Ultraviolet u	Green g	Red r	Near Infrared i	Infrared z
3531	4627	6140	7467	8887

Herein, not to be confused with *redshift* (z)!

Central wavelengths $\lambda_{\rm eff}$ (Å) from Doi et al. (2010), Table 2.



photo credit: *Smithsonian National Air and Space Museum*

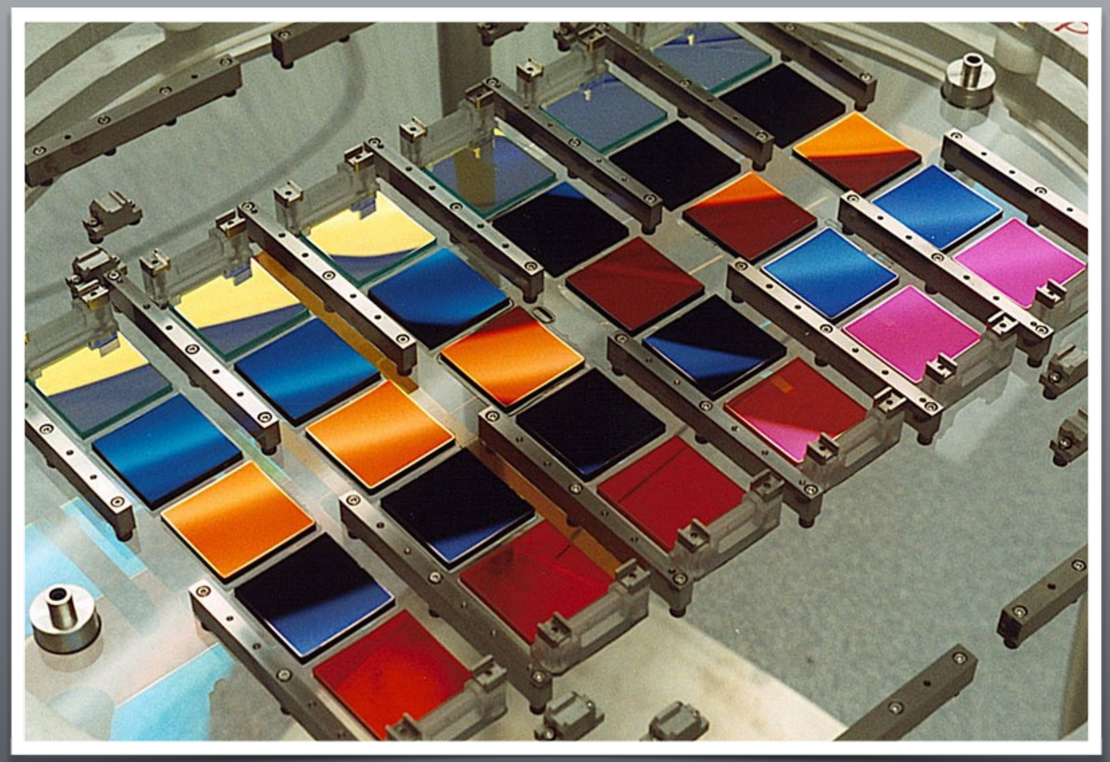


photo credit: *Michael Carr*

skyserver.sdss.org/dr14/en/home.aspx

SLOAN DIGITAL SKY SURVEY

SkyServer DR14

SciServer

afmayer Help Logout

Home | Data | Schema | Education | Astronomy | SDSS | Contact Us | Download | Site Search | Help | History NEW!

NEW: SciServer Betelgeuse (v2.0.0)!

We are proud to announce a new release of the SciServer online science platform! The new "Betelgeuse" release has many new features to manage and share big data resources. Learn about the changes on the **SciServer website**!

SDSS is supported by

Powered by SciServer Microsoft

Site Traffic
Privacy Policy

Welcome to the **DR14 site**!!!

This website presents data from the Sloan Digital Sky Survey, a project to make a map of a large part of the universe. We would like to show you the beauty of the universe, and share with you our excitement as we build the largest map in the history of the world.

News

The site hosts data from **Data Release 14 (DR14)**. **What's new in DR14**, and **known problems**.
More...

Data Access

Navigate | Finding Chart
Quick Look | Explore
Image List
Search
IQS | SQS | IRSQS
SQL Search
Cross-ID
SkyQuery CrossMatch NEW!
CasJobs

Education

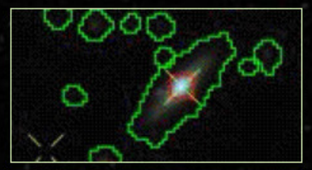
For Educators
Lesson Plans
College Lab Activities
Instructor Guides
Student/Public Research
Galaxy Zoo
Zooniverse
Voyages

Links

sdss.org
Data Release 14
Surveys | Instruments
SDSS Science
Science Archive Server
About Astronomy
About SkyServer
Credits

Help

Start Here | FAQ
Glossary
Algorithms
Cooking with Sloan
SQL Tutorial
About the Database
Schema Browser
Sample SQL Queries






Contact Us

URL
skyserver.sdss.org

Catalog Archive Server (CAS)

skyserver.sdss.org/CasJobs/SubmitJob.aspx

SDSS Query / CasJobs

SciServer

Query tab

afmayer Help Logout

Help Tools Query History MyDB Import Groups Output Schema Browser Queues SkyServer

Context: DR14 | MyScratch: default | Table (optional): petroR50_g | Task Name

Data goes into MyDB."TableName"

Samples Recent Clear [1 s] Syntax OK Syntax Plan Quick Submit

```
SELECT
    s.z
,   s.zErr
,   g.petroR50_g                        -- Change "_g" to "_" with r , i , z
,   g.petroR50Err_g                     -- to get data for those filters.
FROM                                    -- Change "R50" to "Rad" for that data.
    Galaxy  g
,   SpecObj s
WHERE
    s.programname IN ('legacy', 'boss')  -- disallow minor surveys
AND s.zWarning = 0                      -- disallow redshifts with warnings
AND s.zErr >= 0                         -- disallow -n error codes
AND ABS(s.zErr/s.z) <= 0.01             -- max. redshift error is 1%
AND s.z > 0                             -- disallow [÷ 0], above
AND g.clean = 1                         -- clean photometry
AND (g.flags_g & 0x100) = 0             -- disallow NOPETRO flag
AND (g.flags_g & 0x200) = 0             -- disallow MANYPETRO flag
AND g.petroR50_g > 0                    -- disallow -9999 error code
AND g.petroR50Err_g >= 0                -- disallow -1000 error code
AND g.petroR50Err_g / g.petroR50_g < 0.20 -- max. measurement error is 20%
AND g.specObjID = s.specObjID           -- join tables on specObjID key
```

Run SQL statements on "DR14" database (Data Release 14).

SDSS data releases are cumulative. DR 15 (10 Dec. 2018) includes new, additional data that should not alter the prior SDSS data (DR 14) and its analysis that are presented herein.

Contact

sciserver-v2.0.0

skyserver.sdss.org/CasJobs/MyDB.aspx

SDSS Query / CasJobs

MyDB tab

SciServer

afmayer Help Logout

Help Tools Query History MyDB Import Groups Output Schema Browser Queues SkyServer

MyDB | Local Only

Views
Tables
Functions
Procedures

Sort by... | All selected...

	Rows	kB	Name
☐	806,483	20,040	**petroR50_g**

(1) click on the filename

petroR50_g

Contains ~806,483 rows (~20,040 kB)

(2) get the .csv file for graphing

Notes | Sample | Job | Plot | Download | Publish | Rename | Drop

Table Schema type [size]

z	zErr	petroR50_g	petroR50Err_g
real [4]	real [4]	real [4]	real [4]

Notes

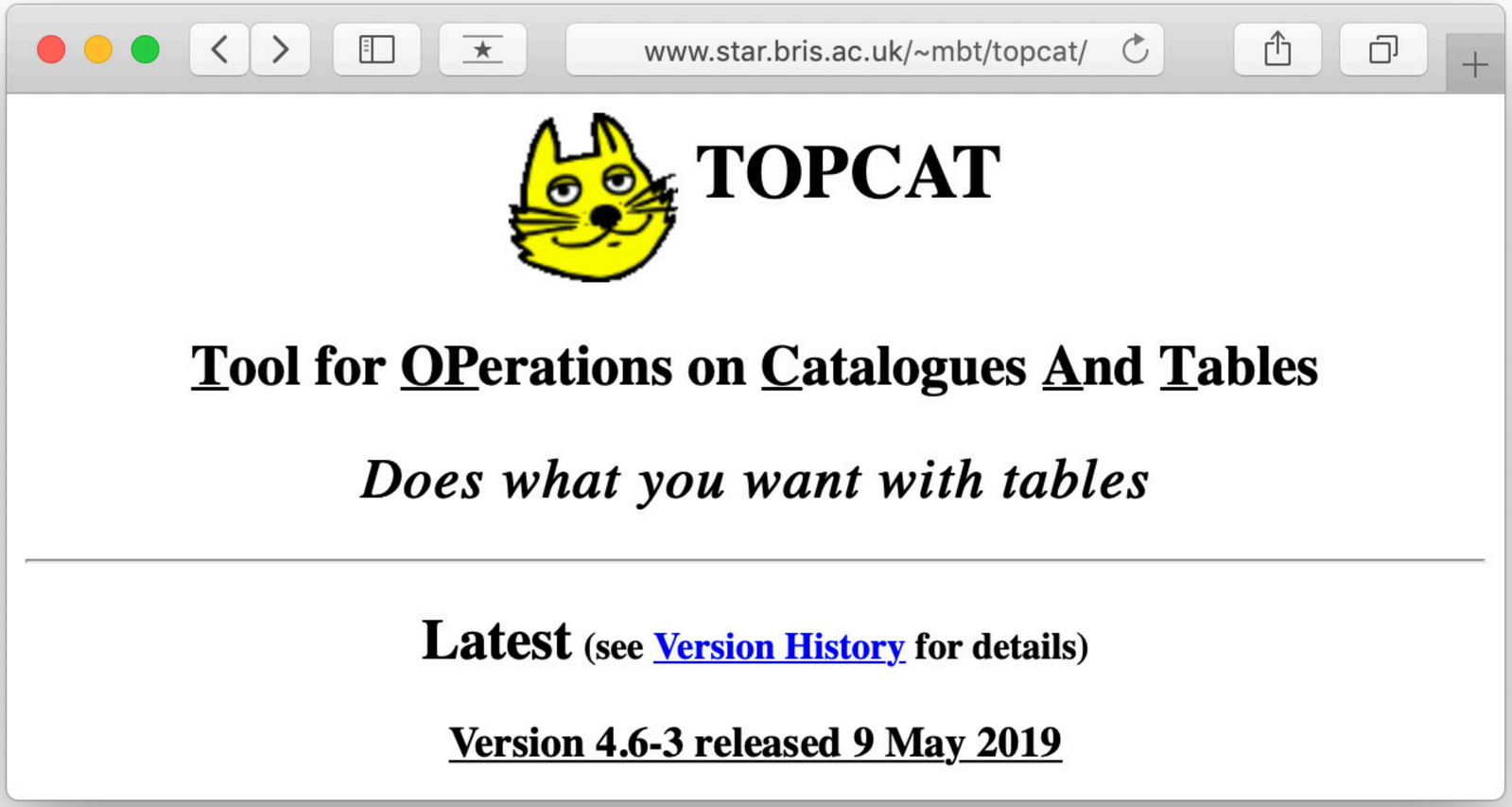
No notes found

New Note

Add Note

Free, cross-platform **astrophysical plotting package**

http://www.star.bris.ac.uk/~mbt/topcat/



TOPCAT Creative



Dr. Mark Taylor
Ph.D. (Bristol)

Astrophysics group
University of Bristol

Free and cross-platform

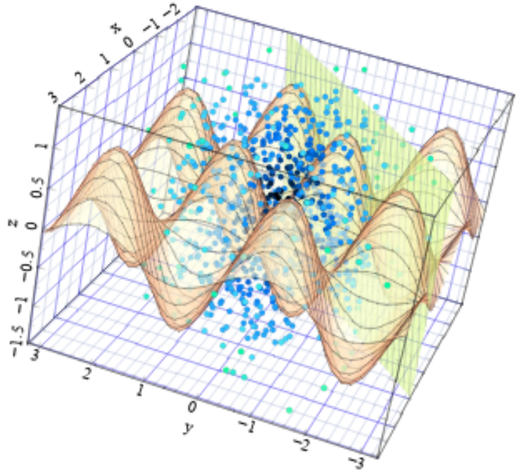
https://veusz.github.io

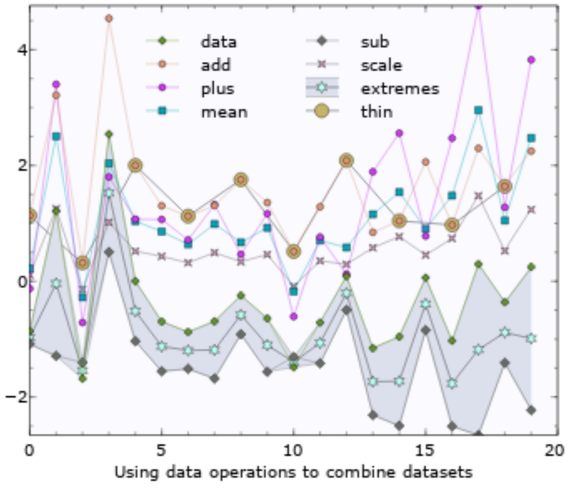
Veusz – a scientific plotting package

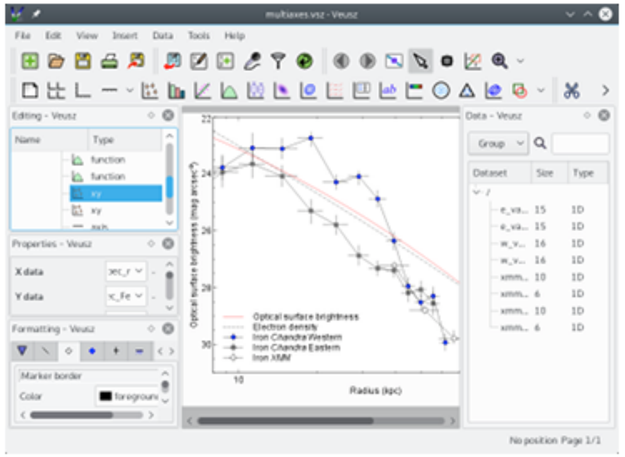
Veusz is a scientific plotting and graphing program with a graphical user interface, designed to produce publication-ready 2D and 3D plots. In addition it can be used as a module in Python for plotting. Veusz is multiplatform, running on Windows, Linux/Unix and macOS. It supports vector and bitmap output, including PDF, Postscript, SVG and EMF. Veusz is Free Software.

With the help of a tutorial the program can be used by the novice user and is flexible for advanced work. In Veusz plots are created by building up plotting widgets with a consistent object-based interface, where the user sets the properties of the widgets. There are many options for customization of plots. See features, 2D examples and 3D examples to see what can be done with the program.

It allows data to be imported from text, CSV, HDF5 and FITS files. Datasets can also be entered within the program and new datasets can be created via the manipulation of existing datasets using mathematical expressions and more. The program can also be extended, by adding plugins supporting importing new data formats, different types of data manipulation or for automating tasks.







Veusz Creative



Dr. Jeremy Sanders
Ph.D. (Cambridge)

High Energy
Astrophysics group
Max Plank (MPE)

PART I – SDSS THETA-Z DATA

Note: slides 16–28 are a precursor to analysis.

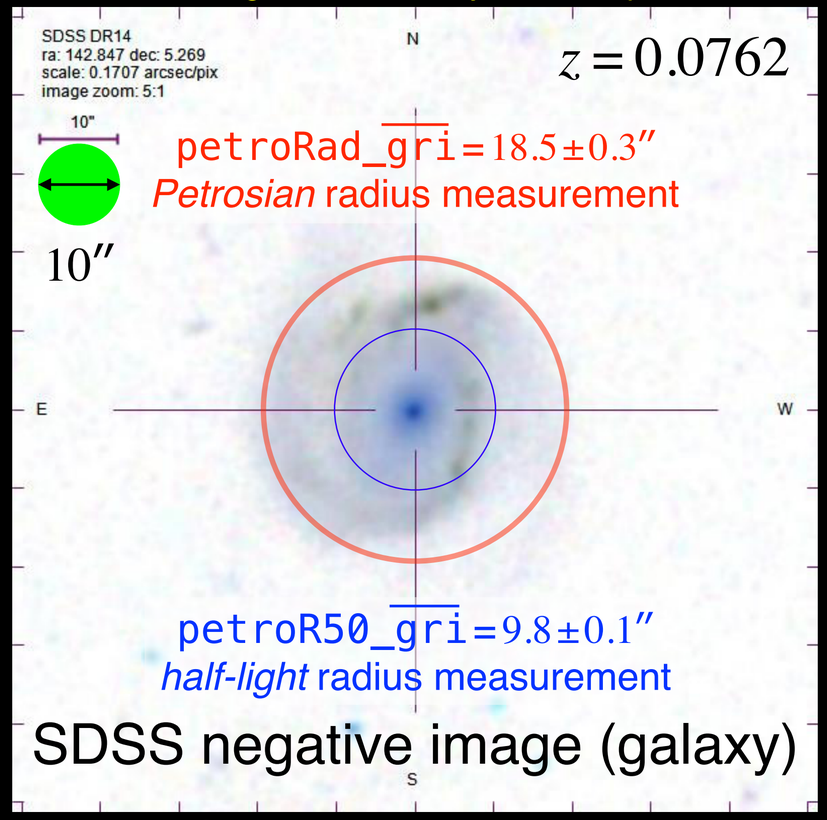
Click to go back to Table of Contents…

Understanding SDSS angular resolution (“*theta*” measurement)

The *average* apparent diameter of the full Moon is $31.1' = 1866''$.



Click image for SDSS SkyServer Explorer.



ObjID: 1237658298990330048

The midline shown has a width of $10''$ (i.e., 10 arcseconds), and the green dot at 6 o’clock position has a $10''$ diameter, as compared to the average apparent size of the full Moon.

SDSS glossary reference

petroRad

The Petrosian radius. A measure of the angular size of an image, most meaningful for galaxies. Units are seconds of arc. The Petrosian radius (and related measures of size called `petroR50` and `petroR90`) are derived from the surface brightness profile of the galaxy, as described in Algorithms.

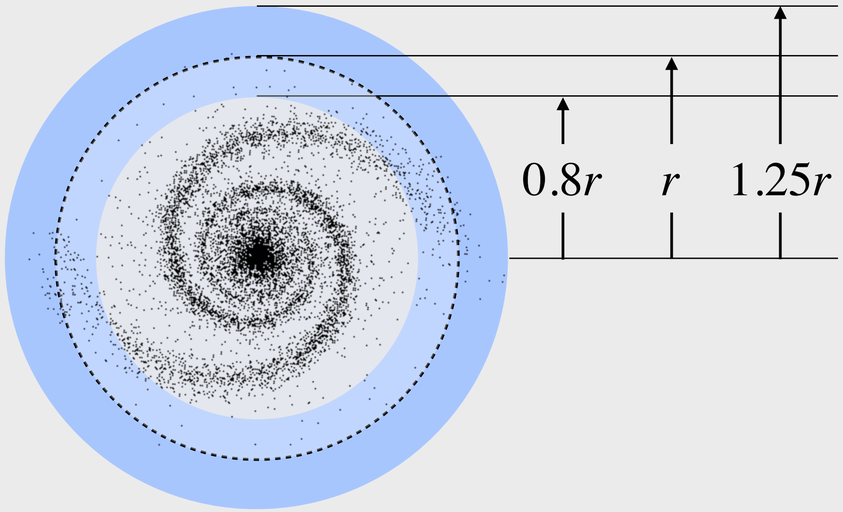
Surface Brightness

The frames pipeline also reports the radii containing 50% and 90% of the Petrosian flux for each band, `petroR50` and `petroR90` respectively.

Source: https://www.sdss.org/dr14/help/glossary/#P

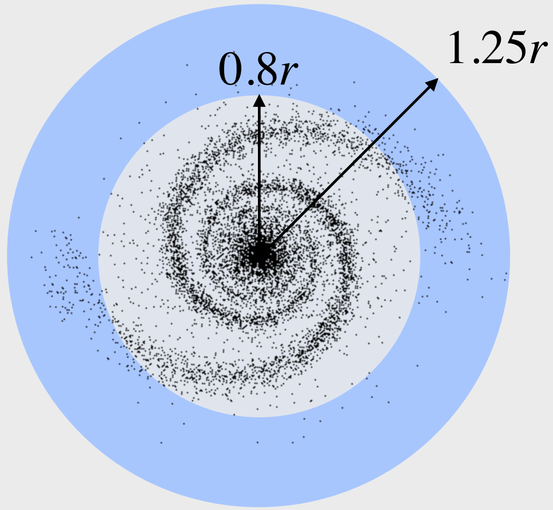
© A. F. Mayer

Petrosian radius



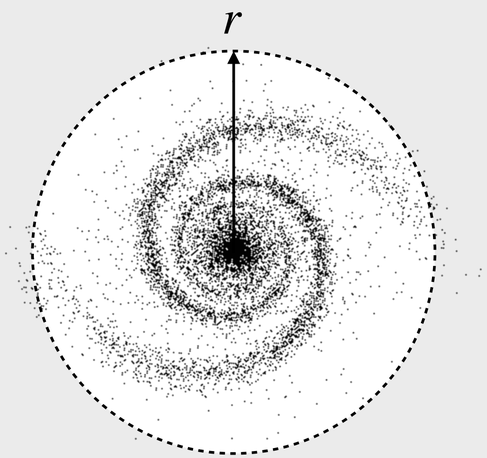
Here, r is a variable measurement;
it is not a recorded measurement.

DEFINITION: "Petrosian ratio," $\mathscr{R}_{\rm P}(r) =$



local surface brightness
in annulus (blue region)

÷



mean surface brightness
measured inside radius r

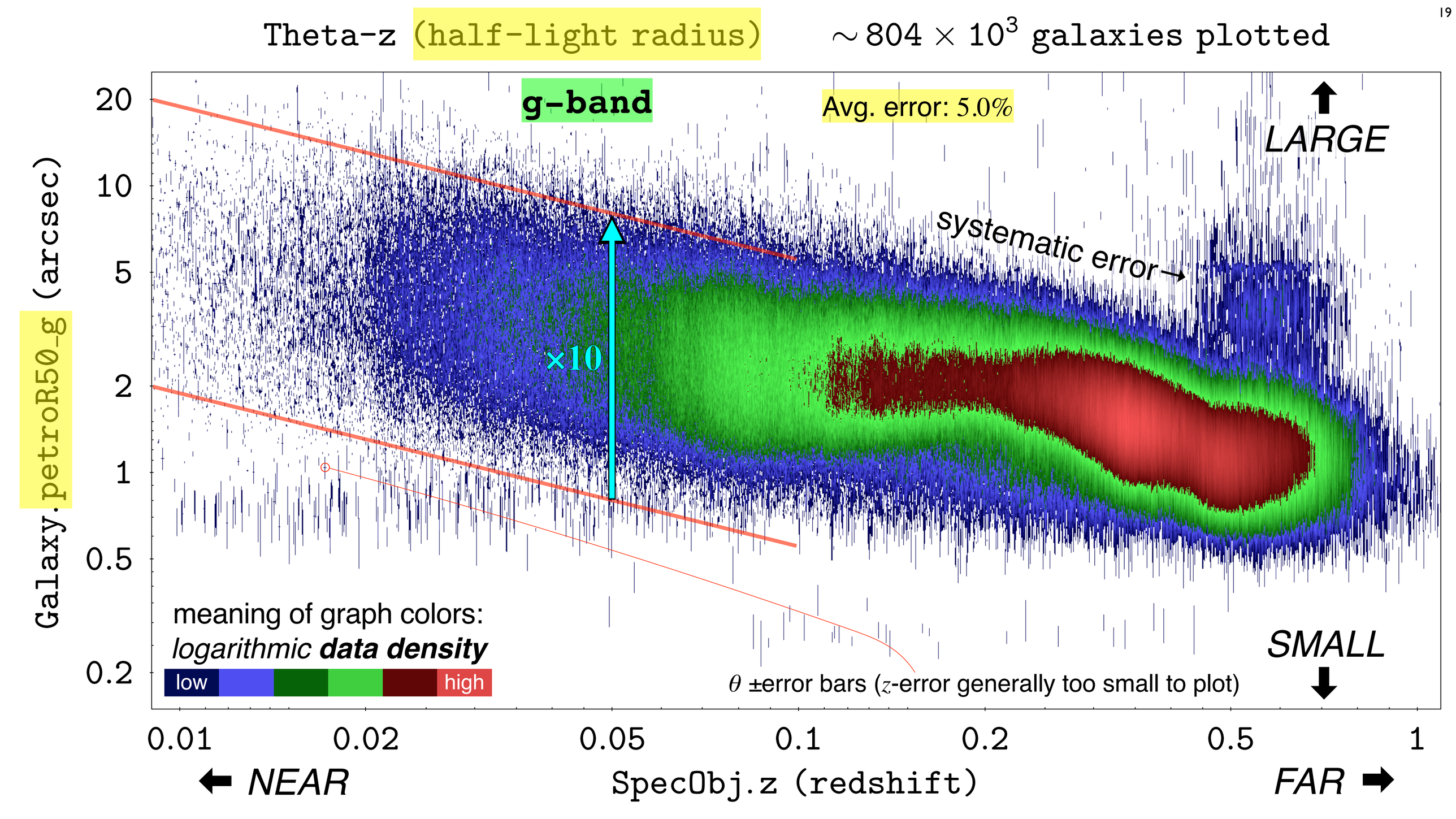
Define $\mathscr{R}_{\rm P,lim}$ as $\mathscr{R}_{\rm P}(r_{\rm P}) = \mathscr{R}_{\rm P,lim}$ where $r_{\rm P}$ is the measured and recorded Petrosian radius. $\mathscr{R}_{\rm P,lim} = 0.2$ for the SDSS:

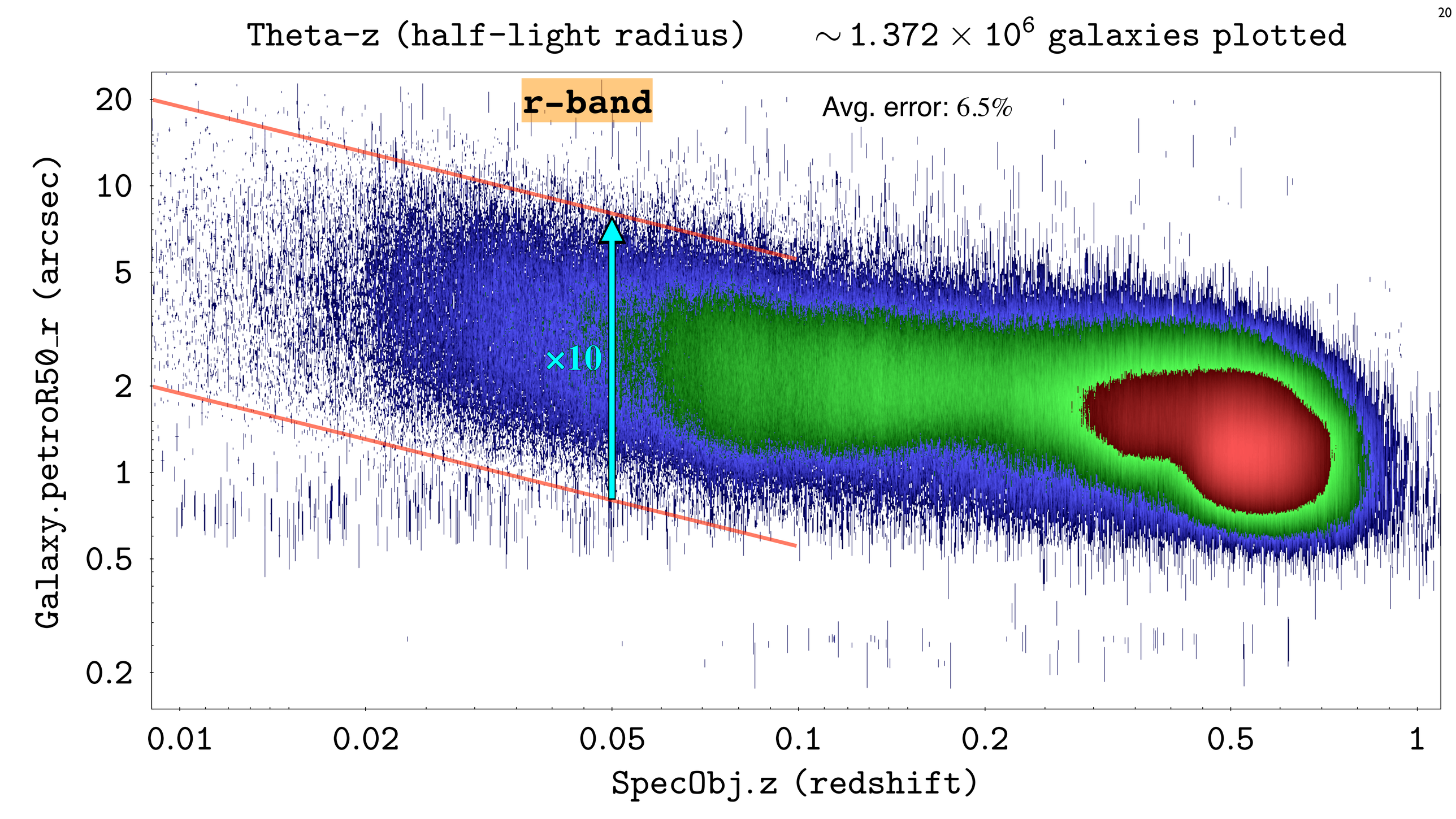
Varying r, when $\mathscr{R}_{\rm P}(r) = 0.2$, then $r_{\rm P} = r$.

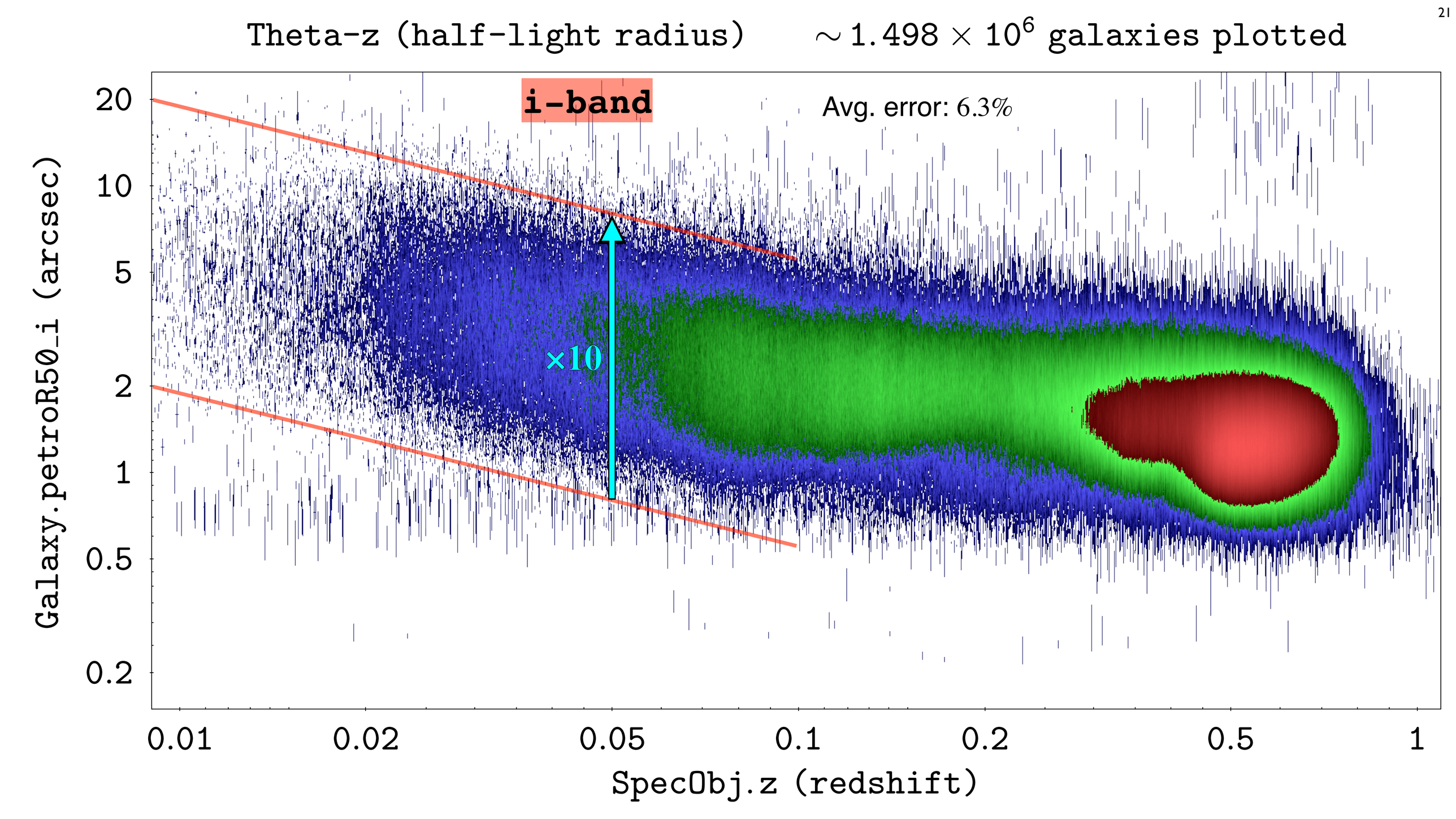
$$\mathscr{R}_{\rm P}(r) \equiv \frac{\int_{0.8r}^{1.25r} {\rm d}r' 2\pi r' I\left(r'\right) / \pi\left(1.25^2 - 0.8^2\right) r^2}{\int_0^r {\rm d}r' 2\pi r' I\left(r'\right) / \pi r^2}$$

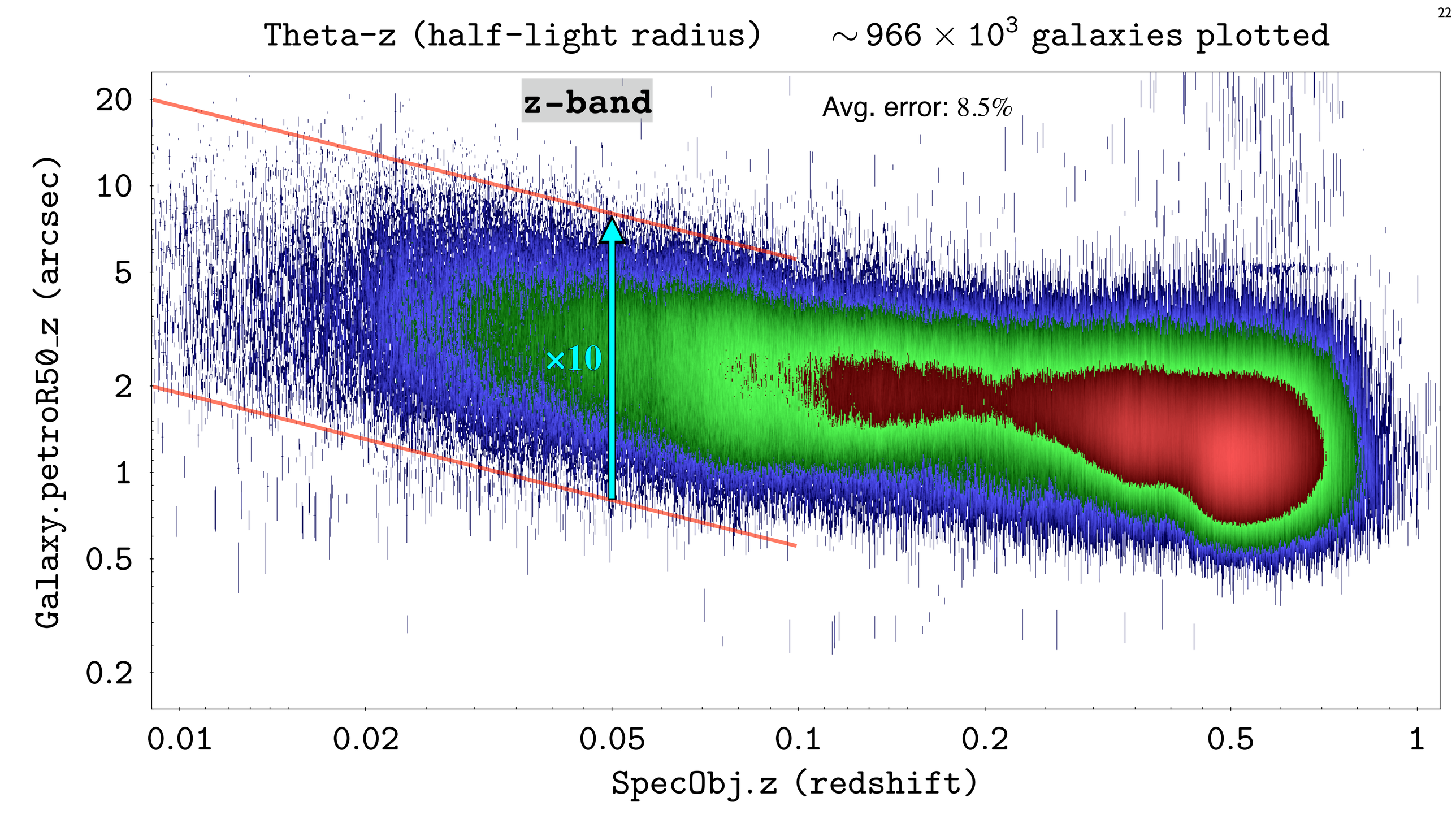
The observed radial galaxy brightness profile [$I(r')$] is "azimuthally averaged" (i.e., averaged over 2π radians).

Reference: https://www.sdss.org/dr14/algorithms/magnitudes/#mag_petro


Theta-z (half-light radius)
~804 × 10^3 galaxies plotted
g-band
Avg. error: 5.0%
LARGE
systematic error
×10
SMALL
meaning of graph colors:
logarithmic data density
low
high
θ ±error bars (z-error generally too small to plot)
Galaxy.petroR50_g (arcsec)
20
10
5
2
1
0.5
0.2
0.01
0.02
0.05
0.1
0.2
0.5
1
NEAR
SpecObj.z (redshift)
FAR

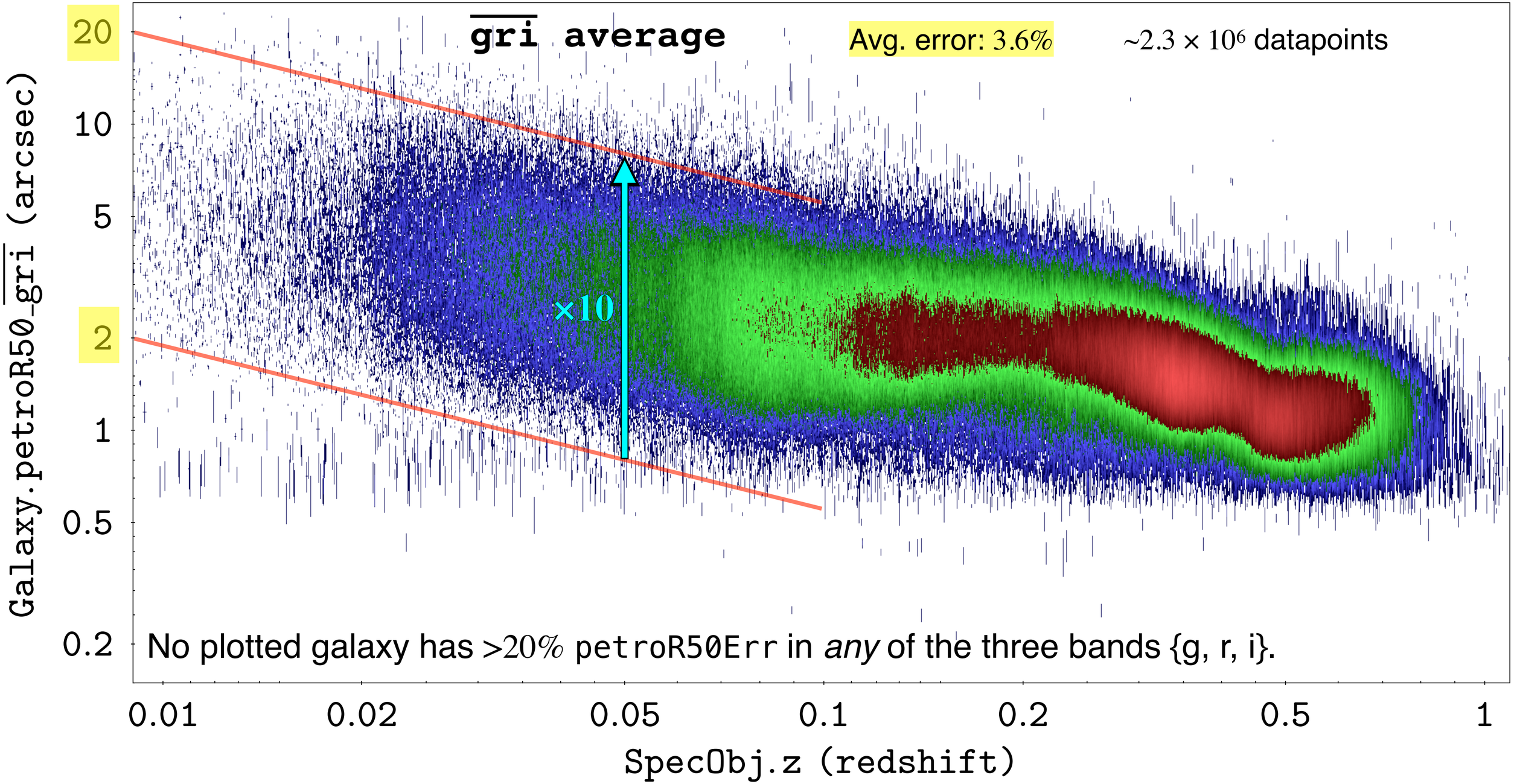

Theta-z (half-light radius)
$\sim 1.372 \times 10^6$ galaxies plotted
r-band
Avg. error: 6.5%
×10
Galaxy.petroR50_r (arcsec)
20
10
5
2
1
0.5
0.2
0.01
0.02
0.05
0.1
0.2
0.5
1
SpecObj.z (redshift)


Theta-z (half-light radius)
$\sim 1.498 \times 10^6$ galaxies plotted
i-band
Avg. error: 6.3%
×10
Galaxy.petroR50_i (arcsec)
20
10
5
2
1
0.5
0.2
0.01
0.02
0.05
0.1
0.2
0.5
1
SpecObj.z (redshift)


Theta-z (half-light radius)
∼966 × 10^3 galaxies plotted
z-band
Avg. error: 8.5%
×10
Galaxy.petroR50_z (arcsec)
20
10
5
2
1
0.5
0.2
0.01
0.02
0.05
0.1
0.2
0.5
1
SpecObj.z (redshift)

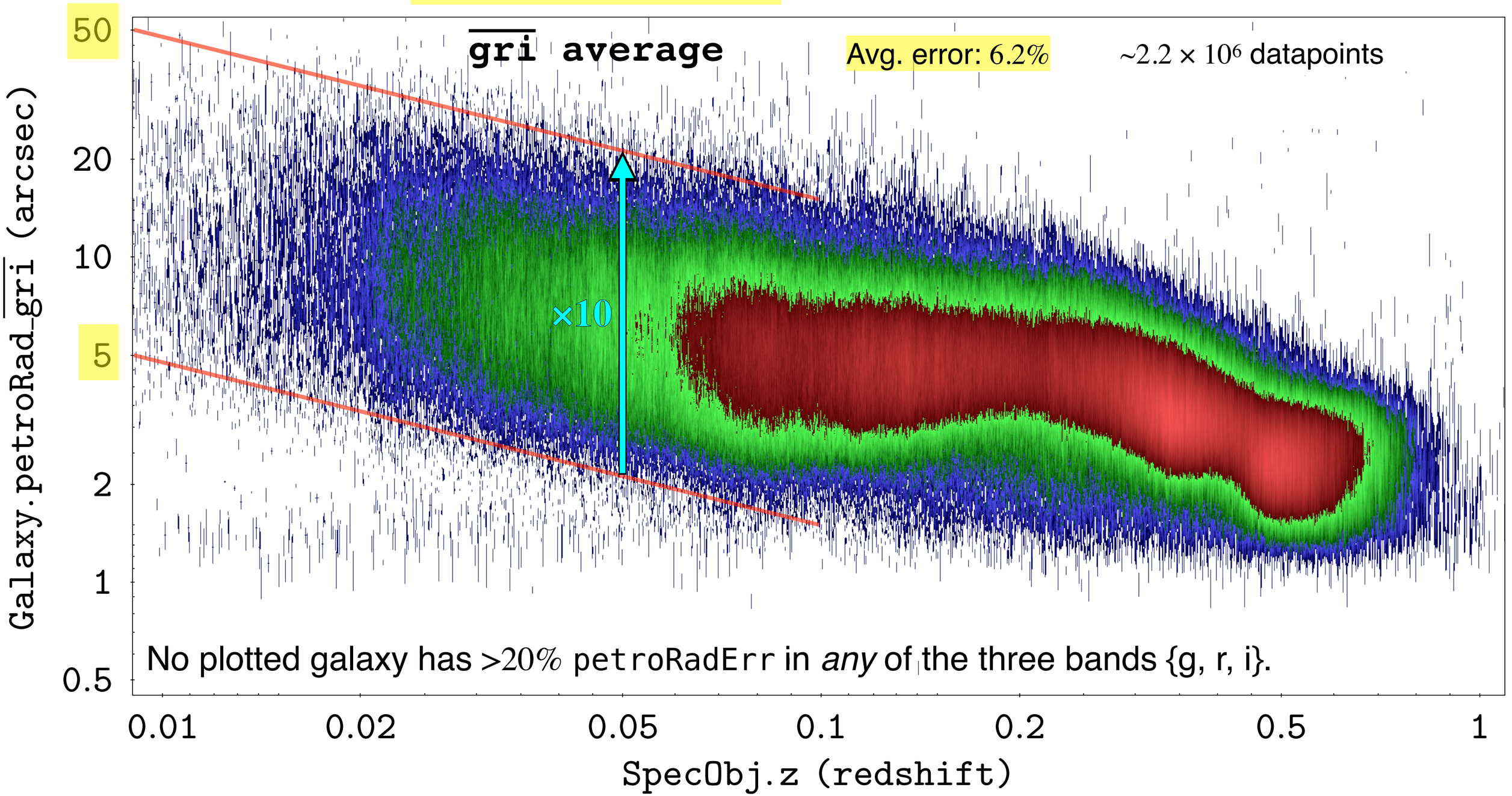
Theta-z (half-light radius)

$\sim 755 \times 10^3$ galaxies plotted



Theta-z (Petrosian radius)

$\sim 719 \times 10^3$ galaxies plotted



Empirical inference

①

The *intrinsic* radial size of *typical* galaxies, including all morphologies, varies by about one order of magnitude (i.e., $\times 10$). That decadal range excludes the statistically-unlikely outliers.

SQL query for theta-z data…

```
SELECT
    s.z
,   s.zErr
,   g.petroR50_g                                -- Change "_g" to "_" with r , i , z
,   g.petroR50Err_g                             -- to get data for those filters.
FROM                                            -- Change "R50" to "Rad" for that data.
    Galaxy  g
,   SpecObj s
WHERE
    s.programname IN ('legacy', 'boss')         -- disallow minor surveys
AND s.zWarning = 0                              -- disallow redshifts with warnings
AND s.zErr >= 0                                 -- disallow -n error codes
AND ABS(s.zErr/s.z) <= 0.01                     -- max. redshift error is 1%
AND s.z > 0                                     -- disallow [÷ 0], above
AND g.clean = 1                                 -- clean photometry
AND (g.flags_g & 0x100) = 0                     -- disallow NOPETRO flag
AND (g.flags_g & 0x200) = 0                     -- disallow MANYPETRO flag
AND g.petroR50_g > 0                            -- disallow –9999 error code
AND g.petroR50Err_g >= 0                        -- disallow –1000 error code
AND g.petroR50Err_g / g.petroR50_g < 0.20       -- max. measurement error is 20%
AND g.specObjID = s.specObjID                   -- join tables on specObjID key
```

SQL modifications for _$\overline{gri}$ (average of {g, r, i})

```
SELECT
    s.z
,   s.zErr
,   (g.petroR50_g + g.petroR50_r + g.petroR50_i) / 3 AS petroR50_gri
,   (g.petroR50Err_g + g.petroR50Err_r + g.petroR50Err_i) / 3 AS petroR50Err_gri

...
```

Add to WHERE clause:

```
AND (g.flags_r & 0x100) = 0                 -- disallow NOPETRO flag
AND (g.flags_r & 0x200) = 0                 -- disallow MANYPETRO flag
AND g.petroR50_r > 0                        -- disallow -9999 error code
AND g.petroR50Err_r >= 0                    -- disallow -1000 error code
AND g.petroR50Err_r / g.petroR50_r < 0.20 -- max. measurement error is 20%

AND (g.flags_i & 0x100) = 0                 -- disallow NOPETRO flag
AND (g.flags_i & 0x200) = 0                 -- disallow MANYPETRO flag
AND g.petroR50_i > 0                        -- disallow -9999 error code
AND g.petroR50Err_i >= 0                    -- disallow -1000 error code
AND g.petroR50Err_i / g.petroR50_i < 0.20 -- max. measurement error is 20%
```

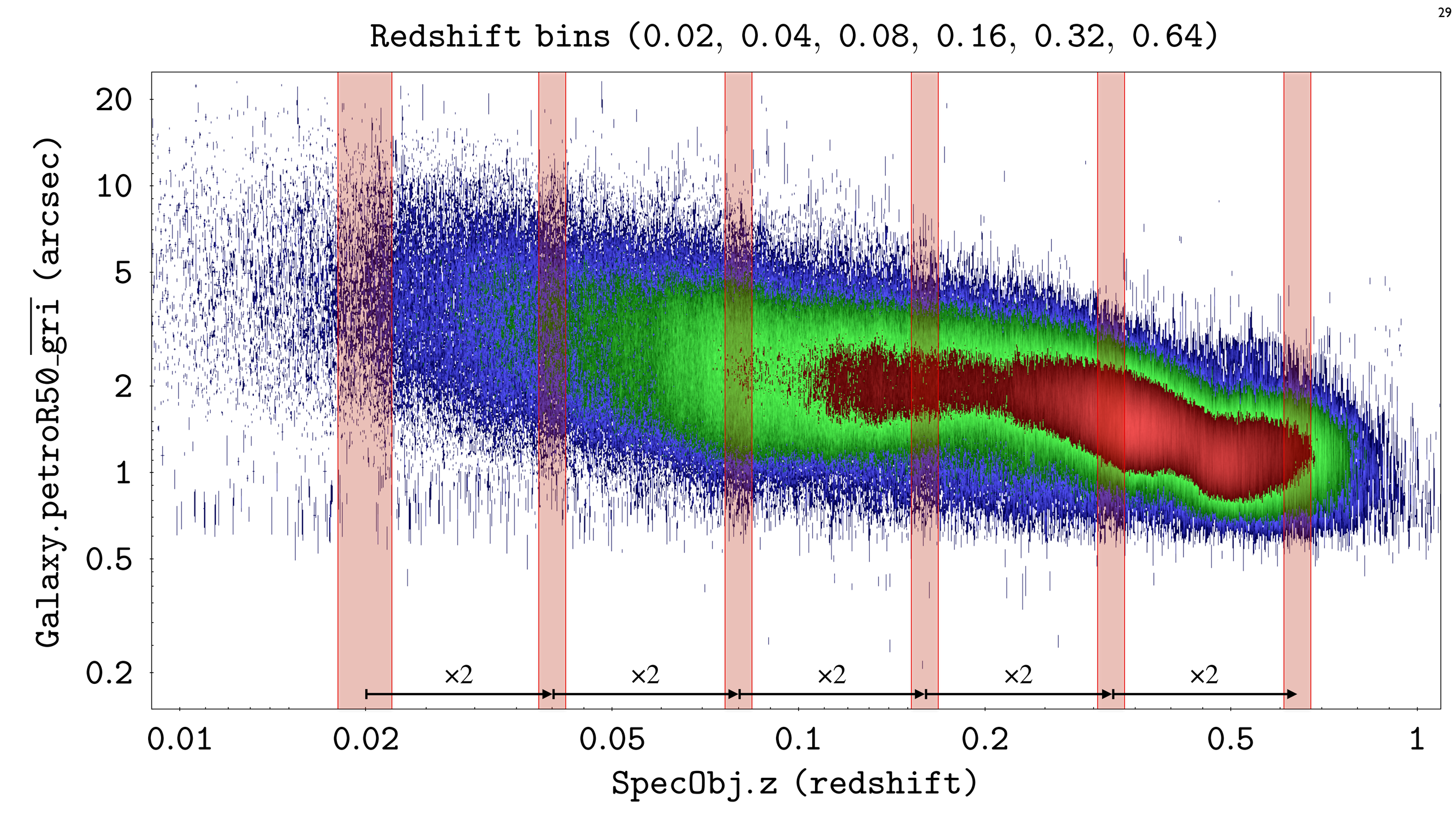
SQL modifications for average error statistic

```
SELECT
    AVG(petroR50Err_z / petroR50_z) * 100 AS AVGpetroR50Err_z

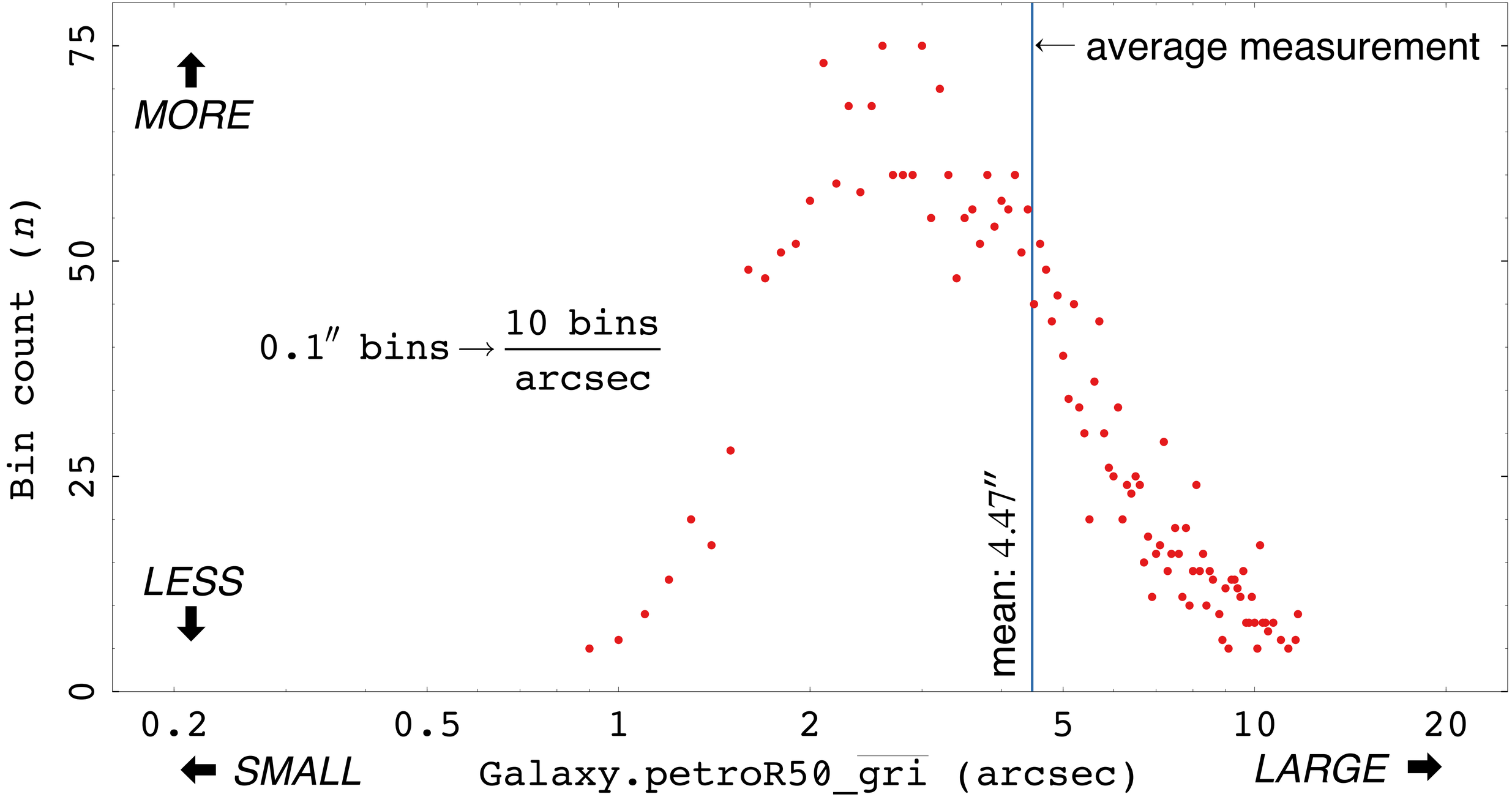
...
```

```
-- When averaging the three filters {g, r, i} use:
SELECT
    AVG((petroR50Err_g / petroR50_g + petroR50Err_r / petroR50_r + petroR50Err_i / petroR50_i) / 3)
                                    * 100 AS AVGpetroR50Err_gri

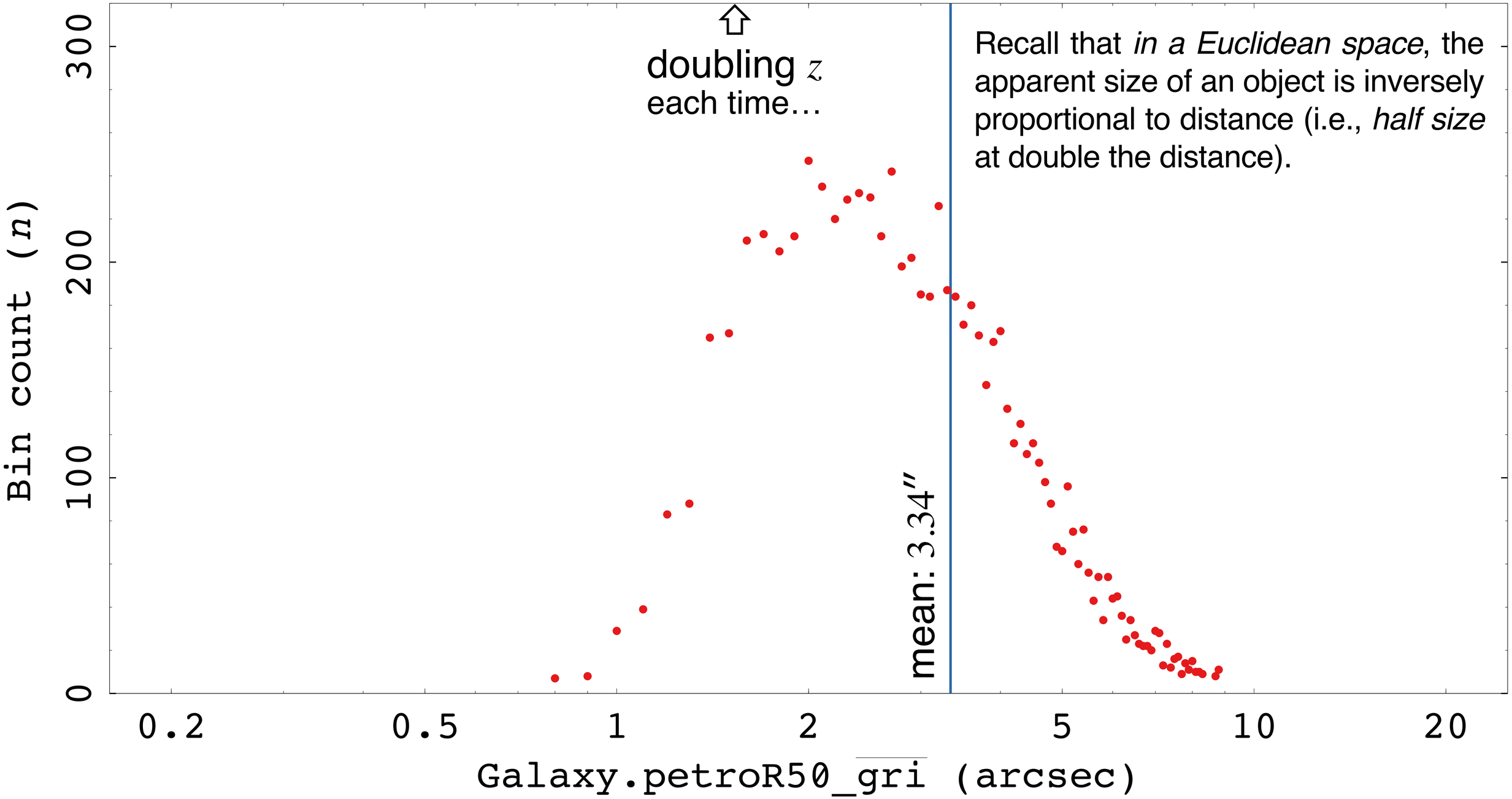
...
```


Redshift bins (0.02, 0.04, 0.08, 0.16, 0.32, 0.64)
Galaxy.petroR50_gri (arcsec)
20
10
5
2
1
0.5
0.2
×2
×2
×2
×2
×2
0.01
0.02
0.05
0.1
0.2
0.5
1
SpecObj.z (redshift)

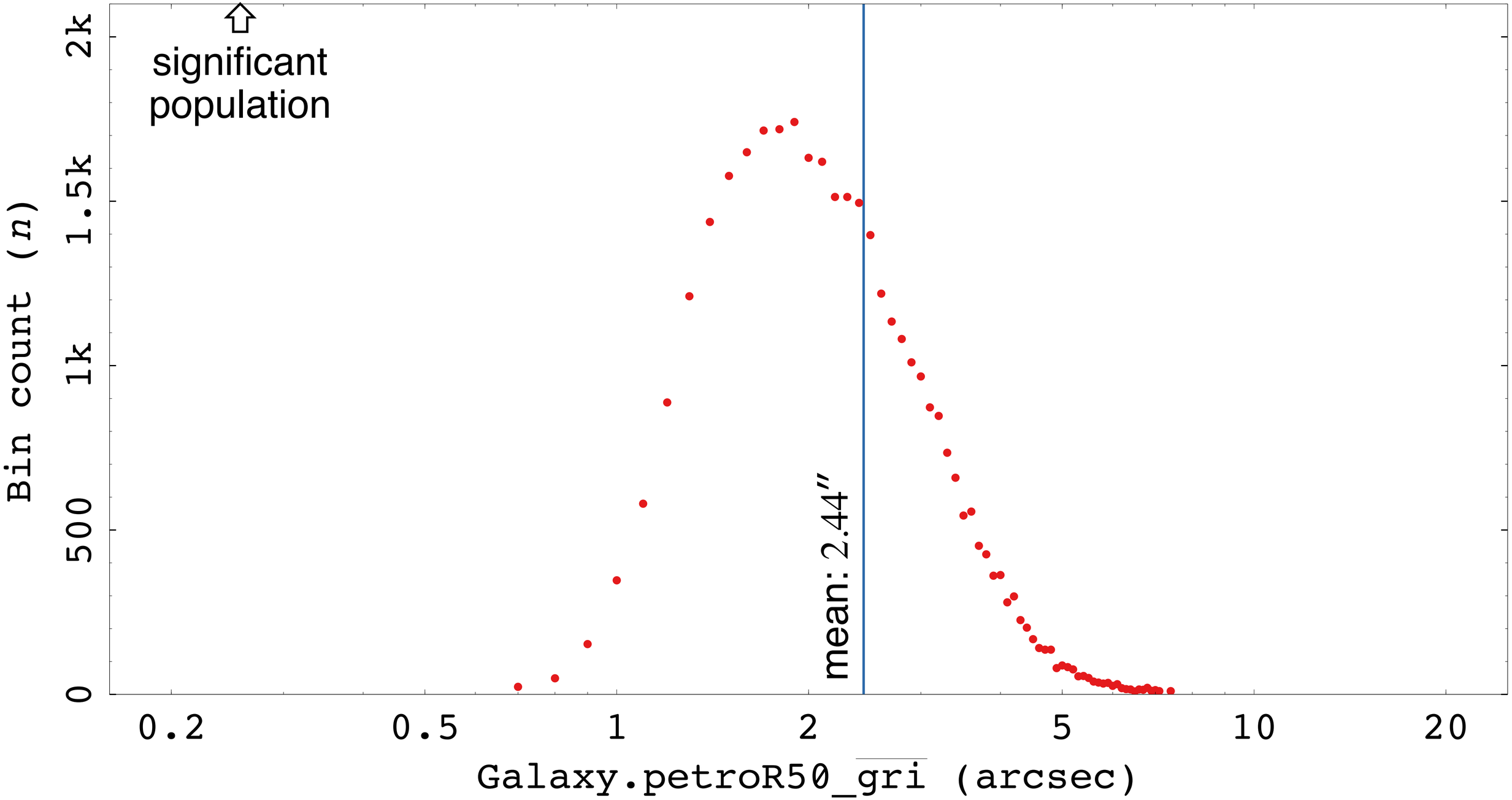
$\sum n = 3071$ $z \approx 0.02$ $(0.018 \leq z \leq 0.022)\ \&\ n > 4$



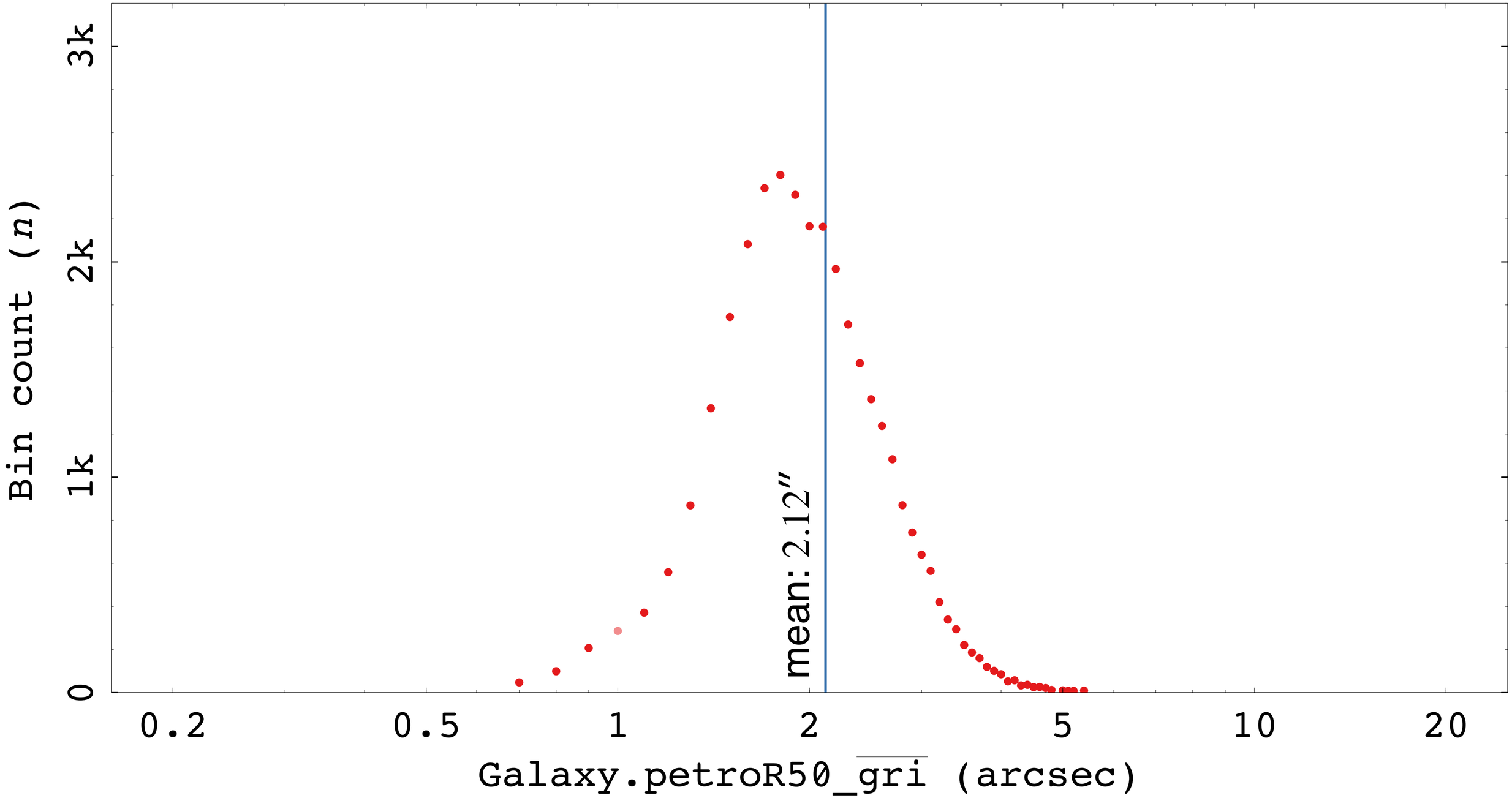
$\sum n = 7738$ $z \approx 0.04$ $(0.038 \leq z \leq 0.042)\ \&\ n > 6$



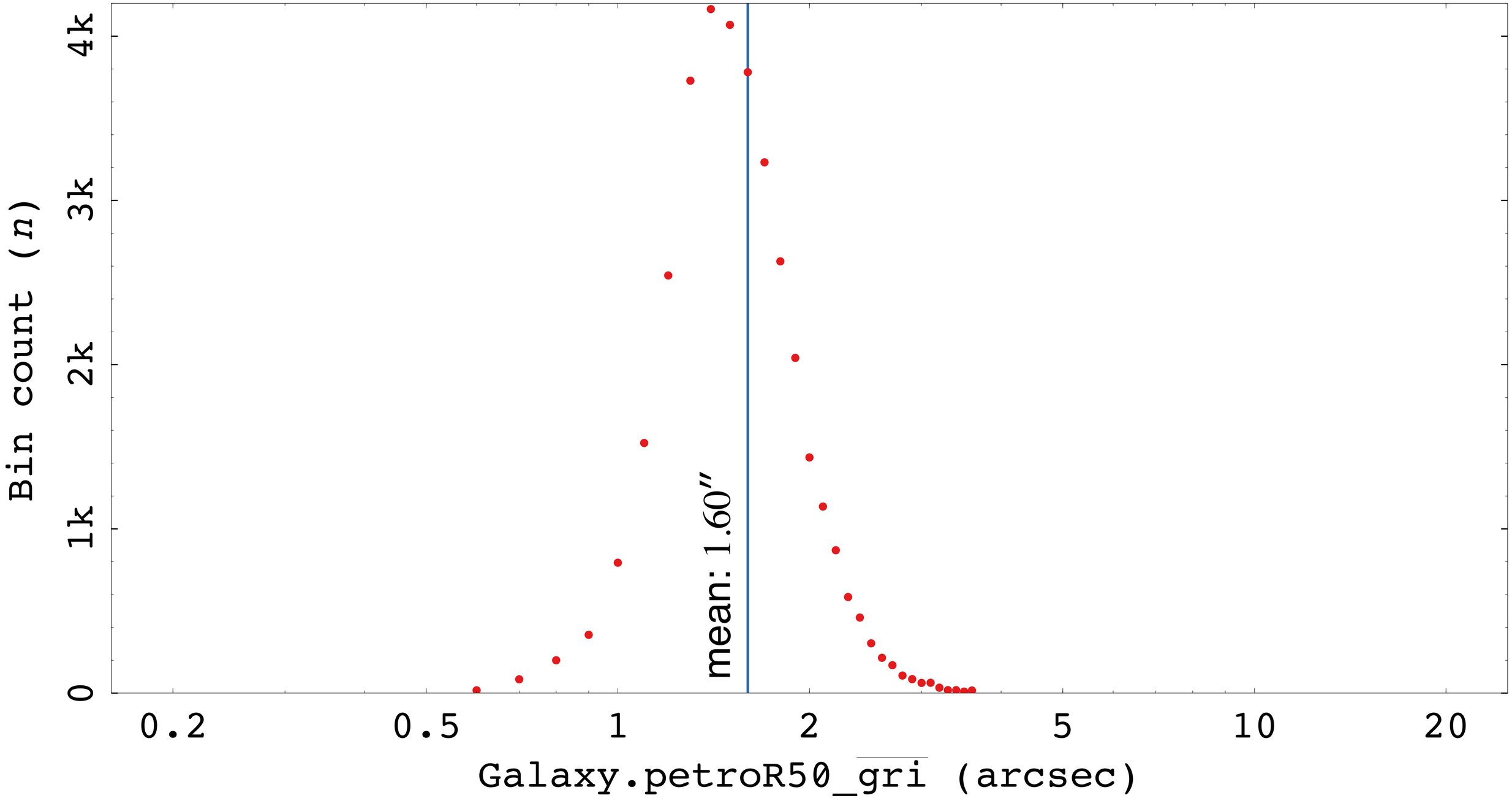
$\sum n \approx 36.0\text{k}$ $z \approx 0.08$ $(0.076 \leq z \leq 0.084)\ \&\ n > 6$



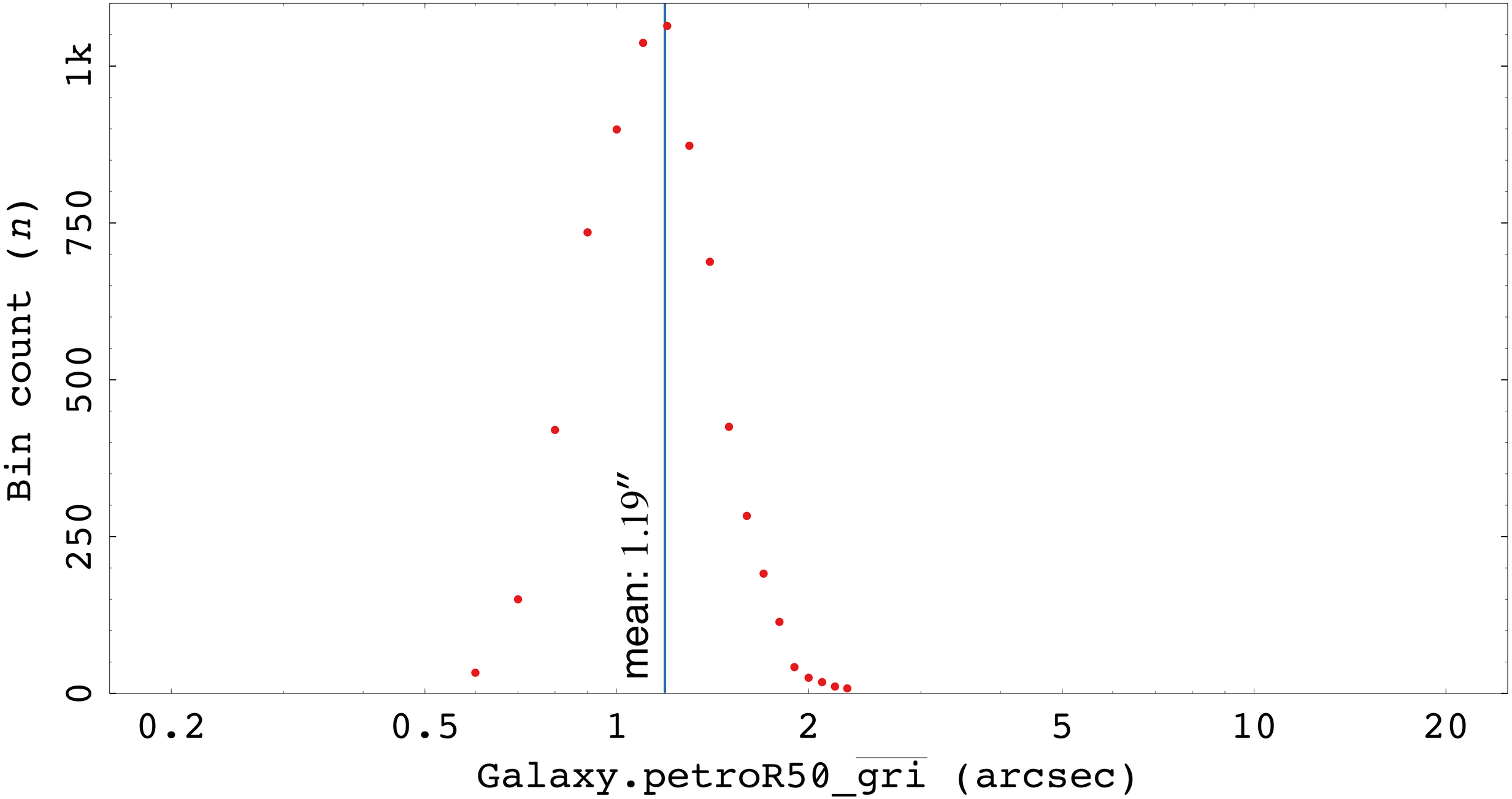
$\sum n \approx 32.9\text{k}$ $z \approx 0.16$ $(0.152 \leq z \leq 0.168)\ \&\ n > 6$



$\sum n \approx 34.7\text{k}$ $z \approx 0.32$ $(0.304 \leq z \leq 0.336)\ \&\ n > 6$



$\sum n = 7016$ $z \approx 0.64$ $(0.608 \leq z \leq 0.672)\ \&\ n > 6$



SQL for redshift-bin histograms

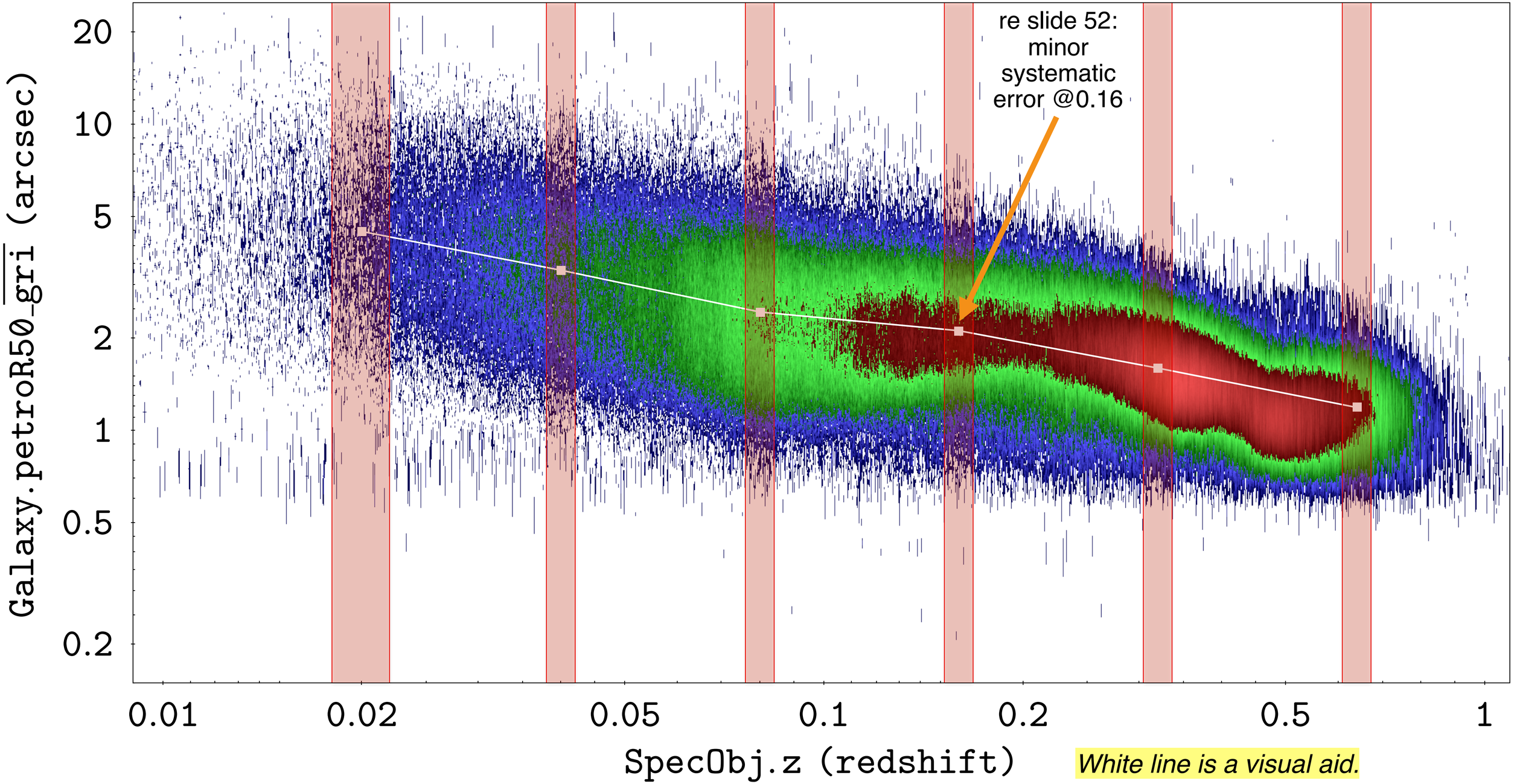
```
SELECT
    ROUND((petroR50_g + petroR50_r + petroR50_i) / 3 , 1) AS petroR50_gri
,   COUNT(1) AS n

...
```

Append to _$\overline{\text{gri}}$ WHERE clause:

```
AND s.z BETWEEN 0.018 AND 0.022 -- CHANGE THIS FOR EACH BIN.
GROUP BY
    ROUND((petroR50_g + petroR50_r + petroR50_i) / 3, 1)
    HAVING COUNT(1) > 3          -- CHANGE THIS AS NEEDED.
ORDER BY 1
```

Mean measurement of Galaxy.petroR50_$\overline{gri}$ within each redshift bin



White line is a visual aid.

Quantitative analysis of galaxy-size statistical distribution ($z = 0.08$)

```
SELECT
    ROUND(AVG(z), 3) AS AVGz
,   ROUND(AVG((petroR50_g + petroR50_r + petroR50_i) / 3), 2) AS ArithMean
,   ROUND(STDDEV((petroR50_g + petroR50_r + petroR50_i) / 3), 2) AS StdDev
,   ROUND(AVG(LN((petroR50_g + petroR50_r + petroR50_i) / 3)), 4) AS mu
,   ROUND(STDDEV(LN((petroR50_g + petroR50_r + petroR50_i) / 3)), 4) AS sigma
,   COUNT(1) AS n

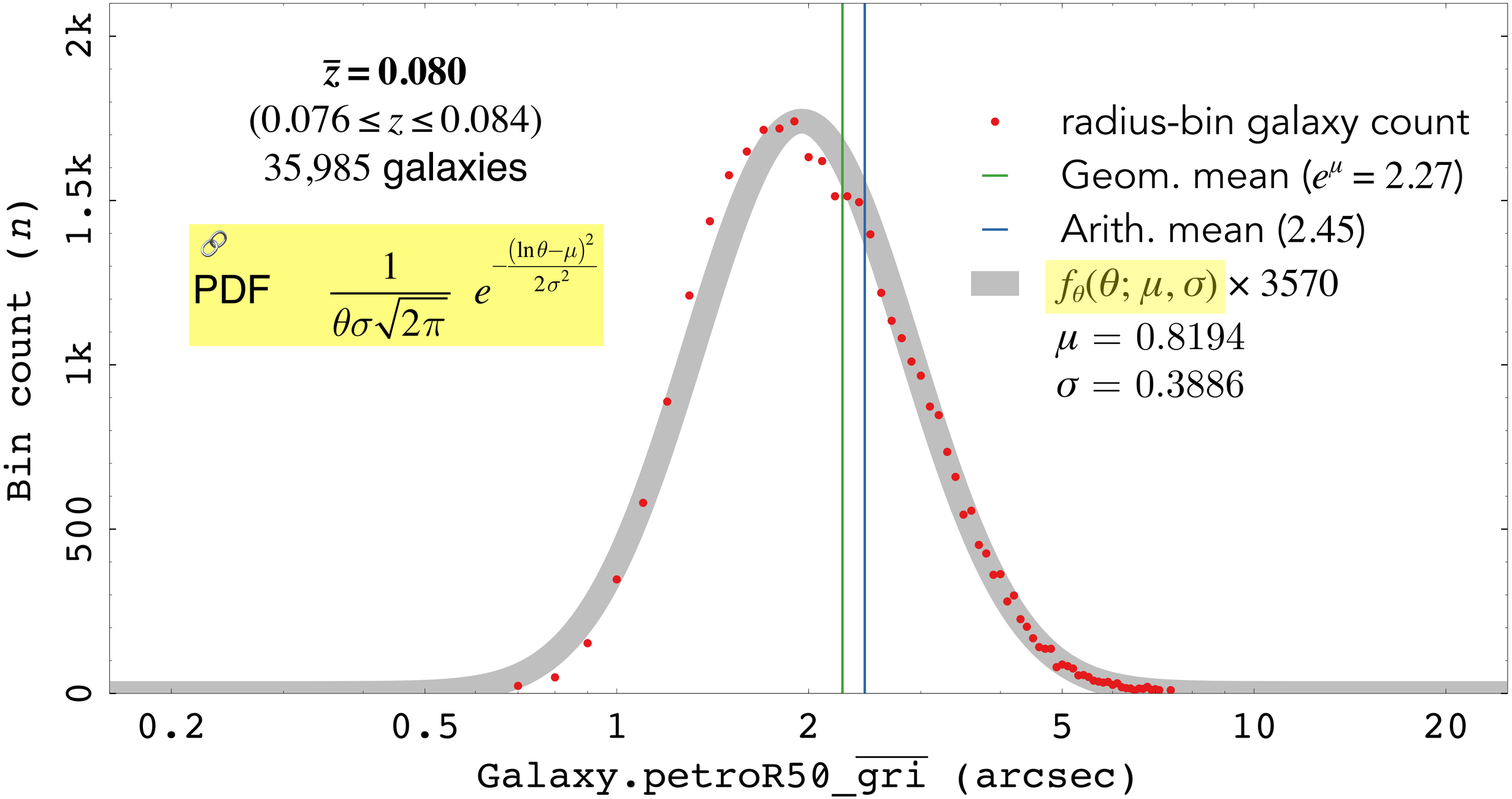
...
```

Append to _$\overline{\text{gri}}$ WHERE clause:

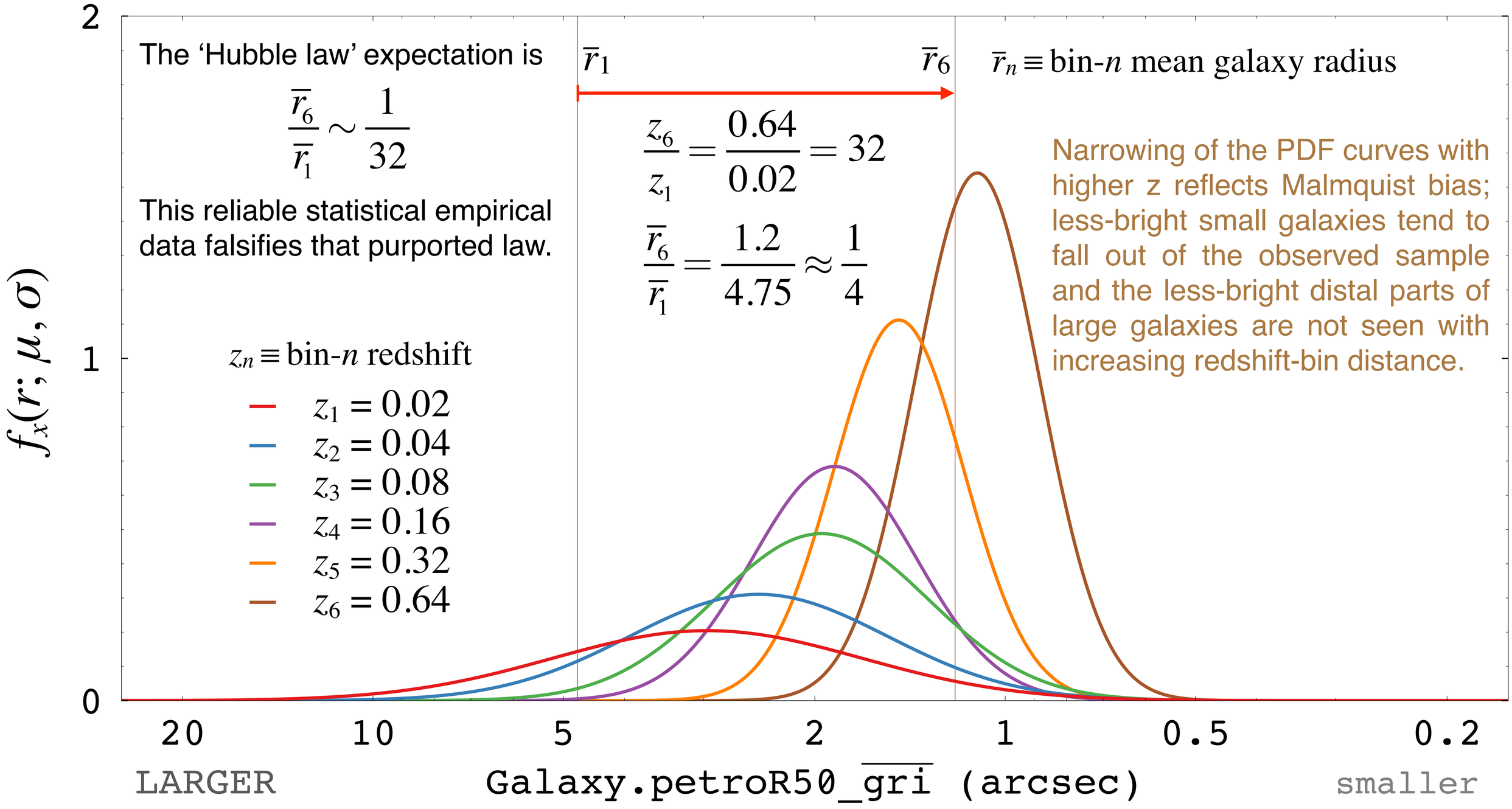
```
AND s.z BETWEEN 0.076 AND 0.084 -- z = 0.08 bin
```

AVGz	ArithMean	StdDev	mu	sigma	n
0.080	2.45	1.01	0.8194	0.3886	35985

Empirical distribution vs. log-normal probability density function (PDF)



Quantitative analysis of galaxy-size statistical distribution (all z-bins)



QQ plot confirmation of log-normal galaxy-size distribution

QQ Plot.nb

```
In[1]:= (* QQ plot to check log-normal distribution of redshift bin 0.08 *)

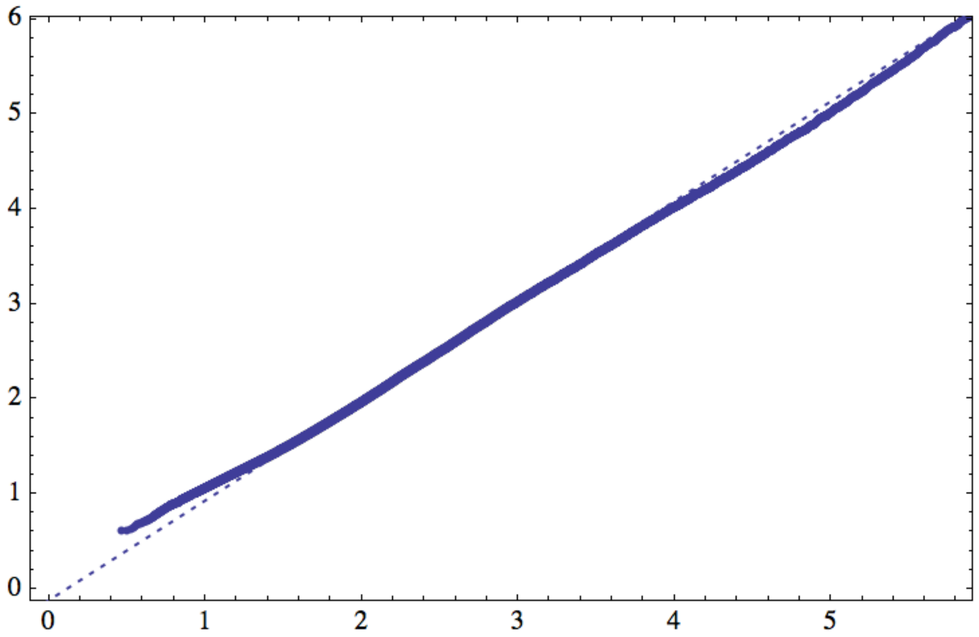
In[2]:= μ = 0.8194;

In[3]:= σ = 0.3886;

In[4]:= Import["/Users/alex/IWARA2018/AVGpetroR50_gri_Bin008.csv", "List"];

In[5]:= QuantilePlot[%, LogNormalDistribution[μ, σ]]
```

Out[5]=



Wolfram Mathematica

200%

SQL for QQ plot

```
SELECT
    (petroR50_g + petroR50_r + petroR50_i) / 3), 2) AS petroR50_gri
```

...

Append to _gri WHERE clause:

```
-- Uncomment one line, below, to choose that bin for analysis.
-- AND s.z BETWEEN 0.018 AND 0.022 -- z = 0.02 bin
-- AND s.z BETWEEN 0.038 AND 0.042 -- z = 0.04 bin
AND s.z BETWEEN 0.076 AND 0.084 -- z = 0.08 bin
-- AND s.z BETWEEN 0.152 AND 0.168 -- z = 0.16 bin
-- AND s.z BETWEEN 0.304 AND 0.336 -- z = 0.32 bin
-- AND s.z BETWEEN 0.608 AND 0.672 -- z = 0.64 bin
```

Quantitative analysis of galaxy-size statistical distribution (all z-bins)…

AVGz	ArithMean	StdDev	mu	sigma	n
0.020	4.75	2.83	1.4014	0.5627	3186
0.040	3.41	1.68	1.1178	0.4688	7834
0.080	2.45	1.01	0.8194	0.3886	35985
0.160	2.13	0.66	0.7114	0.2994	32942
0.320	1.60	0.39	0.4436	0.2367	34769
0.636	1.20	0.28	0.1533	0.2278	7036

Empirical inference

②

Galaxies have a log-normal size distribution, which is clearly observable over a wide range of redshift.

Empirical inference

③

To *good approximation*, the mean apparent galaxy size in each redshift bin can be expected to represent the same standard rod (i.e., to be very nearly the same *intrinsic* size). To assume otherwise would require some unphysical ad hoc explanation.

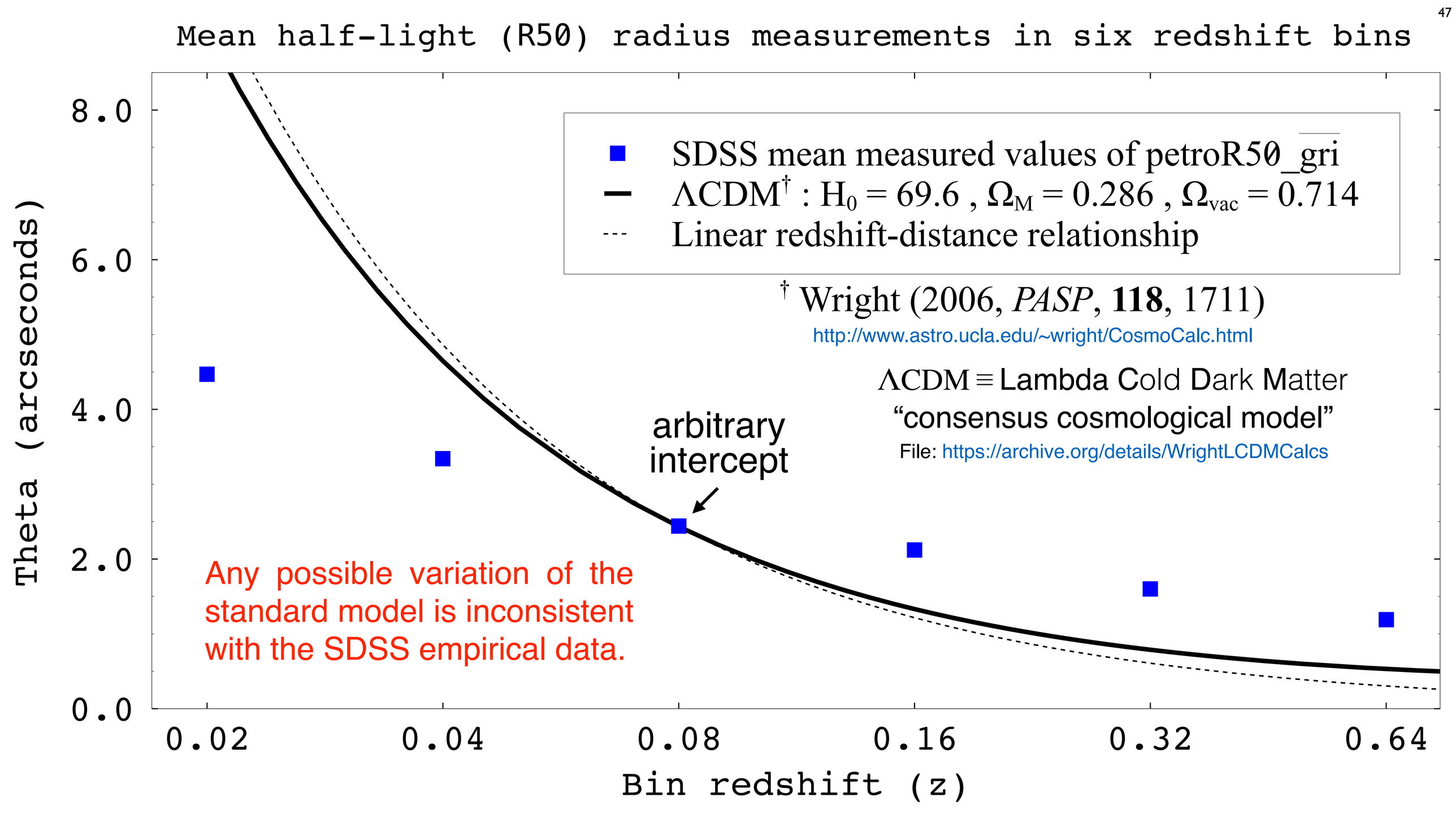
With a sample population across six redshift bins of $\sim 122\mathrm{k}$ galaxies, an increase in redshift of $32\times$ (z: $0.02 \rightarrow 0.64$) is correlated to a smooth and continuous decrease in mean apparent half-light radius of about $4\times$. This is eight times less than expected as per the ‘Hubble law’ predictive model.

"And where science gets *tough*, tough in the sense that you can be wrong, even if you passionately believe something, is that a good scientific theory makes predictions and those predictions can be tested."

🔗 Online Lecture: *The Nature of Space and Time* (1:05:50 / 1:28:25)

– Lee Smolin, *Perimeter Institute for Theoretical Physics*




Mean half-light (R50) radius measurements in six redshift bins
Theta (arcseconds)
8.0
6.0
4.0
2.0
0.0
0.02
0.04
0.08
0.16
0.32
0.64
Bin redshift (z)
SDSS mean measured values of petroR50_gri
ΛCDM† : H0 = 69.6 , ΩM = 0.286 , Ωvac = 0.714
Linear redshift-distance relationship
† Wright (2006, PASP, 118, 1711)
http://www.astro.ucla.edu/~wright/CosmoCalc.html
ΛCDM ≡ Lambda Cold Dark Matter
"consensus cosmological model"
File: https://archive.org/details/WrightLCDMCalcs
arbitrary intercept
Any possible variation of the standard model is inconsistent with the SDSS empirical data.

Let's be clear about what that graph means, as it is non-trivial:

First, we confirm that the empirical SDSS theta-z data is objective and that there is no systematic error or any other problem that invalidates logical inferences that may be drawn from that data.

The graph means that the empirical redshift-distance relationship is inconsistent with the 'Hubble law.' If that is true, then the Universe is not expanding, regardless of what we may *believe* or want to believe. The data is unambiguous; it is based on $\sim 2 \times 10^6$ objective high-quality measurements that are not affected by confirmation bias.

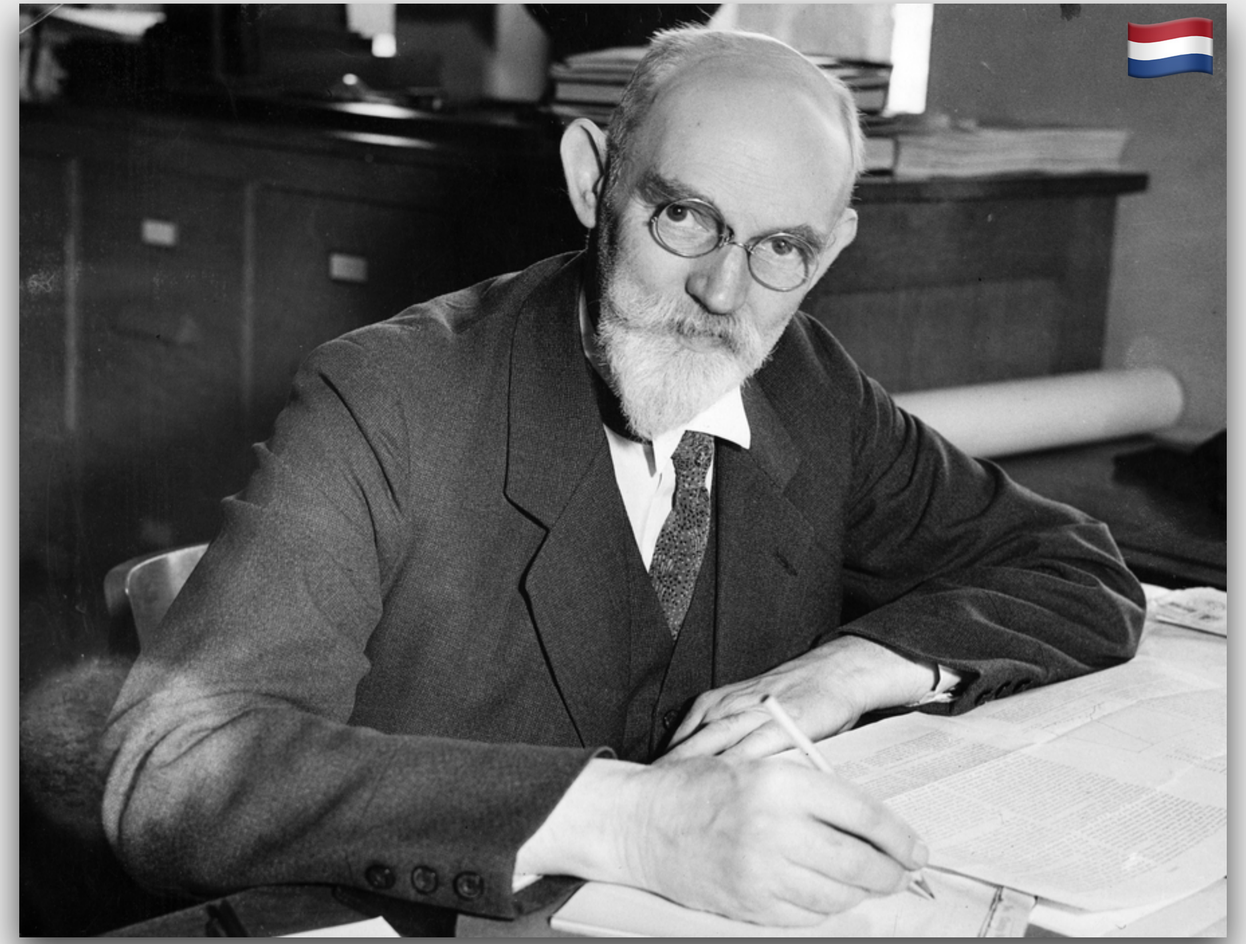
Accordingly, we have a major *scientific crisis* (confirmed by several other independent, corroborating empirical observations, shown later). To find a resolution, there is only one place to look for guidance…

The Einstein Field Equations

$$G_{\mu\nu} + \Lambda g_{\mu\nu} = 8\pi T_{\mu\nu}$$

(The physical constants are normalized.)

Willem de Sitter (6 May 1872 – 20 Nov 1934) was a Dutch mathematician, physicist, and astronomer.



publications link
dwc.knaw.nl ⇨

dwc KNAW Digital Library

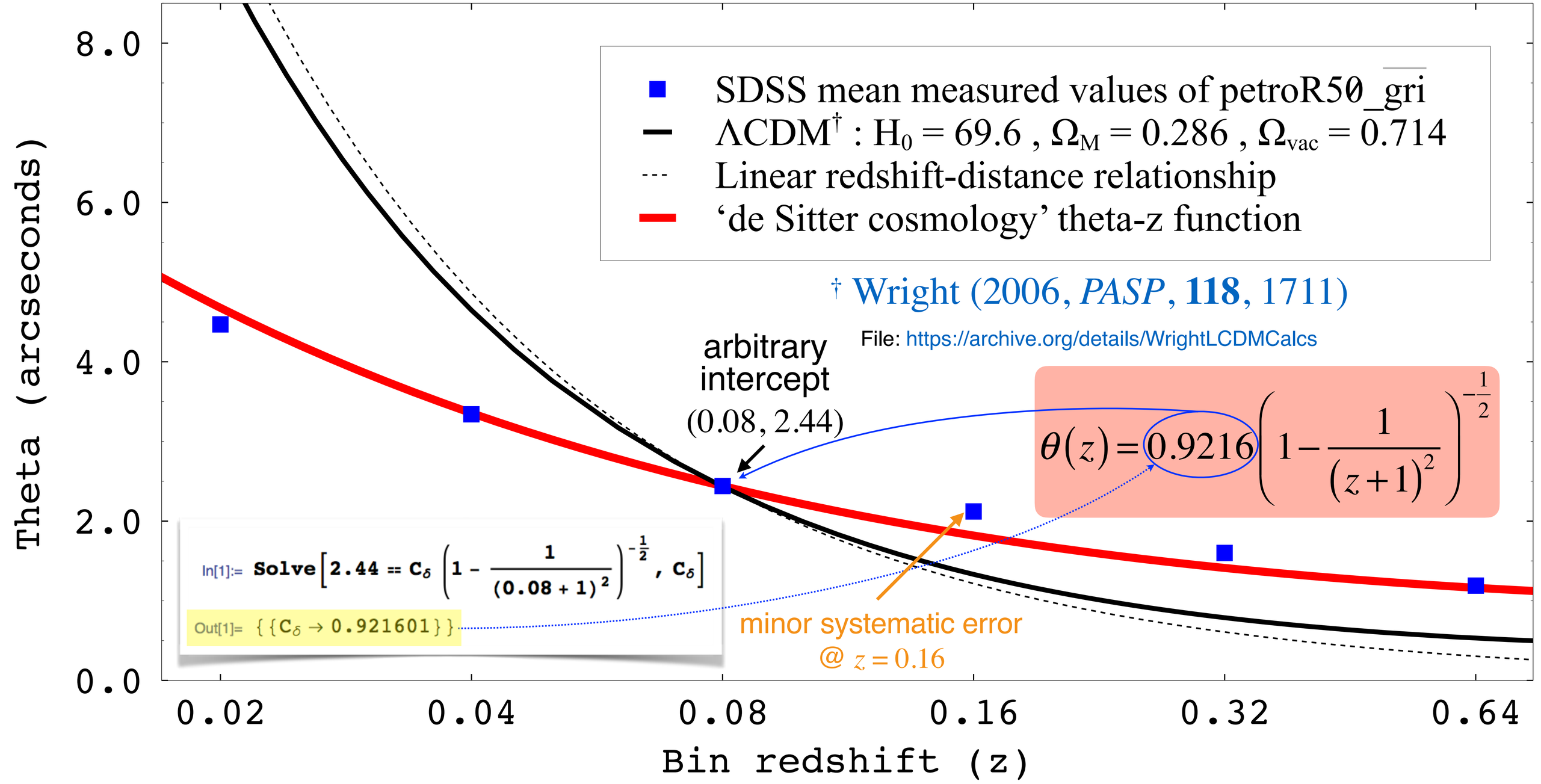
In a nutshell, we go back to Willem de Sitter's exact solution to the Einstein field equations (EFE) circa 1917 and gain a clear and rational understanding of its *physical interpretation*, which new interpretation *supersedes* that of the Einstein-de Sitter debate.[1] This leads to the derivation of a new set of predictive formulas, which rest on first principles and are consistent with the EFE. Among these formulas is:

$$\theta(z) = C_\delta \left(1 - \frac{1}{(z+1)^2} \right)^{-\frac{1}{2}} \quad \text{radians}$$

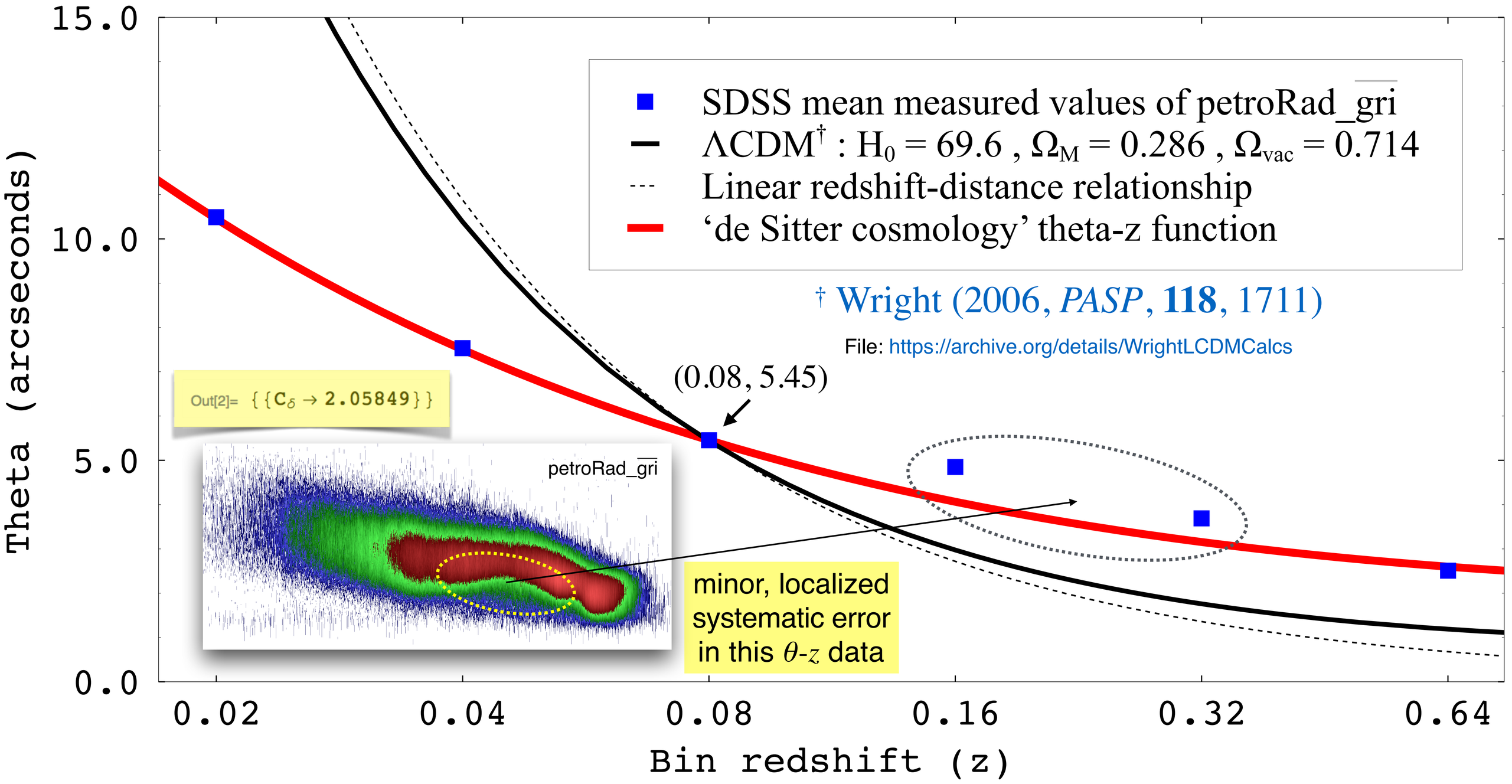
C_δ is an arbitrary *scaling* constant that is proportional to the intrinsic diameter (δ) of the astrophysical standard rod under consideration. Thus, changing C_δ *shifts* the predictive curve up or down to match an arbitrary object size, but it does not modify that curve in any way: With regard to relative measurements, *there are no free parameters in any of the new predictive formulas*. For absolute measurements, the single shared free parameter is the estimated Cosmic radius R.

1. C. O'Raifeartaigh, M. O'Keeffe, W. Nahmb and S. Mitton, "Einstein's cosmology review of 1933: a new perspective on the Einstein-de Sitter model of the cosmos," *Euro. Phys. J. H.* **40**, 301 (2015); arXiv:1503.08029 [physics.hist-ph].

Mean half-light (R50) radius measurements in six redshift bins



Mean Petrosian radius measurements in six redshift bins



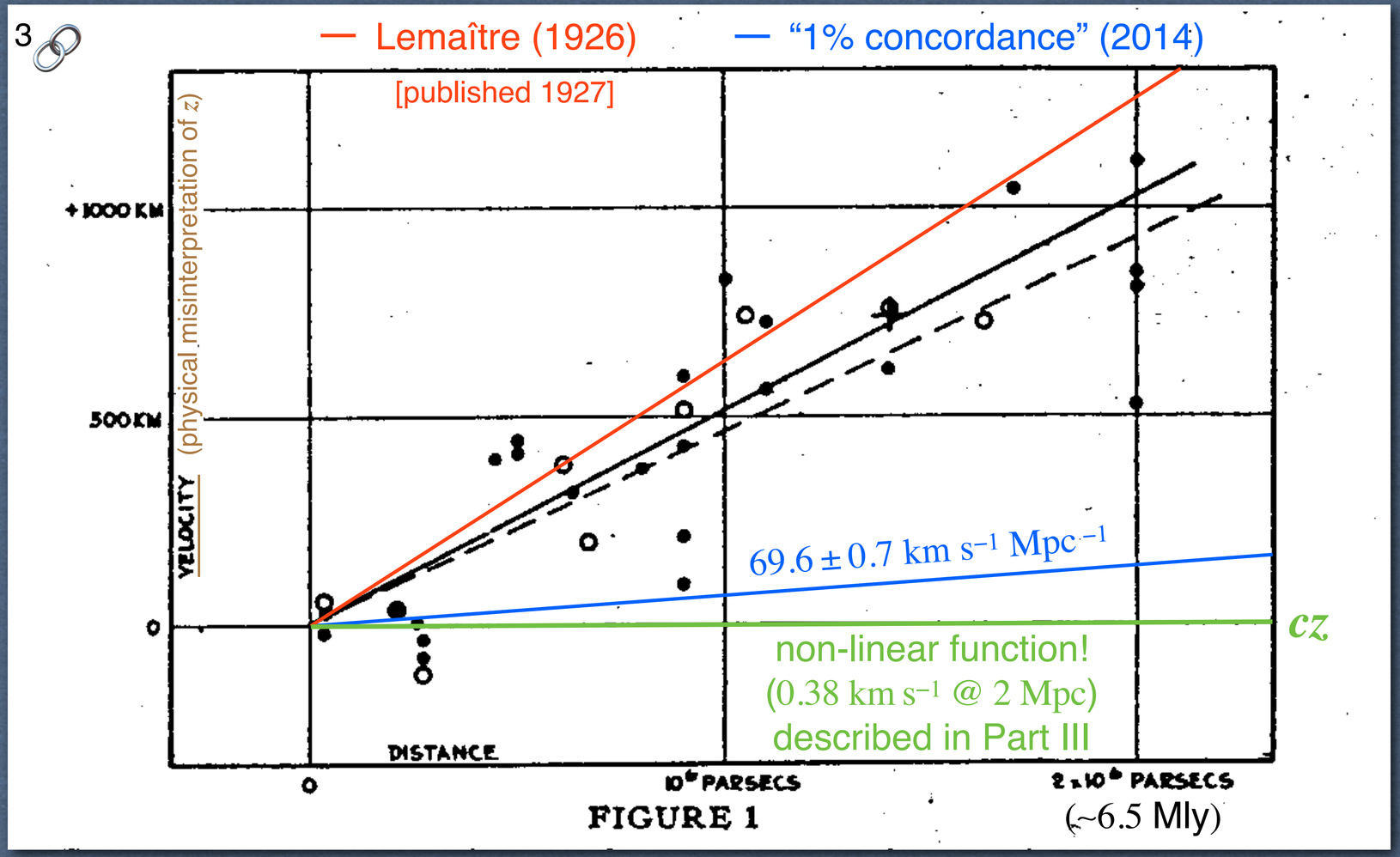
Let's be clear about what the red curves on the prior two slides mean, as it is non-trivial:

As an accurate predictive model of empirical observations, they mean that the Universe is not expanding, regardless of what we may *believe* or want to believe. Over a century ago, de Sitter *unequivocally* pursued the right idea (galaxy redshifts are caused by cosmological spacetime geometry and not by expansion-induced recession). However, he did not adequately interpret (and further develop) his own mathematics.

Quoted from Edwin Hubble's last paragraph; *PNAS* **15**, 168 (1929)

The outstanding feature, however, is the possibility that the velocity-distance relation may represent the de Sitter effect, and hence that numerical data may be introduced into discussions of the general curvature of space. … it may be emphasized that the linear relation found in the present discussion is a first approximation representing a restricted range in distance.

1929 Hubble diagram (annotated)



PART II – SDSS REDSHIFT-MAGNITUDE DATA

Click to go back to Table of Contents…

The astronomical magnitude scale

Apparent magnitude is quantified in terms of the radiation *flux ratio* within a given spectral band (x):

$$m = -2.5 \cdot \log_{10}\left(\frac{F_x}{F_{x,0}}\right)$$

observed / reference

- *Brighter* objects have a *smaller* magnitude.
- -5 “mags” is exactly $100\times$ brighter.
- -1 mag is $\sqrt[5]{100} \approx 2.512\times$ brighter.
- Δm mags is a change in brightness of $2.512^{-\Delta m}\times$

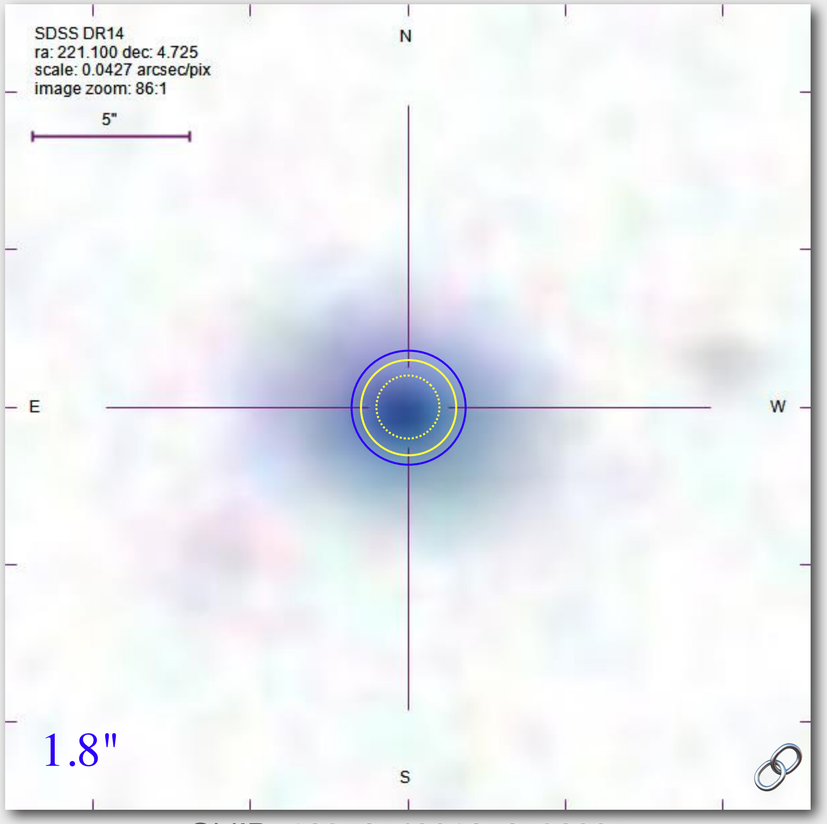
Three among the typical, smaller galaxies in the redshift bin (petroR50_$\overline{gri}$ = 1.8″)

◯ petroR50_$\overline{gri}$ (± 0.1″)

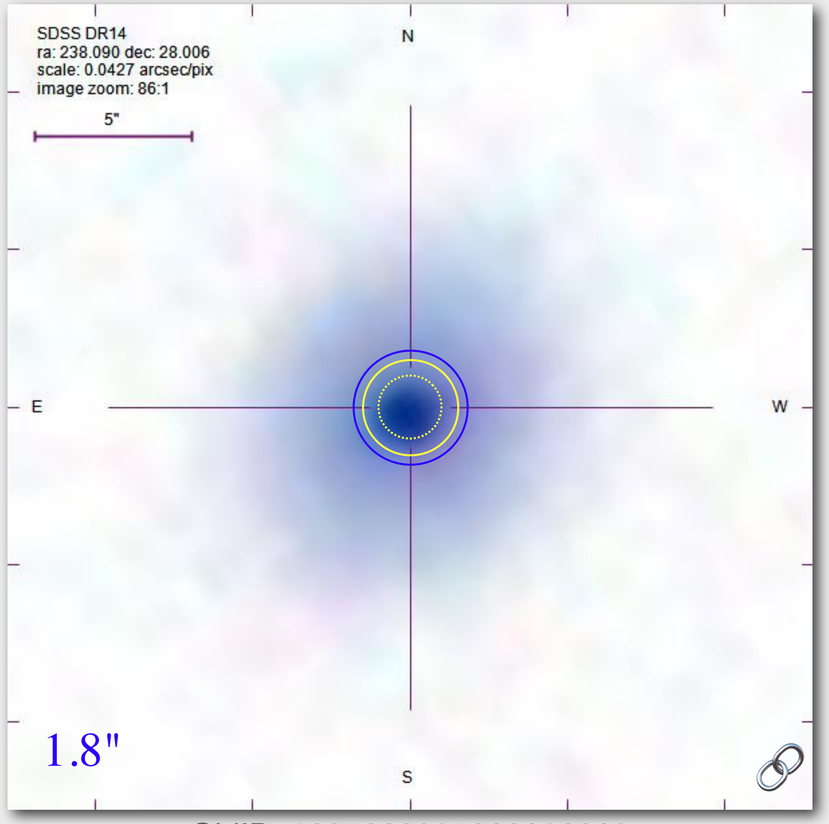
◯ 3″-diameter SDSS fiber

◯ 2″-diameter SDSS fiber

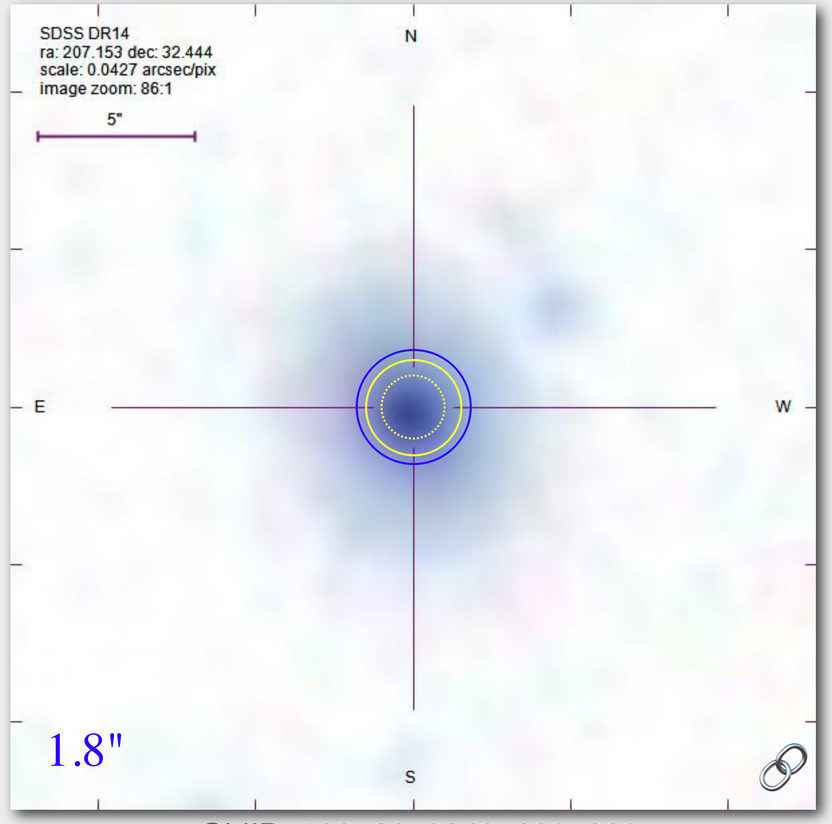
$z = 0.080 \pm 0.004$ (±5%)



ObjID: 1237654881276592335



ObjID: 1237662305662206269



ObjID: 1237665024376307880

SCALE: 0.0427 arcsec/pixel

Click images for SDSS SkyServer Explorer.

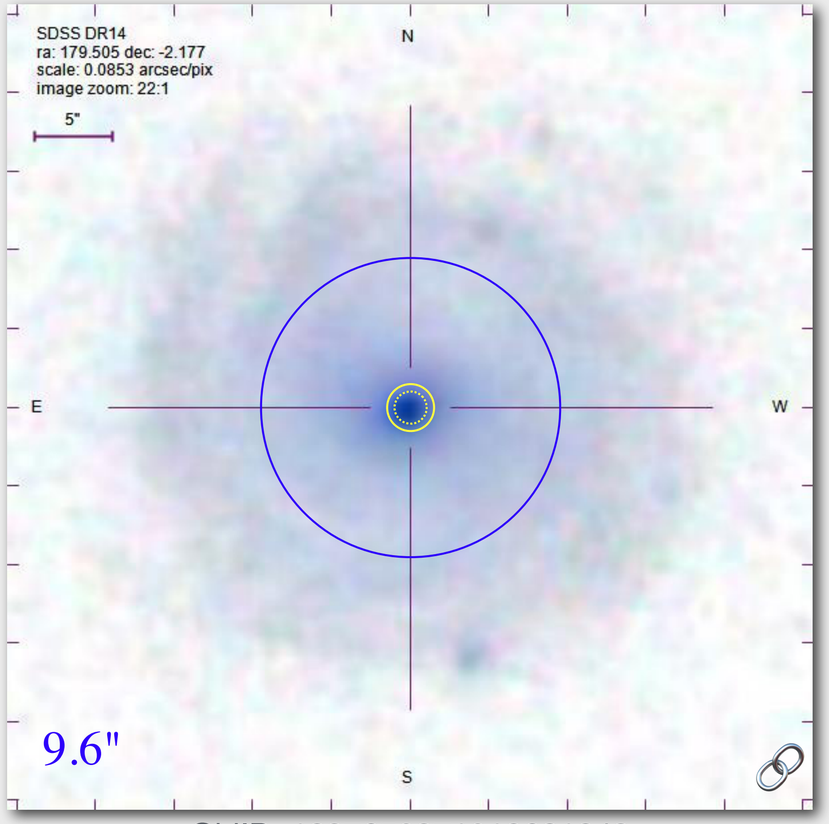
Three among the largest galaxies in the redshift bin, including the extreme outlier

◯ petroR50_gri ($\pm 0.1''$)

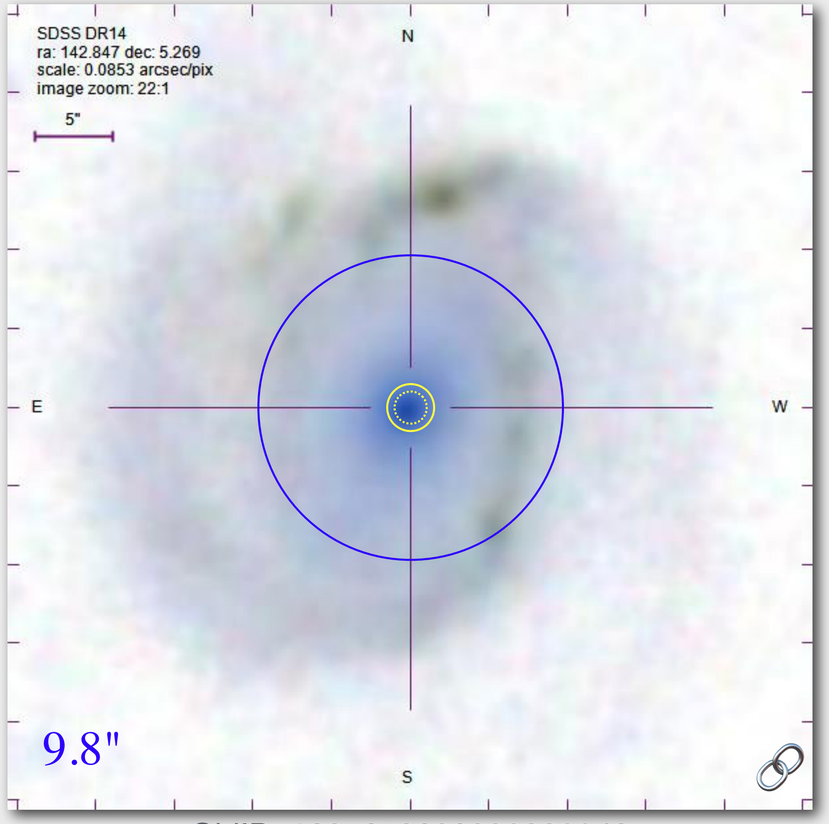
◯ 3″-diameter SDSS fiber

◯ 2″-diameter SDSS fiber

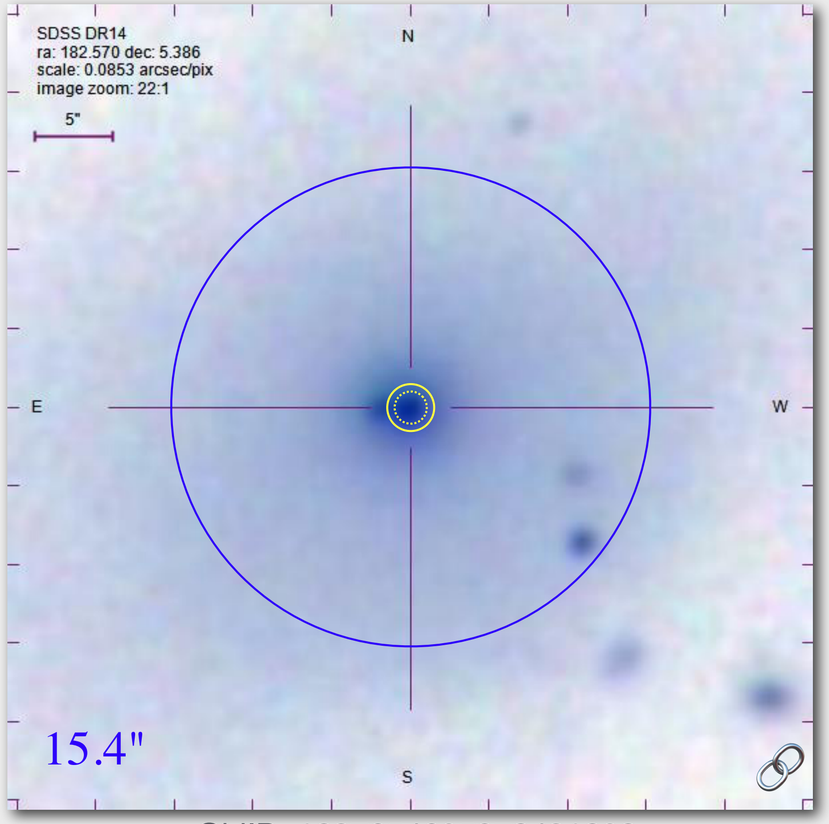
$z = 0.080 \pm 0.004$ ($\pm 5\%$)



ObjID: 1237650371018621243



ObjID: 1237658298990330048



ObjID: 1237654605872431202

Change of scale (demagnified 2×) → SCALE: 0.0853 arcsec/pixel

Click images for SDSS SkyServer Explorer.

Empirical inference

④

By inspection* : to close approximation, the intrinsic diameter of galactic nuclei are constant and independent of host-galaxy size.

Also, down to about $z \sim 0.08$, a $3''$-diameter fixed aperture encloses the apparent diameter of galactic nuclei, thus measuring their flux. Any distal regions of more distant galaxies so enclosed will add a much smaller contribution to the total flux measured by the fiber.

* (of numerous randomly-selected SDSS galaxy images)

Fixed-aperture fiber magnitudes

Fixed-aperture fiber magnitudes are a *byproduct* of the optical spectroscopy measurements (e.g., redshift)—as such, they were not previously considered to be photometric "science data." However, by serendipitous correlation, the $3''$- and $2''$-diameter (Legacy and BOSS spectrograph fibers, respectively) measure (to good approximation over $0.08 \leq z \leq 0.5$) the apparent brightness of galactic nuclei, which dominate the total light flux of galaxies. Just like stars, these ubiquitous objects have a span of intrinsic brightness; given data on $\sim 10^6$ objects, *population statistics* can be exploited for scientific discovery.

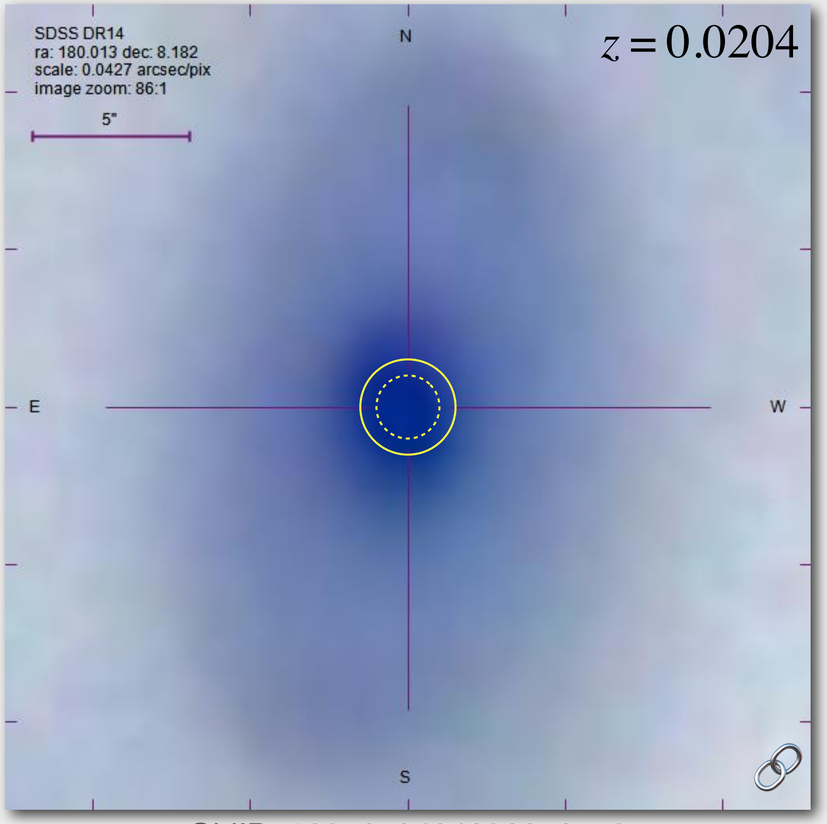
These data are important because they are *independent* of the photometric-pipeline magnitude measurements (e.g., Petrosian magnitudes), with which they shall be shown to be in agreement as concerns empirical *interpretation*.

Fixed-aperture effect over a wide range of redshift $(0.02, 0.08, 0.60)$

○ 3″-diameter SDSS fiber

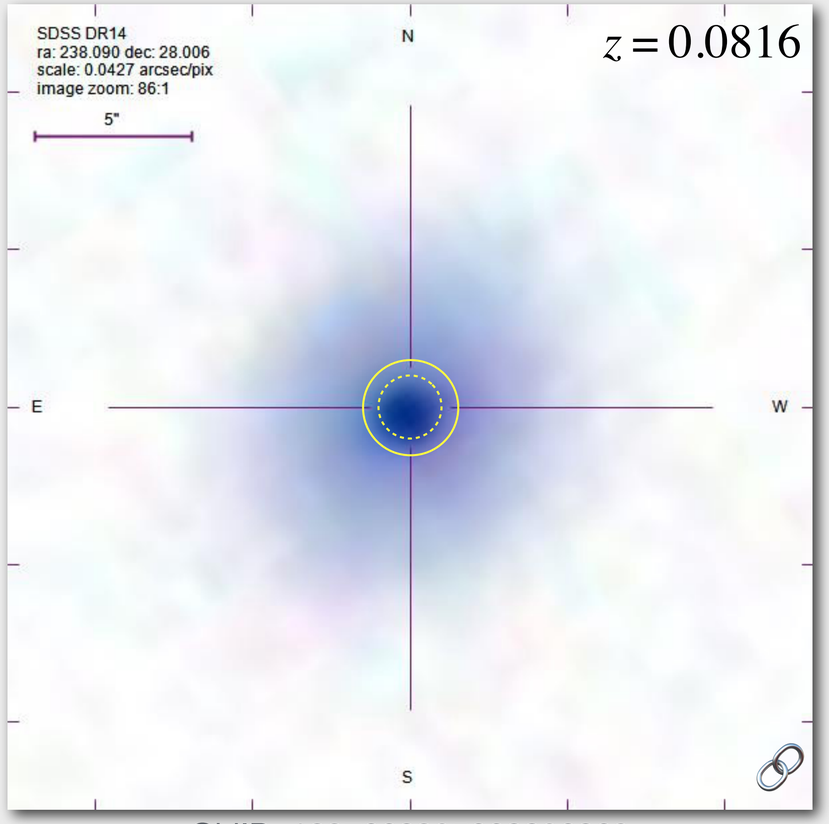
◌ 2″-diameter SDSS fiber

Aperture too small for nucleus:
measured magnitude too high.



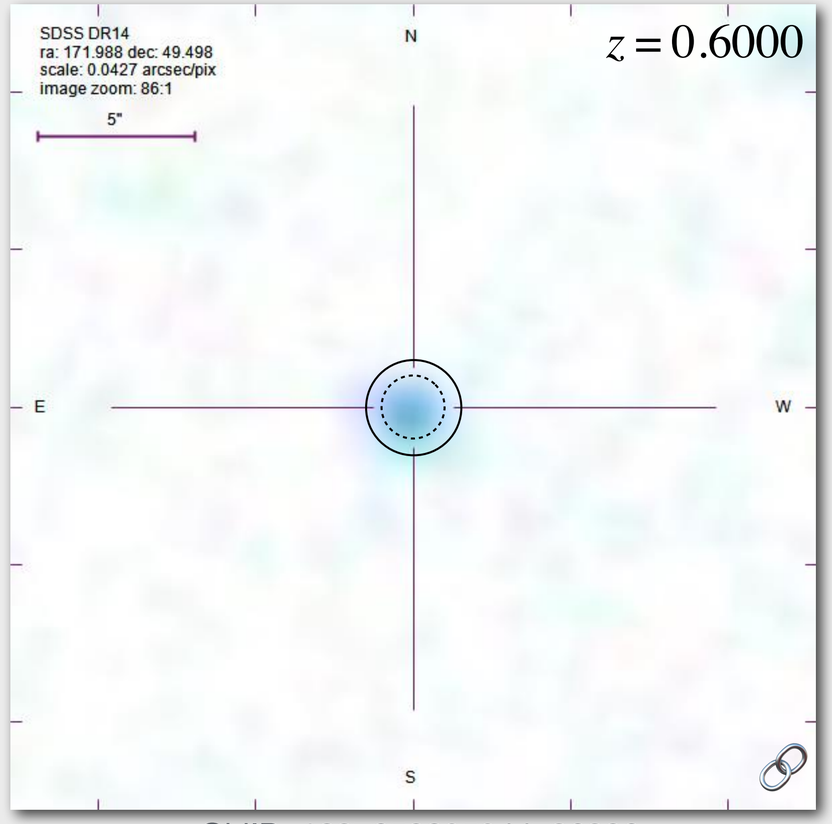
ObjID: 1237658424636276773

Aperture encloses nucleus:
good measured magnitude.



ObjID: 1237662305662206269

Aperture too large for nucleus:
measured magnitude too low.



ObjID: 1237658205044736386

SCALE: 0.0427 arcsec/pixel

Click images for SDSS SkyServer Explorer.

SDSS documentation reference

Fiber Magnitudes: fiberMag and fiber2Mag

Fiber magnitudes reflect the flux contained within the aperture of a spectroscopic fiber in each band. In the case of `fiberMag` we assume an aperture appropriate to the SDSS spectrograph (3″ in diameter). In the case of `fiber2Mag` we assume an aperture appropriate to the BOSS spectrograph (2″ in diameter).

Notes

- For children of deblended galaxies, some of the pixels within a 1.5″ radius may belong to other children; we now measure the flux of the parent at the position of the child; this properly reflects the amount of light which the spectrograph will see.
- Images are convolved to 2″ seeing before fiberMags are measured. This also makes the fiber magnitudes closer to what is seen by the spectrograph.
- Addendum to the above from DR7 notes: There is a cut in 3″ fiber magnitude at g=15, r=15, and i=14.5 (to prevent saturation and cross-talk in the spectrographs).[1]

Source: https://www.sdss.org/dr14/algorithms/magnitudes/#mag_fiber

1. http://classic.sdss.org/dr7/products/general/target_quality.html

SDSS glossary reference

Fiber

The SDSS spectrograph uses optical fibers to direct the light at the focal plane from individual objects to the slithead. Each object is assigned a corresponding `fiberID`. The fibers for SDSS-I/II were 3 arcsecs in diameter in the source plane; they are 2 arcsecs in diameter for BOSS. Each fiber is surrounded by a large sheath which prevents any pair of fibers from being placed closer than 55 arcsecs on the same plate (62 arcsecs for BOSS).

fiberMag

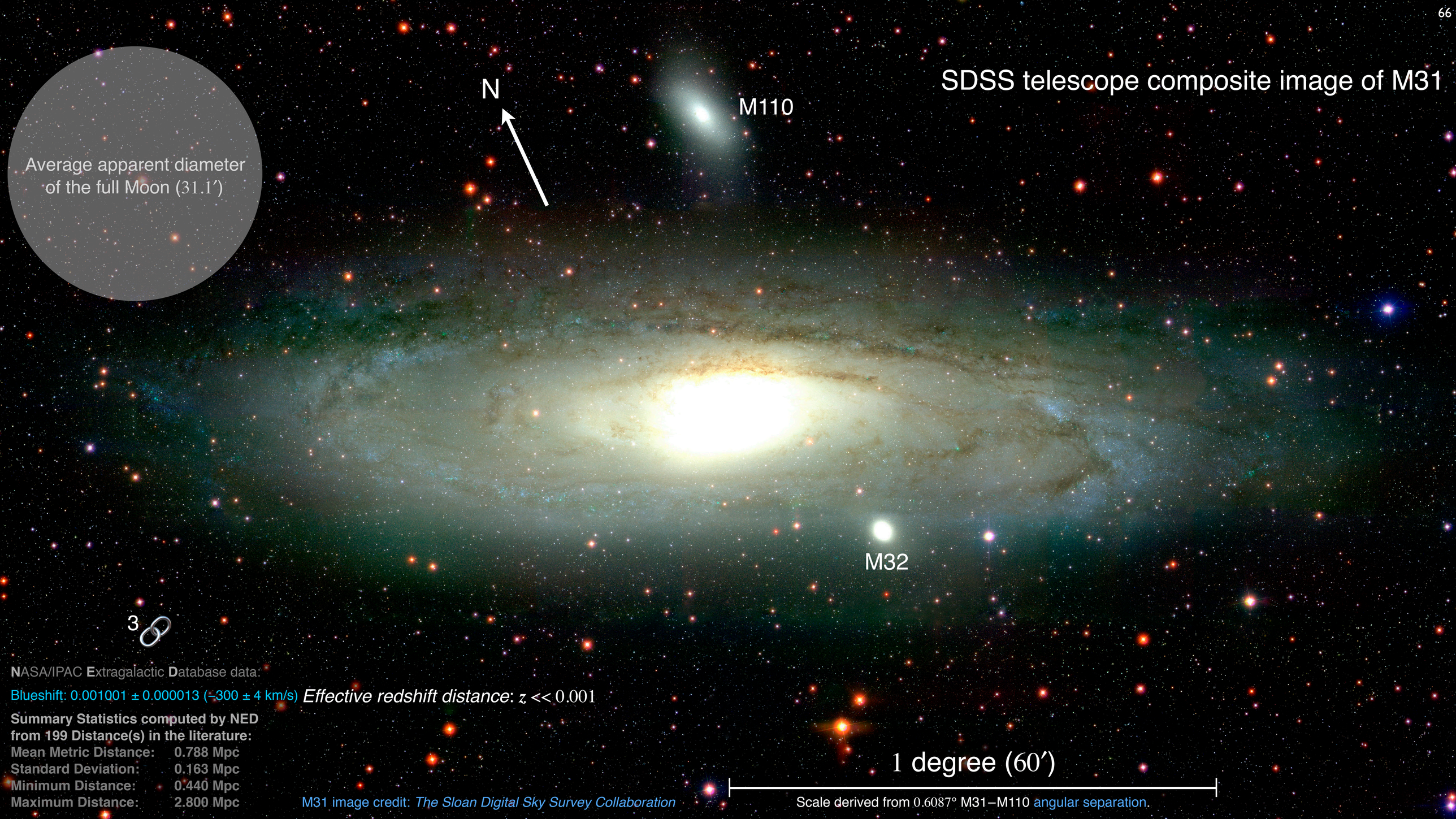
The magnitude measured by the frames pipeline to simulate the flux that would fall into a 3″ fiber in typical seeing. Similarly, `fiber2Mag` simulates the 2″ fiber magnitude.

Plate

Each spectroscopic exposure employs a large, thin, circular metal plate that positions optical fibers via holes drilled at the locations of the images in the telescope focal plane. These fibers then feed into the spectrographs. Each plate has a unique serial number, which is called *plate* in views such as `SpecObj` in the CAS.

Source: https://www.sdss.org/dr14/help/glossary/#F

SDSS telescope composite image of M31



NASA/IPAC **E**xtragalactic **D**atabase data:

Blueshift: 0.001001 ± 0.000013 (–300 ± 4 km/s) *Effective redshift distance*: $z << 0.001$

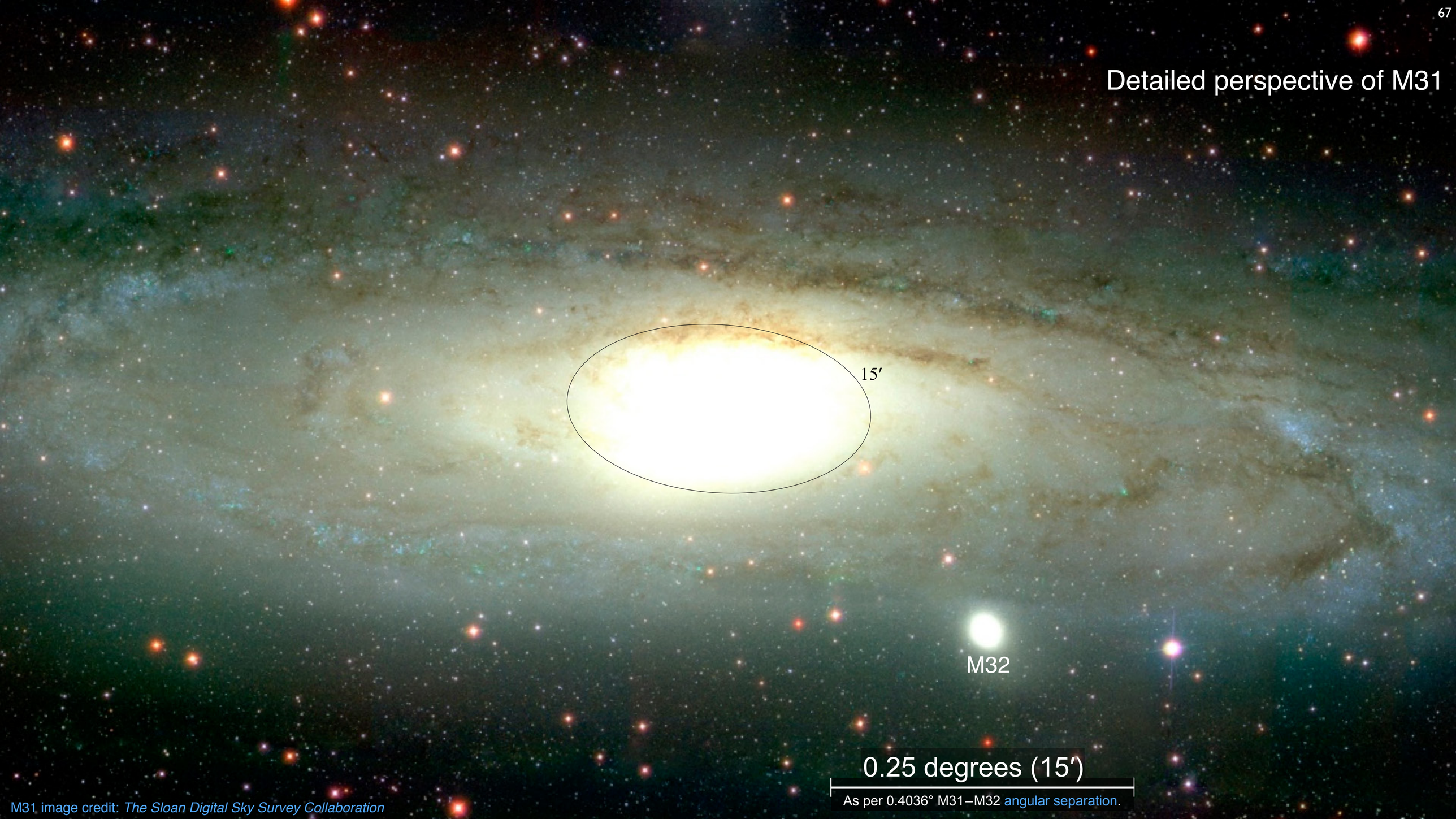
Summary Statistics computed by NED from 199 Distance(s) in the literature:

Mean Metric Distance:	**0.788 Mpc**
Standard Deviation:	**0.163 Mpc**
Minimum Distance:	**0.440 Mpc**
Maximum Distance:	**2.800 Mpc**

M31 image credit: *The Sloan Digital Sky Survey Collaboration*

Scale derived from 0.6087° M31–M110 angular separation.

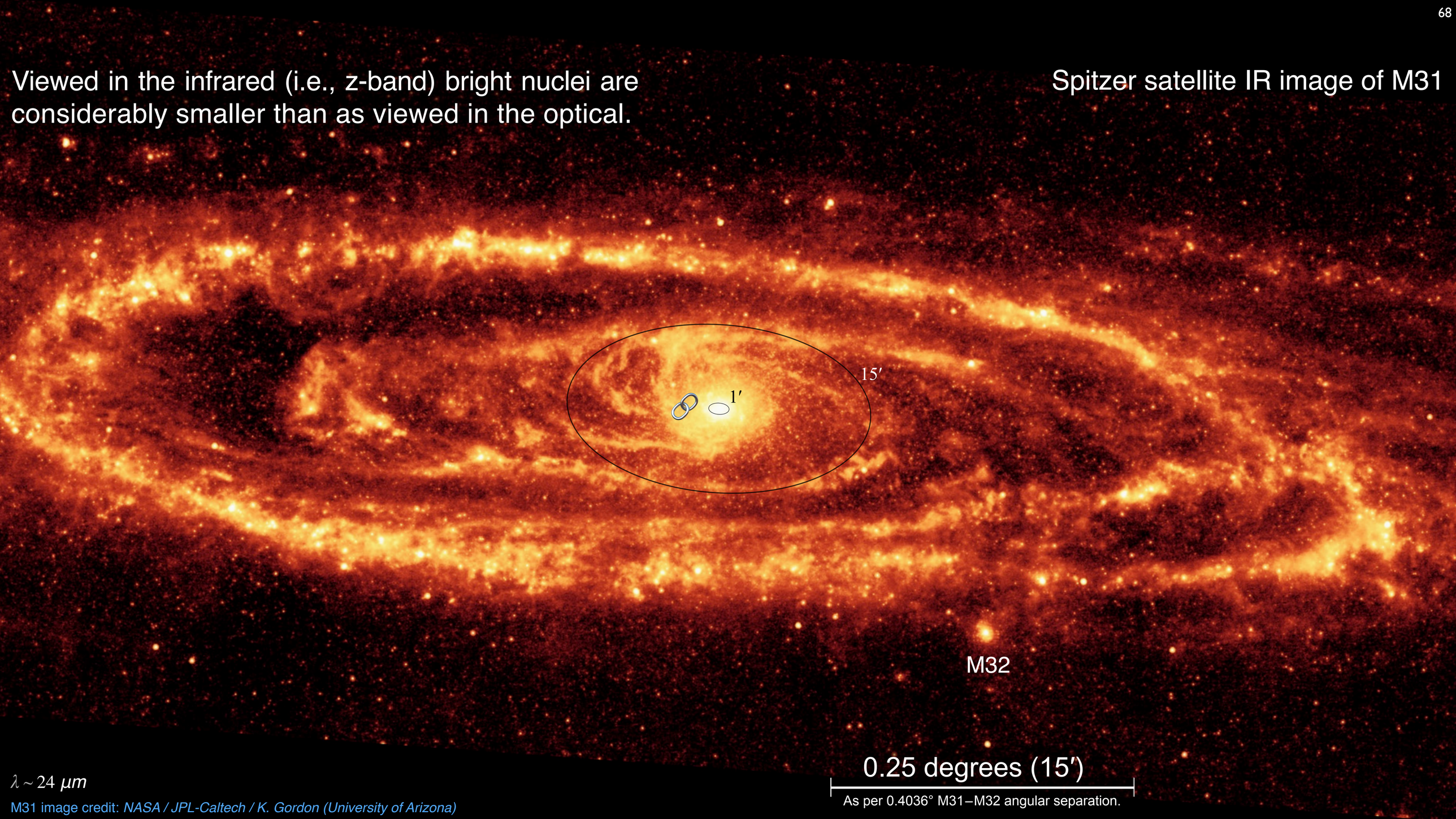
Detailed perspective of M31



M31 image credit: *The Sloan Digital Sky Survey Collaboration*

Viewed in the infrared (i.e., z-band) bright nuclei are considerably smaller than as viewed in the optical.

Spitzer satellite IR image of M31

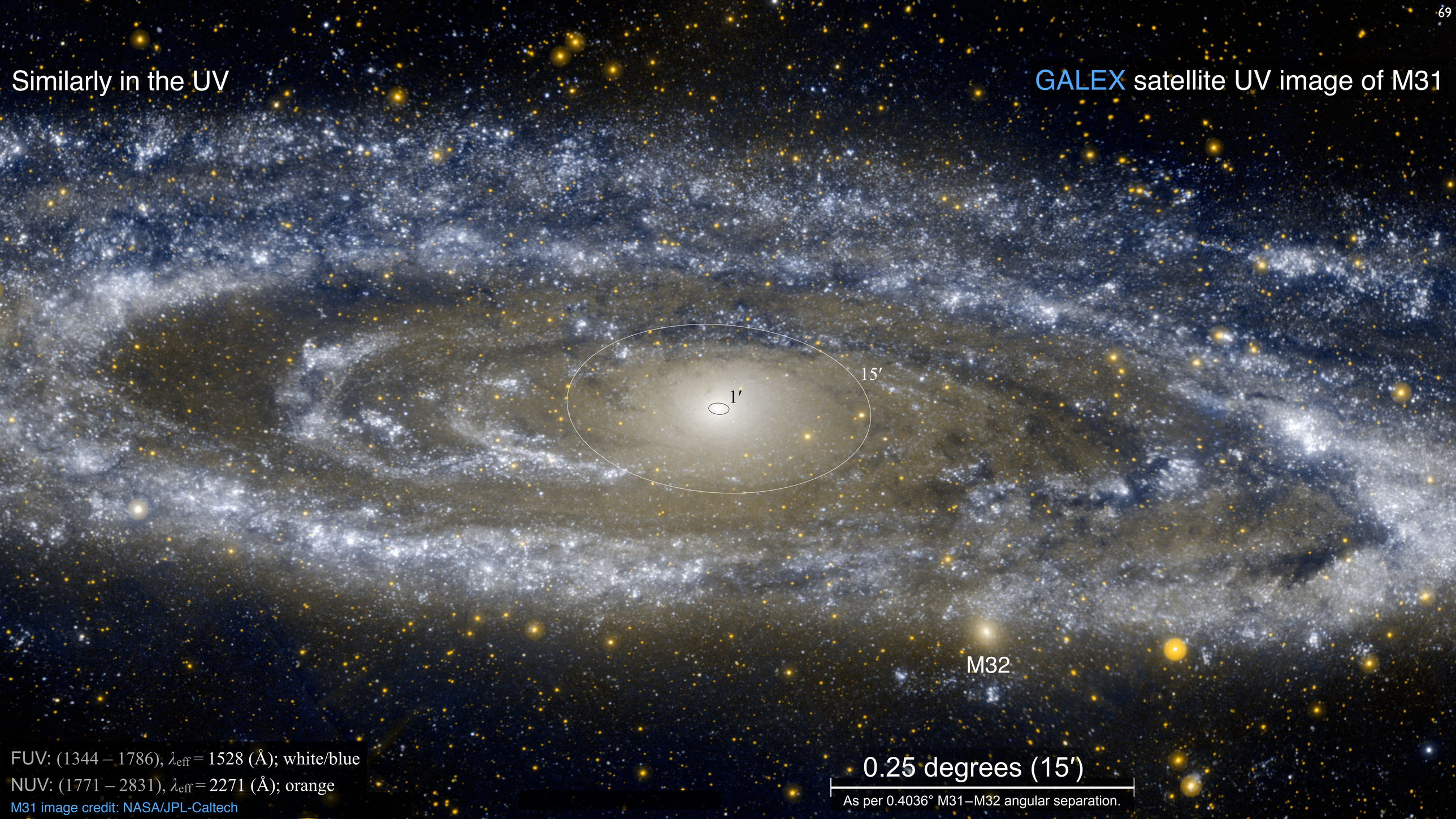


$\lambda \sim 24\ \mu m$

M31 image credit: *NASA / JPL-Caltech / K. Gordon (University of Arizona)*

Similarly in the UV

GALEX satellite UV image of M31



FUV: (1344 – 1786), λ_{eff} = 1528 (Å); white/blue

NUV: (1771 – 2831), λ_{eff} = 2271 (Å); orange

M31 image credit: NASA/JPL-Caltech

0.25 degrees (15′)

As per 0.4036° M31–M32 angular separation.

Similarly in the UV

SWIFT satellite UV image of M31

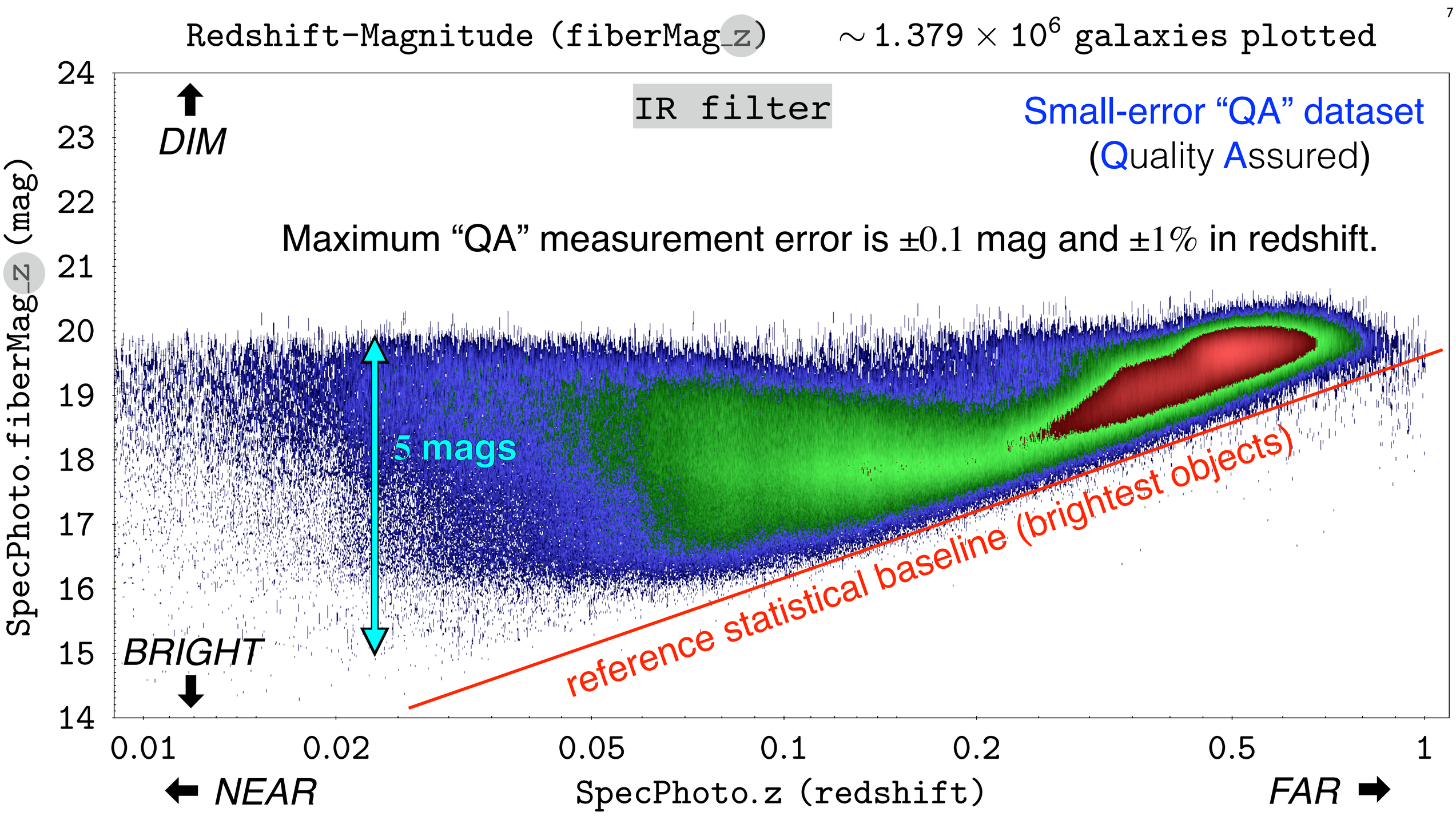


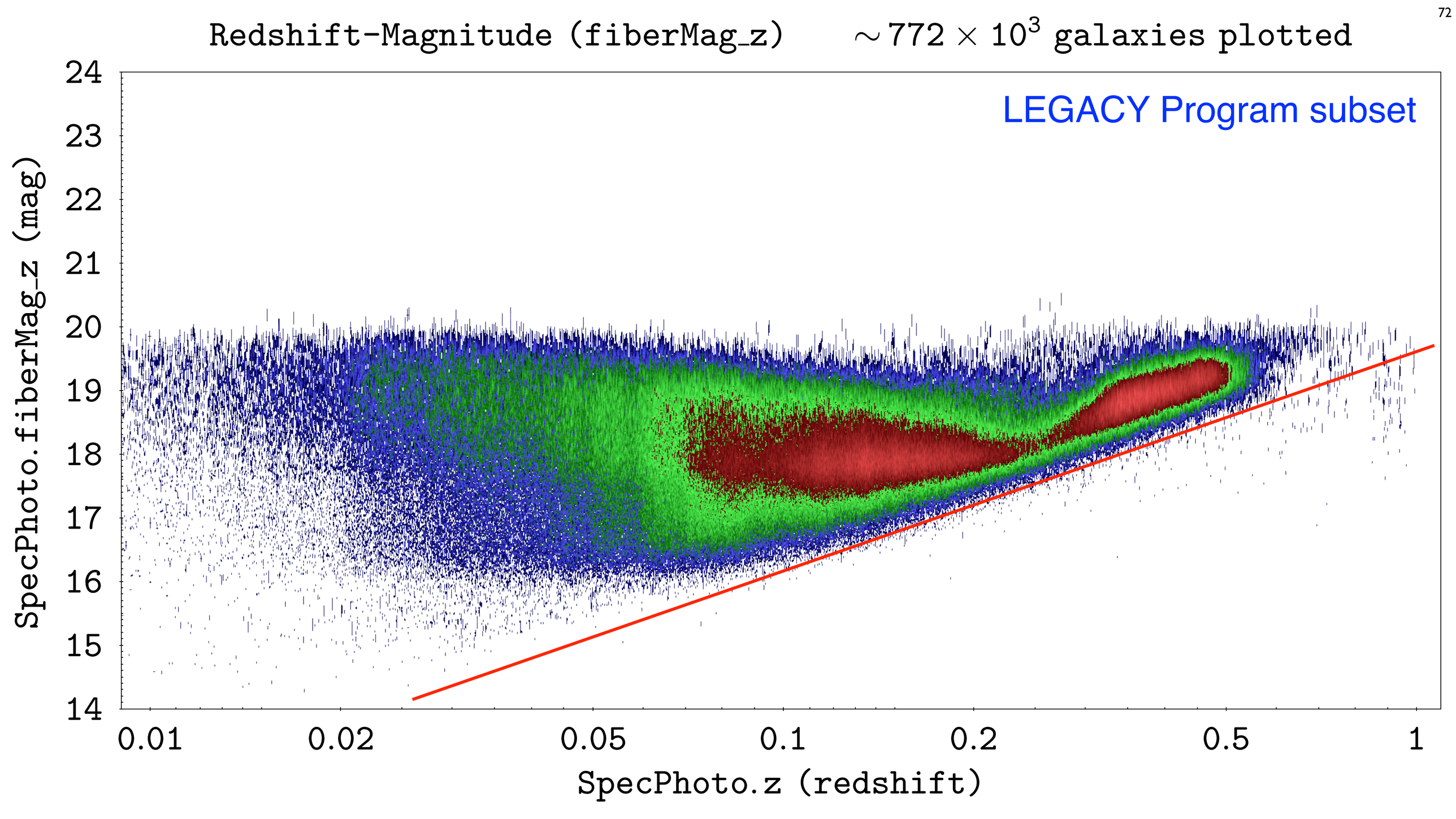
λ : 1700 – 6000 Å

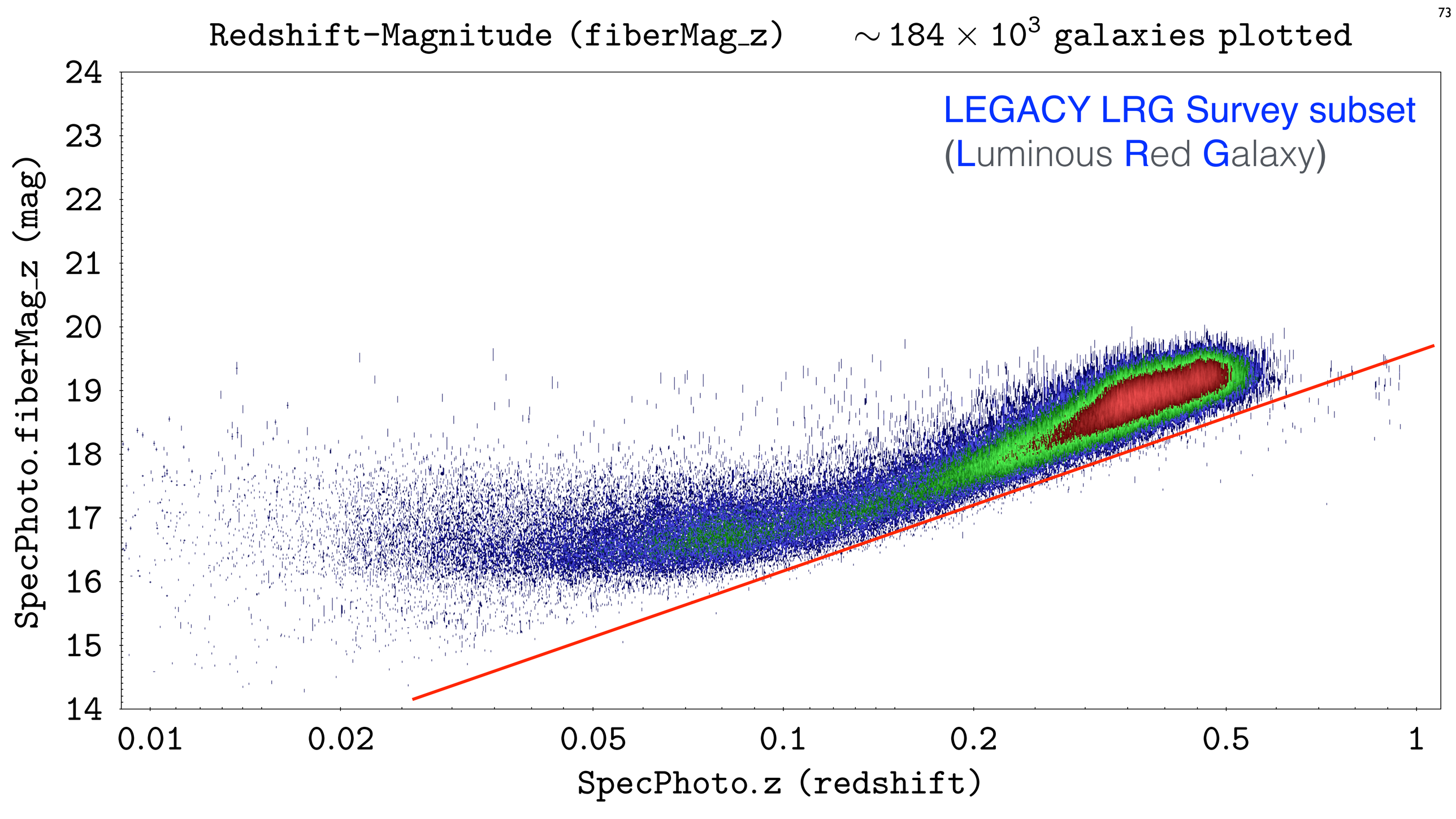
M31 image credit: NASA/Swift/Stefan Immler (GSFC) and Erin Grand (UMCP)

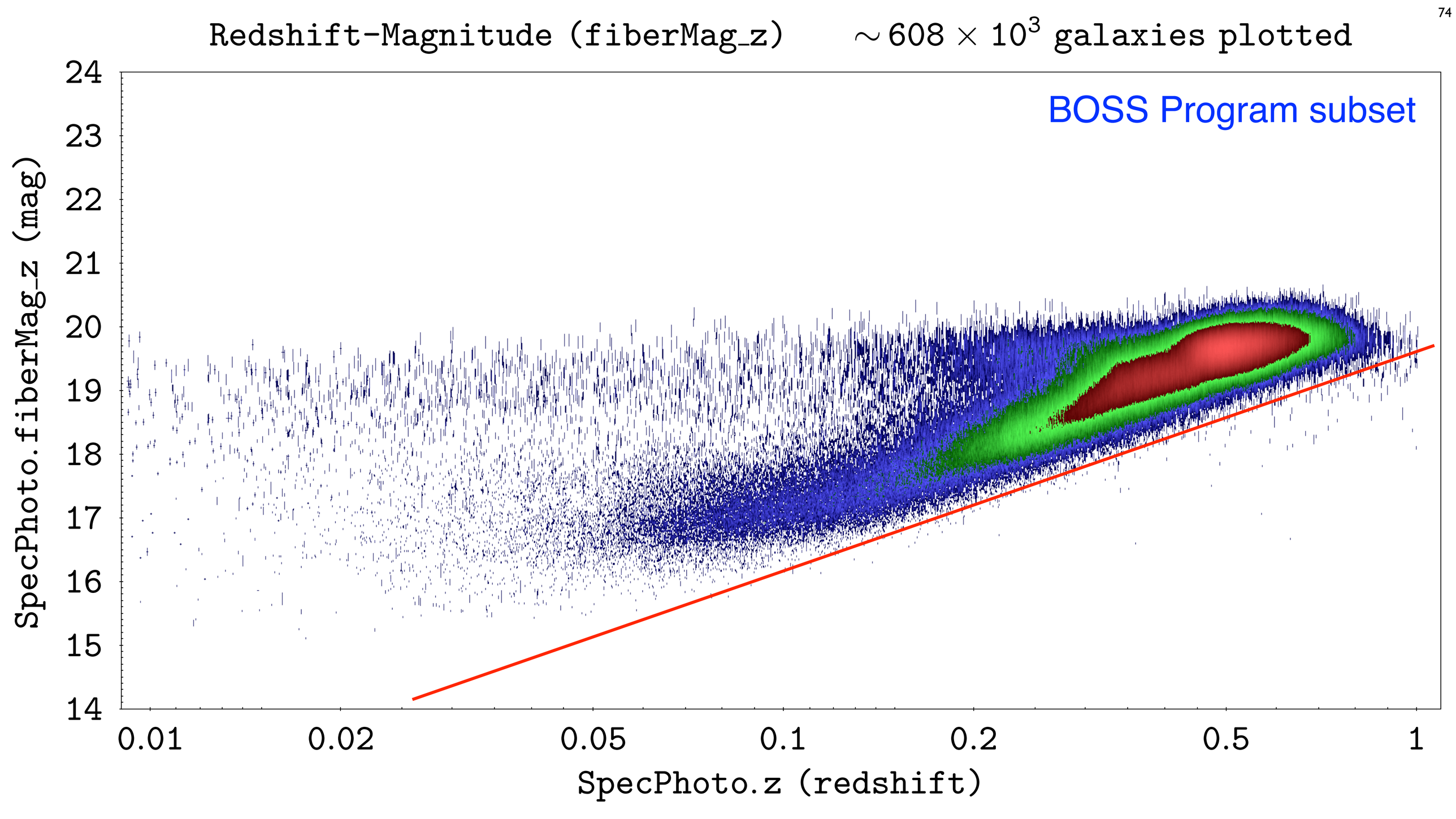
0.25 degrees (15′)

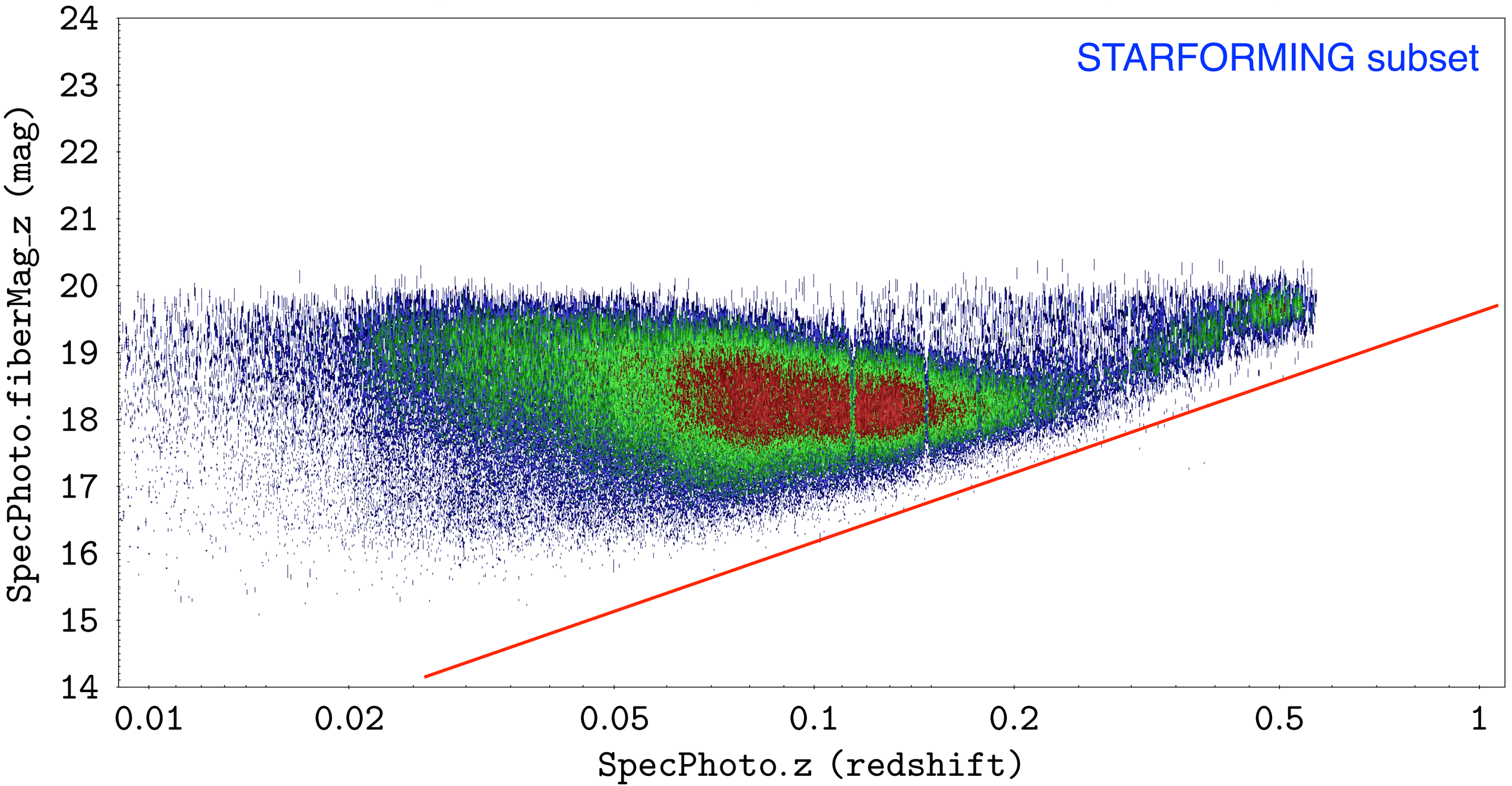
As per 0.4036° M31–M32 angular separation.

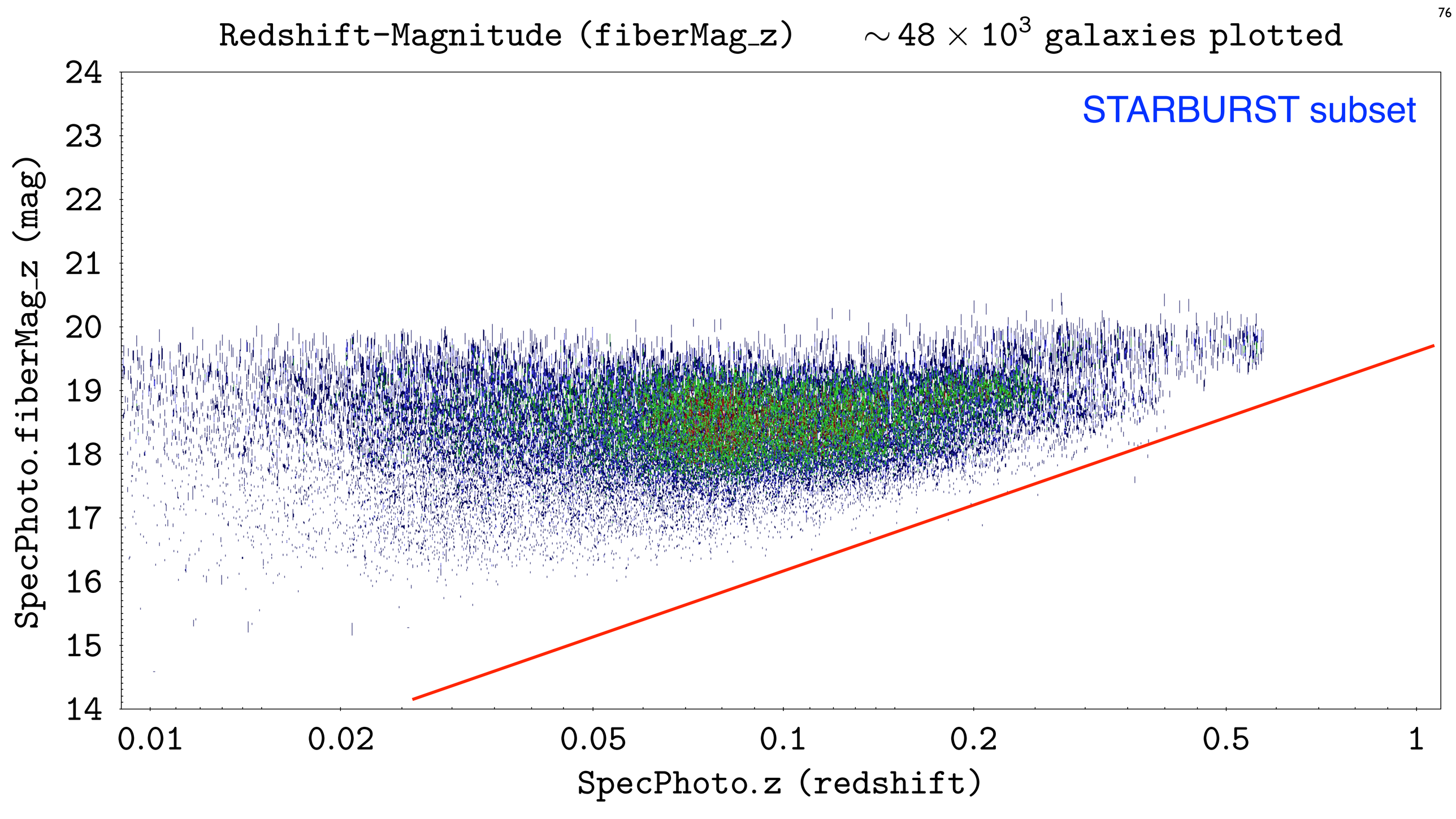

Redshift-Magnitude (fiberMag_z)
~ 1.379 × 10^6 galaxies plotted
IR filter
Small-error "QA" dataset
(Quality Assured)
Maximum "QA" measurement error is ±0.1 mag and ±1% in redshift.
DIM
BRIGHT
5 mags
reference statistical baseline (brightest objects)
SpecPhoto.fiberMag_z (mag)
24
23
22
21
20
19
18
17
16
15
14
0.01
0.02
0.05
0.1
0.2
0.5
1
← NEAR
SpecPhoto.z (redshift)
FAR →

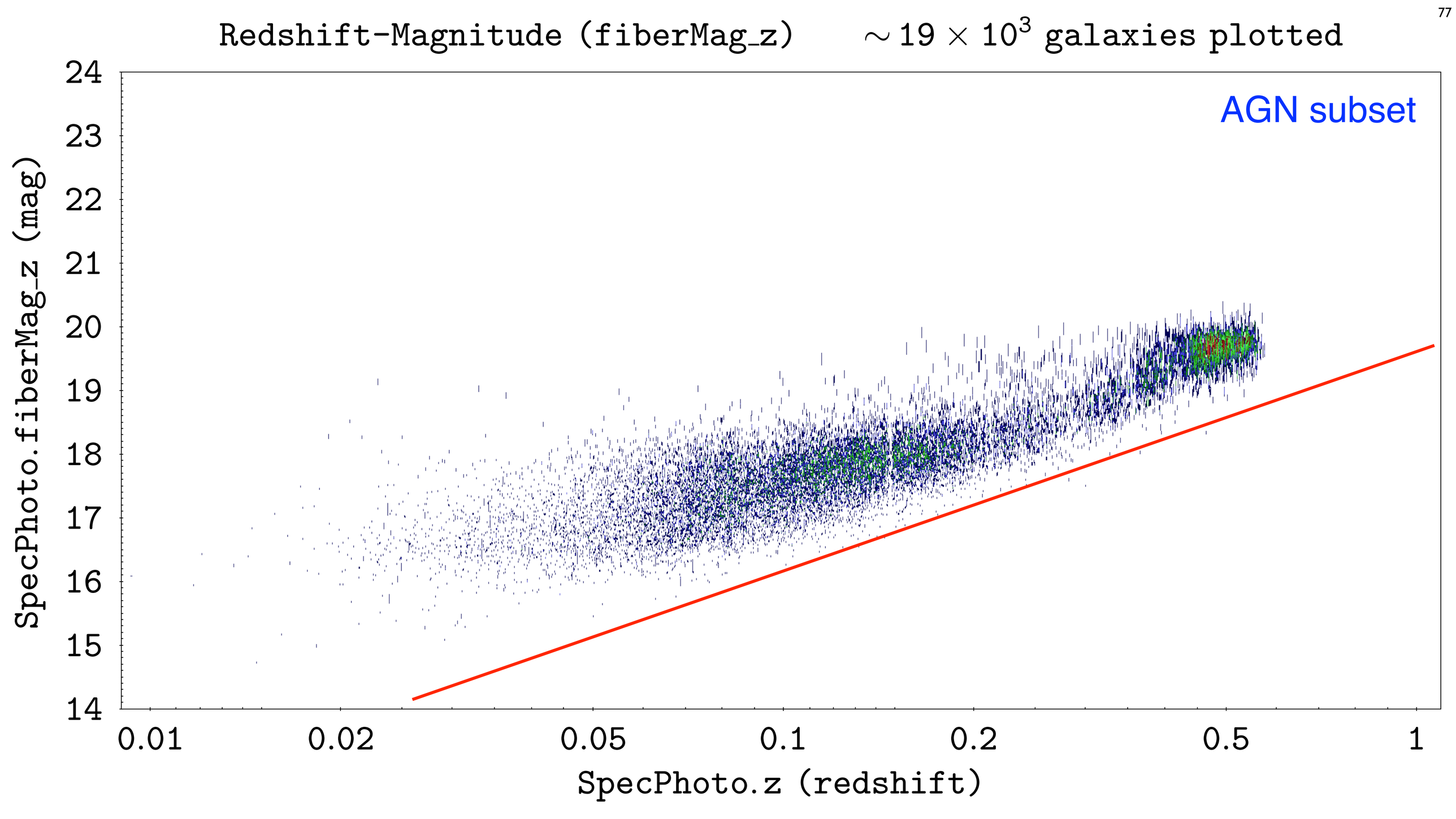

Redshift-Magnitude (fiberMag_z)
$\sim 772 \times 10^3$ galaxies plotted
LEGACY Program subset
SpecPhoto.fiberMag_z (mag)
24
23
22
21
20
19
18
17
16
15
14
0.01
0.02
0.05
0.1
0.2
0.5
1
SpecPhoto.z (redshift)

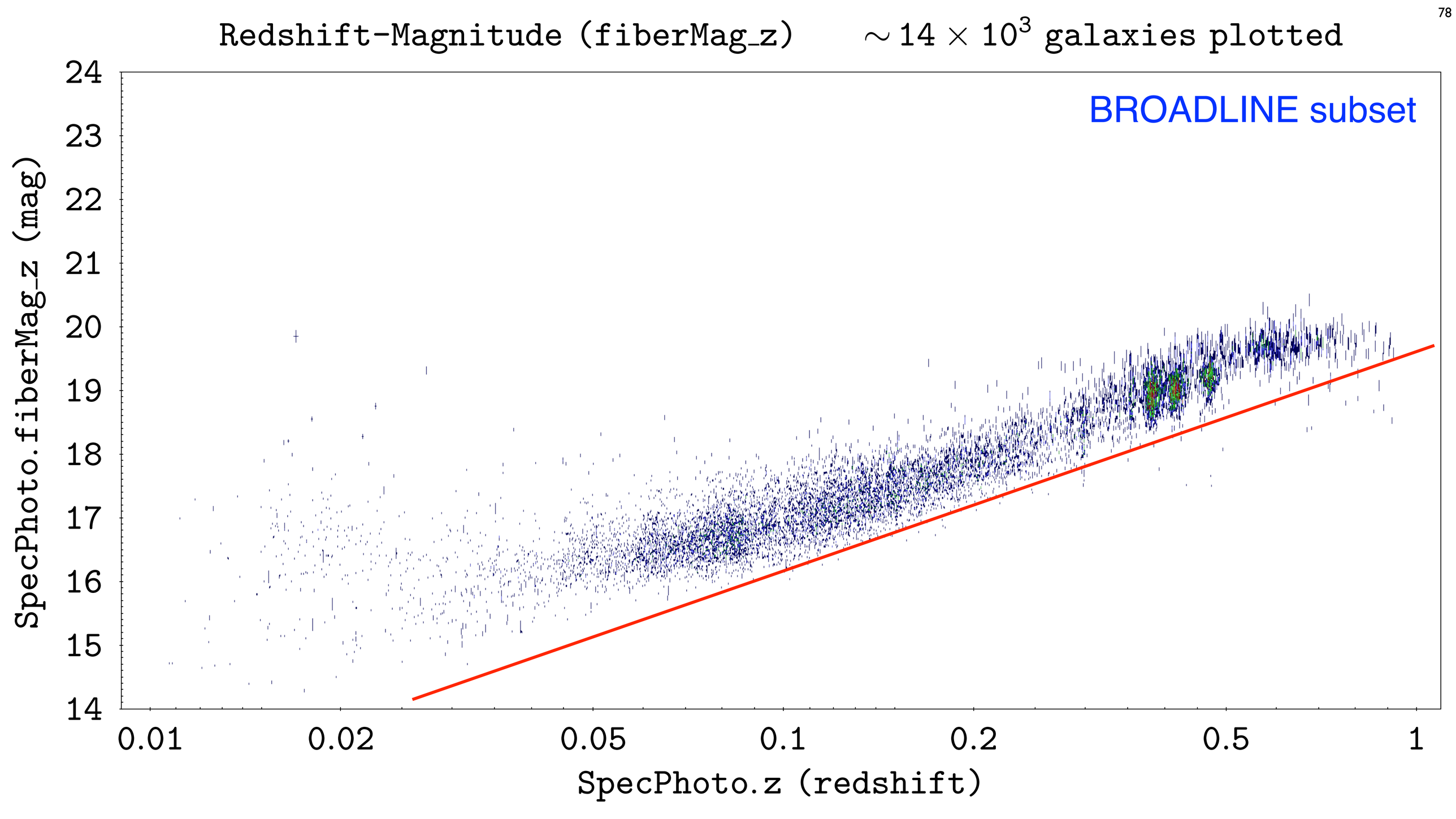

Redshift-Magnitude (fiberMag_z)
$\sim 184 \times 10^3$ galaxies plotted
LEGACY LRG Survey subset
(Luminous Red Galaxy)
SpecPhoto.fiberMag_z (mag)
24
23
22
21
20
19
18
17
16
15
14
0.01
0.02
0.05
0.1
0.2
0.5
1
SpecPhoto.z (redshift)

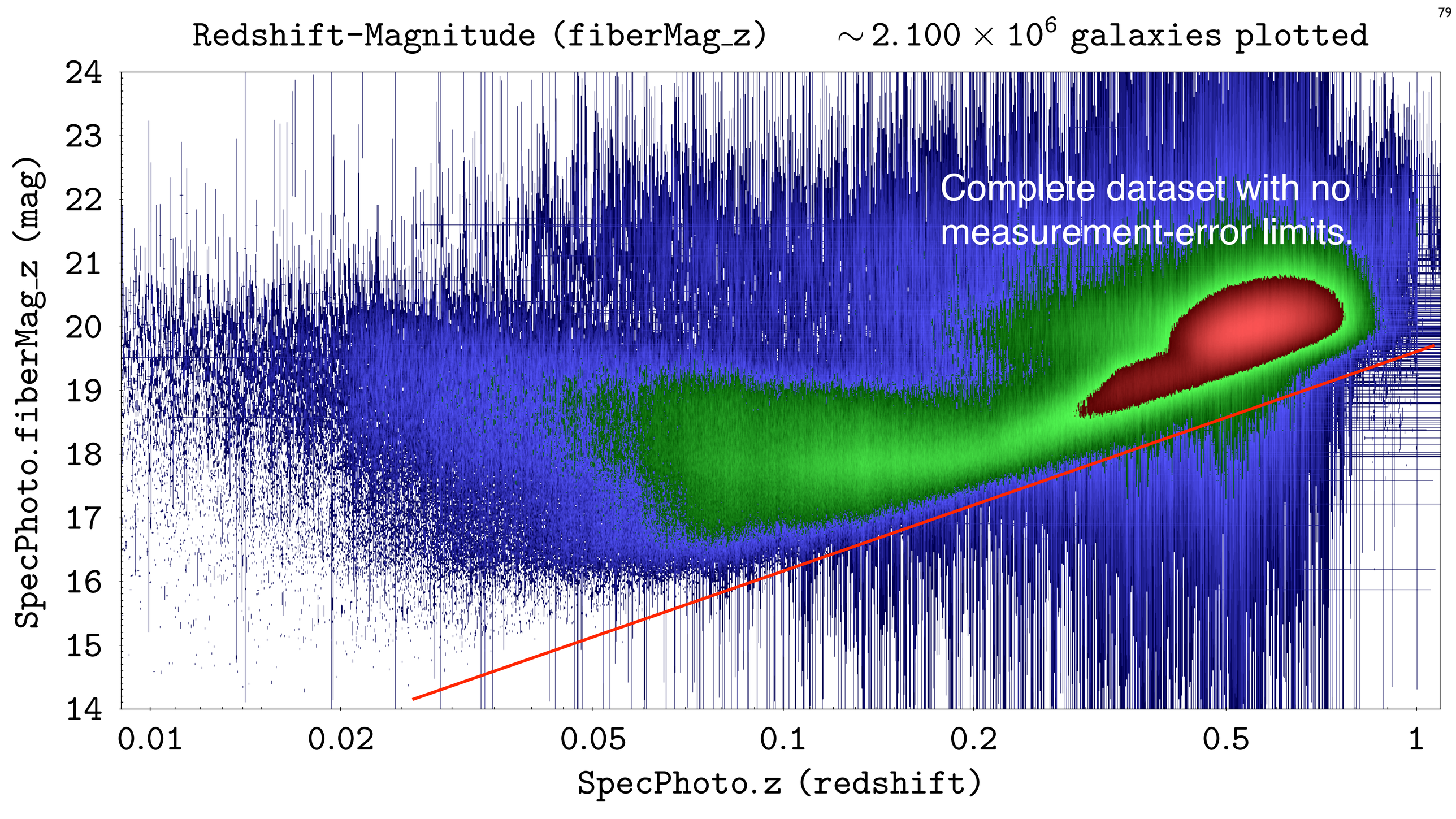

Redshift-Magnitude (fiberMag_z)
$\sim 608 \times 10^3$ galaxies plotted
BOSS Program subset
SpecPhoto.fiberMag_z (mag)
24
23
22
21
20
19
18
17
16
15
14
0.01
0.02
0.05
0.1
0.2
0.5
1
SpecPhoto.z (redshift)


Redshift-Magnitude (fiberMag_z)
$\sim 220 \times 10^3$ galaxies plotted
STARFORMING subset
SpecPhoto.fiberMag_z (mag)
24
23
22
21
20
19
18
17
16
15
14
0.01
0.02
0.05
0.1
0.2
0.5
1
SpecPhoto.z (redshift)


Redshift-Magnitude (fiberMag_z)
$\sim 48 \times 10^3$ galaxies plotted
STARBURST subset
SpecPhoto.fiberMag_z (mag)
SpecPhoto.z (redshift)
24
23
22
21
20
19
18
17
16
15
14
0.01
0.02
0.05
0.1
0.2
0.5
1


Redshift-Magnitude (fiberMag_z)
$\sim 19 \times 10^3$ galaxies plotted
AGN subset
SpecPhoto.fiberMag_z (mag)
24
23
22
21
20
19
18
17
16
15
14
0.01
0.02
0.05
0.1
0.2
0.5
1
SpecPhoto.z (redshift)


Redshift-Magnitude (fiberMag_z)
$\sim 14 \times 10^3$ galaxies plotted
BROADLINE subset
SpecPhoto.fiberMag_z (mag)
24
23
22
21
20
19
18
17
16
15
14
0.01
0.02
0.05
0.1
0.2
0.5
1
SpecPhoto.z (redshift)


Redshift-Magnitude (fiberMag_z)
$\sim 2.100 \times 10^6$ galaxies plotted
Complete dataset with no measurement-error limits.
SpecPhoto.fiberMag_z (mag)
24
23
22
21
20
19
18
17
16
15
14
0.01
0.02
0.05
0.1
0.2
0.5
1
SpecPhoto.z (redshift)

Redshift-Magnitude (fiberMag_z) $\sim 1.379 \times 10^6$ galaxies plotted

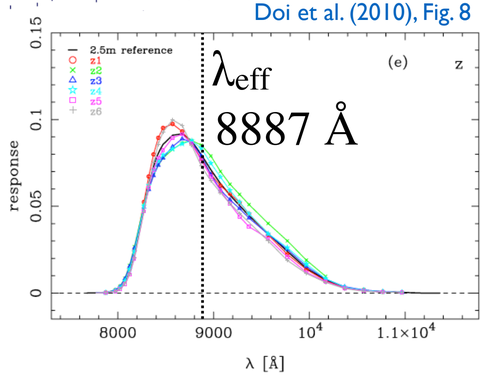
Small-error "QA" dataset

~34% of data does not pass the stringent QA requirements, but that QA process obviously does not alter the data in any way that would significantly affect its physical interpretation. Intrinsic 'noise' around the baseline is less than ±0.2 mag.

linear approximation of brightest galaxy nuclei ±0.2 mag

filter response curve →

Doi et al. (2010), Fig. 8

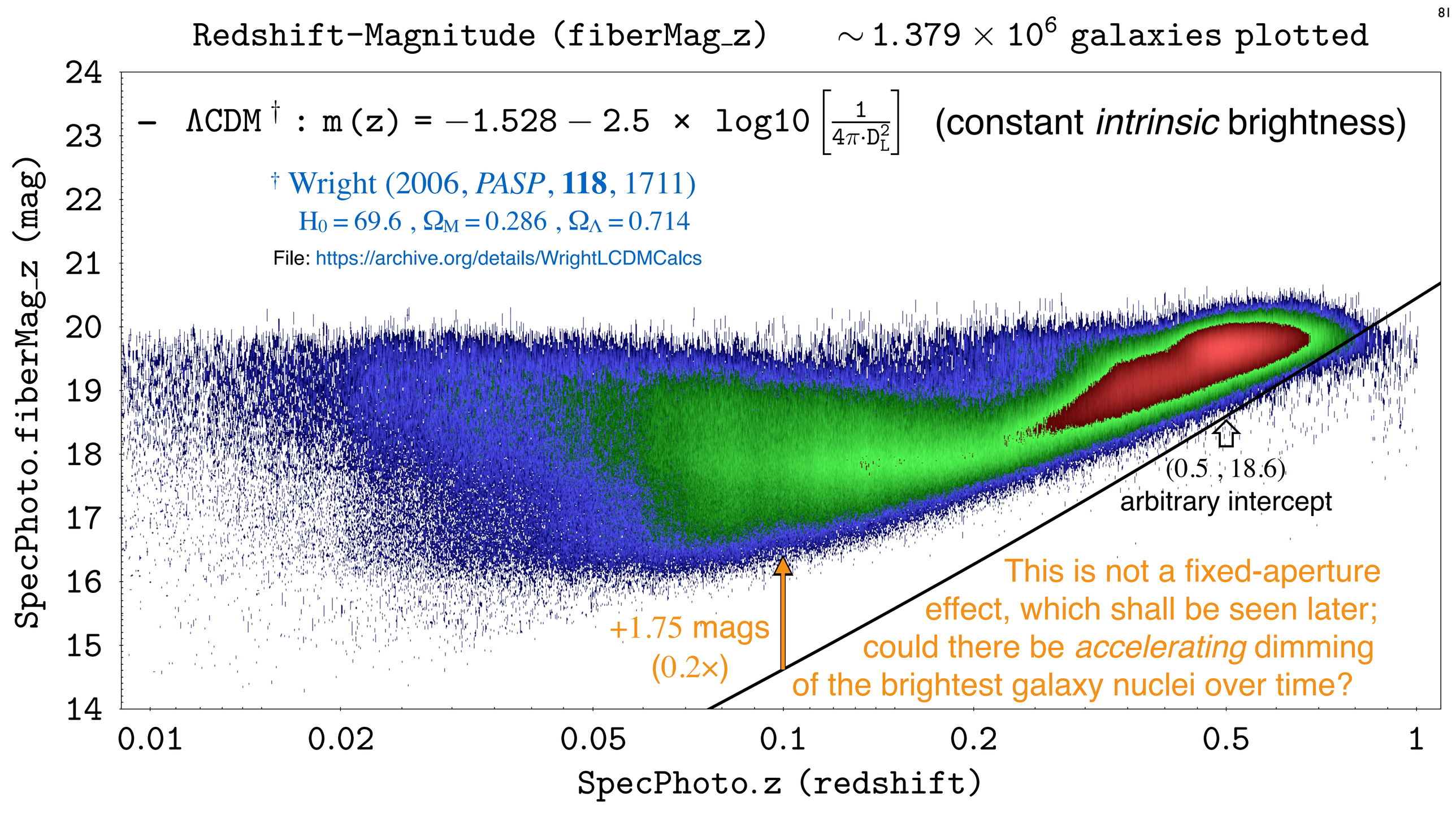


SpecPhoto.fiberMag_z (mag)

24 23 22 21 20 19 18 17 16 15 14

0.01 0.02 0.05 0.1 0.2 0.5 1

SpecPhoto.z (redshift)


Redshift-Magnitude (fiberMag_z)
∼ 1.379 × 10^6 galaxies plotted
– ΛCDM † : m(z) = −1.528 − 2.5 × log10 [1/(4π·D_L^2)] (constant *intrinsic* brightness)
† Wright (2006, *PASP*, **118**, 1711)
H0 = 69.6 , ΩM = 0.286 , ΩΛ = 0.714
File: https://archive.org/details/WrightLCDMCalcs
(0.5 , 18.6)
arbitrary intercept
+1.75 mags
(0.2×)
This is not a fixed-aperture effect, which shall be seen later; could there be *accelerating* dimming of the brightest galaxy nuclei over time?
SpecPhoto.fiberMag_z (mag)
SpecPhoto.z (redshift)
24
23
22
21
20
19
18
17
16
15
14
0.01
0.02
0.05
0.1
0.2
0.5
1

Standard candles, redshift-magnitude, and K-correction

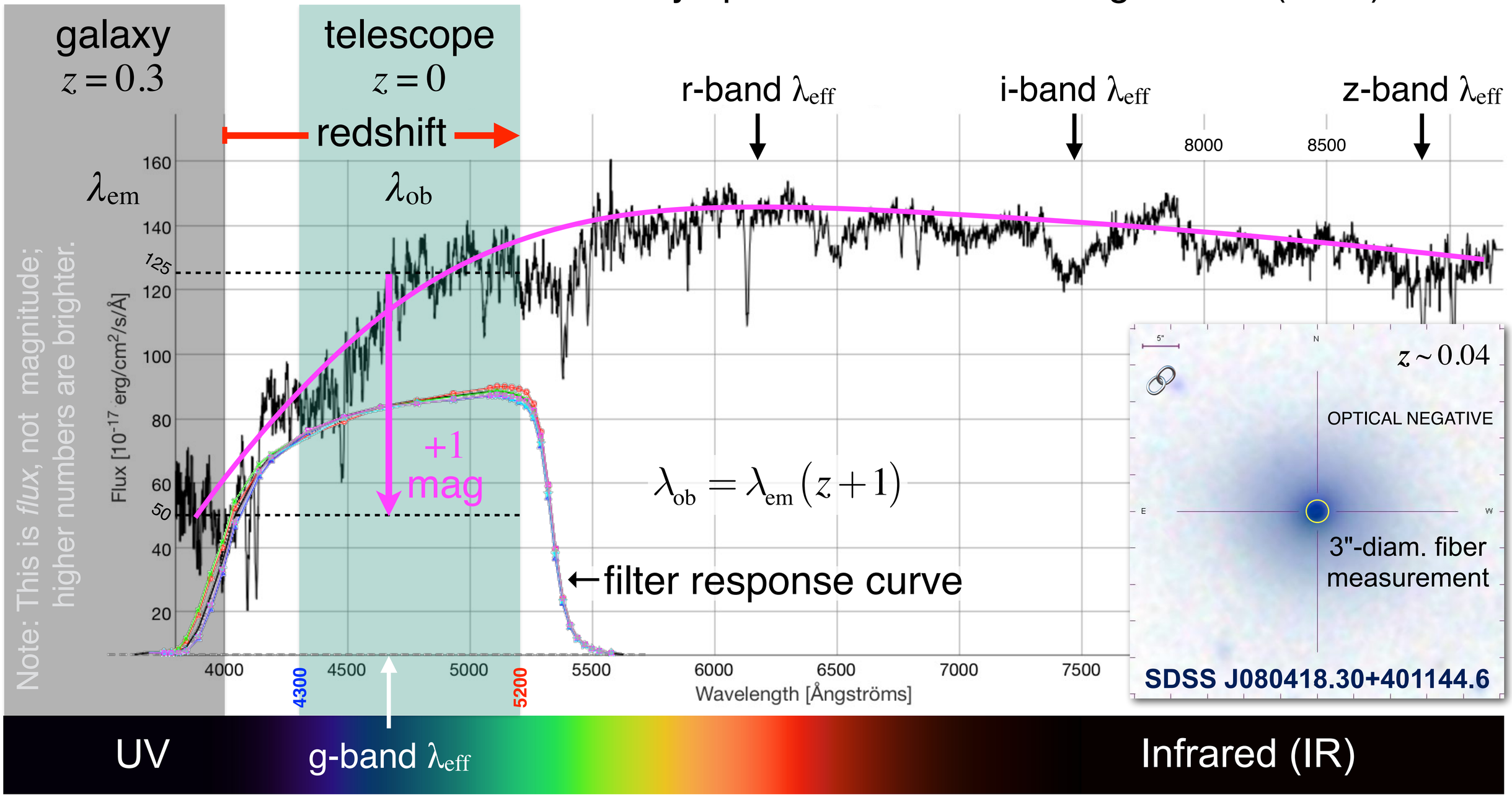
Interpreted in the context of the ΛCDM consensus cosmological model, the graph means that from 5.1 to 1.3 Gyr ago (z: $0.5 \rightarrow 0.1$) the intrinsic brightness of galaxy nuclei, as measured by SDSS fiber magnitudes over this redshift range with good accuracy and consistency, decreased by a factor of about five (i.e., $0.2\times$) at an accelerating rate, and that this phenomenon has continued to date. Such an interpretation defies rational explanation; accordingly, one may conclude that this predictive redshift-magnitude model curve is inconsistent with the empirical data, which is to be expected given the radical failure of the correlated theta-z model.

An accurately-modeled redshift-magnitude curve represents the apparent luminosity of a standard candle over redshift, with an empirical cosmic standard candle being expected to exhibit imperfection in the form of a *narrow range* of intrinsic brightness. In turn, such a cosmic standard candle, observed through a particular bandpass filter, must trace the applicable K-correction curve for that filter.[1] The K-correction curve reflects redshift-induced observation of the *typical* variation in galaxy flux as a function of emission wavelength, which is graphed in the following slide…

1. I. V. Chilingarian, A-L Melchior, & I. Y. Zolotukhin, *MNRAS* **405**, 1409 (2010).

© A. F. Mayer

Galaxy spectrum demonstrating 4000-Å (Ca II) break



Follow the data…

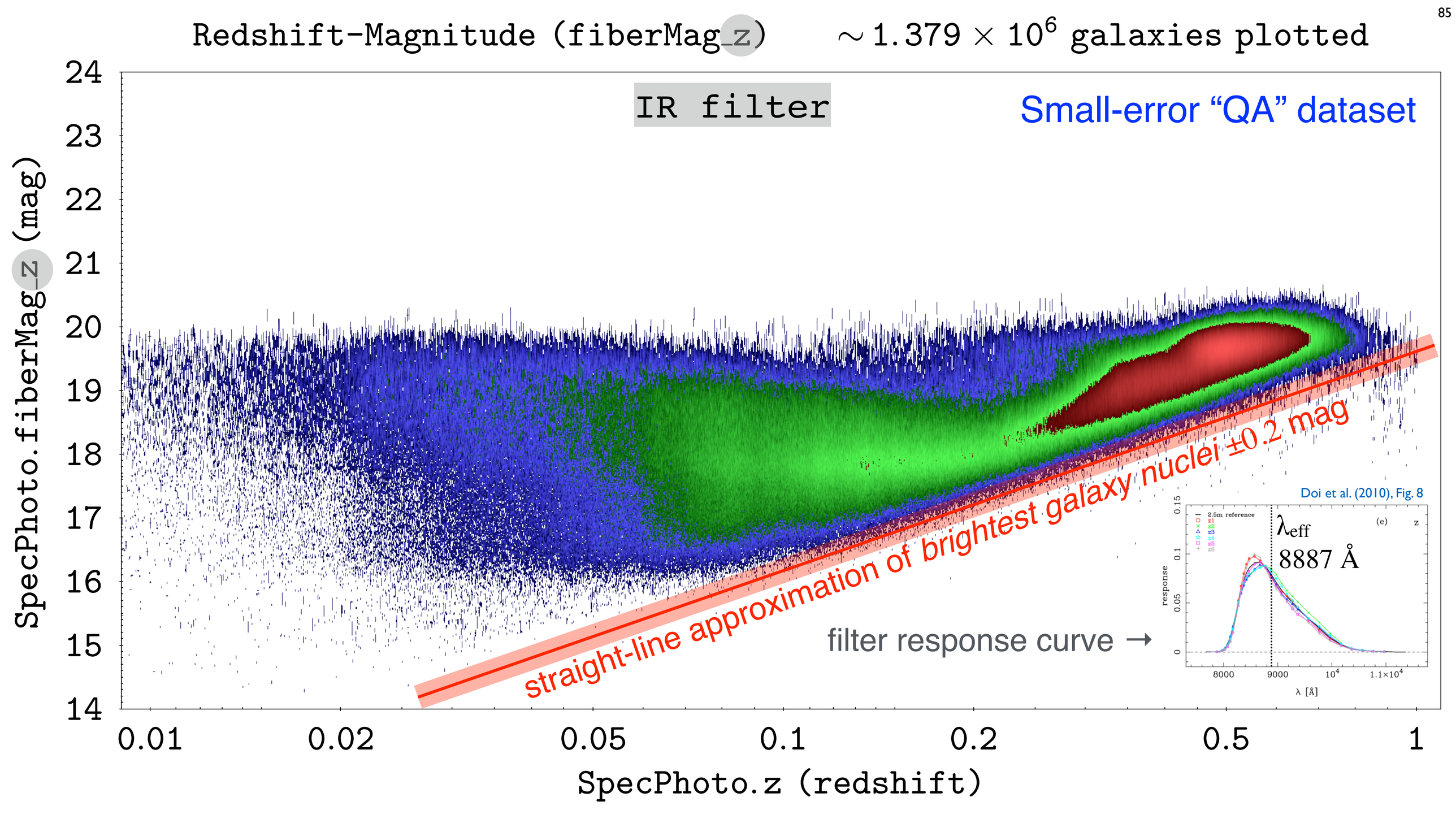
According to conventional thinking in cosmology, the idea that a class of standard-candle galaxies might exist may seem to be a “wild hypothesis” that is inconsistent with what are assumed to be ‘known facts,’ so confusion and misunderstanding are to be expected. However, those problems can be resolved:

If a class of cosmic object is observed to trace the known K-correction curve over redshift, then, *by definition*, that class of object *must* be a standard candle. Confronted with such empirical data, one is not “hypothesizing” the existence of a galactic standard candle, one is *objectively observing* the phenomenon.

The statistical (fuzzy)[1] baseline of the SDSS redshift-magnitude measurements represents the class of brightest galaxies (Petrosian magnitudes for an entire galaxy or their nuclei as measured to good approximation by the spectrograph fiber magnitudes). If that baseline traces the K-correction curve, then we may infer with complete certainty that those objects are also a class of standard candle, without regard for any redshift-magnitude model.

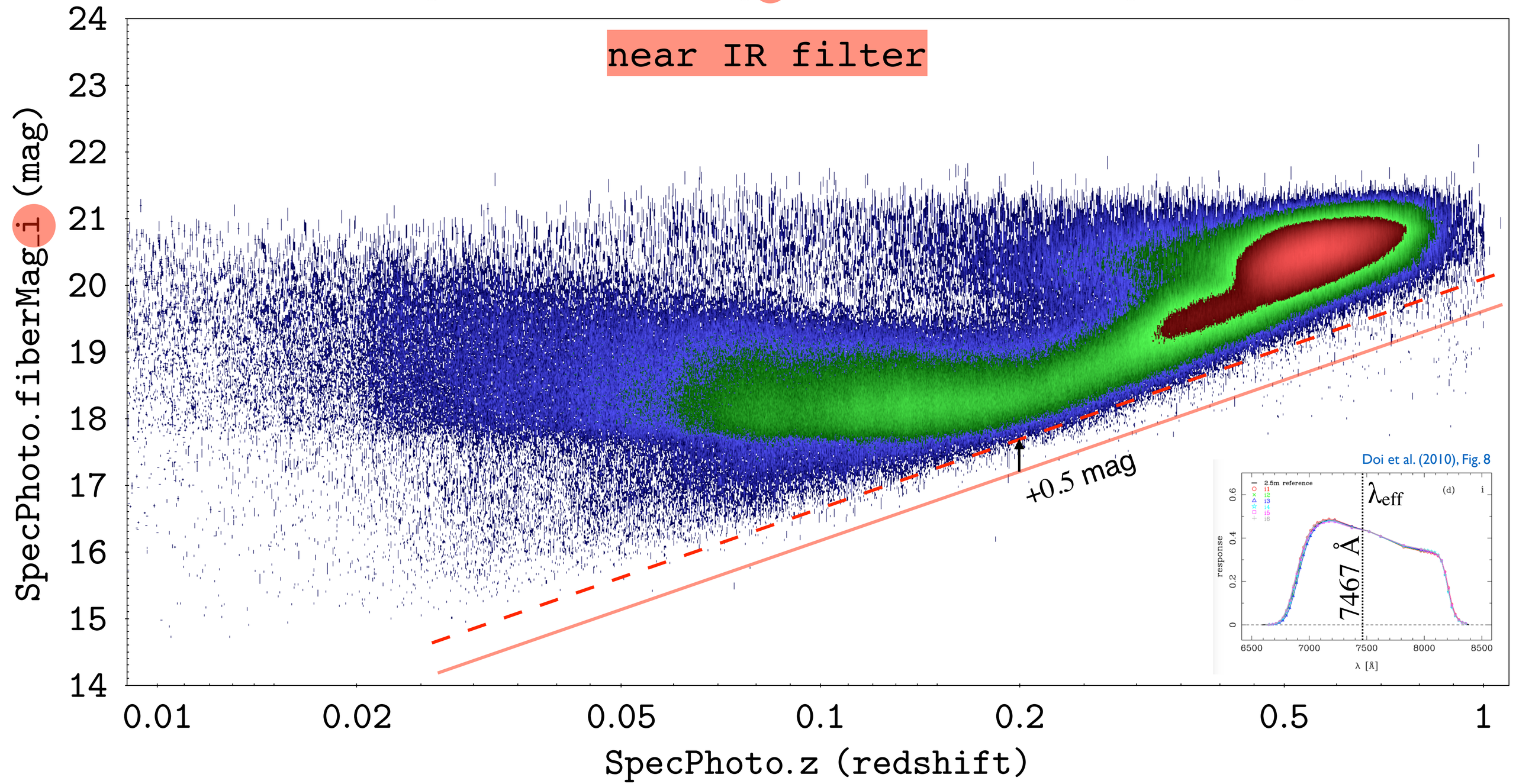
SO, LET US FOLLOW THE *RELIABLE* SDSS DATA AND SEE WHERE IT LEADS…

1. R. Viertl, *Statistical Methods for Fuzzy Data* (Wiley, Chichester, 2011).


Redshift-Magnitude (fiberMag_z)
~ 1.379 × 10^6 galaxies plotted
IR filter
Small-error "QA" dataset
straight-line approximation of brightest galaxy nuclei ±0.2 mag
filter response curve →
Doi et al. (2010), Fig. 8
2.5m reference
z1
z2
z3
z4
z5
z6
λeff
8887 Å
(e)
z
response
λ [Å]
SpecPhoto.fiberMag_z (mag)
SpecPhoto.z (redshift)
24
23
22
21
20
19
18
17
16
15
14
0.01
0.02
0.05
0.1
0.2
0.5
1

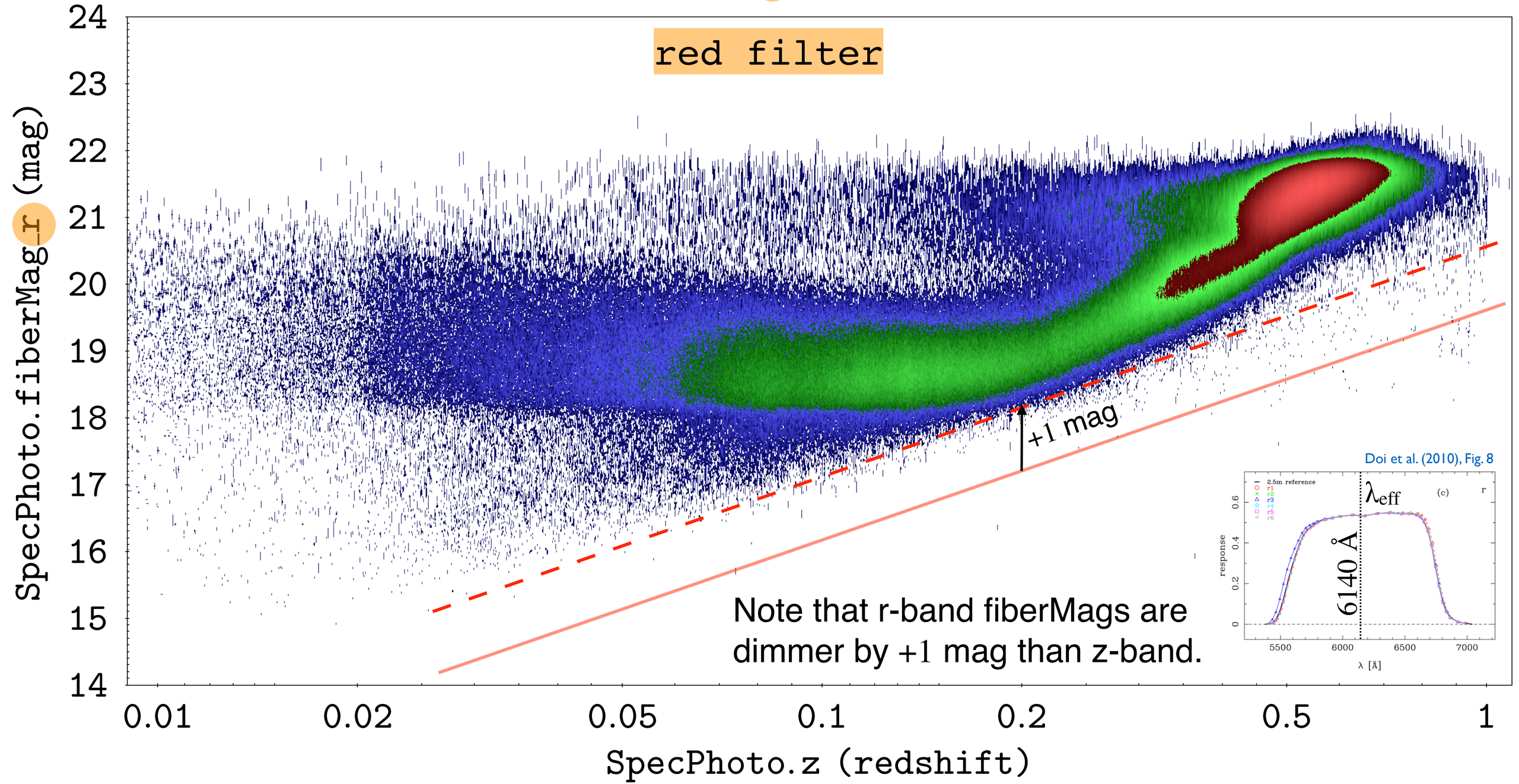
Redshift-Magnitude (fiberMag_i)

$\sim 2.032 \times 10^6$ galaxies plotted



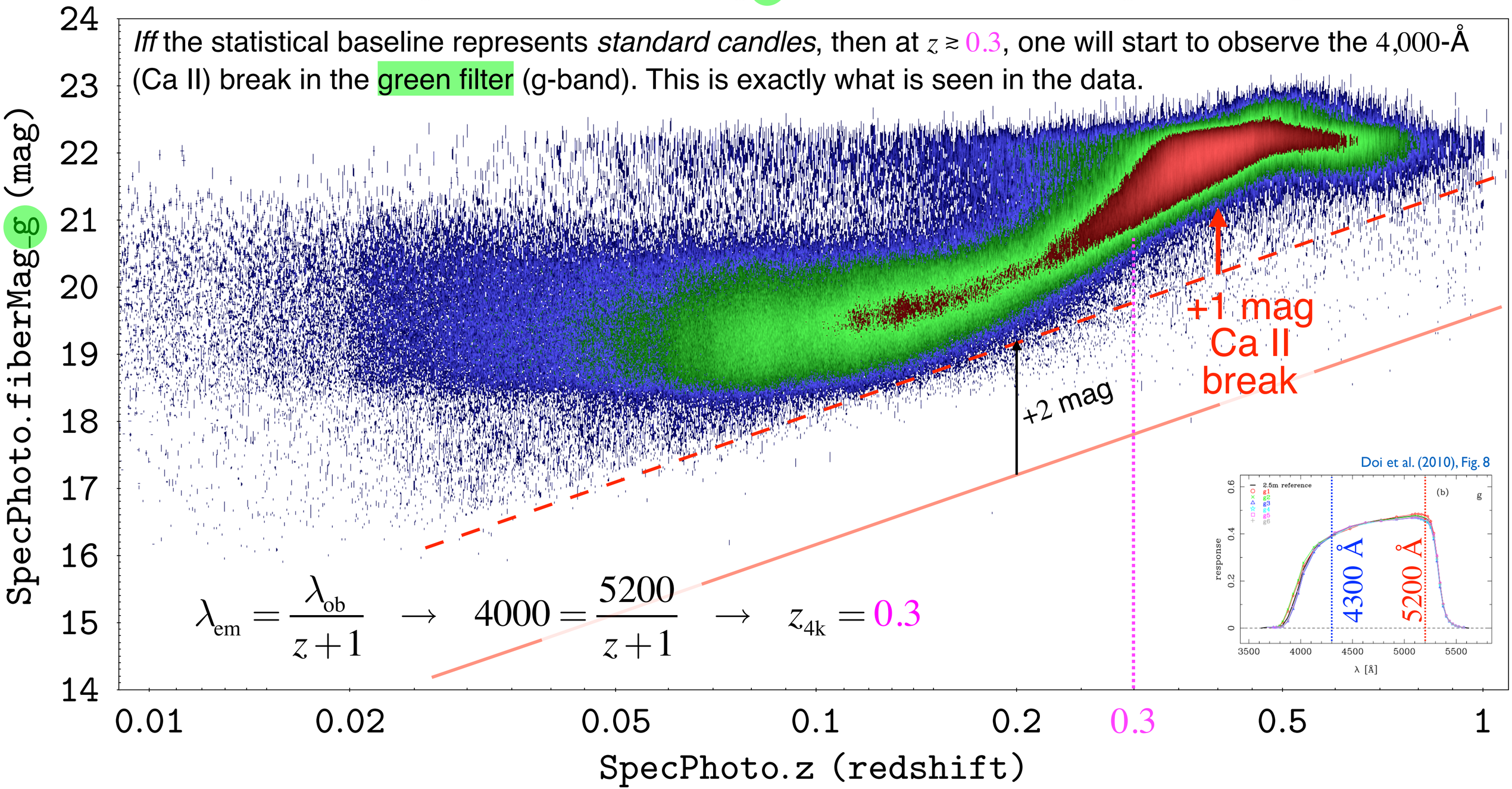
Redshift-Magnitude (fiberMag_r)

$\sim 1.843 \times 10^6$ galaxies plotted



Redshift-Magnitude (fiberMag_g) $\sim 1.115 \times 10^6$ galaxies plotted

Iff the statistical baseline represents *standard candles*, then at $z \approx 0.3$, one will start to observe the 4,000-Å (Ca II) break in the green filter (g-band). This is exactly what is seen in the data.



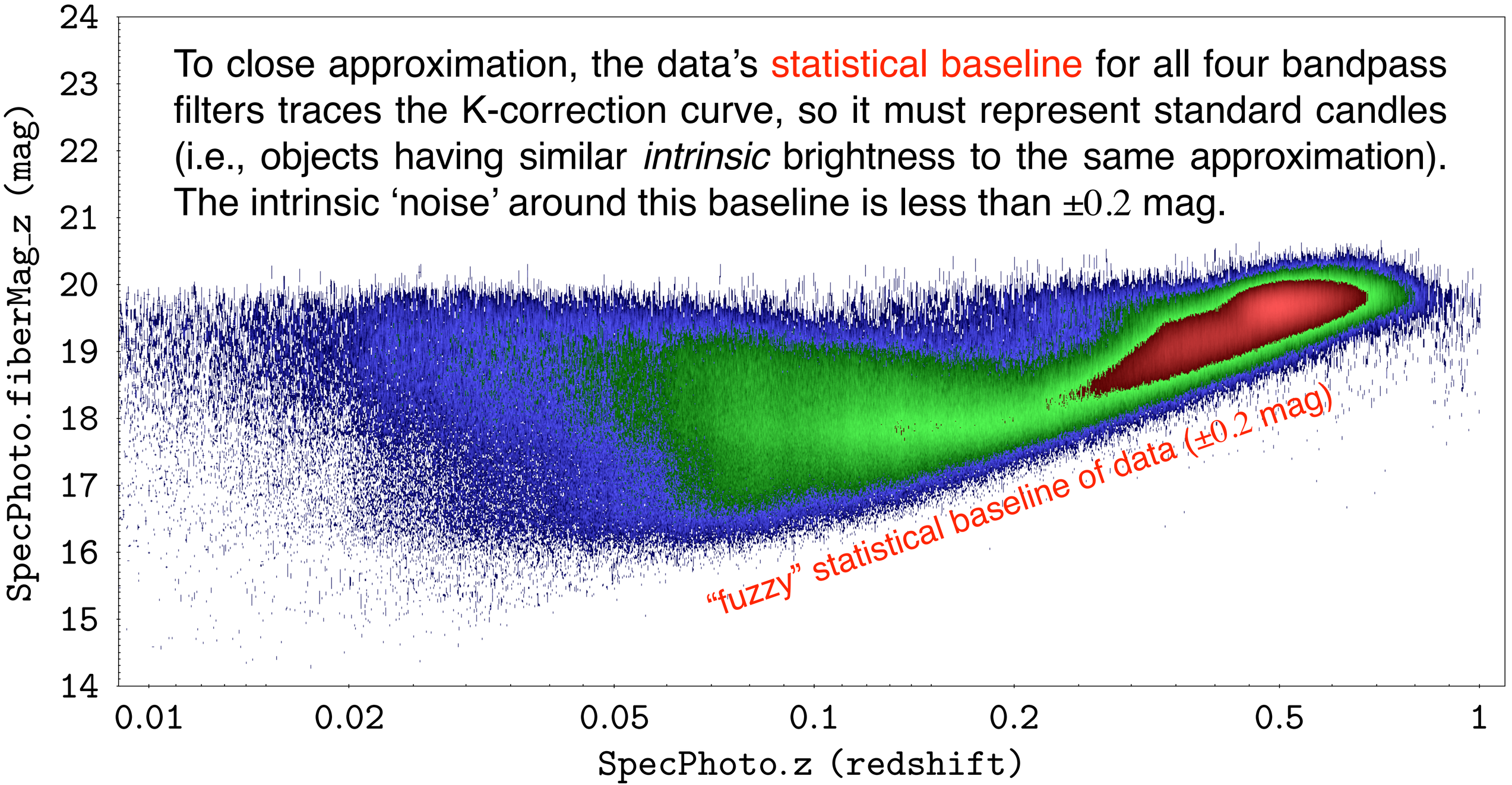
A fundamental assumption associated with the current standard cosmological model is galaxy evolution over lookback time (i.e., galaxies observed at higher redshift are expected to be *intrinsically* younger). However, if that assumption is true, one should not see “red and dead” (i.e., intrinsically very old) high-redshift galaxies $(1 < z < 2)$, yet we do.[1]

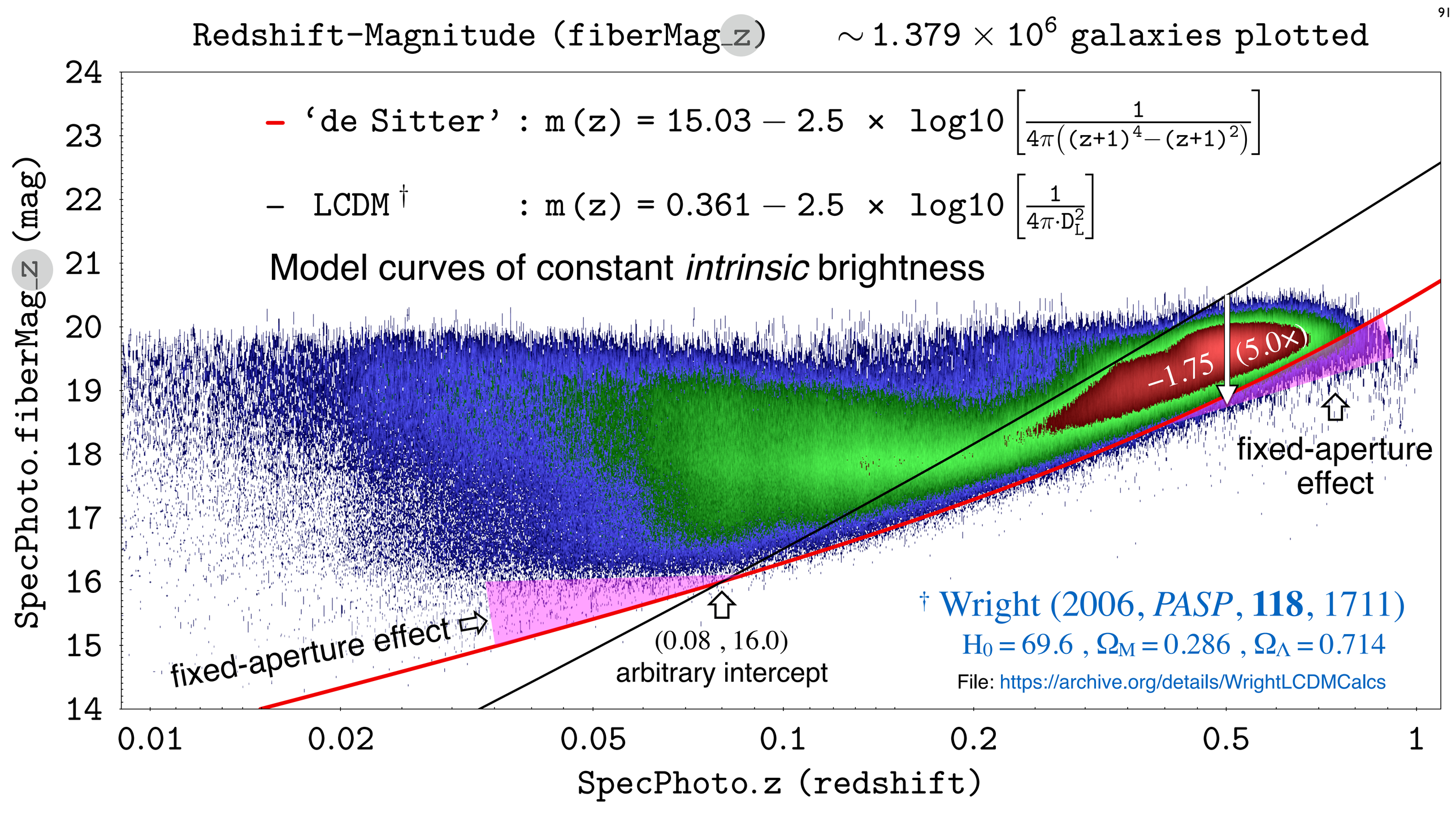
Observation of an *empirical* $m(z)$ “K-correction” curve as seen in the last four slides is a dependable *empirical signature* of a galactic cosmic standard candle. Observation of the $+1$-mag 4000-Angstrom break, which initiates at $z \sim 0.3$ in the g-band as illustrated in the prior slide, *positively* identifies the dataset baseline as a set of *very-nearly-consistent* cosmic ‘standard candles’ (i.e., having minor intrinsic-brightness variation in the set); no “hypothesis” is involved.

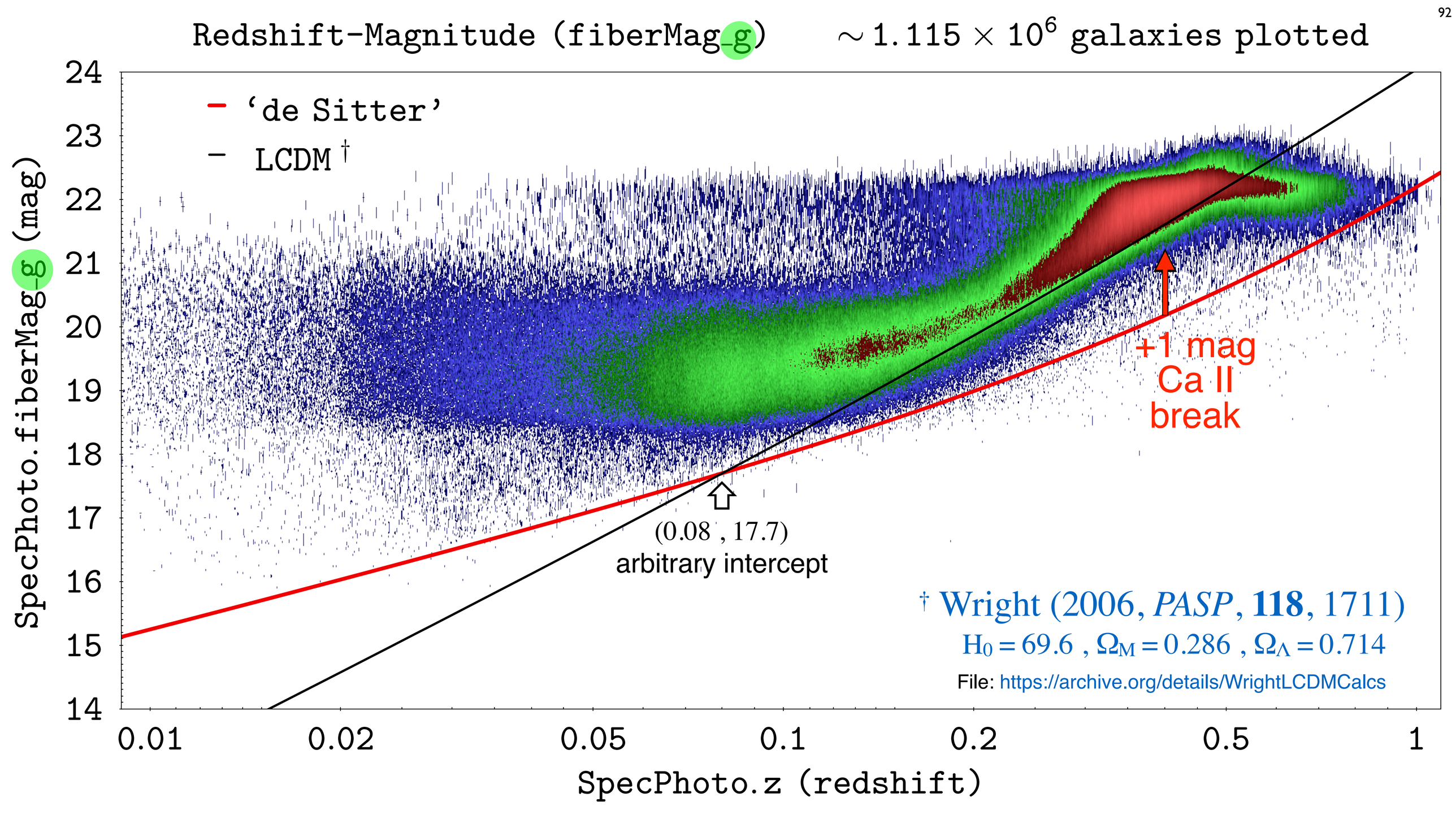
Note: $\mathrm{LCDM} \equiv \Lambda\mathrm{CDM}$ — Lambda Cold Dark Matter [consensus model]

1. R. G. Abraham et al., Star-Forming, Recently Star-Forming, and “Red and Dead” Galaxies at 1<Z<2, in: R. De Grijs and R. M. González Delgado (eds), *Starbursts,* Astrophysics and Space Science Library, vol 329, (Springer, Dordrecht 2005).

Redshift-Magnitude (fiberMag_z) $\sim 1.379 \times 10^6$ galaxies plotted




Redshift-Magnitude (fiberMag_z)
~ 1.379 × 10^6 galaxies plotted
– 'de Sitter' : m(z) = 15.03 – 2.5 × log10 [1 / 4π((z+1)^4 – (z+1)^2)]
– LCDM † : m(z) = 0.361 – 2.5 × log10 [1 / 4π·D_L^2]
Model curves of constant intrinsic brightness
–1.75
(5.0×)
fixed-aperture effect
fixed-aperture effect
(0.08 , 16.0)
arbitrary intercept
† Wright (2006, PASP, 118, 1711)
H0 = 69.6 , ΩM = 0.286 , ΩΛ = 0.714
File: https://archive.org/details/WrightLCDMCalcs
SpecPhoto.fiberMag_z (mag)
SpecPhoto.z (redshift)
24
23
22
21
20
19
18
17
16
15
14
0.01
0.02
0.05
0.1
0.2
0.5
1


Redshift-Magnitude (fiberMag_g)
~ 1.115 × 10^6 galaxies plotted
'de Sitter'
LCDM †
+1 mag
Ca II
break
(0.08 , 17.7)
arbitrary intercept
† Wright (2006, PASP, 118, 1711)
H0 = 69.6 , ΩM = 0.286 , ΩΛ = 0.714
File: https://archive.org/details/WrightLCDMCalcs
SpecPhoto.fiberMag_g (mag)
SpecPhoto.z (redshift)
24
23
22
21
20
19
18
17
16
15
14
0.01
0.02
0.05
0.1
0.2
0.5
1

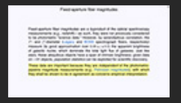
SDSS glossary reference

Magnitude, Petrosian

Stored as `petroMag`. For galaxy photometry, measuring flux is more difficult than for stars, because galaxies do not all have the same radial surface brightness profile, and have no sharp edges. In order to avoid biases, we wish to measure a constant fraction of the total light, independent of the position and distance of the object. To satisfy these requirements, the SDSS has adopted a modified form of the Petrosian (1976) system, measuring galaxy fluxes within a circular aperture whose radius is defined by the shape of the azimuthally averaged light profile. Details can be found in the Photometry section of the Algorithms pages and the Strauss et al. (2002) AJ paper on galaxy target selection. Model magnitudes share most of the advantages of Petrosian magnitudes, and have higher S/N; they are therefore used instead of Petrosian magnitudes for target selection in BOSS.

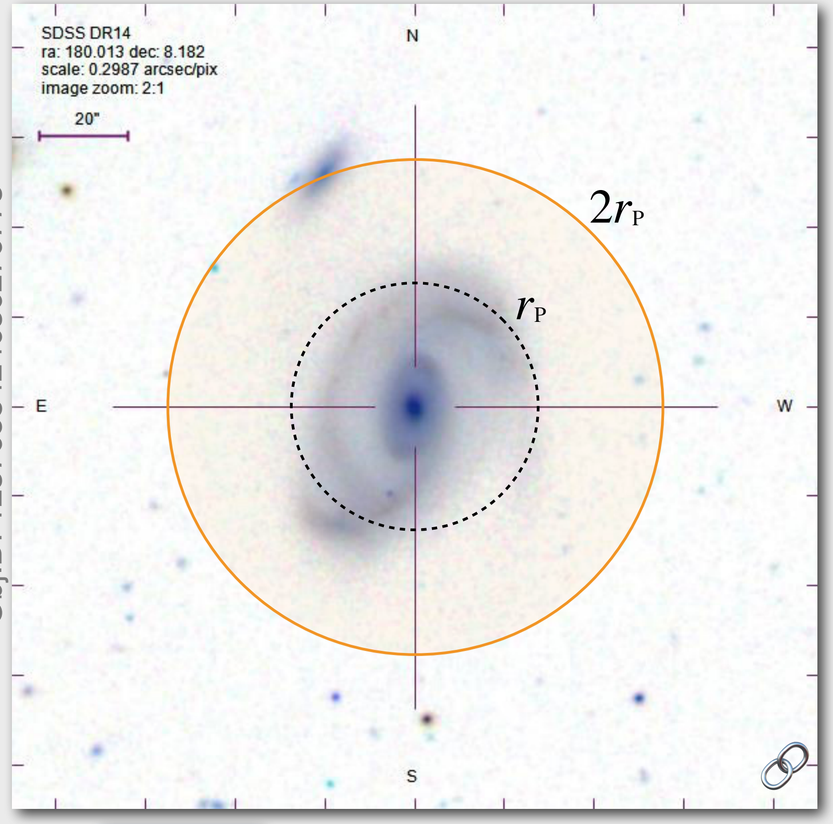
Source: https://www.sdss.org/dr14/help/glossary/#M

If you jumped here, click to go back to *Fixed-aperture fiber magnitudes*…



DEFINITION: “Petrosian flux”

$$F_{\mathrm{P}} \equiv \int_0^{N_{\mathrm{P}} r_{\mathrm{P}}} \mathrm{d}r' 2\pi r' I(r') \quad \left[N_{\mathrm{P}} = 2.0\right]$$

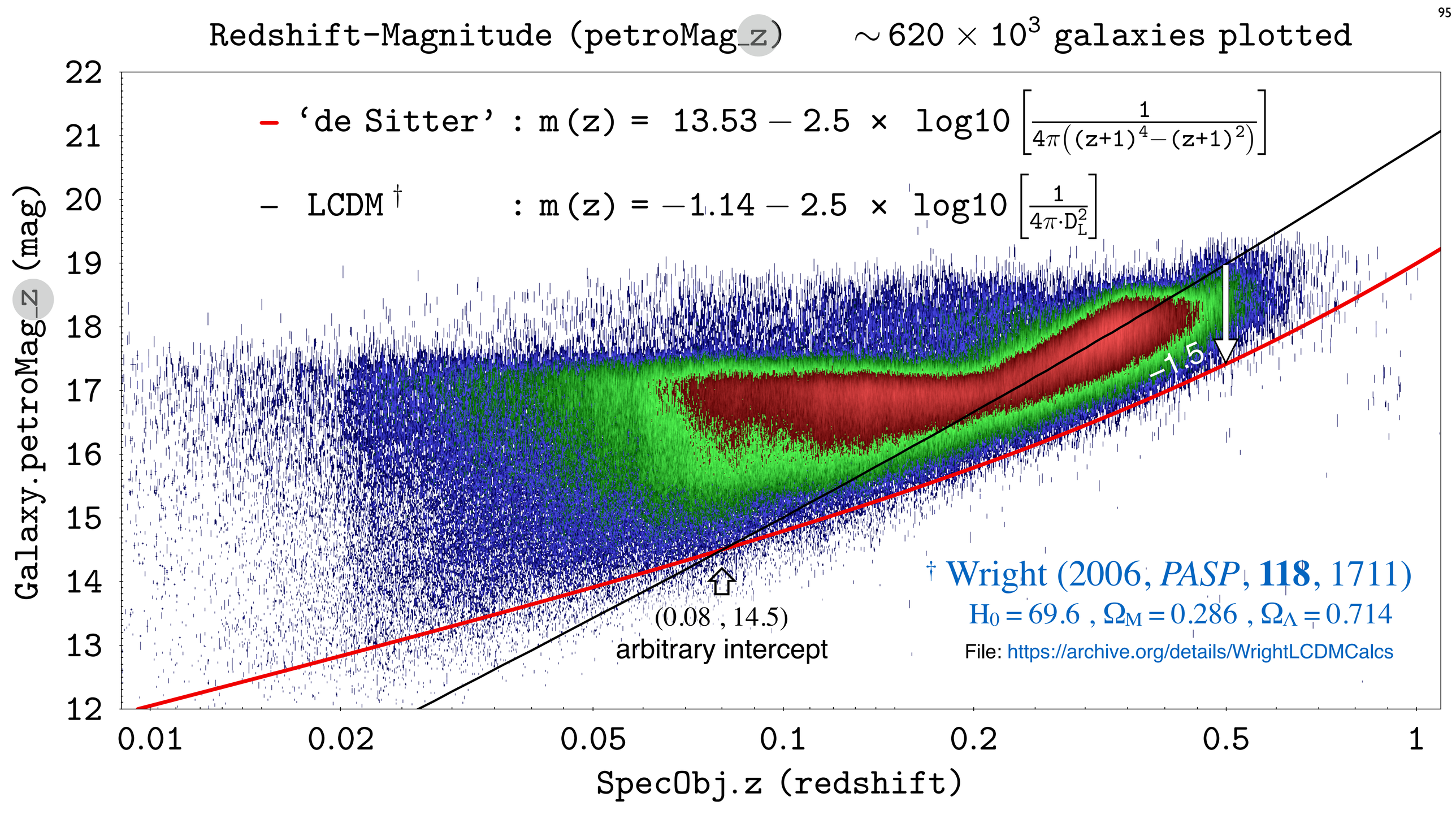


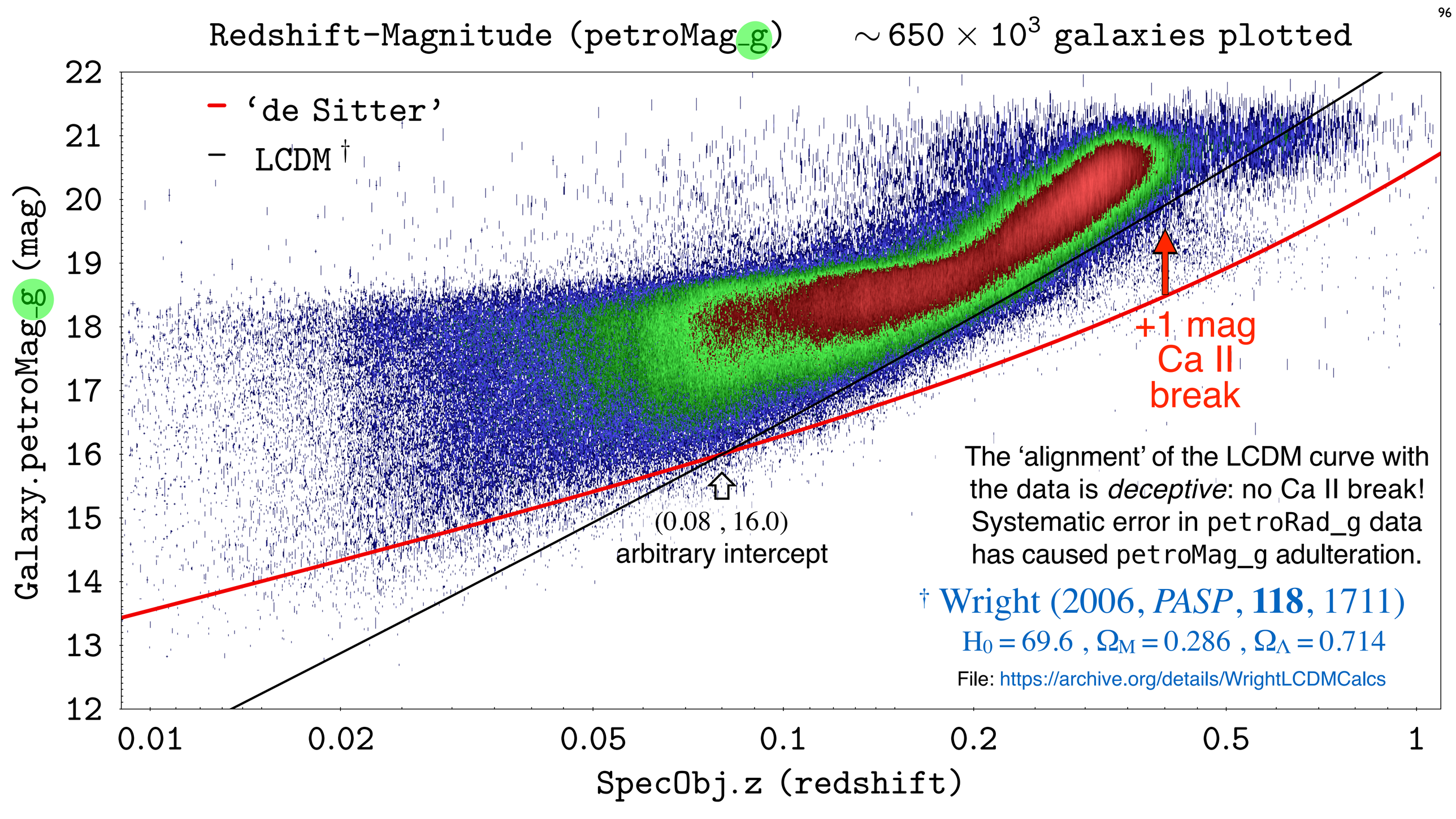
r′-band petroRad_r: $r_{\mathrm{P}} = 27.5''$

The SDSS Petrosian flux in any band is defined as the flux within two Petrosian radii ($2r_{\mathrm{P}}$).

“In the SDSS five-band photometry, the aperture in all bands is set by the profile of the galaxy in the r band alone. This procedure ensures that the color measured by comparing the Petrosian flux F_{P} in different bands is measured through a consistent aperture.”

Reference: https://www.sdss.org/dr14/algorithms/magnitudes/#mag_petro

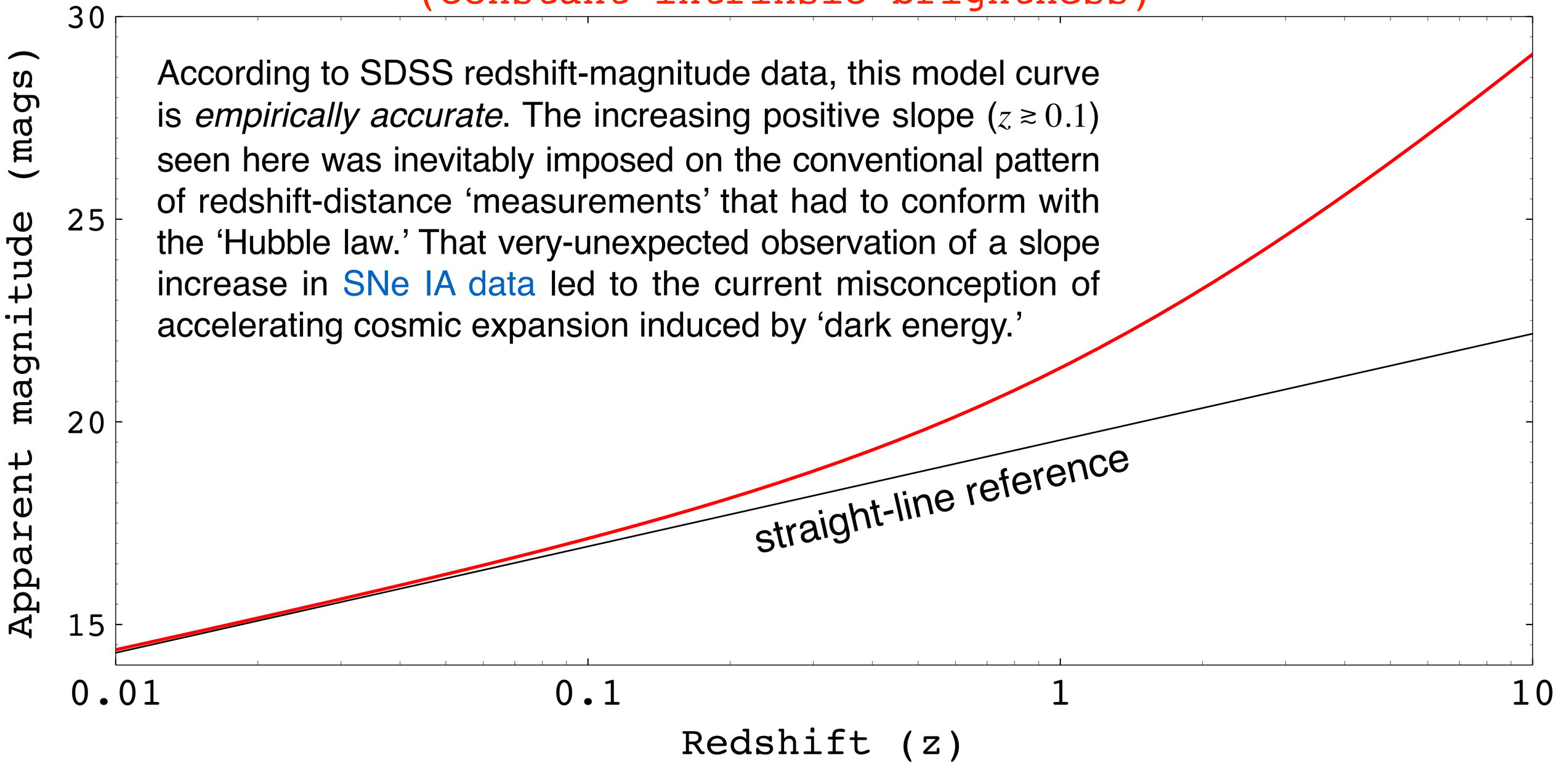

Redshift-Magnitude (petroMag_z)
~620 × 10^3 galaxies plotted
– 'de Sitter' : m(z) = 13.53 – 2.5 × log10 [1 / 4π((z+1)^4 – (z+1)^2)]
– LCDM † : m(z) = –1.14 – 2.5 × log10 [1 / 4π·D_L^2]
–1.5
(0.08 , 14.5)
arbitrary intercept
† Wright (2006, PASP, 118, 1711)
H0 = 69.6 , ΩM = 0.286 , ΩΛ = 0.714
File: https://archive.org/details/WrightLCDMCalcs
Galaxy.petroMag_z (mag)
SpecObj.z (redshift)
22
21
20
19
18
17
16
15
14
13
12
0.01
0.02
0.05
0.1
0.2
0.5
1


Redshift-Magnitude (petroMag_g)
~650 × 10^3 galaxies plotted
– 'de Sitter'
– LCDM †
Galaxy.petroMag_g (mag)
SpecObj.z (redshift)
22
21
20
19
18
17
16
15
14
13
12
0.01
0.02
0.05
0.1
0.2
0.5
1
+1 mag
Ca II
break
(0.08 , 16.0)
arbitrary intercept
The 'alignment' of the LCDM curve with the data is *deceptive*: no Ca II break! Systematic error in petroRad_g data has caused petroMag_g adulteration.
† Wright (2006, *PASP*, **118**, 1711)
H0 = 69.6 , ΩM = 0.286 , ΩΛ = 0.714
File: https://archive.org/details/WrightLCDMCalcs

SQL query for all redshift-magnitude data

```
SELECT -- Change "_z" to "_" with i , r , g to get data for those filters.
    z
,   zErr
,   fiberMag_z -- Change "fiber" to "petro" for that data.
,   fiberMagErr_z
,   CASE (legacy_target1 & 0x20) WHEN 0 THEN 0 ELSE 1 END AS fLRGsurvey
,   programname
,   subClass
FROM
    SpecPhoto
WHERE
    programname IN ('legacy', 'boss') -- disallow minor surveys
AND class = 'GALAXY'                  -- remove QSO and STARs
AND zWarning = 0                      -- disallow redshifts with warnings
AND zErr >= 0                         -- disallow -n error codes
AND ABS(zErr/z) <= 0.01               -- max. redshift error is 1%
AND z > 0                             -- disallow [÷ 0], above
AND fiberMagErr_z BETWEEN 0 AND 0.1   -- disallow errors >0.1 mag and -9999 error code
ORDER BY
    z
```

‘de Sitter’ model redshift-magnitude curve
(constant intrinsic brightness)

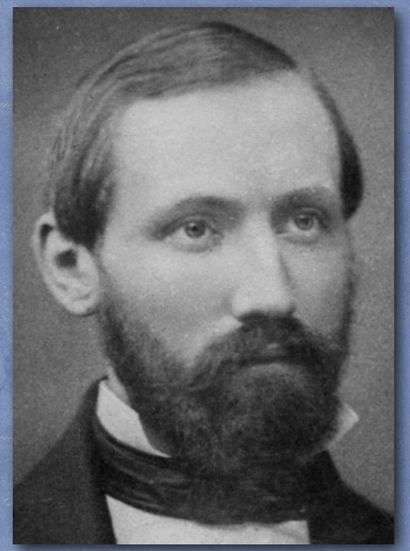


According to SDSS redshift-magnitude data, this model curve is *empirically accurate*. The increasing positive slope ($z \gtrapprox 0.1$) seen here was inevitably imposed on the conventional pattern of redshift-distance ‘measurements’ that had to conform with the ‘Hubble law.’ That very-unexpected observation of a slope increase in SNe IA data led to the current misconception of accelerating cosmic expansion induced by ‘dark energy.’

PART III – DE SITTER COSMOLOGY REVISITED

Click to go back to Table of Contents…

The Main Characters



Bernhard Riemann
(1826 – 1866)

Lifetime list of 11
published papers



Albert Einstein
(1879 – 1955)

List of scientific publications
by Albert Einstein (Wikipedia)

4



Hermann Minkowski
(1864 – 1909)

Space and Time
Minkowski's Papers on Relativity



Willem de Sitter
(1872 – 1934)

Leiden Observatory Archives,
Willem de Sitter papers (WdS)

"It is known that geometry assumes, as things given, both the notion of space and the first principles of constructions in space.

…

This leads us into the domain of another science, of physic [sic], into which the object of this work does not allow us to go to-day."

– G. F. Bernhard Riemann (1854)

G. F. B. Riemann, "On the Hypotheses which lie at the Bases of Geometry," *Göttingen Inaugural Lecture* (1854).

$$\frac{\mathrm{d}t}{\mathrm{d}\tau} = \frac{1}{\sqrt{1-\dfrac{\mathrm{v}^2}{c^2}}}$$

Time measurement is only *locally* valid;
time is a strictly-local phenomenon.

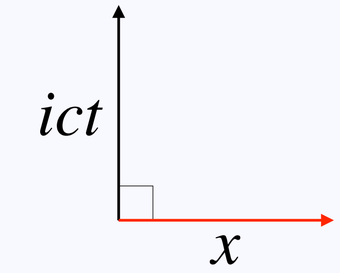
– Albert Einstein (1905)

A. Einstein, “On the Electrodynamics of Moving Bodies,” *Annalen der Physik* **17**, 891 (1905).

$$\mathrm{d}\tau^2 = -c^2\mathrm{d}t^2 + \mathrm{d}x^2 + \mathrm{d}y^2 + \mathrm{d}z^2$$

Space and time are locally-orthogonal coordinates in *the absolute* [4D] *world*.

– Hermann Minkowski (1908)



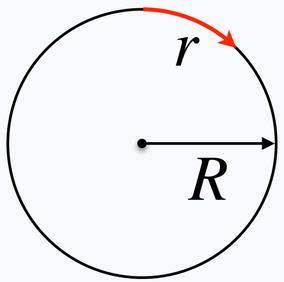
H. Minkowski, “Space and Time,” *A Lecture delivered in Cologne* (21 Sept. 1908).

An exact solution to the field equations

$$ds^2 = -dr^2 - R^2 \sin^2\left(\frac{r}{R}\right)\left[d\psi^2 + \sin^2(\psi)\, d\theta^2\right] + c^2 dt^2$$

The Universe is finite, yet has no boundary.

– Albert Einstein (1917)





A. Einstein, “Cosmological Considerations in the General Theory of Relativity,” *SPAW*, 142 (1917).

Einstein's cosmological considerations

The objective of this paper is not simply to present an historical overview of Einstein's cosmological considerations, but to discuss the central role they played in shaping the paradigm of relativistic cosmology. This, we'll show, was a result of both his actions and, perhaps more importantly, his inactions. Accordingly, discussion won't simply be restricted to Einstein's considerations, as we'll analyse relevant contributions to the relativistic expansion paradigm during the approximately twenty years following Slipher's first redshift measurements in 1912. Our aim is to shed some light on why we think some of the things we do, with the idea that a better understanding of the reasoning that fundamentally influenced the common idea of our expanding universe might help to resolve some of the significant problems that modern cosmology now faces; and we eventually use this knowledge to probe the foundations of the standard model. Much of the information we present, including many of the historical details, we expect will be news to modern practitioners.

Cosmology is in a crisis state unprecedented in the history of science. For while we now possess a model describing the large-scale evolution of our Universe whose parameters have been constrained with significant precision [unsurprisingly not actually so in hindsight], many aspects of the universe that this model seems to describe simply don't meet our theoretical expectations—and a number of 'big questions' have therefore arisen along with the great scientific progress that's taken place this past century.

D. Janzen, "Einstein's cosmological considerations" (2014); arXiv:1402.3212 [physics.hist-ph].

Daryl Janzen, Lecturer in Physics, *Dept. of Physics and Engineering Physics*, Univ. of Saskatchewan



EINSTEIN only assumes *three*-dimensional space to be finite. It is in consequence of this assumption that in (2A) g_{44} remains 1, instead of becoming zero with the other $g_{\mu\nu}$. This has suggested the idea [1]) to extend EINSTEIN'S hypothesis to the *four*-dimensional time-space. We then find a set of $g_{\mu\nu}$ which at infinity degenerate to the values [(2B)]. Moreover we find the remarkable result, that now no "world-matter" is required.

[1]) The idea to make the four-dimensional world spherical in order to avoid the necessity of assigning boundary-conditions, was suggested several months ago by Prof. EHRENFEST, in a conversation with the writer. It was, however, at that time, not further developed.

$$\begin{bmatrix} 0 & 0 & 0 & 0 \\ 0 & 0 & 0 & 0 \\ 0 & 0 & 0 & 0 \\ 0 & 0 & 0 & 1 \end{bmatrix} \qquad \begin{bmatrix} 0 & 0 & 0 & 0 \\ 0 & 0 & 0 & 0 \\ 0 & 0 & 0 & 0 \\ 0 & 0 & 0 & 0 \end{bmatrix}$$

(2A) (2B)

– Willem de Sitter (31 March 1917)

W. de Sitter, "On the relativity of inertia. Remarks concerning Einstein's latest hypothesis," *KNAW Proceedings* **19**(2), 1217 (1917).

Willem de Sitter had this very important critical insight…

"We thus find that in [Einstein's metric] the time has a separate position. That this must be so, is evident a priori. … Such a fundamental difference between the time and the space-coordinates seems to be somewhat contradictory to the complete symmetry of the field-equations…"

– Willem de Sitter (31 March 1917)

W. de Sitter, "On the relativity of inertia. Remarks concerning Einstein's latest hypothesis," *KNAW Proceedings* **19**(2), 1217 (1917).

but then he got confused and found no physical interpretation.

"All this shows that the postulate of the invariance of $g_{\mu\nu}$ *at infinity* [emphasis added] has no real physical meaning. It is purely mathematical."

– Willem de Sitter (31 March 1917)

W. de Sitter, "On the relativity of inertia. Remarks concerning Einstein's latest hypothesis," *KNAW Proceedings* **19**(2), 1217 (1917).

W. de Sitter,
"Einstein's theory of gravitation and its astronomical consequences. Third paper,"
MNRAS **78**, 3 (1917).

Also see the 1918 *KNAW* paper covering a 30 June 1917 lecture on the next slide (quoted reference).

If we neglect all pressures and other internal forces, and if we suppose all matter to be at rest, then the tensor $T_{\mu\nu}$ becomes

(5) $$T_{44} = g_{44}\rho, \qquad \text{all other } T_{\mu\nu} = 0,$$

ρ being the density in natural measure. We can put

(6) $$\rho = \rho_0 + \rho_1,$$

where ρ_0 is the average density of the world-matter. If ρ_0 is positive, then ρ_1 may be positive or negative; but in the latter case the numerical value must not exceed ρ_0.

If we wish to neglect gravitation, we must neglect ρ_1, and take ρ_0 constant. The equations (3) then become

(7) $$\begin{cases} G_{ij} - (\lambda + \frac{1}{2}\kappa\rho_0)g_{ij} = 0. \\ G_{44} - (\lambda + \frac{1}{2}\kappa\rho_0)g_{44} = -\kappa\rho_0 g_{44}. \end{cases}$$

These can be satisfied by the $g_{\mu\nu}$ implied by the line-element

Einstein ➡

(8A) $$ds^2 = -dr^2 - R^2 \sin^2\frac{r}{R}[d\psi^2 + \sin^2\psi d\theta^2] + c^2dt^2,$$

if

(9A) $$\kappa\rho_0 = 2\lambda, \qquad \lambda = \frac{1}{R^2}.$$

This is Einstein's new solution.

The equations are also satisfied by

de Sitter ➡

(8B) $$ds^2 = -dr^2 - R^2 \sin^2\frac{r}{R}[d\psi^2 + \sin^2\psi d\theta^2] + \cos^2\frac{r}{R}c^2dt^2,$$

if

(9B) $$\rho_0 = 0, \qquad \lambda = \frac{3}{R^2};$$

Another exact solution to the field equations

$$\mathrm{d}s^2 = -\mathrm{d}r^2 - R^2 \sin^2\left(\frac{r}{R}\right)\left[\mathrm{d}\psi^2 + \sin^2(\psi)\,\mathrm{d}\theta^2\right] + \cos^2\left(\frac{r}{R}\right)c^2\mathrm{d}t^2$$

"…we have $\varrho_0 = 0$ and consequently all $T_{\mu\nu} = 0$."

$\varrho_0 \equiv$ "average matter density"

– Willem de Sitter (30 June 1917)

A Universe with '*zero average* density' (i.e., *net zero* energy) seems absurd—or is it?

W. de Sitter, "On the curvature of space," *KNAW Proceedings* **20**(1), 229 (1918).

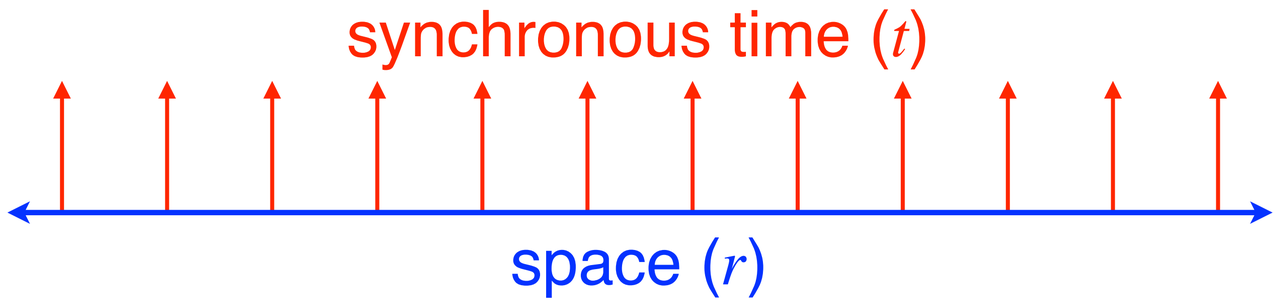
Distance-induced time dilation [$f(r)$] in the de Sitter-metric

$$\mathrm{d}s^2 = -\cancelto{0}{\mathrm{d}r^2} - R^2 \sin^2\left(\frac{r}{R}\right)\left[\cancelto{0}{\mathrm{d}\psi^2} + \sin^2(\psi)\,\cancelto{0}{\mathrm{d}\theta^2}\right] + \cos^2\left(\frac{r}{R}\right)c^2\mathrm{d}t^2$$

$$\mathrm{d}s^2 \equiv \mathrm{d}\tau^2 = \cos^2\left(\frac{r}{R}\right)c^2\mathrm{d}t^2 \qquad \underbrace{(R = c = 1)}_{\text{normalized}}$$

$$\frac{\mathrm{d}t}{\mathrm{d}\tau} = \frac{1}{\cos r}$$

The distinct physical interpretations of Einstein's and de Sitter's "g_{44}" *



$+c^2\mathrm{d}t^2$

Einstein

animation…

* (by modern convention, now "g_{00}")

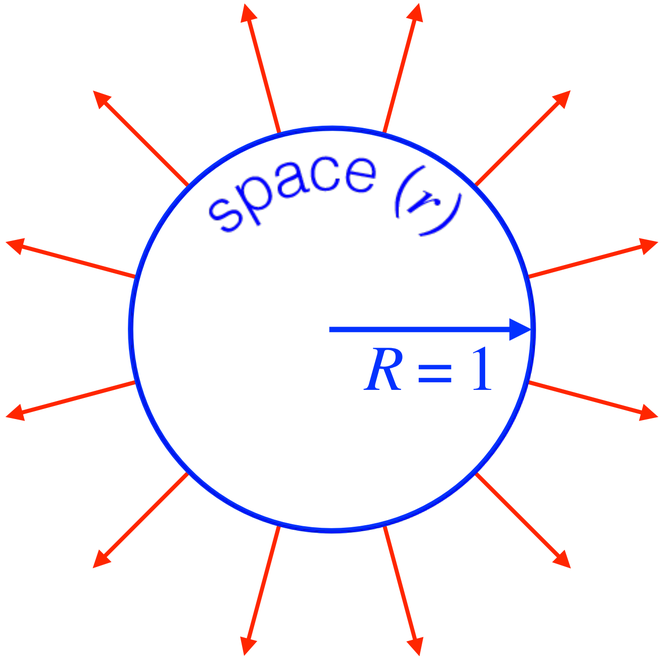
The distinct physical interpretations of Einstein's and de Sitter's "g_{44}" *

p - 1
page #
in PDF

Note that this model derives independently of the EFE from symmetry (i.e., the 3-sphere) and local orthogonality of space and time (Minkowski).

asynchronous time $[\tau(r)]$

$t \equiv \tau(0)$



$$+\cos^2\left(\frac{r}{R}\right)c^2\mathrm{d}t^2$$

de Sitter

animation completed

View the animation (YouTube)
https://youtu.be/kswjXqnNEs0

Change quality to 1080p.

* (by modern convention, now "g_{00}")

Time reversal and energy polarity

An idea arising from mathematical physics, which involves symmetry and the Planck equation ($E = h\nu$), is that *time reversal* yields *negative energy*.

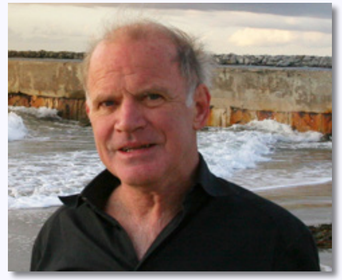
From any observer's arbitrary location in the Cosmos, local proper time in the fundamentally-invisible antipodal volumetric half of the Universe is systemically (i.e., azimuthally averaged) *relativistically reversed* as compared to local proper time in the adjacent visible half, which is bounded by the cosmological redshift horizon (see next slide).

The average matter density of both halves (A, B) is equal, so the two energy *magnitudes* are equal: $|E_A| = |E_B|$. However, *relativistically*, $E_A = -E_B$; therefore *the net cosmic energy is zero*: $E_A + E_B = 0$.

A remarkably-insightful speculation dating back fifty years was on the right track!

K. Mullis, "Cosmological Significance of Time Reversal," *Nature* **218**, 663 (1968).

photo credit: Kent Clemenco

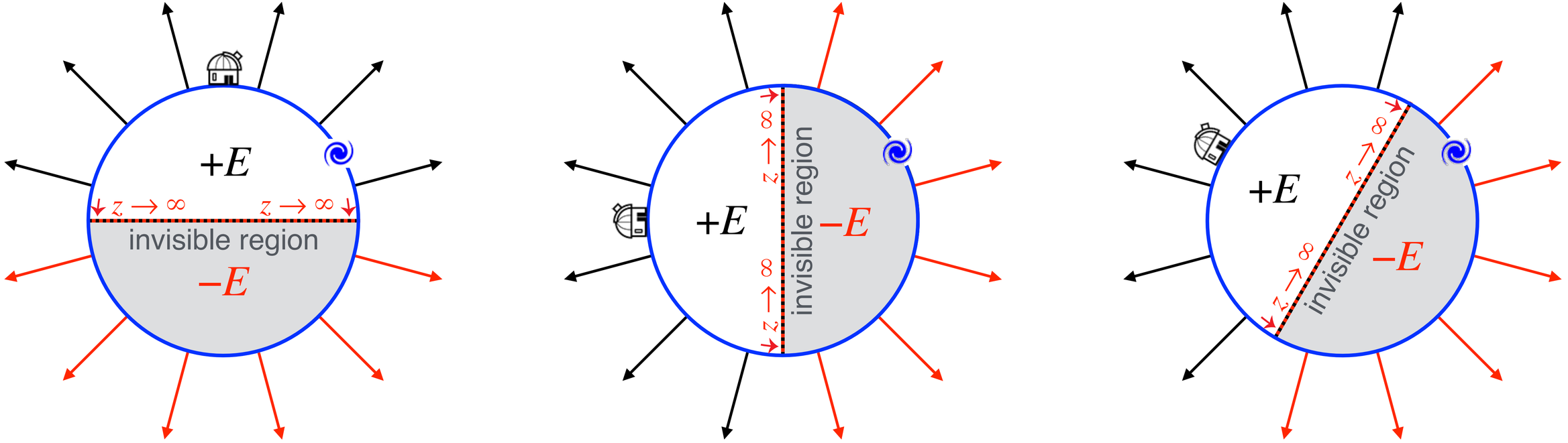


Kary Mullis

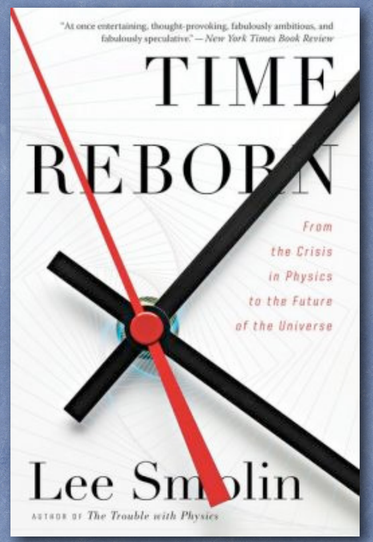
Cosmic antipodal energy polarity is a temporal *relativity* phenomenon.

Same galaxy, different observer location. Radial arrows represent local proper time.

Locally, the laws of physics (e.g., the second law of thermodynamics) are identical.



Relativistically, the *net* energy of the Universe is always *zero*: $(E - E = 0)$ from the point of view of an observer at any arbitrary Cosmic location.



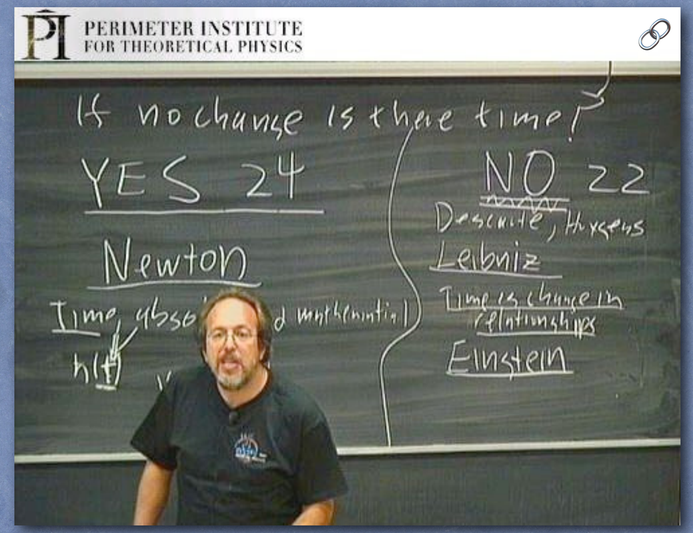
From Chapter 19, "The Future of Time"

"To make further progress in cosmology (and in fundamental physics as well), we need a new conception of a law of nature, valid on the cosmological scale, which avoids the fallacies, dilemmas, and paradoxes and answers the questions that the old framework cannot address."

– Lee Smolin, *Time Reborn* (2013), p. 240.

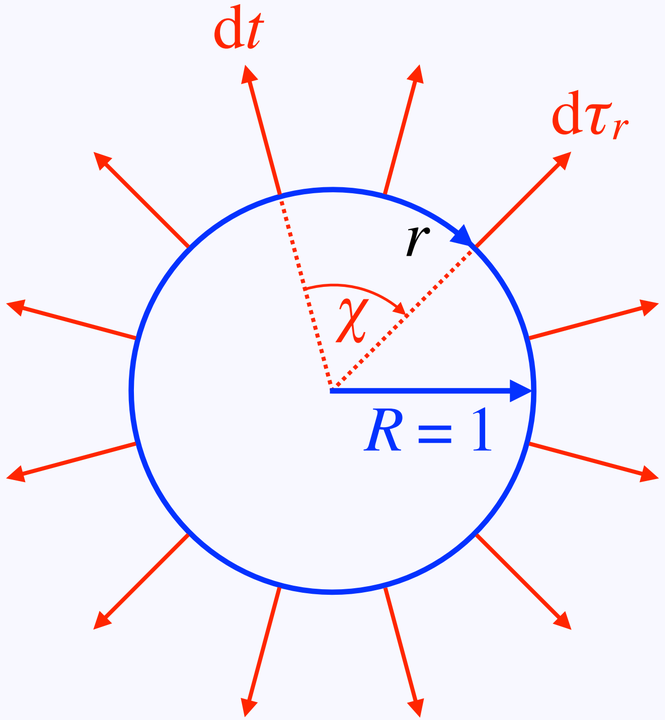
"The nature of space and time is *the* basic subject in physics."

Online Lecture: *The Nature of Space and Time* (0:01:15 / 1:28:25)



Redshift-distance relationship

R is the normalized cosmic radius; r is the distance from the observer; χ is the "cosmic latitude" $[0 \le \chi \le \pi]$.*



$$\chi = \frac{r}{R}$$

$$\frac{\mathrm{d}t}{\mathrm{d}\tau} = \frac{1}{\cos\chi} = \frac{1}{\cos r}$$

$$z+1 = \frac{1}{\cos r}$$

$$\cos r = \frac{1}{z+1}$$

frequency measurement

$$\frac{f_0}{f} = z+1 = \frac{\mathrm{d}t}{\mathrm{d}\tau}$$

$$\rightarrow r(z) = R\cos^{-1}\left(\frac{1}{z+1}\right)$$

redshift-distance relationship

* $\chi \equiv 0$ (where $\mathrm{d}t \equiv \mathrm{d}\tau_0$) is defined for an observer at *any arbitrary location* in the Universe (e.g., the Milky Way).

R cosmos.nb

In[1]:= $\theta = \frac{2.0}{3600} * \frac{\pi}{180}$; (* 2 arcseconds in radians *)

In[2]:= $\rho = \frac{15}{\theta}$; (* ESTIMATE 15 kly per 2 arcseconds @ z = 0.08 *) galaxy nuclei

estimated **intrinsic diameter** and empirically-observed **apparent diameter**

In[3]:= $R = \text{SetPrecision}\left[\rho * \left(1 - \frac{1}{(0.08+1)^2}\right)^{-\frac{1}{2}} * 1*\text{^}-6,\ 2\right]$ (* estimated Cosmic radius in Gly *)

as per new theta-z formula

Out[3]= 4.1

In[4]:= $\frac{\pi}{2} * R$ (* estimated distance to redshift horizon in Gly *)

Out[4]= 6.4

In[5]:= $V = \pi^2 * (R * 1*\text{^}9)^3$ (* volume of visible Universe in ly^3 *)

Out[5]= $7. \times 10^{29}$

In[6]:= $v = \frac{V}{1*\text{^}12}$ (* average volume per galaxy in ly^3 for 10^{12} galaxies *)

Out[6]= $7. \times 10^{17}$

In[7]:= $2\sqrt[3]{\frac{v}{\frac{4}{3}\pi}}$ (* average distance between 10^{12} galaxies in ly *)

Out[7]= 1.1×10^{6}

150%

The Cosmic Radius

In the previous slide, the theta-z predictive formula was used to determine the Cosmic radius (R) as the single unknown. In that formula, the two directly-measurable values are the redshift (z) and the apparent angular diameter (θ) of an observed distant object. The remaining empirical variable, which must be estimated, is the intrinsic diameter (δ) of that object, and $\delta/\theta = \rho$, where this Euclidean effective radius (*rho*) is illustrated on slide 137.

According to the empirical data in the form of visually-analyzed SDSS galaxy images, ubiquitous galaxy nuclei are all of approximately the same intrinsic diameter, which diameter is independent of the widely-varying (by about an order of magnitude) host-galaxy size. Based on observation of the Milky Way and M31 (Andromeda), that diameter is estimated to be about 15 kly.

Though not shown for notebook brevity, $\rho(0.08) \approx 1.55$ Gly. At this redshift, the range in Petrosian radius is $7 \leq r_P \leq 17$, which correlates to a range in *typical* galaxy diameter of $\rho \cdot 2r_P \sim 25\text{–}250$ kly. This is a “reality check” (with good results) on the estimated value of ρ, from which we derive R.

As concerns *absolute* measurements, the single free empirical parameter shared by all predictive formulas is the estimated Cosmic radius R. As such, its accurate measurement by the above method warrants a precision astronometric program (e.g., using the light curves of galactic nuclei) and a more precise measurement of δ than the round estimate of 15 kly.

Prior “redshift-independent” distance measurements

The astronomical reference literature dating back more than a half-century includes numerous “redshift-independent” extragalactic distance measurements, including error bars. For nearby galaxies (out to an estimated 100 Mly) the primary measurement method is the period-luminosity relation of Cepheid variables. For more distant galaxies, in which Cepheids cannot be resolved, the assumed characteristics of Type IA supernovae, the Tully-Fisher relation (an adopted correlation between galaxy luminosity and rotational velocity), and the Faber-Jackson relation (an adopted correlation between elliptical-galaxy luminosity and nuclear stellar velocity dispersion) have been the primary such measurement methods.

In reality, all of these extragalactic distance indicators were tied to the purported ‘Hubble constant,’ which was interpreted as a rigorous empirical constraint on the redshift-distance relationship, recently thought to have 1% error bars.[1] Extragalactic distance measurements contradicting such a generally-accepted (albeit false) ‘empirical law’ were thus considered to be ‘impossible.’

As it is consistent with SDSS and other statistically-significant empirical data, the new redshift-distance relationship is expected to yield absolute distance measurements that are correct to the accuracy of the estimated Cosmic radius R. Corrections to prior distance measurements can be attributed to the ‘impossibility’ of those measurements to have disagreed with the ‘Hubble law.’

1. C. L. Bennett, D. Larson, J. L. Weiland, & G. Hinshaw, “The 1% Concordance Hubble Constant,” *ApJ* **794**, 135 (2014).

Given $R \sim 4.1$ Gly, then in the 1929 Hubble diagram, which extends to $r = 2^{+}$ Mpc:

$$\overbrace{6.5\ \text{Mly}}^{r} = \overbrace{4.1\ \text{Gly}}^{R} \cdot \cos^{-1}\left(\frac{1}{z+1}\right)$$

redshift-distance relationship

Hubble Diagram cz.nb

```
In[1]:= R = 4.1*^9; (* estimated Cosmic radius is 4.1 Gly *)

In[2]:= r = 6.5*^6; (* 2 Mpc is about 6.5 Mly *)

In[3]:= Clear[z]; (* solve for redshift (z), given R and r *)

In[4]:= {z} = z /. Solve[r == R * ArcCos[1/(z + 1)], z]

Out[4]= {1.25669 × 10^-6}

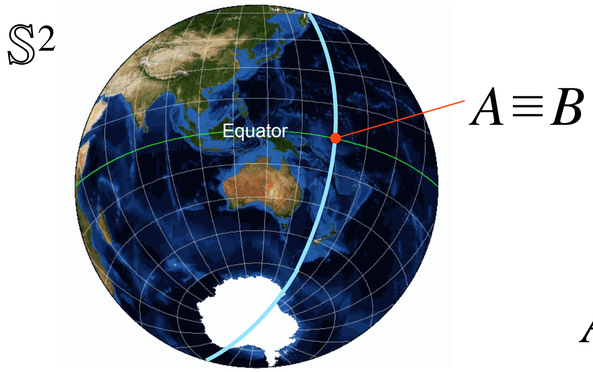
In[5]:= 2.998*^5 * z (* redshift expressed as a recession velocity cz in km s^-1 *)

Out[5]= 0.376757  (Yields y ~ 0 flat green line in slide-56 Hubble diagram, given its "VELOCITY" scale.)
```

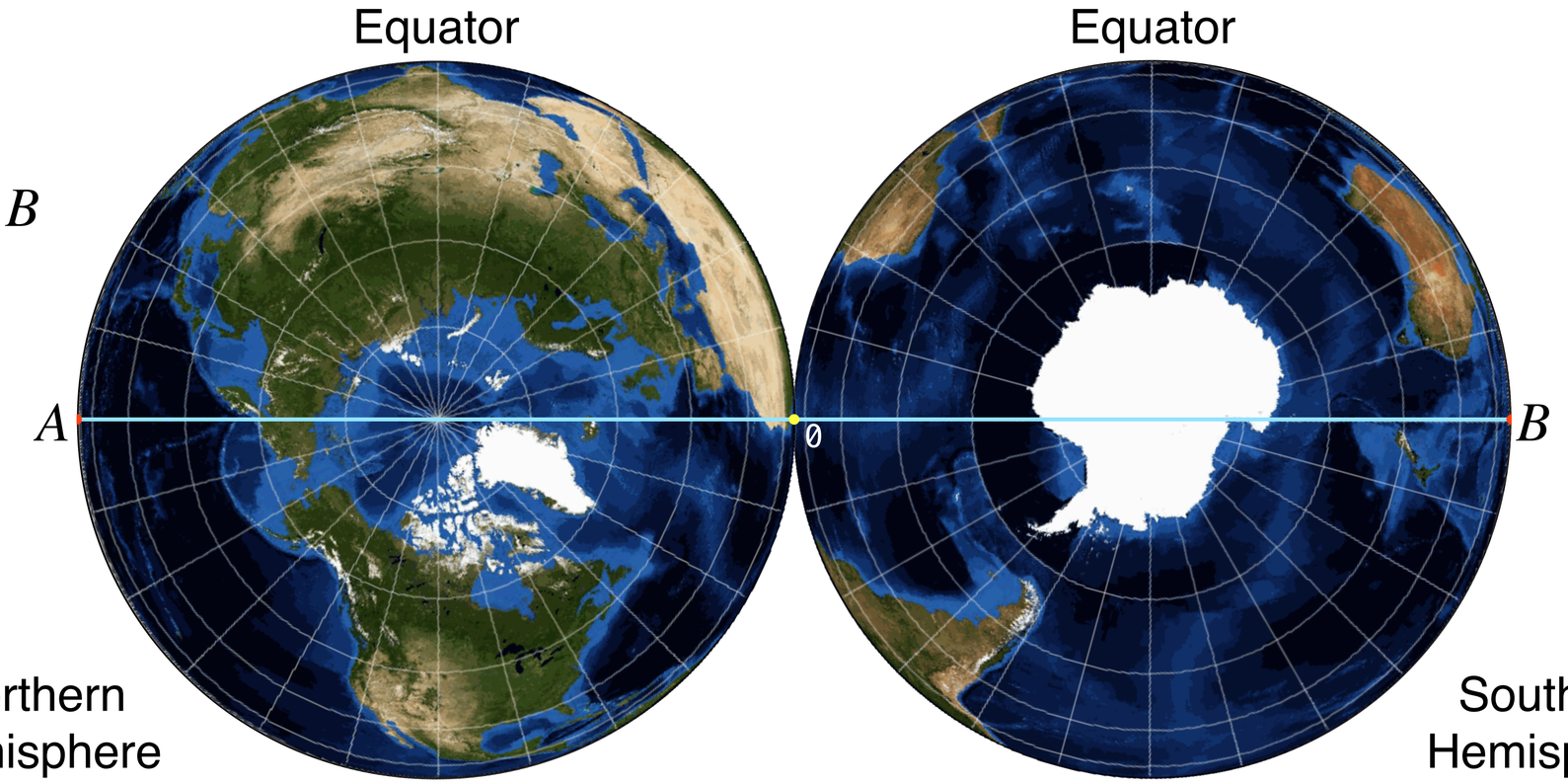
125%

Mapping a finite, boundaryless 2-space…

Every point in a two-dimensional homogeneous, finite, boundaryless space ($\mathbb{S}^2$) can be mapped by an infinite set of great circles ($\mathbb{S}^1$). A more intuitive map of the space is the union of two *disks* ($\mathbb{S}^2$) whose boundary points are duplicate coordinates, whereby a midline (e.g., $\overline{AB}$ where A and B map an identical point) represents one such great circle. Ignoring terrestrial asymmetry, line segments $\overline{0A}$ and $\overline{0B}$ are linear projections of semicircles having 'identical' length to similar paths on the Equator.



Earth idealized as a *sphere*

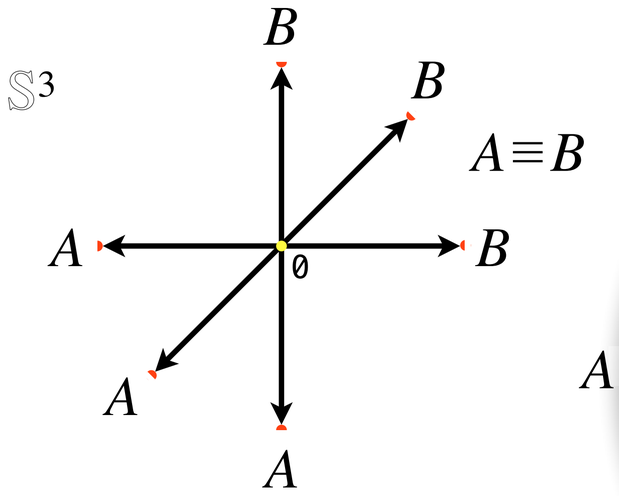


Line $\overline{AB}$ represents a circle.

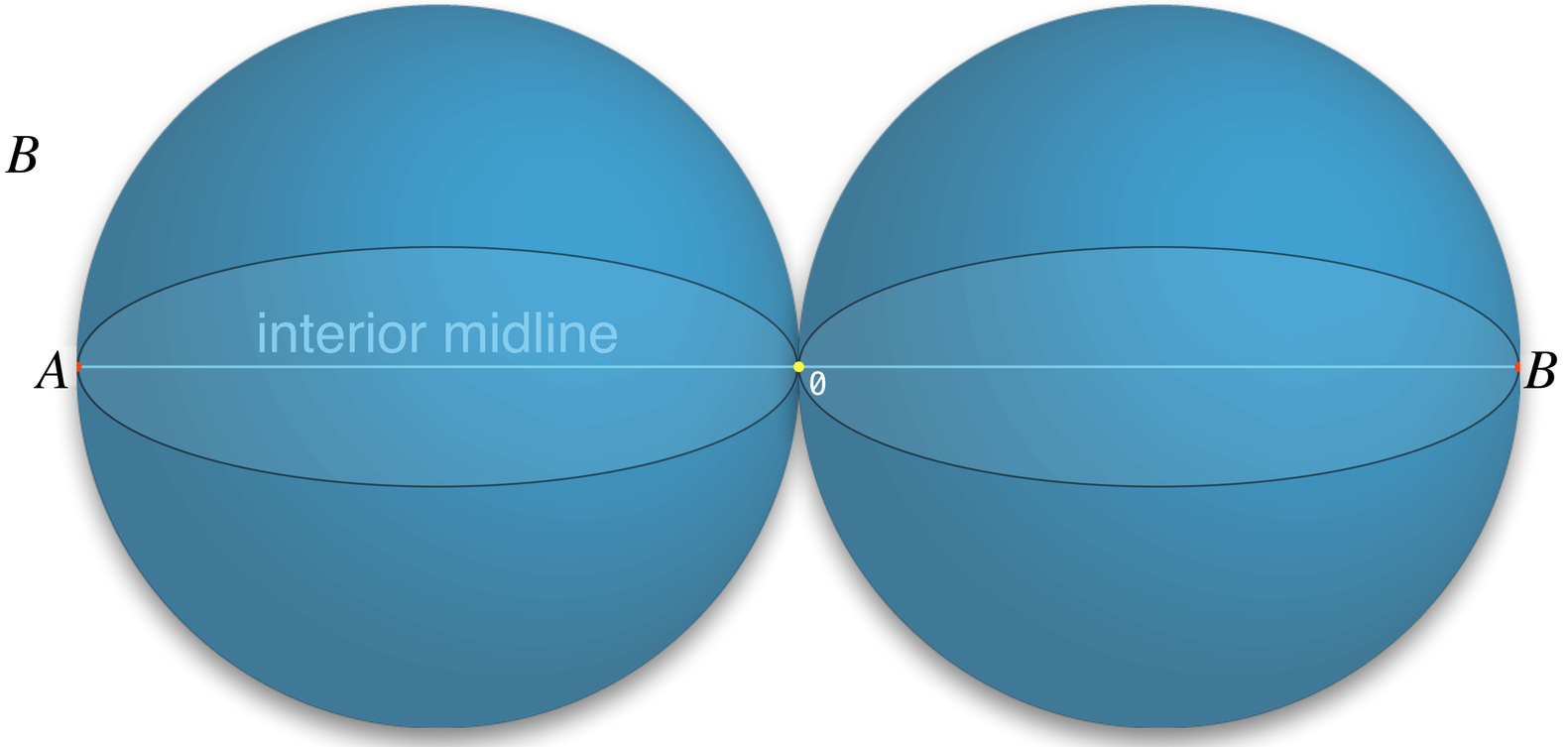
Earth projections source: http://www.icsm.gov.au/education/fundamentals-mapping/projections

Mapping a finite, boundaryless 3-space

Every point in a three-dimensional homogeneous, finite, boundaryless space ($\mathbb{S}^3$) can be mapped by an infinite set of spheres ($\mathbb{S}^2$). A more intuitive map of the space is the union of two *balls* ($\mathbb{S}^3$) whose exterior boundary points are duplicate coordinates. The interior midline $\overline{AB}$ represents a cosmic great circle as A and B map the identical point. The set of interior points uniquely map all of cosmic space, less the set of duplicated points on the map's boundary. Line segments $\overline{0A}$ and $\overline{0B}$ are linear projections of semicircles having identical length to similar paths on the boundary.



Every extended geodesic forms a closed loop.



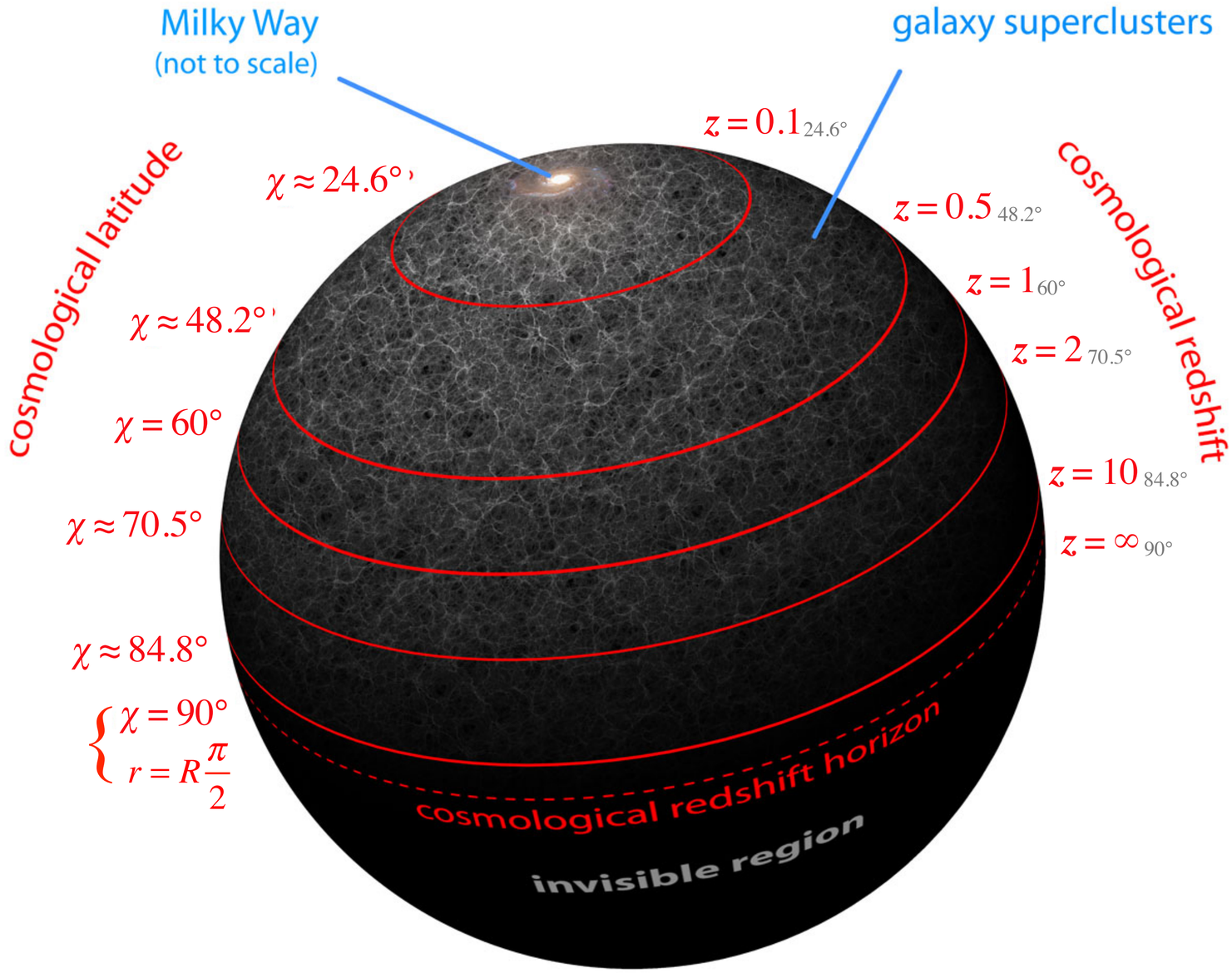
Line $\overline{AB}$ represents a circle.

© A. F. Mayer

A complete cosmological map of the $\mathbb{S}^2$ surface *locally* defined by Galactic latitude $b = 0$ (i.e., the Galactic plane)

$$\chi = \cos^{-1}\left(\frac{1}{z+1}\right)$$

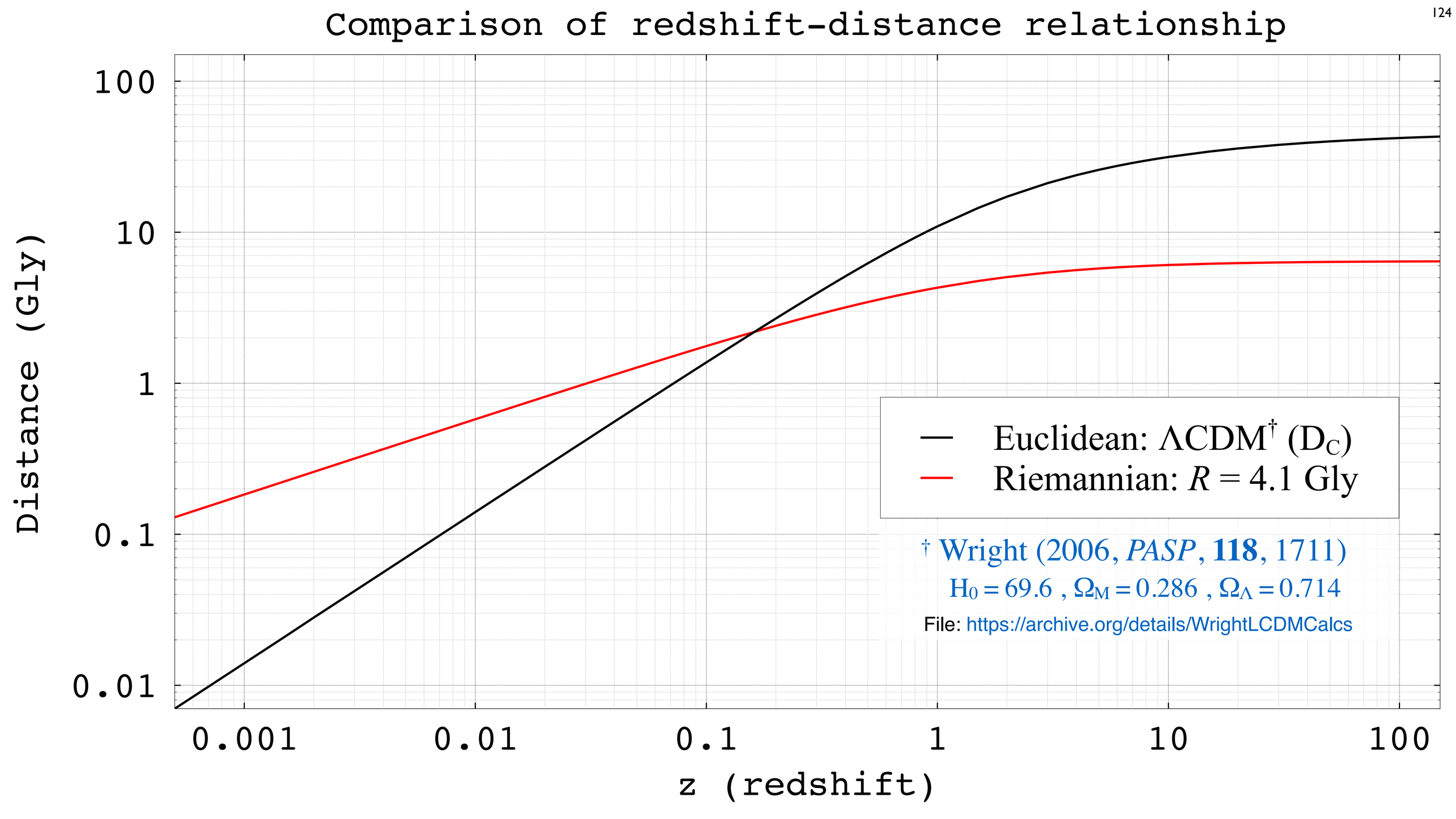
$$z = \frac{1}{\cos\chi} - 1$$



$$r = R\cos^{-1}\left(\frac{1}{z+1}\right)$$

$z = \infty$
@ horizon
$(\chi = \pi/2)$

Graphic by Fabio Basile after an original rendering by Hollin Calloway (2005).


Comparison of redshift-distance relationship
Distance (Gly)
100
10
1
0.1
0.01
0.001
0.01
0.1
1
10
100
z (redshift)
Euclidean: ΛCDM† (D_C)
Riemannian: R = 4.1 Gly
† Wright (2006, PASP, 118, 1711)
H0 = 69.6 , ΩM = 0.286 , ΩΛ = 0.714
File: https://archive.org/details/WrightLCDMCalcs

Reference to the local Universe

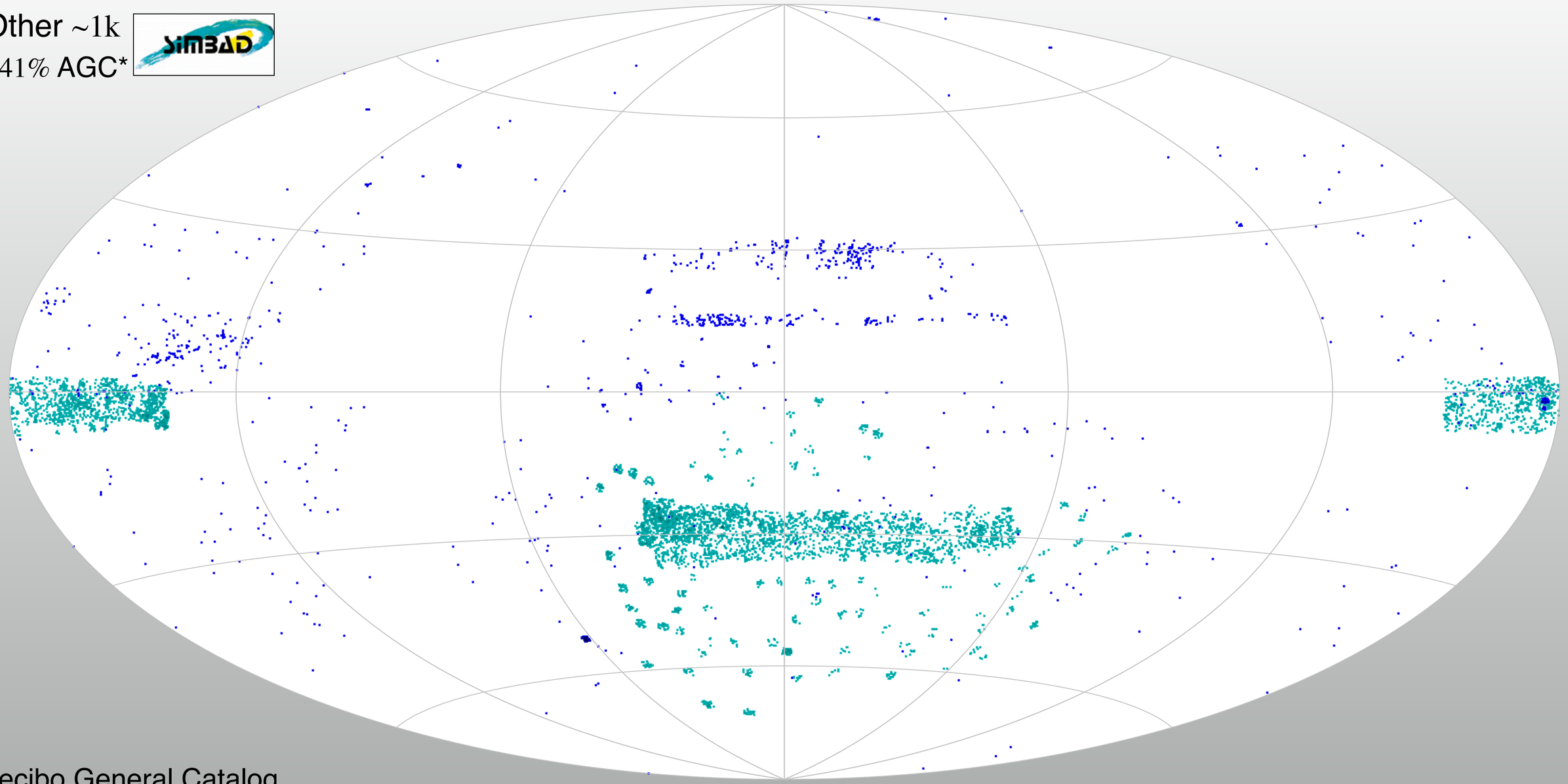
Our closest neighbor, M31 (Andromeda Galaxy) has a mean redshift-independent distance of 0.784 Mpc (~2.6 Mly). According to the consensus ΛCDM cosmological model, with parameter values ($H_0, \Omega_M, \Omega_\Lambda$) shown repeatedly in prior graphs, that distance measurement corresponds to a *distance* redshift $z(d) = 0.000182$. Its *blueshifted* (–) heliocentric relative velocity is recorded as $-300 \pm 4\ \mathrm{km \cdot s^{-1}}$, while its Galactocentric relative velocity (reflecting the Sun's orbital motion) is $-122 \pm 8\ \mathrm{km \cdot s^{-1}}$, the Doppler shift equivalent of the former being $v/c = -0.001$.

According to the following Aitoff projection sky map, such measured galaxy blueshifts, caused by relative-motion ("peculiar-velocity") Doppler shifts overshadowing *distance* redshift, are ubiquitous within the footprint of redshift surveys that faithfully record them. The bar charts on the next slide (127) indicate that measured heliocentric blueshifts rarely exceed $|z| \sim 0.001$, which puts constraints on Doppler-induced variation between measured galaxy shift (±) and *distance* redshift.

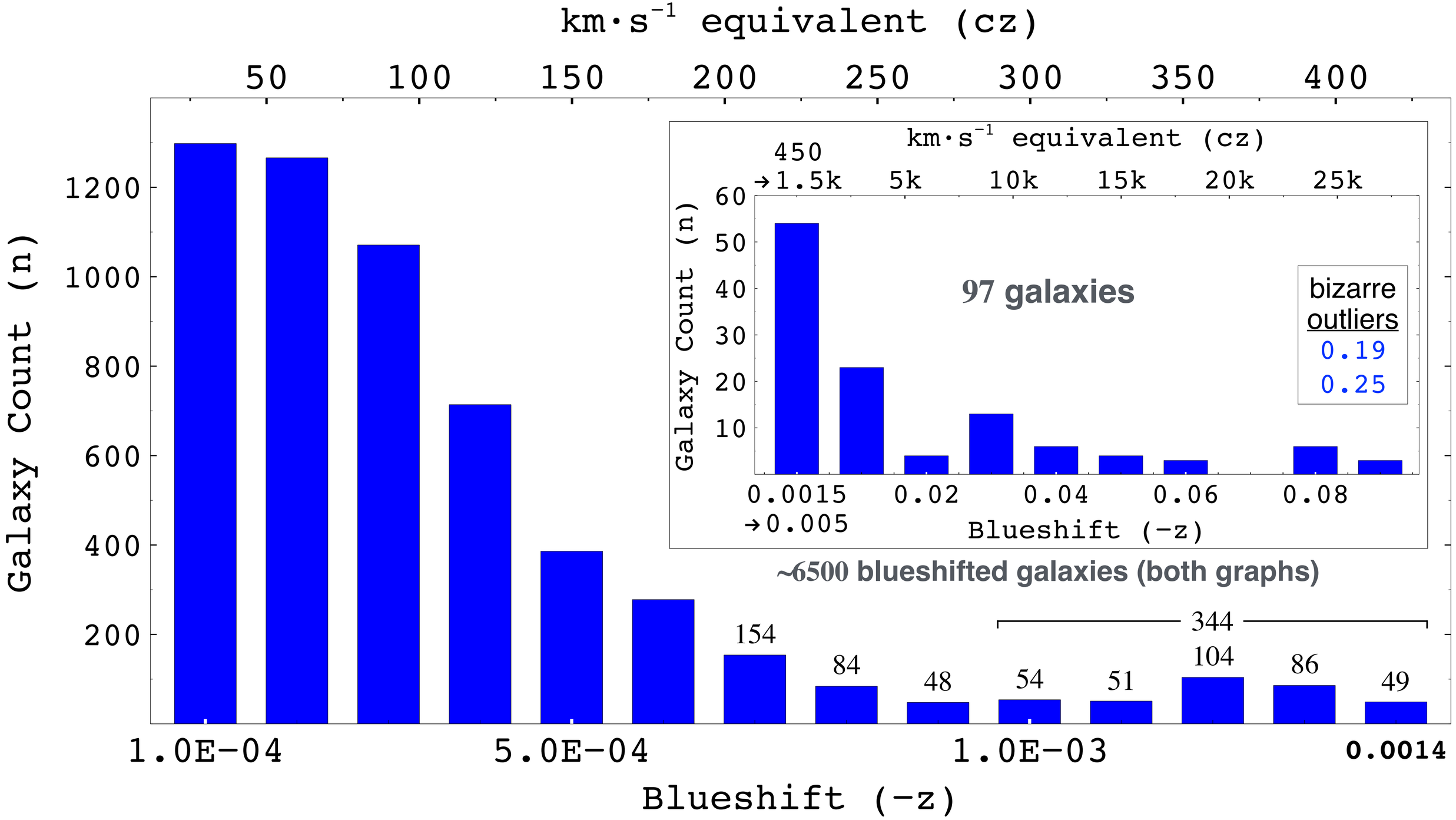
The two redshift-magnitude graphs (128–129), with corresponding distance scales in light years, use M31 as a reference standard candle. Its apparent visual magnitude of 3.4 is in accord with a nominal r-band value of 2.5 mags. Low-redshift data ($z \leq 0.12$), which includes aperture-limited measurements for the nearest galaxies, is sourced from SIMBAD with other data from SDSS. The two graphs compare the Euclidean ΛCDM model to the new, Riemannian 'de Sitter' model. The redshift value of M31 in both graphs is based on its ~2.6 Mly redshift-independent distance.

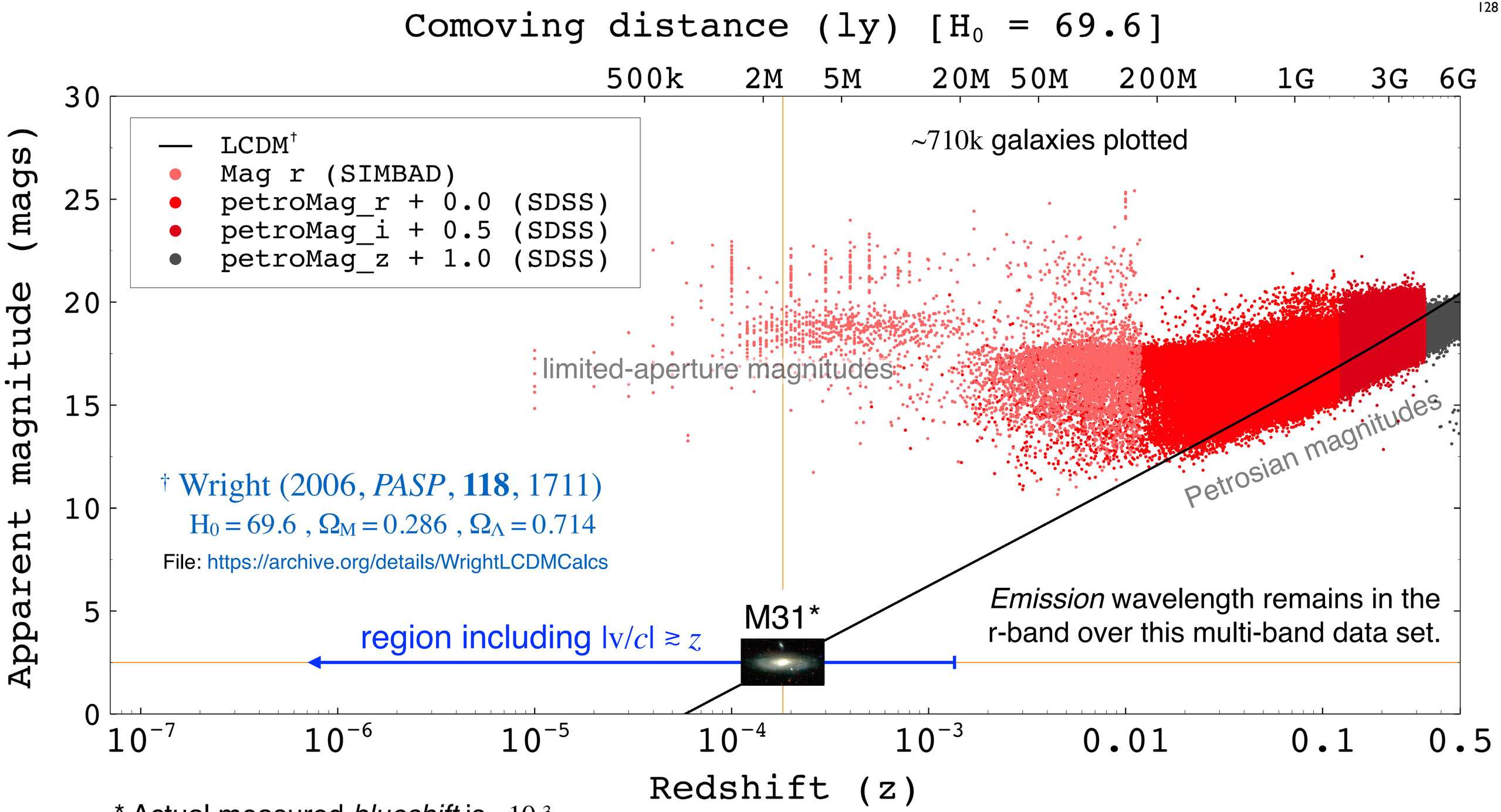
~6500 *blueshifted* galaxies…

- 2dFGRS‡
- Other ~1k
 ~41% AGC*

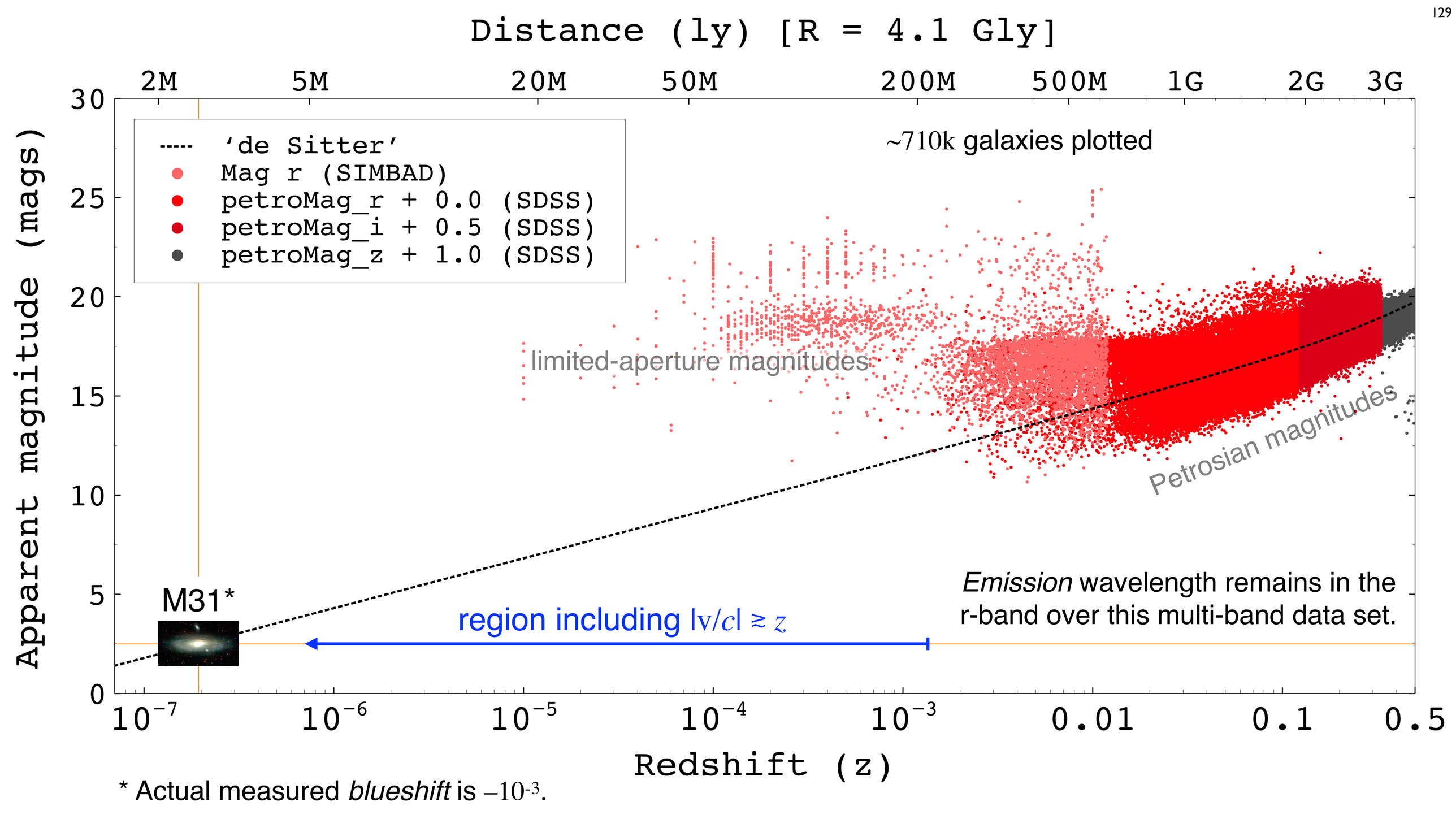


* Arecibo General Catalog
‡ ~5.5k galaxies (2.5% of ~221k w/quality ≥ 3)


km·s⁻¹ equivalent (cz)
50
100
150
200
250
300
350
400
Galaxy Count (n)
1200
1000
800
600
400
200
154
84
48
344
54
51
104
86
49
1.0E−04
5.0E−04
1.0E−03
0.0014
Blueshift (−z)
km·s⁻¹ equivalent (cz)
450
→1.5k
5k
10k
15k
20k
25k
Galaxy Count (n)
60
50
40
30
20
10
97 galaxies
bizarre
outliers
0.19
0.25
0.0015
→0.005
0.02
0.04
0.06
0.08
Blueshift (−z)
~6500 blueshifted galaxies (both graphs)



* Actual measured *blueshift* is -10^{-3}.



* Actual measured *blueshift* is -10^{-3}.

PART IV – NEW PREDICTIVE EQUATIONS

Click to go back to Table of Contents…

The tool implementing the mediation between theory and practice, between thought and observation, is mathematics. Mathematics builds the connecting bridges and is constantly enhancing their capabilities. Therefore it happens that our entire contemporary culture, in so far as it rests on intellectual penetration and utilization of nature, finds its foundations in mathematics.

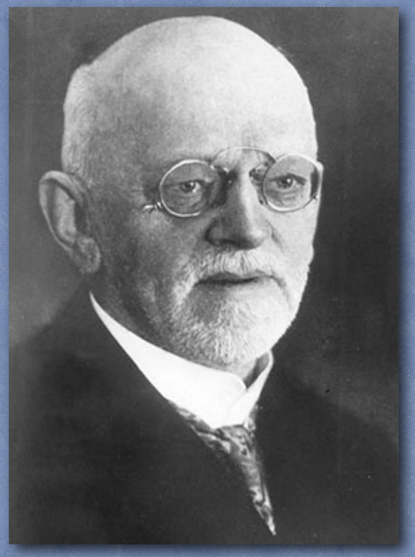
…

For us there is no ignorance, especially not, in my opinion, for the natural sciences.

Instead of this silly ignorance, on the contrary let our fate be:

"We must know, we will know."

– David Hilbert, *Preeminent 20th-century mathematician (1862–1943)*



David Hilbert

Source: *Translation of an address given by David Hilbert in Königsberg*, Fall 1930; translation by Amelia and Joe Ball.

The topological unit 3-sphere (S^3) has a finite, boundaryless *volume*.

line element: $$\mathrm{d}s^2 = \mathrm{d}\psi^2 + \sin^2\psi\left(\mathrm{d}\theta^2 + \sin^2\theta\ \mathrm{d}\phi^2\right)$$

Denotes the topological 3-sphere; not an exponent!

$$S^3 = \int_0^{\pi} \mathrm{d}\psi \int_0^{\pi} \sin\psi\ \ \mathrm{d}\theta\ \int_0^{2\pi} \sin\psi\ \ \sin\theta\ \ \mathrm{d}\phi$$

volume: $$S^3 = 4\pi \int_0^{\pi} \sin^2\psi\ \ d\psi$$

$$S^3 = 2\pi\left(\psi - \cos\psi\sin\psi\right)\Big]_0^{\pi} = 2\pi^2$$

$S^3(\chi)$:

$$\psi \to \chi$$

$$S^3 = 2\pi\left(\chi - \cos\chi\sin\chi\right)$$

"continued on next slide"



Redshift-volume function…

$$S^3(\chi) = 2\pi(\chi - \cos\chi \sin\chi)$$

$\chi(z)$:

$$\begin{cases} \cos\chi = \dfrac{1}{(z+1)} \\ \\ \sin\chi = \sqrt{1-\cos^2\chi} = \left(1 - \dfrac{1}{(z+1)^2}\right)^{\frac{1}{2}} \end{cases}$$

$$S^3(z) = 2\pi\left\{\cos^{-1}\left(\frac{1}{z+1}\right) - \left[\left(\frac{1}{z+1}\right)\left(1 - \frac{1}{(z+1)^2}\right)^{\frac{1}{2}}\right]\right\}$$

$S^3(z)$:

$$S^3(z) = 2\pi\left[\cos^{-1}\left(\frac{1}{z+1}\right) - \left(\frac{1}{(z+1)^2} - \frac{1}{(z+1)^4}\right)^{\frac{1}{2}}\right] \quad \underbrace{R^3 \text{ units}}$$

Volume-element function…

$$S^3(z) = 2\pi\left[\cos^{-1}\left(\frac{1}{z+1}\right) - \left(\frac{1}{(z+1)^2} - \frac{1}{(z+1)^4}\right)^{\frac{1}{2}}\right]$$

$$u = (z+1)^{-1} \qquad \frac{\mathrm{d}u}{\mathrm{d}z} = -(z+1)^{-2} = -u^2$$

$$S^3(z) = 2\pi\left[\cos^{-1} u - \left(u^2 - u^4\right)^{\frac{1}{2}}\right]$$

$$\frac{\mathrm{d}S^3}{\mathrm{d}z} = 2\pi\left[\frac{-1}{\sqrt{1-u^2}}\frac{\mathrm{d}u}{\mathrm{d}z} - \frac{1}{2\sqrt{u^2-u^4}}\left(2u\frac{\mathrm{d}u}{\mathrm{d}z} - 4u^3\frac{\mathrm{d}u}{\mathrm{d}z}\right)\right]$$

Volume-element function…

$$\frac{\mathrm{d}S^3}{\mathrm{d}z} = 2\pi\left[\frac{-1}{\sqrt{1-u^2}}\frac{\mathrm{d}u}{\mathrm{d}z} - \frac{1}{2\sqrt{u^2-u^4}}\left(2u\frac{\mathrm{d}u}{\mathrm{d}z} - 4u^3\frac{\mathrm{d}u}{\mathrm{d}z}\right)\right] \qquad \left(\frac{\mathrm{d}u}{\mathrm{d}z} = -u^2\right)$$

$$= 2\pi\left[\frac{u^2}{\sqrt{1-u^2}} - \frac{1}{2\sqrt{u^2-u^4}}\left(-2u^3+4u^5\right)\right] = 2\pi\left[\frac{u^2}{\sqrt{1-u^2}} + \frac{u^3}{\sqrt{u^2-u^4}} - \frac{2u^5}{\sqrt{u^2-u^4}}\right]$$

$$= 2\pi\left[\frac{u^2}{\sqrt{1-u^2}} + \frac{1}{\sqrt{u^2-u^4}}\left(u^3-2u^5\right)\right] = 2\pi\left\{\frac{1}{\sqrt{1-u^2}}\left[u^2 + \frac{1}{u}\left(u^3-2u^5\right)\right]\right\}$$

$$= 4\pi\left[\frac{1}{\sqrt{1-u^2}}\left(u^2-u^4\right)\right] \qquad \longrightarrow$$

Volume-element function…

$$\frac{\mathrm{d}S^3}{\mathrm{d}z} = 4\pi\left[\frac{1}{\sqrt{1-u^2}}\left(u^2-u^4\right)\right] \qquad \left\{u=(z+1)^{-1}\right\}$$

$$\frac{\mathrm{d}S^3}{\mathrm{d}z} = \frac{4\pi}{\sqrt{1-(z+1)^{-2}}}\left(\frac{1}{(z+1)^2}-\frac{1}{(z+1)^4}\right) \quad \underbrace{R^3 \text{ units}}$$

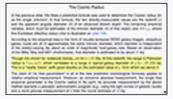
$$S^3(z) = C_V \cdot 2\pi\left[\cos^{-1}\left(\frac{1}{z+1}\right)-\left(\frac{1}{(z+1)^2}-\frac{1}{(z+1)^4}\right)^{\frac{1}{2}}\right] \quad \text{arbitrary units}$$

$$\frac{\mathrm{d}S^3}{\mathrm{d}z} = C_{\mathrm{d}V} \cdot \frac{4\pi}{\sqrt{1-(z+1)^{-2}}}\left(\frac{1}{(z+1)^2}-\frac{1}{(z+1)^4}\right) \quad \text{arbitrary units}$$

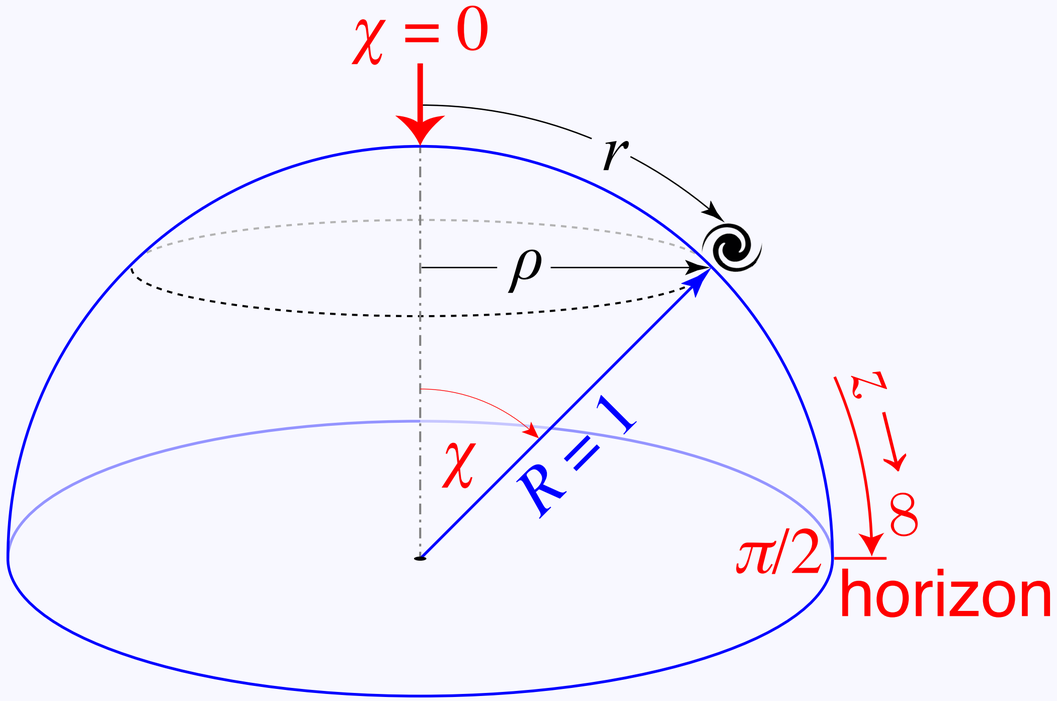
Here, C_V and $C_{\mathrm{d}V}$ are data-dependent arbitrary *scaling* constants.

Theta-z relationship (apparent size of a standard rod)

Jump back to ***The Cosmic Radius***.



observer's arbitrary location
(e.g., the Milky Way Galaxy)



$$\rho = \cancel{R}\sin\chi = \left(1-\frac{1}{(z+1)^2}\right)^{\frac{1}{2}}$$

$$\theta(z) \propto \frac{1}{\rho}$$

$$\theta(z) = C_\delta\left(1-\frac{1}{(z+1)^2}\right)^{-\frac{1}{2}} \text{ radians}$$

Here, C_δ is an arbitrary *scaling* constant that is proportional to the intrinsic diameter of the standard rod (a class of astrophysical object understood to be of approximately the same intrinsic size) under consideration.

Redshift-magnitude function…

$$S^3 = 4\pi \int_0^{\pi} \sin^2 \psi \ \mathrm{d}\psi = 4\pi \int_0^{\pi} \sin^2 \chi \ \mathrm{d}\chi \qquad (\psi \to \chi)$$

$$S^2 = \frac{\mathrm{d}}{\mathrm{d}\chi} S^3 = 4\pi \sin^2 \chi$$

$$\sin \chi = \left(1 - \frac{1}{(z+1)^2} \right)^{\frac{1}{2}}$$

$$S^2 = 4\pi \left(1 - \frac{1}{(z+1)^2} \right) \quad \underbrace{R^2 \text{ units}}$$



Redshift-magnitude function…

$$F\left(S^2\right)=\frac{L}{S^2}=\frac{L}{4\pi\left(1-\frac{1}{\left(z+1\right)^2}\right)} \qquad \left(z>0\right)$$

Time dilation factor : $\left(z+1\right)^{-2}$ Curvature factor : $\left(z+1\right)^{-2}$

$$F\left(z\right)=\frac{L}{4\pi\left(1-\frac{1}{\left(z+1\right)^2}\right)\cdot\left(z+1\right)^4}=\frac{L}{4\pi\left[\left(z+1\right)^4-\left(z+1\right)^2\right]}$$



Redshift-magnitude function…

$$F(z) = \frac{L}{4\pi\left[(z+1)^4 - (z+1)^2\right]}$$

$$m = C_M - 2.5 \cdot \log(b)$$

$$m(z) = C_M - 2.5 \cdot \log\left(\frac{1}{4\pi\left[(z+1)^4 - (z+1)^2\right]}\right) \quad \text{mags}$$

Here, C_M is an arbitrary *scaling* constant that is proportional to the absolute magnitude of the standard candle under consideration.

Redshift-magnitude function

If one wishes to incorporate IGM extinction (light dimming due to absorption and scattering by the intergalactic medium), which is *approximated** to be a linear function of radial distance, then

$$m(z) = C_M - 2.5 \cdot \log\left(\frac{1}{4\pi\left[(z+1)^4 - (z+1)^2\right]}\right) + \underbrace{\varepsilon_\lambda \cos^{-1}\left(\frac{1}{z+1}\right)}_{\text{IGM extinction}} \quad \text{mags}$$

Here, ε_λ is a constant, which may vary with observed wavelength (λ); it is correlated to the average density of the IGM over the line of sight to the target object. This was set to *zero* for the graphed functions.

* *Such approximation does not take into account that IGM extinction is a function of photon wavelength, which varies over the light path due to persistent redshift.*

PART V – GALAXY SPACE DENSITY

Click to go back to Table of Contents…

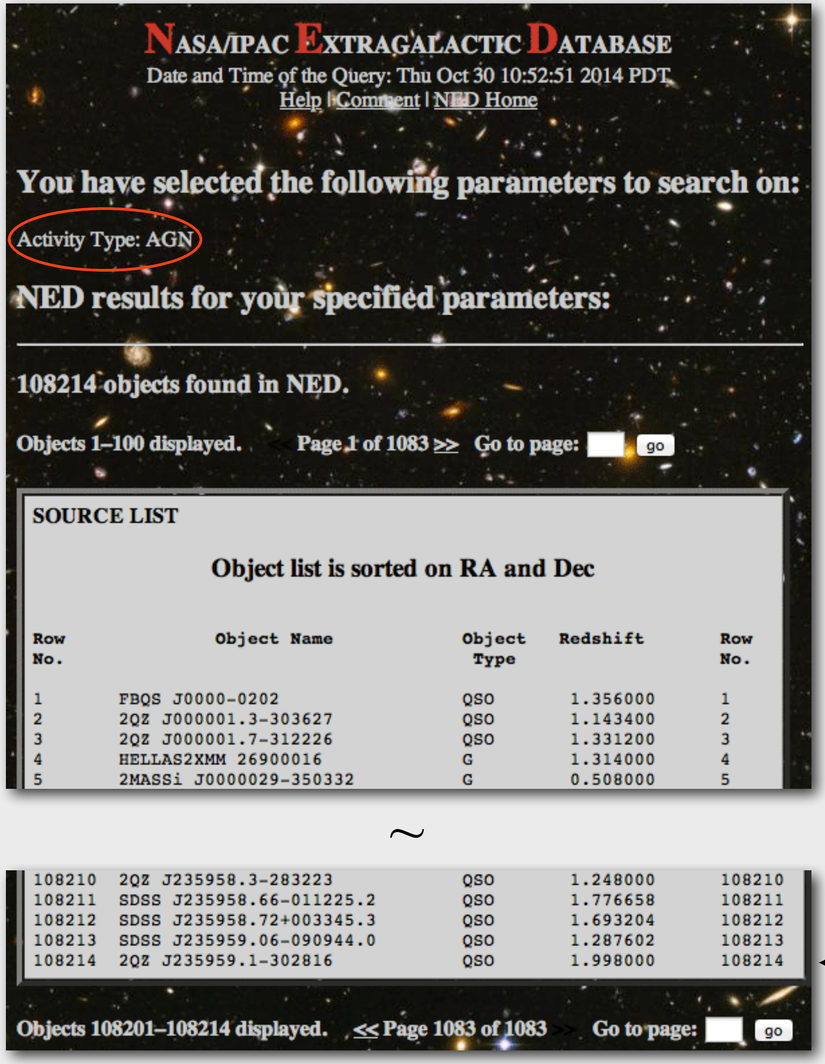
Space-density of active galactic nuclei

A small percentage of galaxies host an active galactic nucleus (AGN), which has a much higher luminosity than normal; the brightest AGN are observed at very high redshift ($z > 6$), so these galaxies are an ideal observable with which to confront theoretical predictions of galaxy space density, including testable assumptions concerning galaxy evolution over lookback time. According to the data and the new cosmological model, AGN constitute a fixed portion of the local regional galaxy population (on large scale) throughout the Universe. According to the ΛCDM model, AGN population density has increased by over four orders of magnitude since the presumed 'primordial universe.'

To counteract any survey selection effects, data for $\sim 108\text{k}$ AGN is sourced from the NASA/IPAC Extragalactic Database (NED); SDSS data constitutes about 72% of the graphed NED AGN dataset, with the balance sourced from numerous other surveys.

NED AGN

Click *image* for source data,
here for precompiled datafile.



NASA/IPAC EXTRAGALACTIC DATABASE

Date and Time of the Query: Thu Oct 30 10:52:51 2014 PDT

Help | Comment | NED Home

You have selected the following parameters to search on:

Activity Type: AGN

NED results for your specified parameters:

108214 objects found in NED.

Objects 1–100 displayed. Page 1 of 1083 >> Go to page: go

SOURCE LIST

Object list is sorted on RA and Dec

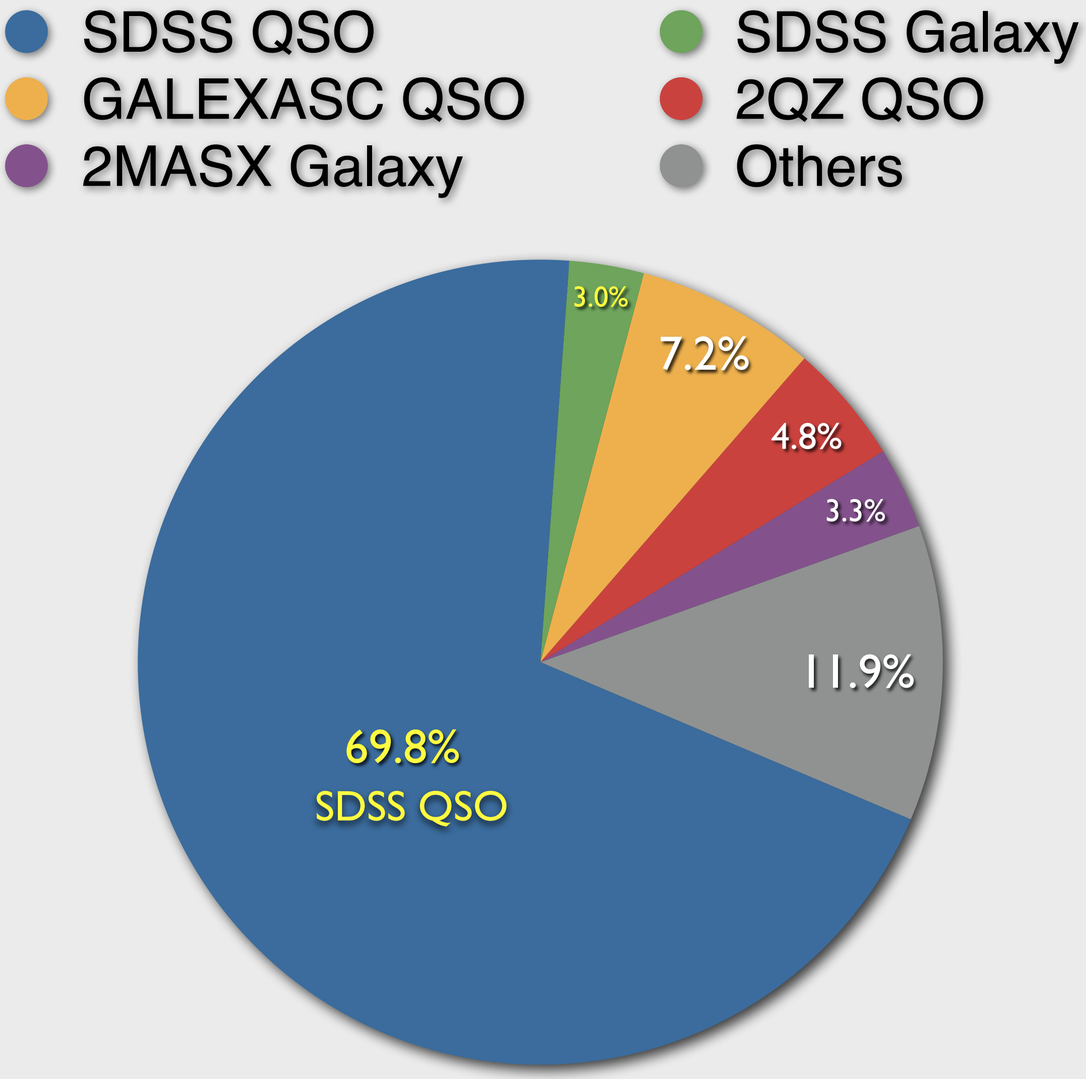
Row No.	Object Name	Object Type	Redshift	Row No.
1	FBQS J0000-0202	QSO	1.356000	1
2	2QZ J000001.3-303627	QSO	1.143400	2
3	2QZ J000001.7-312226	QSO	1.331200	3
4	HELLAS2XMM 26900016	G	1.314000	4
5	2MASSi J0000029-350332	G	0.508000	5

~

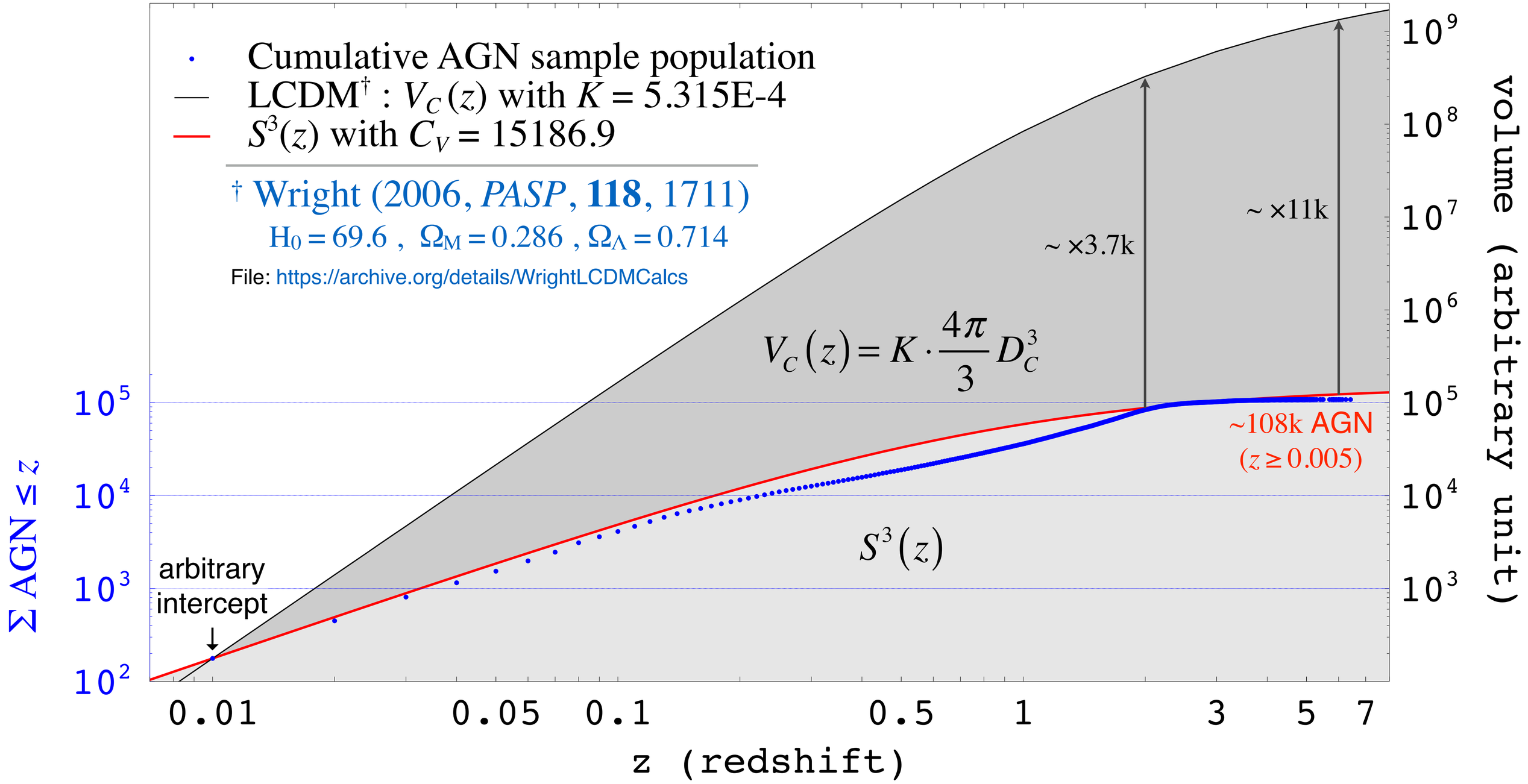
108210	2QZ J235958.3-283223	QSO	1.248000	108210
108211	SDSS J235958.66-011225.2	QSO	1.776658	108211
108212	SDSS J235958.72+003345.3	QSO	1.693204	108212
108213	SDSS J235959.06-090944.0	QSO	1.287602	108213
108214	2QZ J235959.1-302816	QSO	1.998000	108214

Objects 108201–108214 displayed. << Page 1083 of 1083 >> Go to page: go

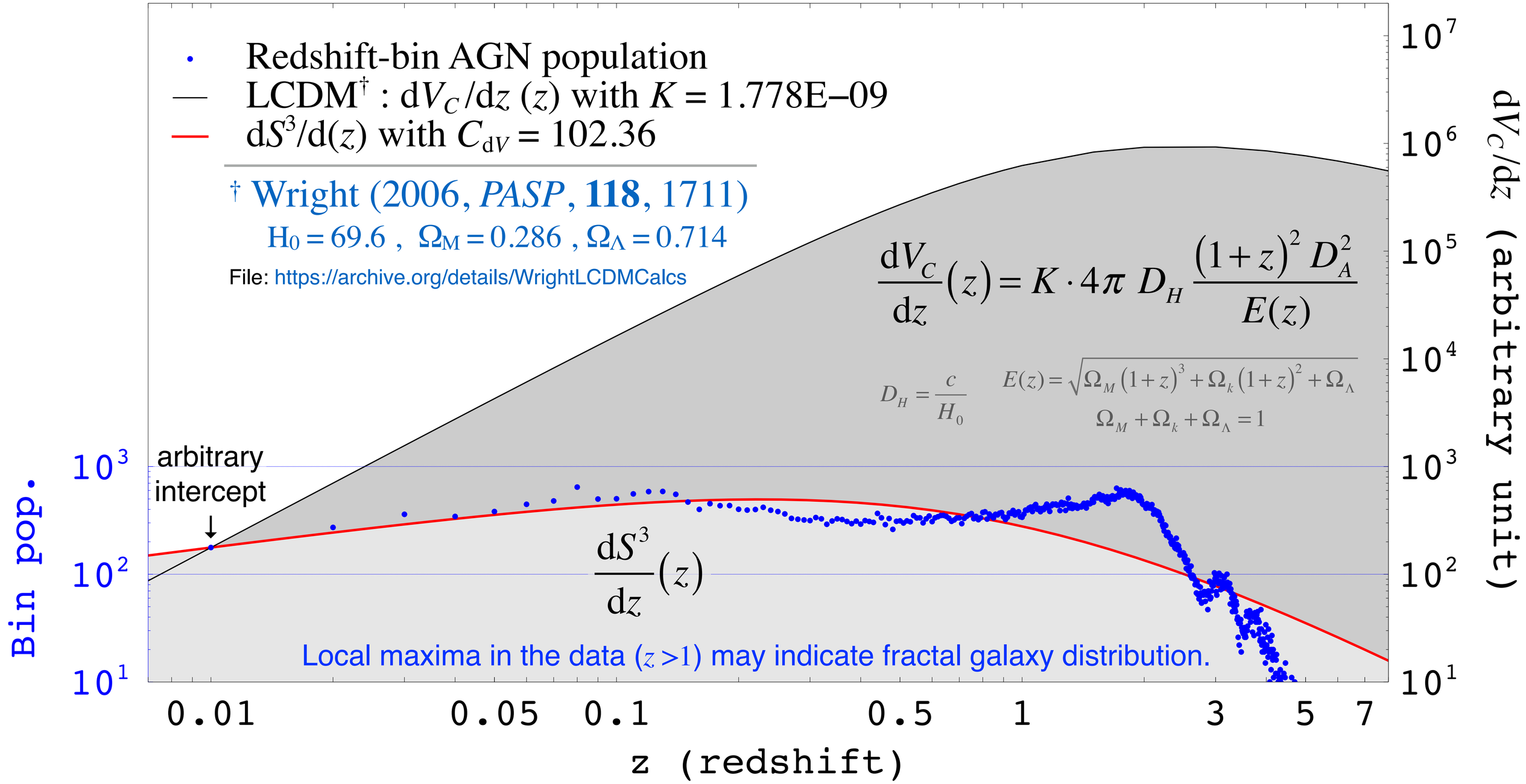
⟸108,214 AGN



Cumulative AGN population ($\sum \mathrm{AGN} \le z$) vs. volume models



AGN redshift-bin population vs. volume-element models

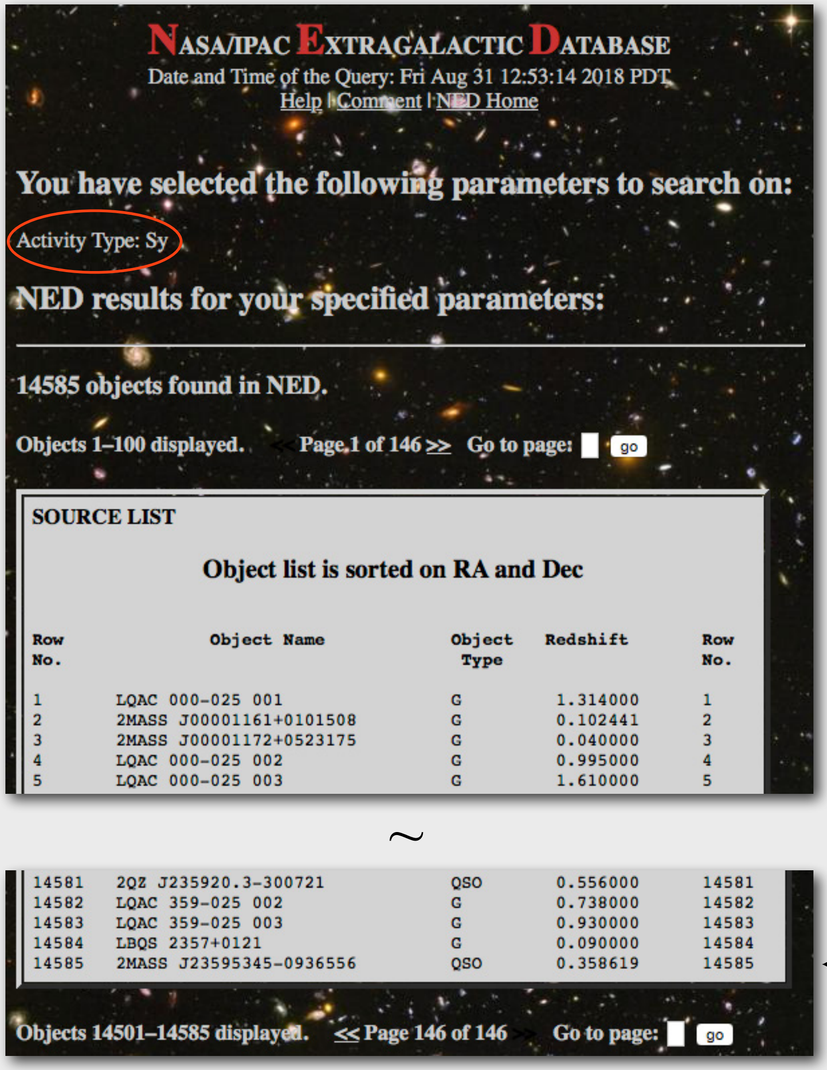


Space-density of Seyfert galaxies

Any uniquely-identifiable subset of the galaxy population that is expected to constitute some fixed percentage of the total galaxy population can be used to confront the volume function with empirical data. One such example are galaxies classified as Seyfert galaxies, which are spiral galaxies with unusually bright nuclei that produce broad emission lines. Referencing NED and using a similar procedure as that used to analyze the general AGN population, the redshift population distribution of Seyfert galaxies is graphed subsequently…

NED Seyferts

Click *image* for source data,
here for precompiled datafile.



NASA/IPAC EXTRAGALACTIC DATABASE

Date and Time of the Query: Fri Aug 31 12:53:14 2018 PDT

Help | Comment | NED Home

You have selected the following parameters to search on:

Activity Type: Sy

NED results for your specified parameters:

14585 objects found in NED.

Objects 1–100 displayed. << Page 1 of 146 >> Go to page: go

SOURCE LIST

Object list is sorted on RA and Dec

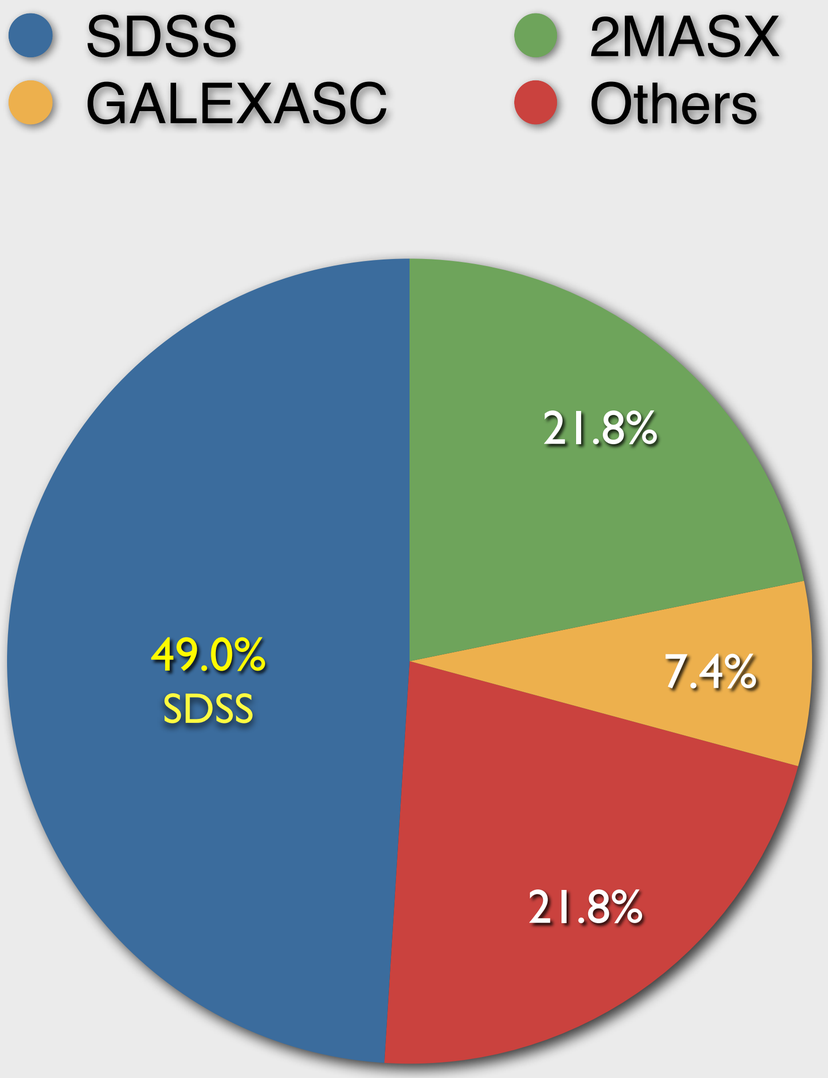
Row No.	Object Name	Object Type	Redshift	Row No.
1	LQAC 000-025 001	G	1.314000	1
2	2MASS J00001161+0101508	G	0.102441	2
3	2MASS J00001172+0523175	G	0.040000	3
4	LQAC 000-025 002	G	0.995000	4
5	LQAC 000-025 003	G	1.610000	5

~

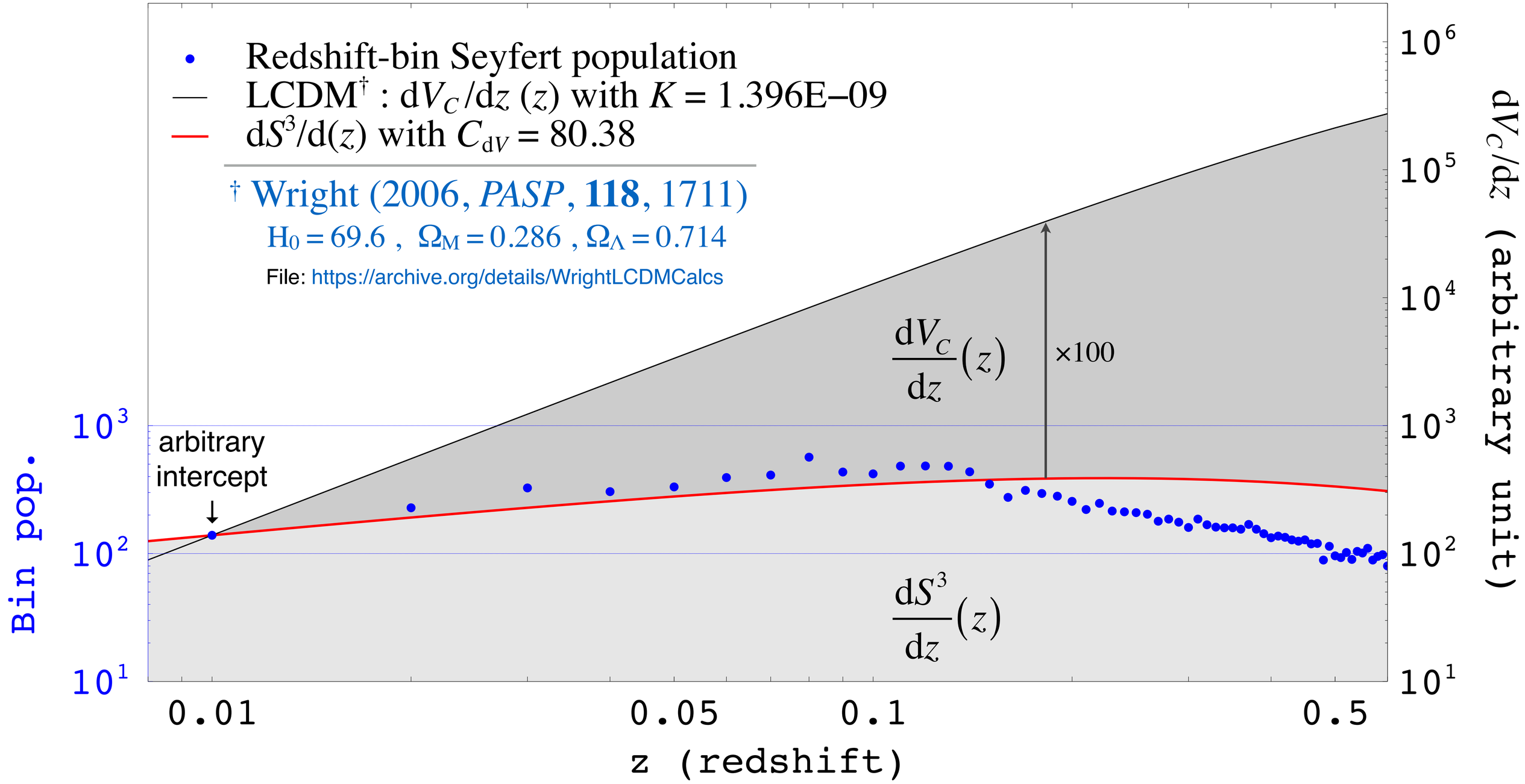
14581	2QZ J235920.3-300721	QSO	0.556000	14581
14582	LQAC 359-025 002	G	0.738000	14582
14583	LQAC 359-025 003	G	0.930000	14583
14584	LBQS 2357+0121	G	0.090000	14584
14585	2MASS J23595345-0936556	QSO	0.358619	14585

Objects 14501–14585 displayed. << Page 146 of 146 >> Go to page: go

⟸14,585 Seyferts



Seyfert redshift-bin population vs. volume-element models



PART VI – CREDITS AND AFTERWORD

Note: Addenda 1–2 (Parts VII & VIII) follow.

Click to go back to Table of Contents…

SDSS-I/II Acknowledgment (Legacy data)

Funding for the SDSS and SDSS-II has been provided by the Alfred P. Sloan Foundation, the Participating Institutions, the National Science Foundation, the U.S. Department of Energy, the National Aeronautics and Space Administration, the Japanese Monbukagakusho, the Max Planck Society, and the Higher Education Funding Council for England. The SDSS Web Site is www.sdss.org.

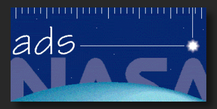
The SDSS is managed by the Astrophysical Research Consortium for the Participating Institutions. The Participating Institutions are the American Museum of Natural History, Astrophysical Institute Potsdam, University of Basel, University of Cambridge, Case Western Reserve University, University of Chicago, Drexel University, Fermilab, the Institute for Advanced Study, the Japan Participation Group, Johns Hopkins University, the Joint Institute for Nuclear Astrophysics, the Kavli Institute for Particle Astrophysics and Cosmology, the Korean Scientist Group, the Chinese Academy of Sciences (LAMOST), Los Alamos National Laboratory, the Max-Planck-Institute for Astronomy (MPIA), the Max-Planck-Institute for Astrophysics (MPA), New Mexico State University, Ohio State University, University of Pittsburgh, University of Portsmouth, Princeton University, the United States Naval Observatory, and the University of Washington.

SDSS-III Acknowledgment (BOSS data)

Funding for SDSS-III has been provided by the Alfred P. Sloan Foundation, the Participating Institutions, the National Science Foundation, and the U.S. Department of Energy Office of Science. The SDSS-III web site is www.sdss3.org.

SDSS-III is managed by the Astrophysical Research Consortium for the Participating Institutions of the SDSS-III Collaboration including the University of Arizona, the Brazilian Participation Group, Brookhaven National Laboratory, Carnegie Mellon University, University of Florida, the French Participation Group, the German Participation Group, Harvard University, the Instituto de Astrofisica de Canarias, the Michigan State/Notre Dame/JINA Participation Group, Johns Hopkins University, Lawrence Berkeley National Laboratory, Max Planck Institute for Astrophysics, Max Planck Institute for Extraterrestrial Physics, New Mexico State University, New York University, Ohio State University, Pennsylvania State University, University of Portsmouth, Princeton University, the Spanish Participation Group, University of Tokyo, University of Utah, Vanderbilt University, University of Virginia, University of Washington, and Yale University.

This research has made use of



NASA's Astrophysics Data System;

•



JPL HORIZONS System;

•

5



the SIMBAD database, CDS, Strasbourg, France
Reference: *A&AS* **143**, 9;

•



the VizieR catalogue access tool, CDS, Strasbourg, France
Reference: *A&AS* **143**, 23;

•



the NASA/IPAC Extragalactic Database (NED) which is operated by the Jet Propulsion Laboratory, California Institute of Technology, under contract with the National Aeronautics and Space Administration.

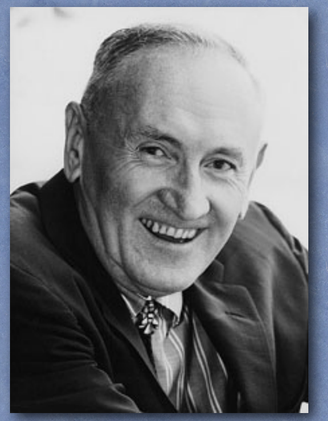
This is a reasonable scientific statement (c. 1960) based on empirical evidence:

"The age of 10^{18} years for rich compact clusters of galaxies may be shortened somewhat by considering certain interactions between galaxies that lead to more inelastic and resonant encounters between galaxies. Unless, however, far greater efficiency for the transfer of energy and momentum is postulated for such interactions than is compatible with our present-day knowledge of physical phenomena, the age of rich spherically symmetrical and compact clusters of galaxies is clearly greater than 10^{15} years."[1]

– Fritz Zwicky, *Preeminent 20th-century astrophysicist* (1898 – 1974)

"If ever a competition were held for the most unrecognized genius of twentieth century astronomy, the winner surely would be Fritz Zwicky."

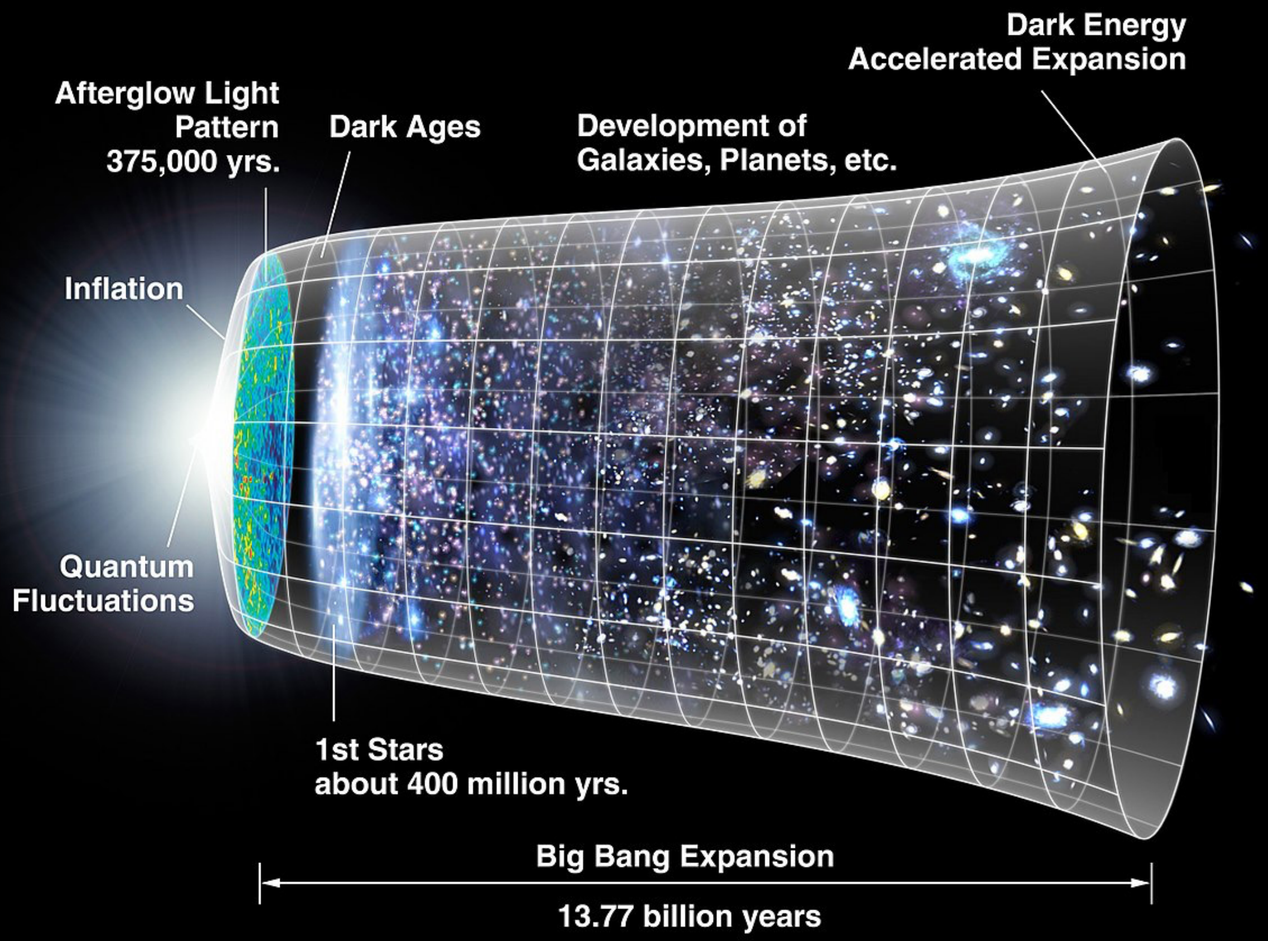
– Steven Soter & Neil deGrasse Tyson,
Cosmic Horizons: Astronomy at the Cutting Edge. New York: The New Press, 2000.

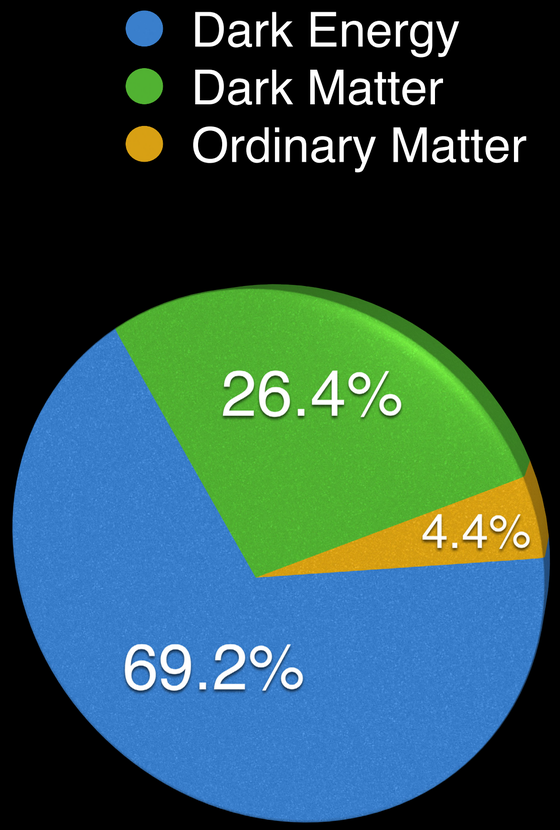


Fritz Zwicky

1. F. Zwicky, "The Age of Large Globular Clusters of Galaxies," *Pub. Astron. Soc. Pacif.* **72** (428), 365 (1960).

A DEFINITIVELY-FALSIFIED MODEL





Plank Collaboration, *Plank* 2015 Results. XIII. Cosmological Parameters; arXiv:1502.01589 [astro-ph.CO]

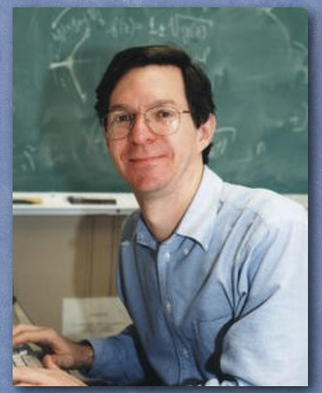
This isn't just *wrong*—it's "*spherically wrong*."

(i.e., the same from every perspective, as per Fritz Zwicky)

The greater meaning of this document beyond its scientific content

I want to argue that clear thinking, combined with a respect for evidence — especially inconvenient and unwanted evidence, evidence that challenges our preconceptions — are of the utmost importance to the survival of the human race* in the twenty-first century, and especially so in any polity that professes to be a democracy.

– Alan Sokal,
Professor of physics at New York University
Professor of mathematics at University College London



Alan Sokal

* One must concede that there is such a thing as “dangerously stupid.”

Source: A. Sokal, “What is science and why should we care? — Part I,” *Scientia Salon* (26 March 2014).



Tycho Brahe*
(1546–1601)

James Edward Gunn,

"Father" of the SDSS

"In 1987 Gunn proposed putting an array of CCDs on a 2.5m-telescope and using it for both images and spectra, scanning the entire visible sky in about five years and building an enormous data archive which could be used for far more than his main interest, determining the three-dimensional structure of the universe of galaxies. This ultimately became the Sloan Digital Sky Survey, and Gunn devoted a large portion of his career to building it and making it work."

Source: http://www.phys-astro.sonoma.edu/brucemedalists/Gunn/index.html

The perfect candidate for the NOBEL PRIZE IN PHYSICS for *real* contributions to science.

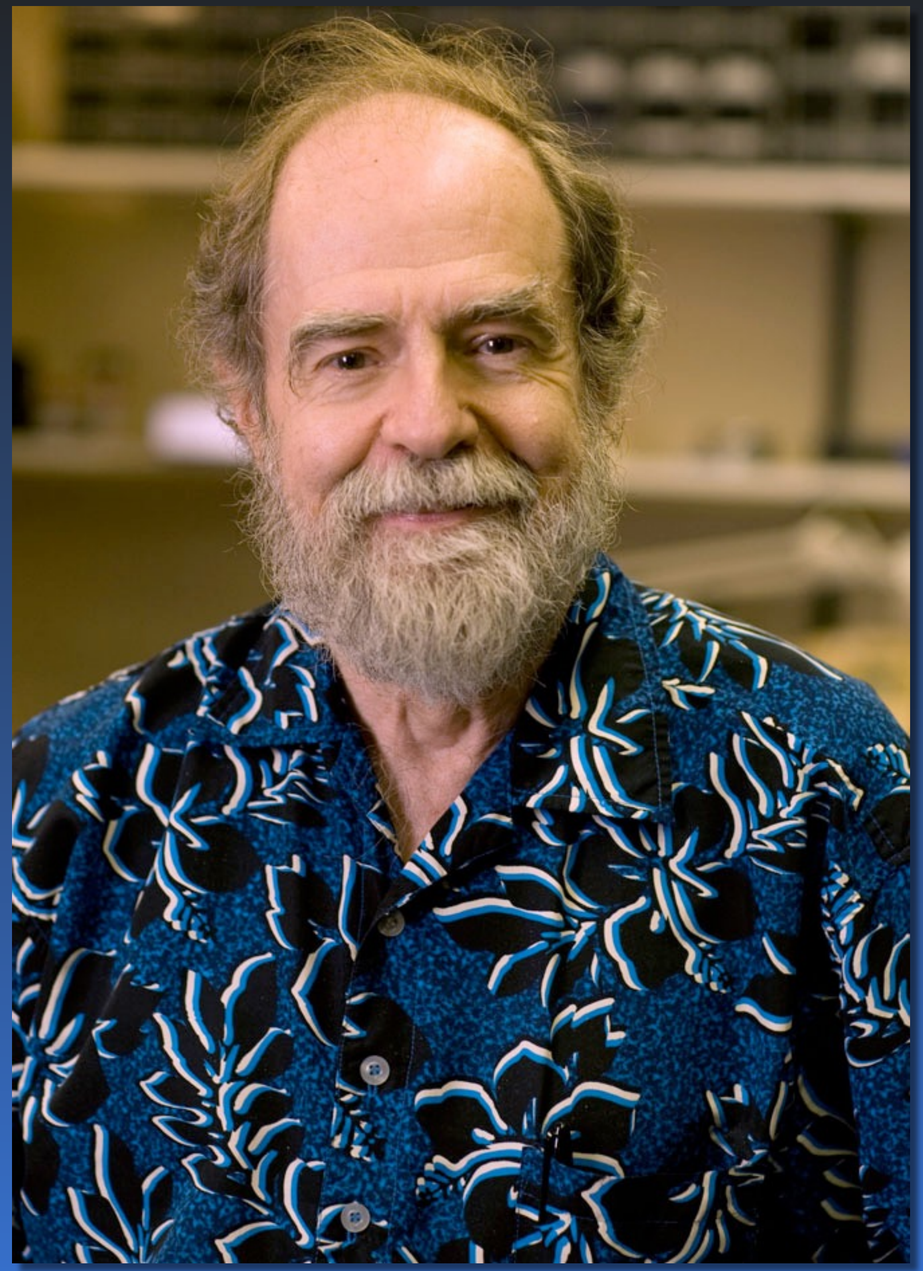


Photo 2009 by Brian Wilson • brianwilsonphotographer.com •

J. E. GUNN ET AL., "THE 2.5 m TELESCOPE OF THE SLOAN DIGITAL SKY SURVEY," THE ASTRONOMICAL JOURNAL, 131:2332–2359, 2006 April

2

* Tycho Brahe's accurate astronomical data allowed Johannes Kepler to discover that the planets moved in elliptical orbits, which led to Isaac Newton's universal law of gravitation. James Gunn's work proves to be of a similar nature.

Impromptu, hand-held, amateur video footage taken during the talk and Q&A:



https://youtu.be/KlQmVdgMv14

I should not have used the phrase, “catastrophic failure of the model” during my talk, as this may be interpreted as a subjective opinion, and it could engender strong negative emotions in certain individuals. People should come to that conclusion on their own from the evidence.

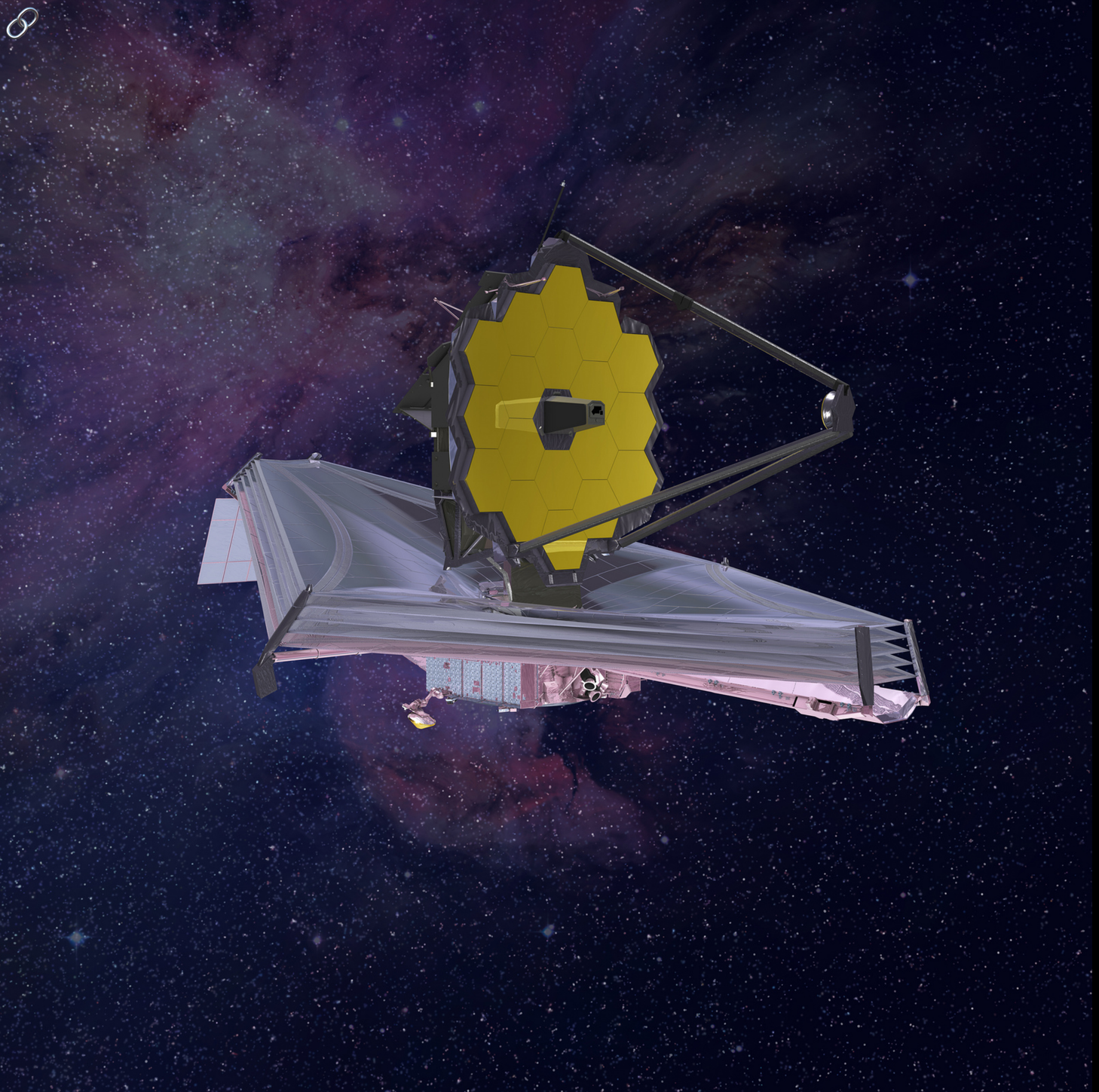
I thank Dr. César Augusto Zen Vasconcellos for the opportunity to present this research at IWARA 2018.

I thank the entire SDSS Team over many years (from DR4 in 2005 to present). I am privileged to have had the opportunity to benefit from their life's work and they share directly in the achievement of scientific discovery that arises from it.

In addition, I thank the engineers, computer scientists, executive management and support staff of Apple Computer, Wolfram (Mathematica), Google, Wikimedia, Adobe, Microsoft (SQL Server), Oracle (MySQL), and PremiumSoft (Navicat) for providing the tools and services that performed essential roles in this research.

Although prior *analysis* of CMBR and supernovae data, of which I am aptly critical, may have been flawed, it is clear that the related projects have contributed in no small measure to this research. I thank the teams of engineers, technicians, and astronomers, in particular the legion of NASA/JPL staff and NASA contractors, who made those challenging observational enterprises possible.

This research is not the work of one person; it is the success of many thousands.



James Webb Space Telescope

Earliest Launch: March 2021

- 6.5-m 18-segment primary mirror
- Near Infrared Camera (NIRCam)
 $0.6 \leq \lambda \leq 5$ microns
- Near Infrared Spectrograph (NIRSpec)
 $0.6 \leq \lambda \leq 5$ microns
- Mid-Infrared Instrument (MIRI)
 $5 \leq \lambda \leq 28$ microns
- Fine Guidance Sensor/Near Infrared Imager and Slitless Spectrograph (FGS/NIRISS)
 $0.8 \leq \lambda \leq 5$ microns

There is no such thing as the “early Universe”; JWST will see that cosmological creation is an eternal process and that the Universe is similar yet different everywhere, as is true for Earth.

PART VII – ADDENDUM 1: RELATED COSMOLOGICAL ISSUES

Click to go back to Table of Contents…

Three cornerstones of the Big-Bang theory and ‘dark matter’

Four important issues require resolution in the context of a ‘de Sitter’ Universe in a state of eternal dynamic equilibrium, having a static volume ($\dot{R} = 0$):

1. Given the mutual gravitational attraction of the total cosmic matter content over an arbitrary amount of time, what prevents general gravitational collapse?
2. Given that a primordial hot, dense state of the Universe is a false inference based on the fallacious idea of an expanding universe, then ‘Big Bang nucleosynthesis’ of the light-element nucleotides (^{1}H, ^{2}H, ^{4}He, ^{3}He, ^{7}Li, ^{7}Be) is certainly another fallacy. As deuterium (^{2}H) is destroyed in the interiors of stars faster than it is produced, its observed cosmic abundance (i.e., its source) requires explanation.
3. Given that galaxy redshifts are accurately modeled by relativistic time dilation induced by uniform, isotropic cosmic spacetime curvature, their prior canonical interpretation as universal expansion is falsified; thus, no primordial compressed, hot, dense state of the Universe approximately 14 Gyr ago can be presumed. Accordingly, a *ubiquitous and continuous energy conversion process* is required to explain the observed cosmic microwave background.
4. What is the nature of purported ‘dark matter’?

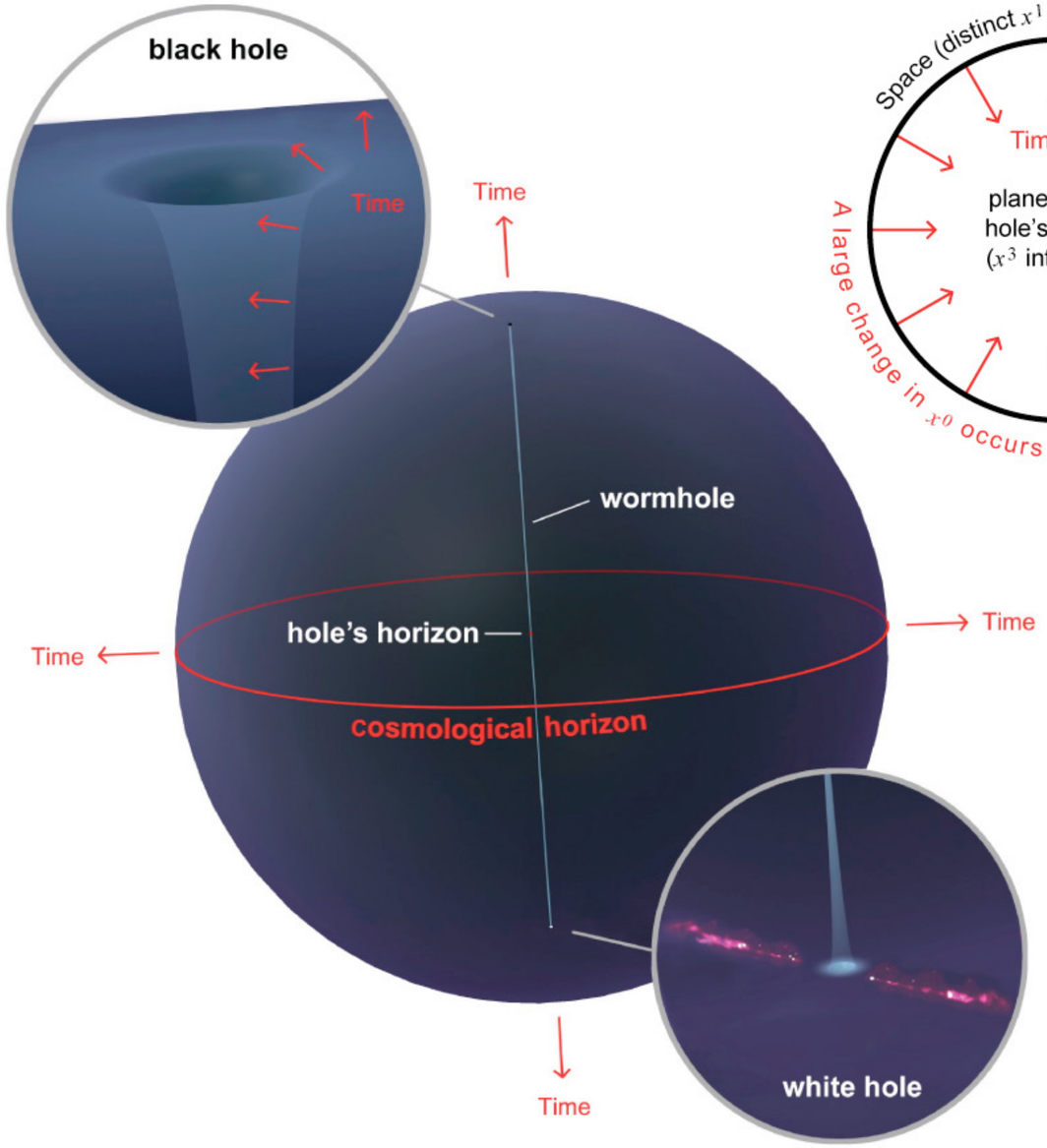
Dynamical cosmic mass-energy redistribution

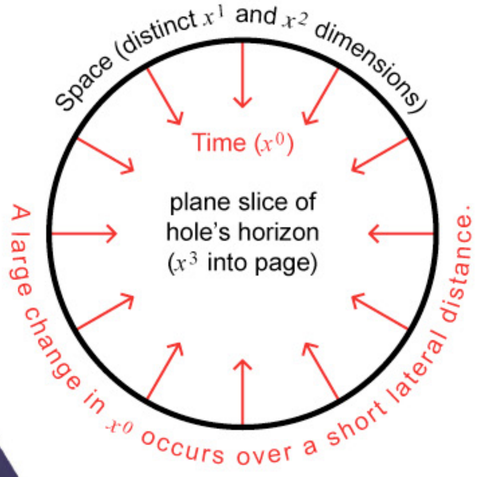
1. Given the mutual gravitational attraction of the total cosmic matter content over an arbitrary amount of time, what prevents general gravitational collapse?

The *geometric* model of relativistic time applicable to the cosmological Riemannian 3-sphere ($\mathbb{S}^3$) is *similarly* applicable in the case of spacetime geometry encountered in the strong-field limit (i.e., a black hole). It is apparent that the present canonical conceptualization of such phenomenon as a compact spatially-localized *object* having a 'singularity' at coordinate $r = 0$ is unphysical. Such a "hole" *necessarily* connects two antipodal regions of cosmological spacetime having relativistically-reversed time coordinates. It is a quasi-stable configuration of spacetime-geometry, which *cosmological structure* is sustained by dynamic mass-energy *flow* through that structure. Every locally-mass-energy-*absorbing* black hole has a corresponding *cosmologically-antipodal* locally-mass-energy-*emitting* "white hole." Such white holes are empirically observed as regions of mass-energy emission far exceeding that which is possible through thermonuclear fusion. While mass-energy conservation holds cosmologically, it does not hold locally in the vicinity of such holes, which transport mass-energy between cosmological antipodes…

© A. F. Mayer

The reciprocal cosmological and energetic relationships between the terminals of a wormhole.





Graphic by Hollin Calloway (2005).

A. Bridle, D. Hough, C. Lonsdale, J. Burns, & R. Laing, "Radio Quasar 3C175"
VLA 4.9 GHz image at 0.35″ resolution

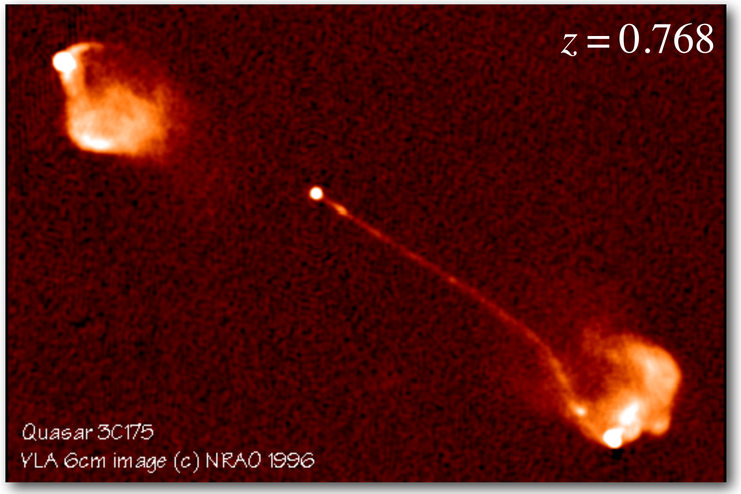


Image courtesy of *NRAO/AUI/NSF*

Wormholes

It proves to be the case that the foundations of general relativity are inconsistent with the Newtonian conception of a gravitational '*equipotential* surface,' which surface is simply defined by a finite coordinate radius about an idealized point source: Having a strictly-locally-defined *geometric* definition according to these foundations, each among the set of distinct local proper time coordinates τ_p, associated with the neighborhood of each point p on such surface, excepting antipodal points, cannot have the identical geometric definition (i.e., they are not parallel in R^4). This distinction correlates to a symmetric time dilation between the τ_p with associated measurable (already measured yet unrecognized) empirical phenomena in the weak field.*

This empirically-verifiable incremental improvement to canonical general relativity radically alters the interpretation of the strong-field limit and eliminates the dubious notion that a physical 'spacetime singularity,' where the known laws of physics break down, exists at coordinate $r = 0$. Rather, as has been long suspected, in particular by the pure mathematics community, spacetime must be smooth and continuous everywhere; catastrophic gravitational collapse leads to the creation of a physically-real so-called "wormhole" connecting distinct regions of spacetime as illustrated in the preceding slide.

* Details to be discussed in a pending series of journal letters by A. F. Mayer.

Cosmic jets

2. Where do observable conditions exist for the production of deuterium (^{2}H)?

A very high-temperature plasma ($\sim 10^9$ K or ~ 0.1 Mev) of free protons and neutrons that cools rapidly is understood to be a process that leads to the nucleosynthesis of the light elements. The necessary high temperatures for the required reaction sequences to take place are not found in stars and deuterium production requires an environment of high energy coupled with low density. The observed existence of the light elements cannot be due to normal processes in stellar evolution, particularly because typical stellar evolution involves destruction of deuterium.

Observed jets, as exemplified in the foregoing image of Radio Quasar 3C175, constitute an ideal environment for nucleosynthesis of the light elements. It is understood that such jets emanate from "white holes," which may be characterized as cosmological-scale particle accelerators. Such jets are the likely progenitors of new (i.e., spiral) galaxies, so one would expect to find an unlikely abundance of ^{2}H at the core of spiral galaxies (e.g., the Milky Way). This is exactly the case, although its presence was attributed to an ad hoc phenomenon.[1]

1. D. A. Lubowich et al., "Deuterium in the Galactic Centre as a result of recent infall of low-metalicity gas," *Nature* **405**, 1025 (2000).

3. What is the source of the cosmic microwave background (CMB)?

As it is now conclusively determined that the Universe is not expanding, it is certain that the CMB does not have a 'primordial origin.' Accordingly, one must identify some continuous and contemporary source for these photons. Controversy about the origins of the CMB is not new.[1] It should now be clear that published analyses of data strongly confirming the Big-Bang theory were fabricated; however, atypical analyses of the *same data* that has been largely ignored to date has yielded important insights:

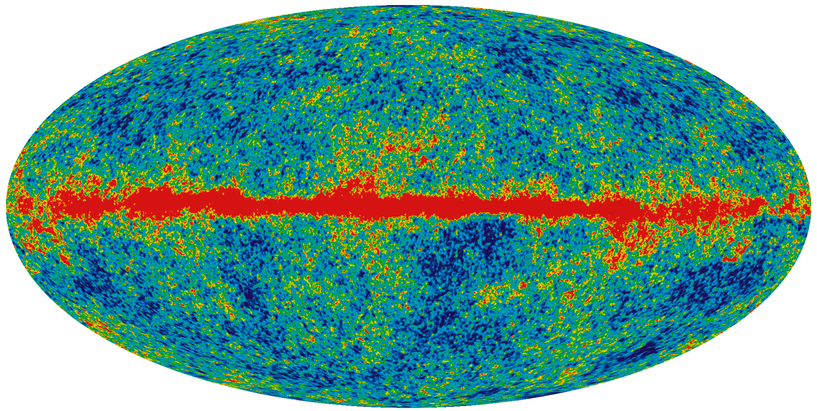
> The cosmic microwave background is often called the echo of the Big Bang, but recent research suggests that some of its features might have their origins much closer to home. Although most cosmologists think that the tiny variations in the temperature of the background are related to quantum fluctuations in the early universe, Glenn Starkman and colleagues at CERN and Case Western Reserve University in the US have now found evidence that some of these variations might have their roots in processes occurring in the solar system. If correct, the new work would require major revisions to the standard model of cosmology. … "Each of these correlations could just be an accident," says Starkman. "But we are piling up accident on accident. Maybe it is not an accident and, in fact, there is some new physics going on." [2]

1. H.-J. Fahr and M. Sokaliwska, "Remaining Problems in Interpretation of the Cosmic Microwave Background," *Phys. Res. Int.* **2015**, 503106.

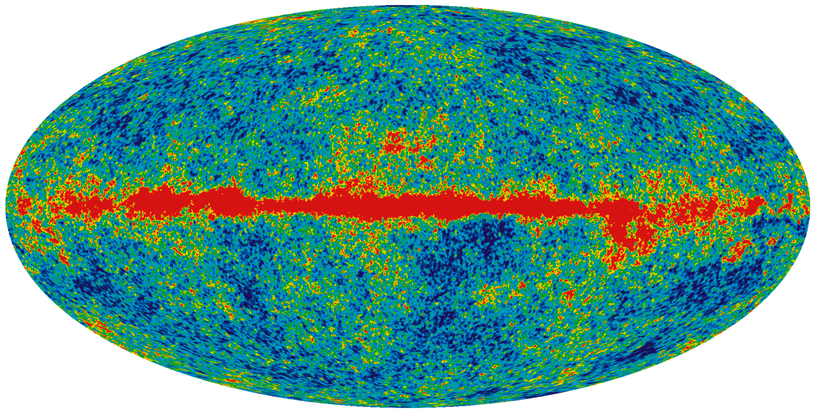
2. E. Cartlidge, "Doubts cast over map of the cosmos," *Physics World* **18(1)**, 5 (2005).

WMAP full-sky temperature maps (linear scale from −200 to +200 μK) — WMAP Science Team

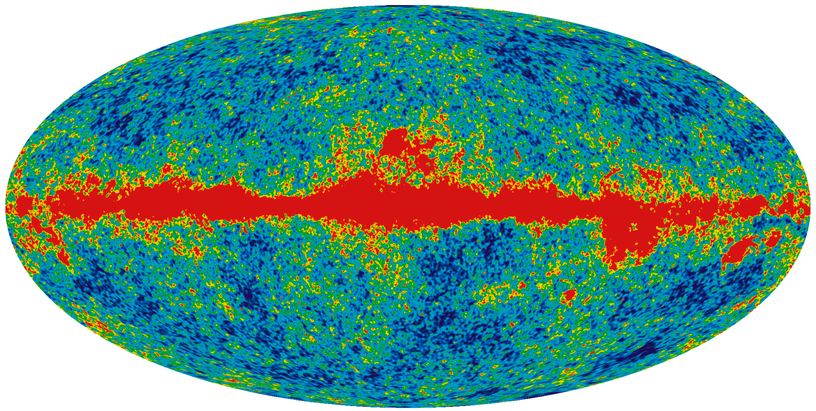
(1) W-Band Map (94 GHz)



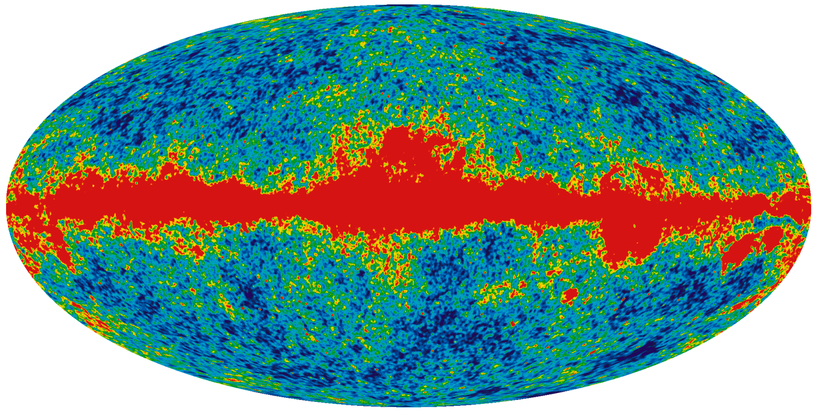
(2) V-Band Map (61 GHz)



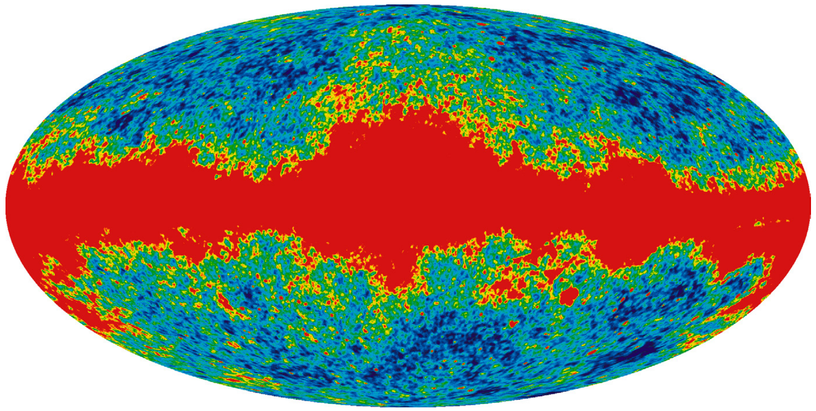
(3) Q-Band Map (41 GHz)



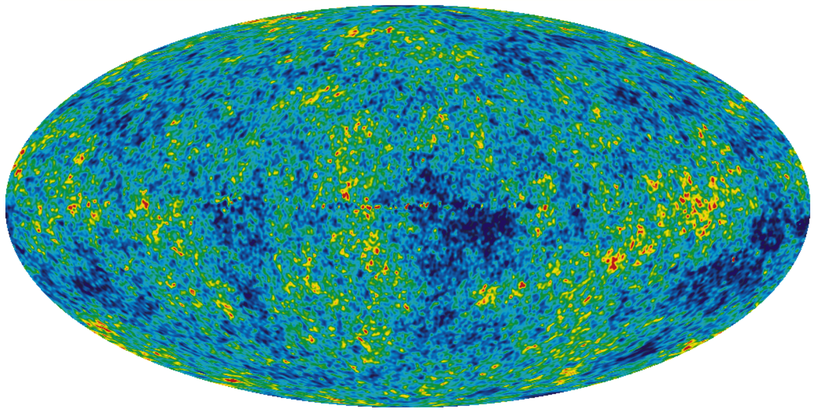
(4) Ka-Band Map (33 GHz)



(5) K-Band Map (23 GHz)



Internal Linear Combination Map



"The Internal Linear Combination Map is a weighted linear combination of the five WMAP frequency maps. The weights are computed using criteria which minimize the Galactic foreground contribution to the sky signal. The resultant map provides a low-contamination image of the CMB anisotropy." – NASA LAMBDA

Some claimed interpretations of WMAP data (source verbatim)

The WMAP science team has…

3. …determined the universe to be 13.77 billion years old to within a half percent.
4. …nailed down the curvature of space to within 0.4% of "flat" Euclidean.
5. …determined that ordinary atoms (also called baryons) make up only 4.6% of the universe.
6. …completed a census of the universe and finds that dark matter (matter not made up of atoms) is 24.0%
7. …determined that dark energy, in the form of a cosmological constant, makes up 71.4% of the universe, causing the expansion rate of the universe to speed up. - "Lingering doubts about the existence of dark energy and the composition of the universe dissolved when the WMAP satellite took the most detailed picture ever of the cosmic microwave background (CMB)." - Science Magazine 2003, "Breakthrough of the Year" article

Source: https://map.gsfc.nasa.gov

An important paper with a prophetic title that challenged these interpretations:

U. Sawangwit & T. Shanks, “Is everything we know about the universe wrong?” *Astronomy & Geophysics* **51**, 5.14 (2010).

“Excess microwave emission”

We now know that there is no such thing as a ‘primordial Big-Bang photon,’ so it is evident that the much-touted analyses of COBE-, WMAP-, and Plank-satellite data, purporting to ‘prove’ various aspects of the Big-Bang theory were fabrications, not unlike the systemic fabrication of data uncovered during the 2008 ‘financial crisis.’ The problem in physics is one of “group-think,” arguably driven by the agendas of a few key ‘authorities,’ who have received high accolades.

From the following quotation, it is clear that the galactic foreground emission was actually never understood, thus requiring unrestrained ad hoc speculation. Then the process of sanitizing the “contaminated” (subjectively bad) empirical data to produce ‘science data’ (subjectively good) involved *arbitrarily* removing theoretically-problematic objective empirical data.

> The cause of observed inner galaxy excess microwave emission is assumed to be synchrotron emission from highly relativistic electron-positron pairs produced by [ad hoc] dark matter particle annihilation as more conventional sources have been ruled out.[1, 2]

1. D. P. Finkbeiner, “WMAP Microwave Emission Interpreted as Dark Matter Annihilation in the Inner Galaxy,” (2 Sep. 2004); arXiv:astro-ph/0409027. → *Phys. Rev. D* **76**, 083012 (2007)
2. D. P. Finkbeiner, “Microwave Interstellar Medium Emission Observed by the Wilkinson Microwave Anisotropy Probe,” *Astrophys J.* **614**, 186–193 (2004).

Vitally-important conventionally-disregarded empirical evidence from WMAP data

Also, in 2003 Hans Kristian Eriksen of the University of Oslo and his co-workers presented more results that hinted at alignments. They divided the sky into all possible pairs of hemispheres and looked at the relative intensity of the fluctuations on the opposite halves of the sky. What they found contradicted the standard inflationary cosmology—the hemispheres often had very different amounts of power. But what was most surprising was that the pair of hemispheres that were the most different were the ones lying above and below the Ecliptic, the plane of the earth's orbit around the sun. This result was the first sign that the CMB fluctuations, which were supposed to be cosmological in origin, with some contamination by emission in our own galaxy, have a solar system signal in them—that is, a type of observational artifact.[1]

— astrophysicists have found that the plane of the solar system threads itself through hot and cold spots in the cosmic microwave background, suggesting that some of the variations in the latter are not caused by events that took place in the early universe.[2]

1. G. D. Starkman and D. J. Schwarz, "Is the Universe Out of Tune?" *SciAm* (Aug. 2005), p. 52.
2. E. Cartlidge, "Doubts cast over map of the cosmos," *Physics World* **18(1)**, 5 (2005).

The large-angle (low-ℓ) correlations of the cosmic microwave background exhibit several statistically significant anomalies compared to the standard inflationary cosmology.

…

We have shown that the planes defined by the octopole are nearly aligned with the plane of the Doppler-subtracted quadrupole, that three of these planes are orthogonal to the ecliptic plane, with normals aligned with the dipole (or the equinoxes), while the fourth plane is perpendicular to the supergalactic plane. Each of these correlations is unlikely at 99% C.L., and at least two of them are statistically independent. We have also seen that the ecliptic threads between a hot and a cold spot of the combined Doppler-subtracted-quadrupole and octopole maps—following a node line across about 1/3 of the sky, and separating the three strong extrema from the three weak extrema of the map.

We find it hard to believe that these correlations are just statistical fluctuations around standard inflationary cosmology's prediction of statistically isotropic Gaussian random $a_{\ell m}$'s. That the quadrupole-octopole correlation just happened to increase by ~5 when the quadrupole was Doppler-corrected seems particularly unlikely. The correlation of the normals with the ecliptic poles suggest an unknown source or sink of CMB radiation or an unrecognized systematic. If it is a physical source or sink in the inner solar system it would cause an annual modulation in the time-ordered data.

…

Physical correlation of the CMB with the equinoxes is difficult to imagine, since the WMAP satellite has no knowledge of the inclination of the Earth's spin axis. (all underlined emphasis added)

D. J. Schwarz, G. D. Starkman, D. Huterer & C. J. Copi,
"Is the Low-ℓ Microwave Background Cosmic?" *Phys. Rev. Lett.* **93**, 221301 (2004); arXiv:astro-ph/0403353.

The primary cause of secular astrophysical spin-down (i.e., “rotation braking”)

The principle of “relativistic temporal geometry,” which has been shown to apply cosmologically, must similarly apply to the local gravitational field. The mathematical expression of the latter phenomenon is off-topic herein. However, to summarize it, just as a redshift occurs due to the homogeneous and isotropic curvature of cosmological space between widely-separated regions *at the same Newtonian potential*, the same principle applies over the curvature incurred in any orbit in a gravitational field, including such orbit at constant radius around an ideal point-mass. Due to a (*geometric*) distinction in proper time at each point on the orbit, by analogy, one may consider a gravitational field to have a kind of ‘resistance,’ causing subtle energy loss for orbiting bodies in the weak field that manifests in the form of electromagnetic radiation, which radiation can be thought of as a kind of ‘heat’ due to that ‘resistance.’ The stronger the field, and the greater the velocity of motion through it, the greater the energy-dissipation effect, per unit mass.

Constituent mass-elements of a rotating astrophysical body effectively ‘orbit’ in the gravitational field of the total source mass, with the highest velocity occuring at its equator. It follows that the temperature of the radiation produced by the effective ‘gravitational resistance’ incurred by that rotational motion is greatest at the equator and falls off to zero at the poles. Note that energy conservation correlated with this phenomenon requires the secular spin-down of all rotating astrophysical bodies. This *universal* ‘gravitational-resistance’ spin-down is particularly noticeable for pulsars, in which case that effect is conventionally attributed to magnetic dipole radiation.

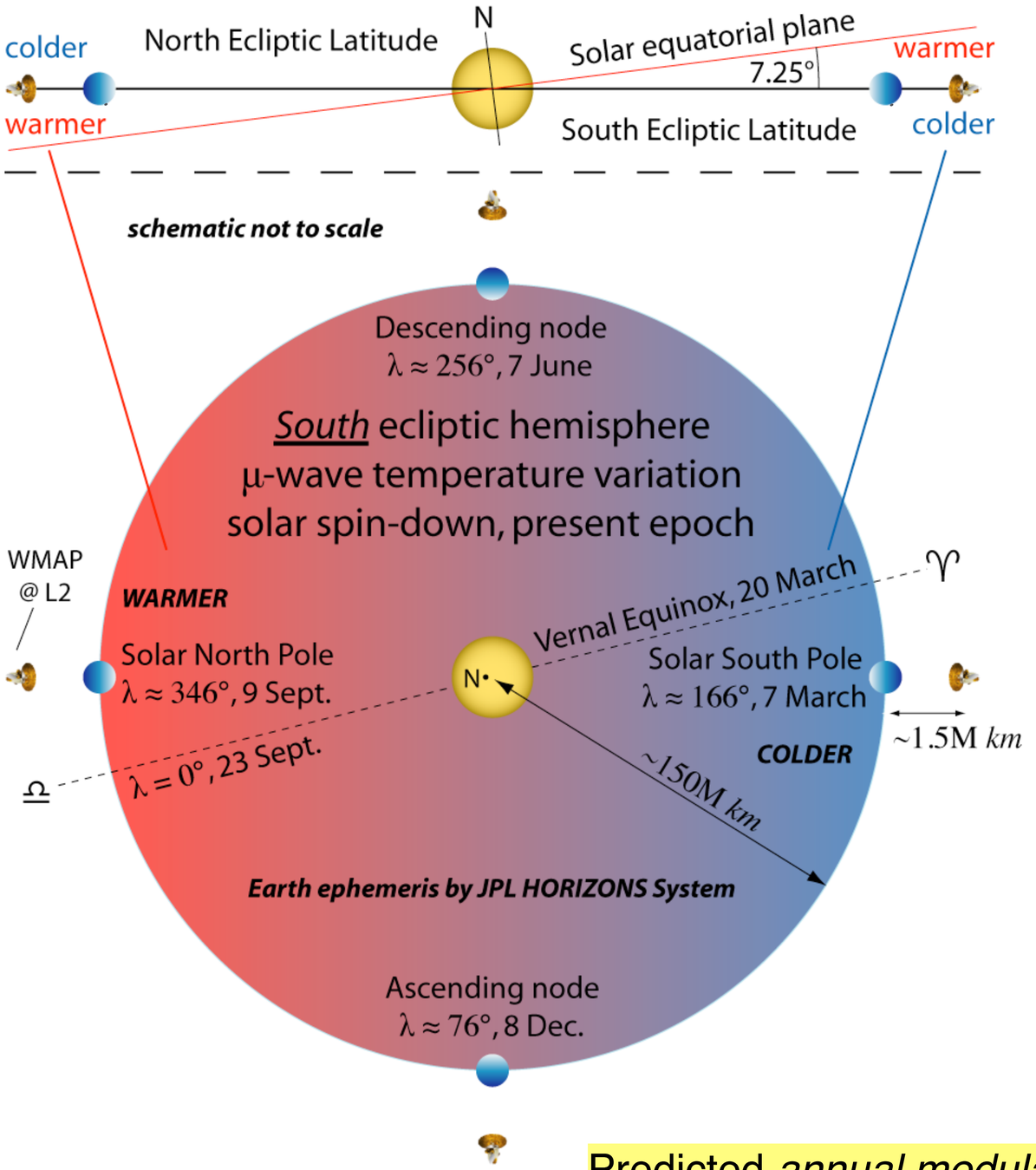
Predicted observable phenomena

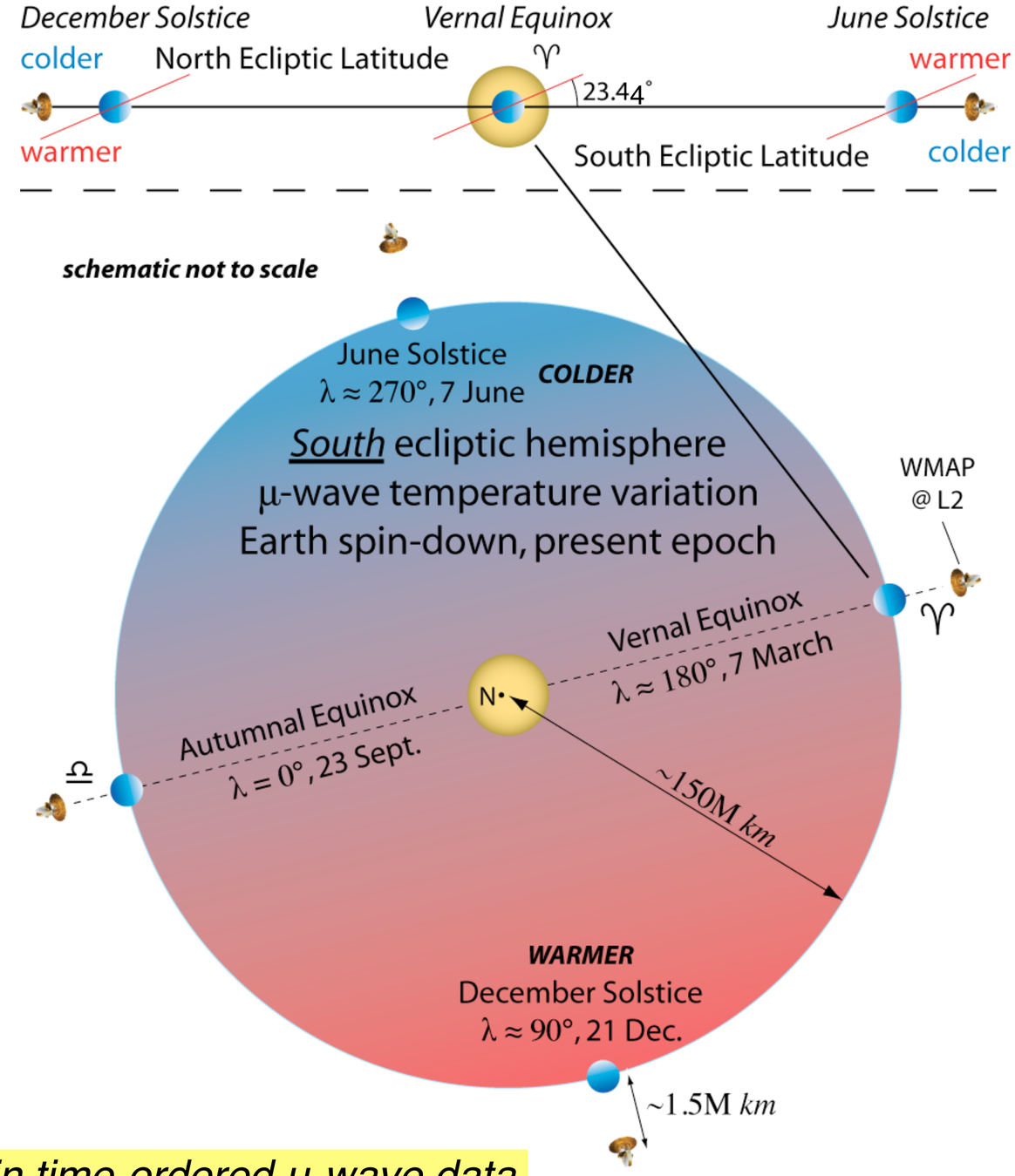
The foregoing assertion concerning the fundamental instability of gravitational systems and the associated radiative phenomenon is subject to empirical verification: The Sun represents 99.86% of Solar System mass, it has an equatorial sidereal rotation period of about 600 hours (longer at higher latitude), and its equatorial plane is inclined 7.25 degrees to the Ecliptic. Due to that obliquity, the South Pole Telescope points toward the solar equatorial plane for six months per year, and then away from it. One may expect to see a correlated annual modulation in microwave temperature in that data (see next slide, *left* diagram).

For a satellite co-orbiting with the Earth at L2 in the Ecliptic (e.g., WMAP), the obliquity of the Earth's spin axis to the Ecliptic ($23.44°$) causes a similar observable effect correlated to the equinoxes (see next slide, *right* diagram). From astronomical records dating back several millennia, the long-term increase in the mean length-of-day has been established to be about 1.8 ms per century,[1] This secular spin-down correlates to an average continuous energy dissipation of 2.8 terawatts. The conventional explanation for terrestrial rotational braking is that Earth's rotational energy is being dissipated as "tidal friction" and also "tidal acceleration" of the Moon. The Sun, rather than Earth, is the Moon's dominant gravitational field and it's differential 'resistive' quality on the Earth-Moon system causes observed lunar acceleration.

1. F. R. Stephenson, L. V. Morrison2, & C. Y. Hohenkerk, "Measurement of the Earth's rotation: 720 BC to AD 2015," *Proc. R. Soc. A* **472**, 20160404.

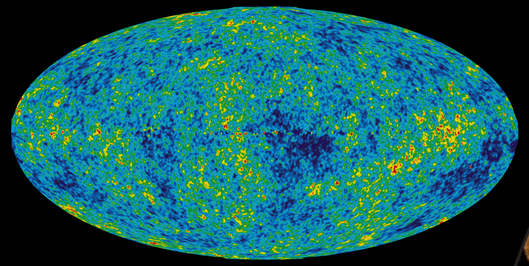
© 2007 A. F. Mayer





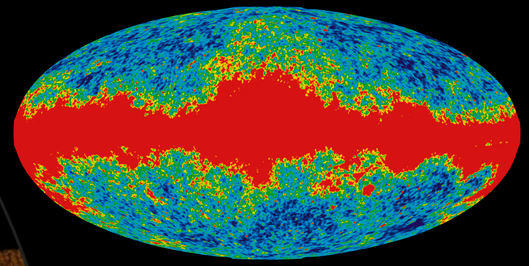
Predicted *annual modulation in time-ordered μ-wave data.*

SDSS terapixel image of the night sky.
Limited to the “Northern Galactic Cap,” this image represents just a portion of the WMAP “full-sky map,” below.



Internal Linear Combination

Every galaxy emits microwave radiation, as does our Galaxy (red foreground, below).



K-Band (23 GHz)

Every point in this image is a galaxy.

This is just ~10^6 galaxies of ~10^{11} cosmologically.

Northern Galactic Cap

Image credit: M. Blanton and the SDSS-III

Ubiquity of ‘gravitational radiation’

With $\sim 10^{11}$ stars orbiting its center, the Galaxy is an obvious source of the identical radiation correlated to the secular spin-down of the Sun and Earth, also each star’s orbital motion in the galactic gravitational field contributes to the radiation. Hence, the huge Galactic signal that had to be removed from the popularized WMAP “Internal Linear Combination Map,” including inexplicable “excess microwave emission.”

Given a total population on the order of 10^{11}–10^{12} galaxies, the Cosmos presents the observer with about 10^{4}–10^{5} galaxies per micro-steradian, that representing $\sim 10^{-7}$ of the celestial sphere. With each galaxy locally producing the same microwave radiation as observed for the Milky Way (e.g., the K-Band Map at 23 GHz), it is clear that this presents the observer with a nearly-isotropic microwave background, with slightly higher temperature for regions of higher density.

The foregoing implies that the phenomenon of “gravitational radiation” is ubiquitous, observably manifesting in the electromagnetic spectrum. Verification of the predicted annual modulation in time-ordered μ-wave data would show that the COBE, WMAP, and Plank satellites were de facto ‘gravitational wave’ detectors and that LIGO and similar instruments are useless white elephants. The purported measurement of “gravitational waves” according to their heretofore canonical theoretical description, and leading to the 2017 Nobel Prize in Physics, was at best bad science, and at worst a fraud, as has been argued by various authors (see next slide)…

Selected supporting references jeopardizing the celebrated LIGO ‘discovery’

J. Creswell, S. von Hausegger, A. D. Jackson, H. Liu, & P. Naselsky, "On the time lags of the LIGO signals," (9 Aug 2017); arXiv:1706.04191v2.

J. Creswell, S. von Hausegger, A. D. Jackson, H. Liu, & P. Naselsky, "Comments on our paper, 'On the time lags of the LIGO signals'," (27 Jun 2017).

D. Christopoulos, "My deepest disappointment for Nobel Prize Physics 2017," RG (Dec 2017).

D. Christopoulos, "A detailed critical review of reported event GW150914 that LIGO/VIRGO collaboration announced as gravitational waves and black holes observation," RG (Mar 2016).

B. R. De, "Casebook of Bibhas De—The Mystery of the Hanford Empaths," eBook (7 Jan 2018).

B. R. De, "Unchallenged privilege: The billion-dollar trilateral gravitational-wave discovery scam," 2nd Ed., Bibhas De (Aug 2017).

W. W. Engelhardt, The LIGO-VIRGO Miracle: A contemplation on the detection of gravitational waves in three different places on August 14, 2017,” RG (Oct 2017).

J. Horgan, "Is the Gravitational-Wave Claim True? And Was It Worth the Cost?," blogs.scientificamerican.com (12 Feb 2016).

Despite claims of authenticity, a telling description of how an artificial signal, indistinguishable from ‘science data,’ was a distinct possibility:
J. Kanner & A. Weinstein, "The Astrophysicists Who Faked It—The inside story of the gravitational wave signal injection," *Naultilus* (3 Nov 2016).

M. Mahin, "LIGO Doubts Will Persist Unless Replication Occurs," futureandcosmos.blogspot.com (19 Feb 2016).

X. Mei, Z. Huang, P Ulianov, & P. Yu, "LIGO Experiments Cannot Detect Gravitational Waves by Using Laser Michelson Interferometers," *J. Mod. Phys.* **7**, 1749 (2016).

S. Sims, "Problems with the LIGO gravitational wave discovery," Plasma Pics (15 Mar 2016).

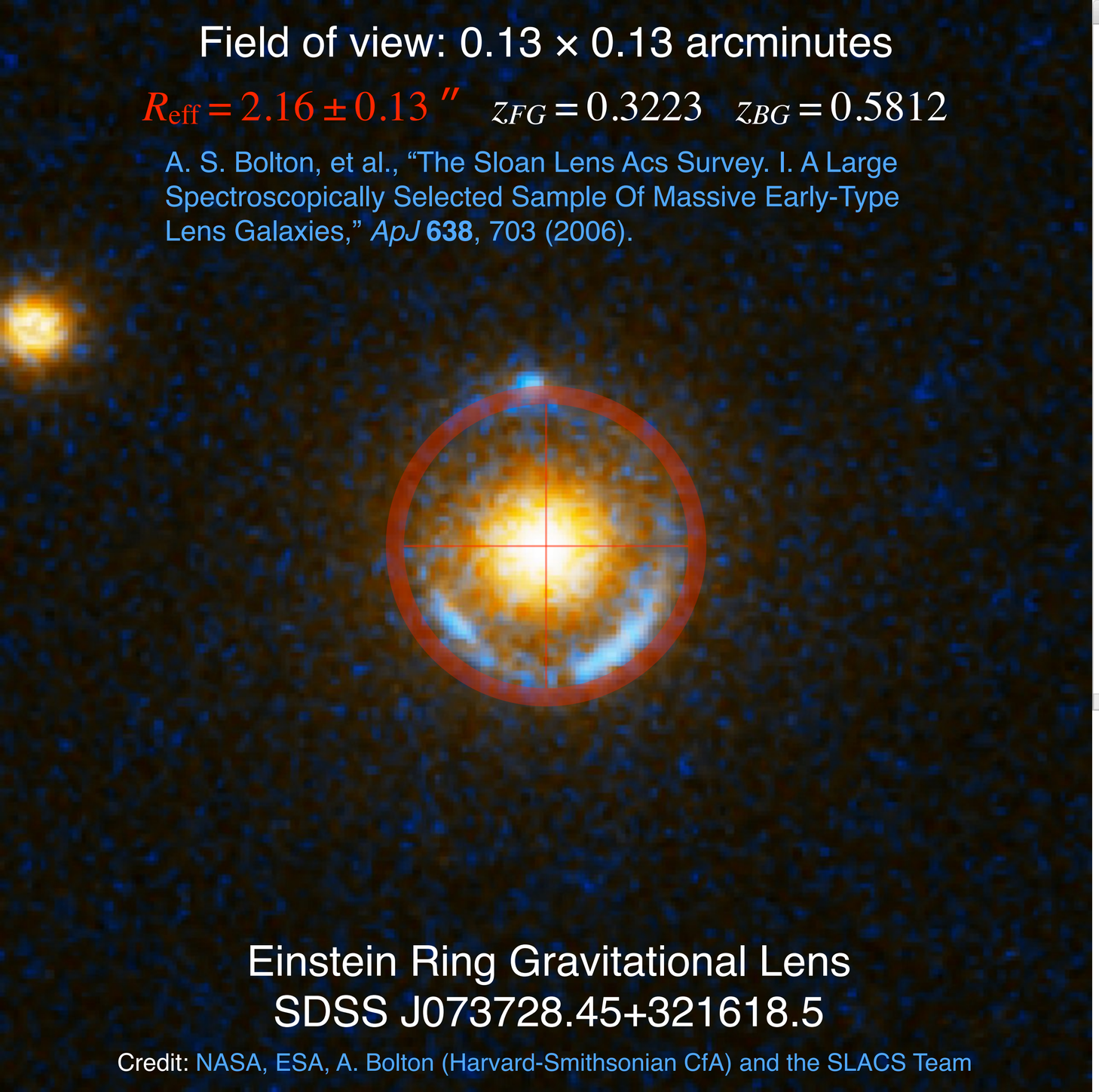
‘Empirical evidence’ can be illusory

4. What is the nature of ‘dark matter’?

Purported empirical evidence for ‘dark matter’ includes apparent excess (otherwise-undetectable) gravitational mass required to bind galaxy clusters, to produce observed gravitational lensing, and to account for spiral-galaxy rotation curves. Rather than the common perception that such rotation curves are “flat,” they actually exhibit radial acceleration (increasing orbital velocity) as per observation of the hydrogen 21-cm line (i.e., orbiting gas) extending far beyond the optical disk.

Observed radial acceleration of spiral galaxy rotation curves is readily explained in the context of the gravitational tidal forces on the disk produced by the host cluster; details are available at gravitysim.net, in particular, this 15-minute video (immediate viewing recommended). A definitive solution to the perplexing winding problem concerning spiral galaxies is also put forward.

Prior calculations based on observed gravitational lenses suffered from application of a faulty redshift-distance relationship and Cosmic geometry (Euclidean versus Riemannian), causing misinterpretation of empirical observables (next slide). In the subsequent slide, redshift distances for the Einstein ring and background galaxy, which are based the new model herein, indicate no non-luminous excess mass within the boundary of the ring.



Einstein Ring.nb

180

```
In[1]:= θE = 2.16`3 / (2 * 3600) * π / 180 ; (* radians *)

In[2]:= G = 6.67408`6*^-11; (* m^3 kg^-1 s^-2 *)

In[3]:= c = 299792458`9; (* m s^-1 *)

In[4]:= R = 4.1`2*^9 * 9.46073*^15 ; (* m *)

In[5]:= DL = R * ArcCos[1 / (0.3233 + 1)];

In[6]:= DS = R * ArcCos[1 / (0.5812 + 1)];

In[7]:= DLS = DS - DL;

In[8]:= Clear[M]

In[9]:= {M} = M /. Solve[θE == Sqrt[(4 G * M / c^2) DLS / (DL * DS)], M];

In[10]:= M = UnitConvert[Quantity[M, "Kilograms"], "SolarMass"]

Out[10]= 6.62313 × 10^11 M⊙
```

150%

The here-calculated value of $6.6{\times}10^{11}$ $M_\odot$ inside the Einstein ring is consistent with conventional matter; no mysterious, non-luminous 'dark matter' need be attributed to the mass of this galaxy or similar ones.

z	ΛCDM* (D_A)	'de Sitter'
0.3223	3.1753 Gly	2.9278 Gly
0.5812	4.4810 Gly	3.6331 Gly
D_{LS}	0.7934 Gly	0.7053 Gly

*

$H_0 = 69.6$

$\Omega_M = 0.286$

$\Omega_\Lambda = 0.714$

Explanation of following Mathematica notebook and correlated graph

The Coma cluster contains $\sim 1\text{k}$ galaxies observed within apparent diameter $\sim 100'$. For $R = 4.1$ Gly, 1^{rad} corresponds to ~ 872 Mly at the reference redshift for Coma ($z_{\text{ref}} = 0.0234$); so the Coma radius ($50'$) correlates to $r_C = 12.7$ Mly. Relative to z_{ref}, this radius gives near/far boundaries in redshift space for the Coma cluster of $z \approx 0.0227/0.0241$. Accordingly, the highlighted red box represents a ~ 25 Mly-diameter ball roughly centered on NGC 4874.

A*ssuming* that most of the galaxies in the graph are "clustered" inside that ball, then one must interpret most of their redshifts as radial velocities $\sim c(z_n - z_{\text{ref}})$, shown by the scale on the right. If one furthermore assumes that such unlikely configuration is dynamically stable, one must then invent invisible gravitating matter having no electromagnetic signature whatsoever, and having a mass within the ball many times that of the visible baryonic matter. Some time ago, this purported 'dark matter' was given the prophetic British acronym FAIRIE DUST: "Fabricated Ad hoc Invention Repeatedly Invoked in Efforts to Defend Untenable Scientific Theory."

Alternatively, one may interpret the measured redshifts as being predominantly *cosmological*; then the plotted "Coma-cluster" galaxies are distributed along a filament ~ 25 Mly in diameter with a ~ 360 Mly extent. That filament has a higher-to-lower center-to-periphery density gradient that is highlighted by the horizontal (radial-distance scale) background-shading gradient in the graph. Observing Coma, one is looking down a filament, rather than at a roughly-spherical distribution.

Coma.nb

In[1]:= R = 4100`; (* estimated Cosmic radius in Mly *)

In[2]:= z_{ref} = 0.0234`; (* Coma-cluster redshift as per SIMBAD *)

In[3]:= r_c = 3000`; (* observed cluster radius of 50 arcmins in arcsecs *)

In[4]:= $\rho = R\left(1 - \frac{1}{(z_{ref}+1)^2}\right)^{\frac{1}{2}}$ (* 1 radian at z_{ref} in Mly *)

Out[4]= 871.741

$\rho \frac{\pi}{180 * 3600}$ 1*^6 (* ly per arcsecond @ z_{ref} for top x-axis *)

Out[5]= 4226.32

In[6]:= $r_c = r_c \frac{\pi}{180 * 3600} \rho$ (* r_c converted to radians → Mly *)

Out[6]= 12.679

In[7]:= $D_m = R * \text{ArcCos}\left[\frac{1}{0.0234 + 1}\right]$ (* z = 0.0234; Coma-cluster z_{ref} distance in Mly *)

Out[7]= 878.446

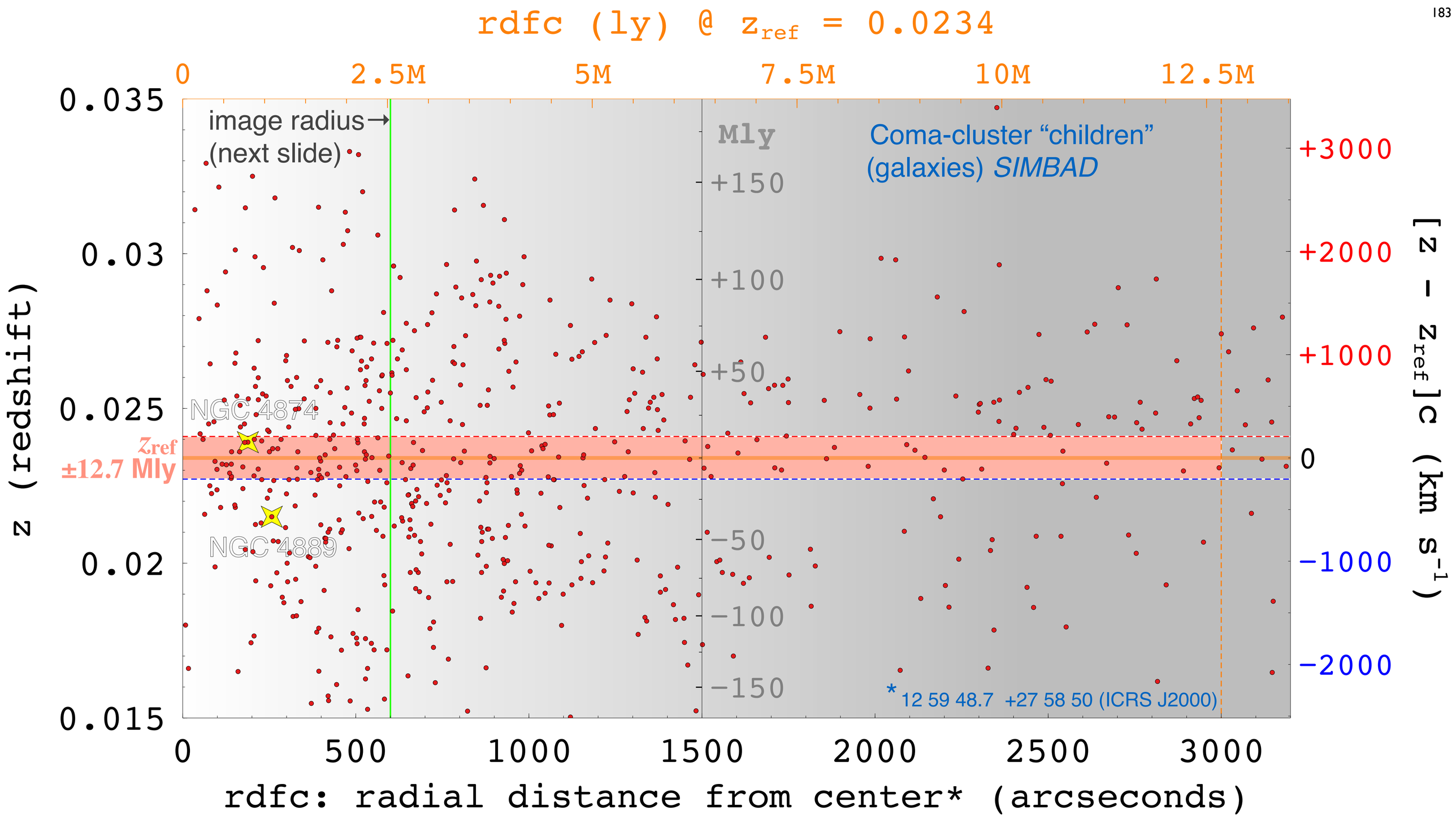
In[8]:= $\text{Solve}\left[D_m - r_c == R * \text{ArcCos}\left[\frac{1}{z+1}\right], z\right]$ (* matching Coma-cluster far redshift *)

Out[8]= {{z → 0.0227167}}

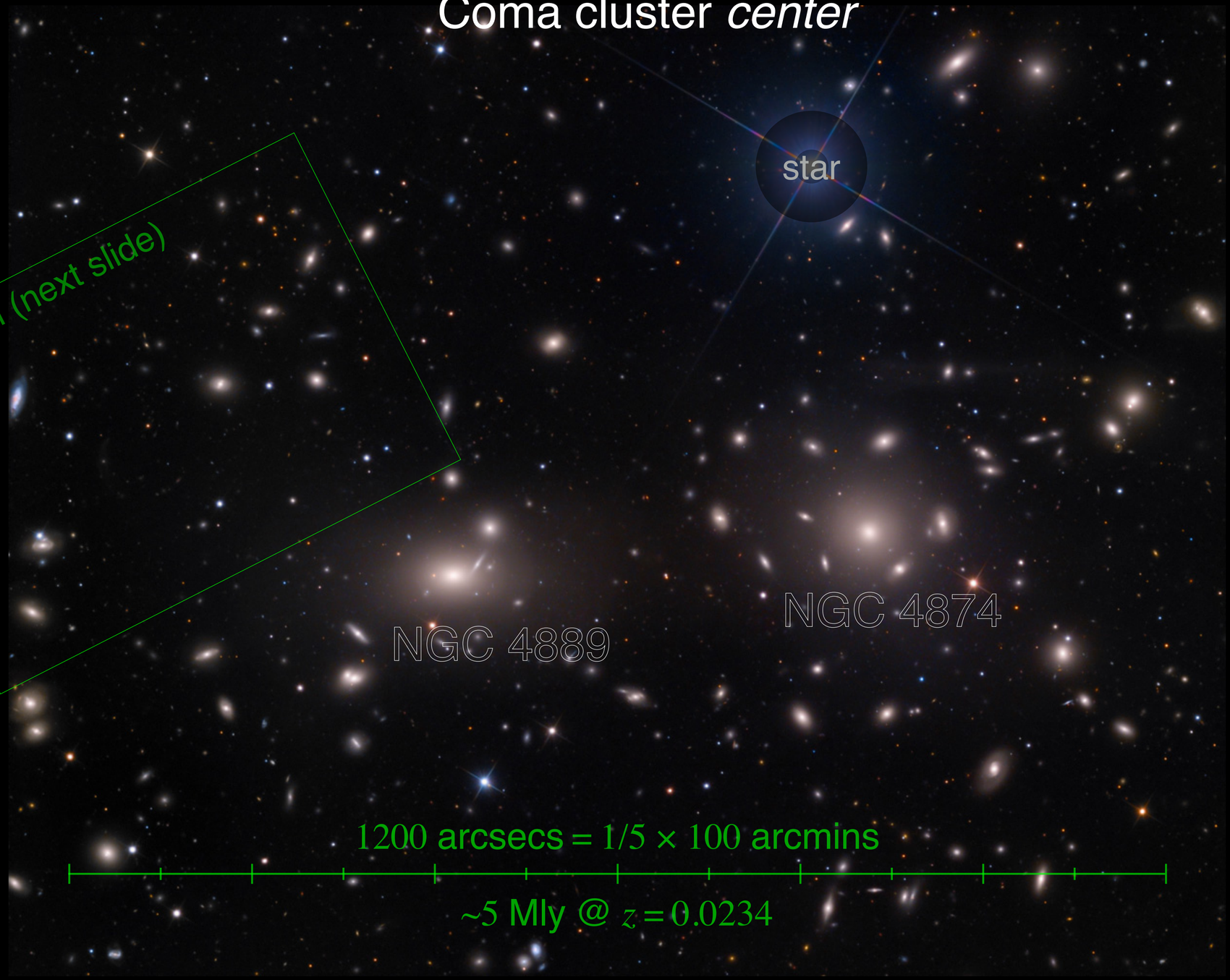
In[9]:= $\text{Solve}\left[D_m + r_c == R * \text{ArcCos}\left[\frac{1}{z+1}\right], z\right]$ (* matching Coma-cluster far redshift *)

Out[9]= {{z → 0.024094}}

125%


rdfc (ly) @ z_ref = 0.0234
0
2.5M
5M
7.5M
10M
12.5M
image radius→
(next slide)
Mly
+150
+100
+50
−50
−100
−150
Coma-cluster "children"
(galaxies) SIMBAD
NGC 4874
NGC 4889
z_ref
±12.7 Mly
* 12 59 48.7 +27 58 50 (ICRS J2000)
0.035
0.03
0.025
0.02
0.015
z (redshift)
+3000
+2000
+1000
0
−1000
−2000
[z − z_ref]c (km s^-1)
0
500
1000
1500
2000
2500
3000
rdfc: radial distance from center* (arcseconds)

Coma cluster *center*

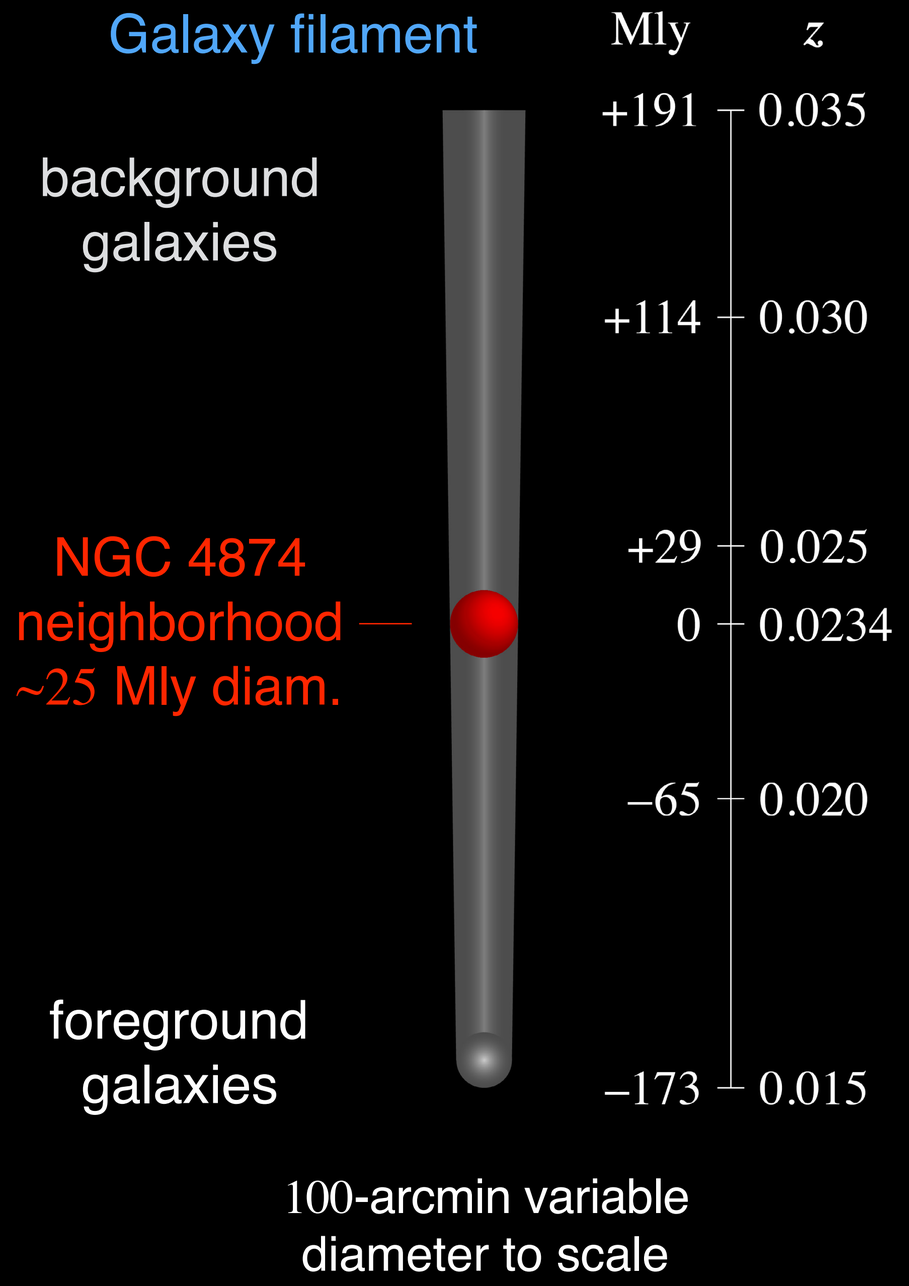


Adam Block/Mount Lemmon SkyCenter/University of Arizona

Coma cluster detail



NASA, ESA, and the Hubble Heritage Team (STScI/AURA)



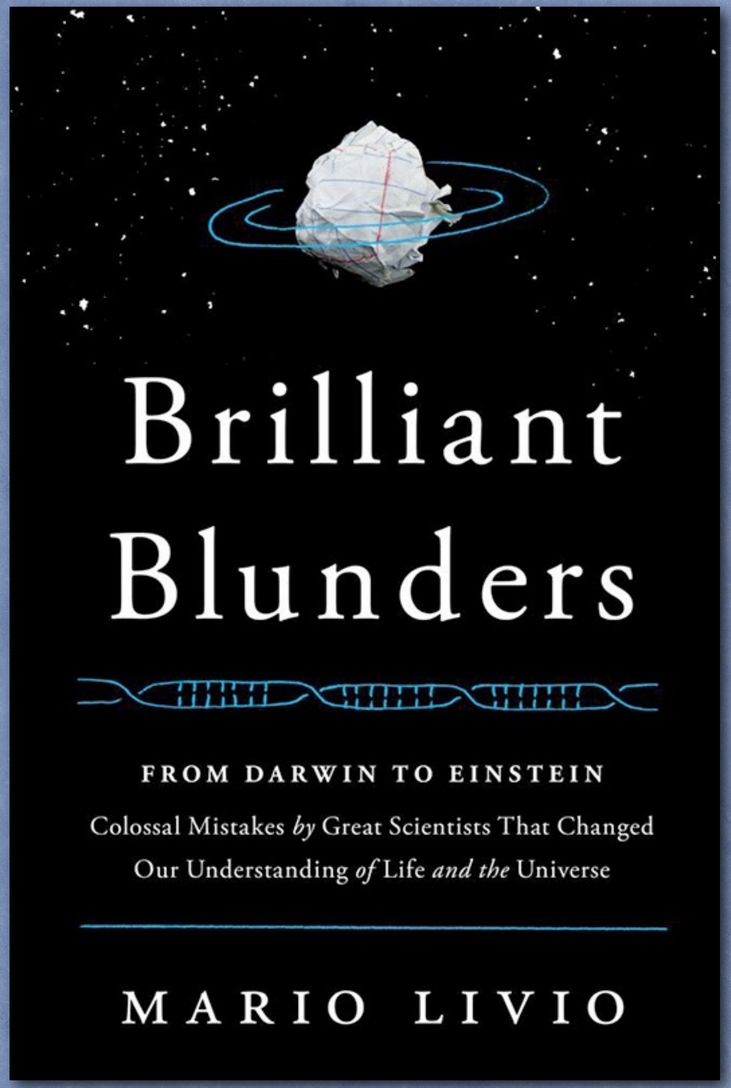
By convention, the word “cluster” generally refers to a roughly spherical clump; then “galaxy cluster” conveys the tacit presumption that the observed group of galaxies is similarly structured—to be sure, one does not refer to a long queue of persons as a *cluster*.

By inspection and analysis, the name “Coma cluster” is a misnomer; one should rather call that region of sky the “Coma filament.” The observed galaxies are distributed over a long and narrow region of space as illustrated to-scale at left. To simply assume that they are “clustered” within the region of the red ball, which requires very high relative velocities that could only be induced by gravitating ‘dark matter,’ is both arbitrary and unphysical.

Being based on the incorrect expanding-universe model, all previous galaxy-evolution models are equally wrong. Galaxies and their groups did not form by local accretion (i.e., “clustering”) of expanding matter.

PART VIII – ADDENDUM 2: RELEVANT HISTORY, ETC.

Click to go back to Table of Contents…



"Physicists sometimes tend to ignore the history of their subject. After all, who cares who discovered what, as long as the discoveries are made widely known? In a few cases, however, discoveries are of such magnitude, that understanding the path that had led to such insights, including the correct attribution, can be of great value."[1]

– Astrophysicist and author, Mario Livio



Mario Livio

About the book:

"Breakthroughs require the willingness to embrace risks and to accept errors as potential portals of discovery."

1. Mario Livio, "Lost in translation: Mystery of the missing text solved," Nature 479, 171 (2011); free HubbleSite version.

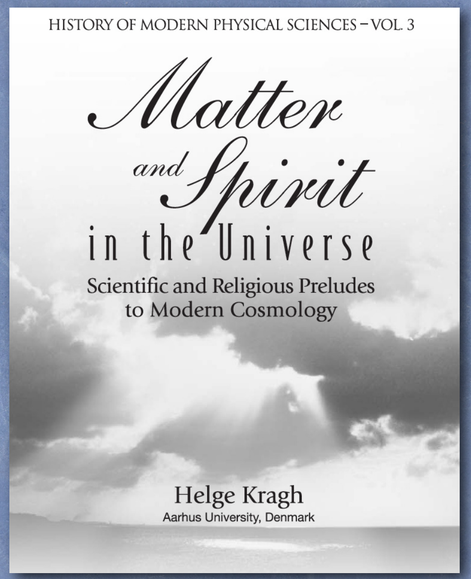
In 1921, a young Belgian mathematics postdoc and seminarian by the name of Georges Henri Lemaître wrote an essay entitled *God's First Three Declarations*.* The author stated that this 1921 essay was "an attempt to describe scientifically the first verses of Genesis." This biblically-inspired essay, discovered in the archives of the Catholic University of Leuven in the late 20th century, is the actual root of the Big-Bang theory. Lemaître (July 1894 – June 1966) was ordained as a Catholic priest in 1923.



Georges Lemaître

* Footnotes: "Les trois premières paroles de Dieu."
The manuscript is reproduced in Stoffel (1996), pp. 107–111.
Lemaître's religious views are discussed in Lambert (1997).

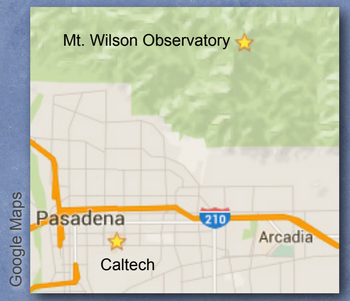
Source: Helge Kragh, *Matter and Spirit in the Universe*
(Imperial College Press, London, 2004), p. 141.



Click the book cover for *Journal for the History of Astronomy* review article by E. McMullin (2005).

In June1925, Lemaître met with Hubble at Mt. Wilson.[1,2]


Courtesy Huntington Library



(1) references Mt. Wilson
(2) references Caltech

1. John Farrell, *The Day Without Yesterday: Lemaître, Einstein, and the Birth of Modern Cosmology*, New York: Thunder's Mouth Press, 2005, p. 78.
2. Jeremiah P. Ostriker & Simon Mitton, *Heart of Darkness: Unraveling the Mysteries of the Invisible Universe*, Princeton: Princeton Univ. Press, 2013, p. 68.

The Lemaître-Hubble connection

In 1926, the year following his special trip to Mt. Wilson, Georges Lemaître submitted a paper to *Annales de la Société scientifique de Bruxelles* that was published in 1927 in Belgium (in French), so it had a limited audience: "A Homogeneous Universe of Constant Mass and Increasing Radius accounting for the Radial Velocity of Extra-galactic Nebulæ."[1]

Lemaître's visit to Mt. Wilson was motivated by his nascent cosmological theory and, three years after this initial meeting in California, Edwin Hubble and Lemaître both attended the 1928 IAU (International Astronomical Union) conference in Holland, giving Hubble an additional opportunity to meet with Lemaître.[2] It is unlikely that Lemaître did not discuss the details of his fantastical expanding-universe theory with Hubble when they met on both occasions (1925 and 1928).

Referencing a 1926 *ApJ* paper by Hubble,[3] Lemaître's paper provided a cosmic expansion-velocity estimate of 625 km s^{-1} Mpc^{-1}, whose inverse implied a 'Hubble time' (i.e., the age of the modeled expanding universe) of about 1.6 Gyr, this at a point in history when geologists were rapidly coming to the conclusion that the planet Earth had existed for at least 2–3 Gyr.

1. M. l'Abbé G. Lemaître, "Un Univers Homogéne de Masse Constante et de Rayon Croissant…," *Annales de la Société Scientifique de Bruxelles* **A47**, 49 (1927).
2. Sidney van den Bergh, "Discovery of the Expansion of the Universe," *J. Roy. Astron. Soc. Can.* **105(5)**, 197 (2011); arXiv:1108.0709 [physics.hist-ph].
3. Edwin Hubble, "Extra-Galactic Nebulae," *ApJ* **64**, 321 (1926).

Grace Lillian Burke Hubble

Edwin Hubble's wife, Grace, was a wealthy and influential socialite,* having inherited two large fortunes, the first from her father and the second from her first husband. That elite status was considerably amplified, as it was concurrent with the Great Depression, and it likely had a strong influence on her husband's media-driven reputation.

* "Grace Hubble, a brilliant woman with a keen wit, led an extraordinary life at the center of Caltech's intellectual community, with members of the British émigré community in Los Angeles and among Hollywood's elite."

🔗 Linda Mollino, "The Story of Grace Lillian Burke Hubble," *San Marino Tribune* (28 Nov. 2016).

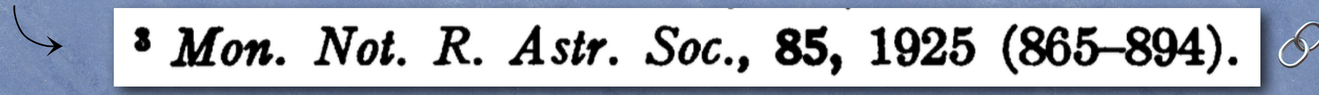
“…a man whose life is cloaked in pathological lies…”

[The screenplay] “Hubble” is the magnificent story of one of history’s greatest and most flawed geniuses and the even more magnificent universe he sought to map. In 1931, Edwin Hubble became the most famous man in the world. He was heralded as the greatest astronomer since Galileo. His discoveries had an irrevocable impact on both Einstein’s Theory of Relativity and religious interpretations of the origins of heaven and earth. But Hubble was a haunted man, dogged by mysterious secrets from the past and by enemies that threatened to destroy everything. How could a man who spoke with a British accent, wore a cape, and carried a cane be from Missouri? Why did none of his stories of his past match the claims of others? How could his wife Grace knowingly perpetuate all of this? Driven by intense ambition and a longing for something that was lost long ago, a man whose life is cloaked in pathological lies paradoxically discovers one of science’s greatest and most enduring truths [that turns out to be one of science’s greatest and most enduring *cons* and a plagiarism of a young priest’s very-misguided, religiously-inspired *fantasy*.]

🔗 Tribeca Film Institute (Alfred P. Sloan Partnership), Comment on the screenplay, “Hubble,” by S. L. Otto (2005).

Oddly, Edwin Hubble is credited for original work by other people…

Quotation from reference 3 of 4 in E. Hubble's 1929 *PNAS* paper; the italics are in the original:



Curtis† seems to have been the first to realise the cosmical importance of the occurrence of Novæ in spiral nebulæ. By assuming equality in absolute magnitude of galactic and spiral Novæ he concluded that the latter, being apparently ten magnitudes fainter, are about one hundred times as far away as are the former. Estimating the mean distance of galactic Novæ to be 100,000 light years, he reached the conclusion that the spirals are galactic systems in size comparable to our own, and *that the closest spirals are millions of light-years away.*

2 † *Journal of the Washington Acad. of Sc.*, **9**, 217 (1919) & *L.O.B.*, **300**, 108 (1917)
(***L**ick **O**bservatory **B**ulletin*)

An excerpt from the referenced *L.O.B.* article appears on the following slide…

Oddly, Edwin Hubble is credited for original work by other people…

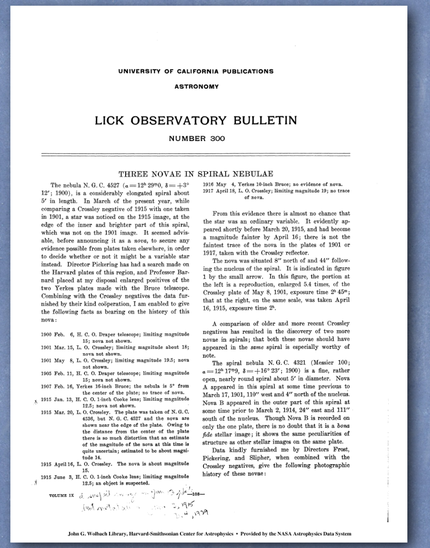
The occurrence of these novae in spiral nebulae must be regraded as a fact bearing very directly on the theories of the constitution of the spirals. It seems to me that they furnish weighty evidence in favor of the well known "island universe" theory of the spiral nebulae. …

… There is thus an average difference of ten magnitudes between galactic novae and spiral novae. Now all the evidence available assigns a great distance to the galactic novae. If we assume equality of absolute magnitude for galactic and spiral novae, then the latter, being apparently ten magnitudes the fainter, are of the order of one hundred times as far away as the former. That is, the spirals containing the novae are far outside our stellar system [i.e., the Milky Way]; and these particular spirals are undoubtedly, judging from their relatively greater angular diameters, the nearer spirals. …

Herber D. Curtis
U.S. Shipping Board Navigation School
San Diego, California, September 8, 1917.

Issued October 16, 1917.

🔗 Quotation: *Lick Observatory bulletin* **300** (1917), p. 110.



UNIVERSITY OF CALIFORNIA PUBLICATIONS

ASTRONOMY

LICK OBSERVATORY BULLETIN

NUMBER 300

THREE NOVAE IN SPIRAL NEBULAE

The nebula N. G. C. 4527 ($\alpha = 12^h\ 29^m0$, $\delta = +4°\ 12'$, 1900), is a considerably elongated spiral about 5′ in length. In March of the present year, while comparing a Crossley negative of 1915 with one taken in 1901, a star was noticed on the 1915 image, at the edge of the inner and brighter part of this spiral, which was not on the 1901 image. It seemed advisable, before announcing it as a nova, to secure any evidence possible from plates taken elsewhere, in order to decide whether or not it might be a variable star instead. Director Pickering has had a search made on the Harvard plates of this region, and Professor Bernard placed at my disposal enlarged positives of the two Yerkes plates made with the Bruce telescope. Combining with the Crossley negatives the data furnished by their kind cooperation, I am enabled to give the following facts as bearing on the history of this nova:

1900 Feb. 6, H. C. O. Draper telescope; limiting magnitude 15; nova not shown.
1901 Mar. 15, L. O. Crossley; limiting magnitude about 16; nova not shown.
1901 May 8, L. O. Crossley; limiting magnitude 15.5; nova not shown.
1905 Feb. 15, H. C. O. Draper telescope; limiting magnitude 15; nova not shown.
1907 Feb. 16, Yerkes 10-inch Bruce; the nebula is 5′ from the center of the plate; no trace of nova.
1915 Jan. 12, H. C. O. 1-inch Cooke lens; limiting magnitude 12.5; nova not shown.
1915 Mar. 20, L. O. Crossley. The plate was taken of N. G. C. 4536, but N. G. C. 4527 and the nova are shown near the edge of the plate. Owing to the distance from the center of the plate there is so much distortion that an estimate of the magnitude of the nova at this time is quite uncertain; estimated to be about magnitude 14.
1915 April 16, L. O. Crossley. The nova is about magnitude 13.
1915 June 3, H. C. O. 1-inch Cooke lens; limiting magnitude 12.5; an object is suspected.
1916 May 4, Yerkes 10-inch Bruce; no evidence of nova.
1917 April 18, L. O. Crossley; limiting magnitude 19; no trace of nova.

From this evidence there is almost no chance that the star was an ordinary variable. It evidently appeared shortly before March 20, 1915, and had become a magnitude fainter by April 16; there is not the faintest trace of the nova in the plates of 1901 or 1917, taken with the Crossley reflector.

The nova was situated 8″ north of and 44″ following the nucleus of the spiral. It is indicated in figure 1 by the small arrow. In this figure, the portion at the left is a reproduction, enlarged 5.4 times, of the Crossley plate of May 8, 1901, exposure time 2^h 45^m; that at the right, on the same scale, was taken April 16, 1915, exposure time 2^h.

A comparison of older and more recent Crossley negatives has resulted in the discovery of two more novae in spirals; that both these novae should have appeared in the *same* spiral is especially worthy of note.

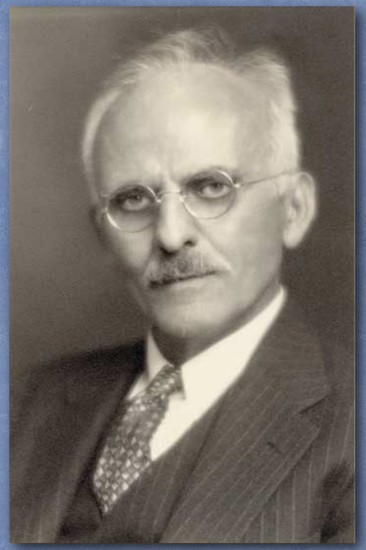
The spiral nebula N. G. C. 4321 (Messier 100; $\alpha = 12^h\ 17^m9$, $\delta = +15°\ 57'$, 1900) is a fine, rather open, nearly round spiral about 5′ in diameter. Nova A appeared in this spiral at some time previous to March 17, 1901, 119″ west and 8″ north of the nucleus. Nova B appeared in the outer part of this spiral at some time prior to March 2, 1914, 24″ east and 111″ south of the nucleus. Though Nova B is recorded on only the one plate, there is no doubt that it is a bona fide stellar image; it shows the same peculiarities of structure as other stellar images on the same plate.

Data kindly furnished me by Directors Frost, Pickering, and Slipher, when combined with the Crossley negatives, give the following photographic history of these novae:

VOLUME IX

John G. Wolbach Library, Harvard-Smithsonian Center for Astrophysics • Provided by the NASA Astrophysics Data System

Click for document.



Herber Curtis

Oddly, Edwin Hubble is credited for original work by other people.

Additionally, Edwin Hubble did not discover that the redshift was increasing with distance; this was published five years earlier by Carl Wilhelm Wirtz in Germany:

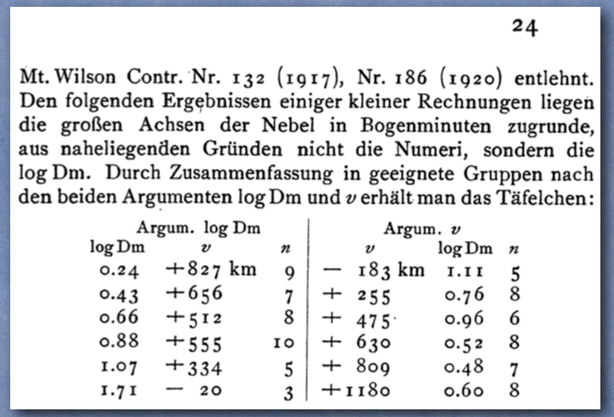
De Sitters Kosmologie und die Radialbewegungen der Spiralnebel. Von C. Wirtz.

"Es bleibt also schon so kein Zweifel, daß die positive Radialbewegung der Spiralnebel mit zunehmender Entfernung ganz erheblich anwächst."

Translation: "So there remains no doubt that the positive radial motion [i.e., *redshift* interpreted as a Doppler shift, cz] of the spiral nebulae grows very considerably with distance."

Carl W. Wirtz, "De Sitter cosmology and the radial motion of the spiral nebulae," *Astronomische Nachrichten* **222**, 21 (1924).

Carl Wilhelm Wirtz (1876 – 1939), the astronomer, should not to be confused with Carl Eugen Julius Wirtz, (1910 – 1994), the nuclear physicist who worked with Werner Heisenberg.



24

Mt. Wilson Contr. Nr. 132 (1917), Nr. 186 (1920) entlehnt. Den folgenden Ergebnissen einiger kleiner Rechnungen liegen die großen Achsen der Nebel in Bogenminuten zugrunde, aus naheliegenden Gründen nicht die Numeri, sondern die log Dm. Durch Zusammenfassung in geeignete Gruppen nach den beiden Argumenten log Dm und v erhält man das Täfelchen:

Argum. log Dm			Argum. v		
log Dm	v	n	v	log Dm	n
0.24	+827 km	9	− 183 km	1.11	5
0.43	+656	7	+ 255	0.76	8
0.66	+512	8	+ 475	0.96	6
0.88	+555	10	+ 630	0.52	8
1.07	+334	5	+ 809	0.48	7
1.71	− 20	3	+1180	0.60	8

Click for document.

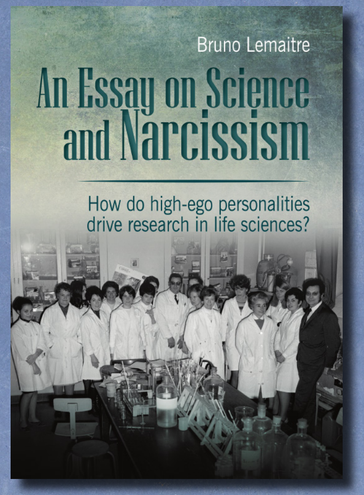


Carl Wilhelm Wirtz

Plus ça change, plus c'est la même chose.

The title, in French, may be translated into familiar colloquial English as "same difference" or "history repeats itself." However, now is the time to *change* history, to boldly stand up and say "No more of this fraudulence!"

> The replication crisis …, in which "sexy" papers fail to stand up to closer scrutiny, can be blamed in part on scientists being motivated by a need for attention and authority as well as curiosity about the natural world…
>
> – Bruno Lemaitre



Quoted from: Hannah Devlin, "Science falling victim to 'crisis of narcissism'," *The Guardian* (20 Jan 2017).

The Need for Freedom in Scientific Research (original essay title)

The history of science teaches that the greatest advances in the scientific domain have been achieved by bold thinkers who perceived new and fruitful approaches that others failed to notice. If one had taken the ideas of these scientific geniuses who have been the promoters of modern science and submitted them to committees of specialists, there is no doubt that the latter would have viewed them as extravagant and would have discarded them for the very reason of their originality and profundity. As a matter of fact, the battles waged, for example by Fresnel and by Pasteur suffice to prove that some of these pioneers ran into a lack of understanding from the side of eminent scholars which they had to fight with vigor before emerging as the winners. More recently, in the domain of theoretical physics, of which I can speak with knowledge, the magnificent novel conceptions of Lorentz and Planck, and particularly Einstein also clashed with the incomprehension of eminent scientists. The new ideas here triumphed; but, in proportion as the organization of research becomes more rigid, the danger increases that new and fruitful ideas will be unable to develop freely.

Let us state in a few words the conclusion to be drawn from the foregoing. While, by the very force of circumstances, research and teaching are weighted down by administrative structures and financial concerns and by the heavy armature of strict regulations and planning, it becomes more indispensable than ever to preserve the freedom of scientific research and the freedom of initiative for the original investigators, because these freedoms have always been and will always remain the most fertile sources for the grand progress of science.

Louis de Broglie, April 25, 1978

Louis de Broglie, *Heisenberg's Uncertainties and the Probabilistic Interpretation of Wave Mechanics*, (Kluwer, Dordrecht, 1990), p. xviii.

For many centuries, astronomers and mathematicians worked on the details of the geocentric cosmology of the Ptolemaic system, which standardized the Geocentric model in the academic world of the second-century CE. Many lifetimes and man-centuries of effort were devoted to this futile effort, as was also the case with alchemy, commonly associated with the “Dark Ages.”

Currently, there are dozens of programs, typically involving enormous public investment and the careers of hundreds of trained scientists and support personnel, investigating ‘dark energy’ and ‘dark matter,’ which are equally futile. Although not certain, prior to required prediction verification, it is likely that “gravitational wave” research, according to the current conventional approach, is similarly futile. In modern times, the Nobel Prize is more than an award for personal achievement; it establishes a line of academic research as requiring decades of effort by the global scientific community, effectively standardizing the awarded work, which then garners the better part of human and capital resources. Accordingly, when such a prize standardizes a futile avenue of research, this inevitably proves to be catastrophic, both for nascent scientific careers and for the advancement of human knowledge; time and resources may be misdirected for many decades.

The predictive equations put forward in this report were first put forward in 2005, when the author was a “Visiting Scholar” at Stanford University. Between 2005 and 2010, most of this report’s content was communicated to authorities at leading academic institutions worldwide (e.g., this 2010 report). The response *included* contrived ad hominem attack (prior to MG12) and, the misleading awards of the 2006 (2005+1) and 2011 (2010+1) Nobel Prizes in Physics.

Detailed online abstract from MG12 (**July 2009**)

COM2 - Dark Energy and Universe Acceleration

Speaker	Mayer, Alexander
Talk Title	Cosmological Implications of the SDSS and 2dF Redshift–Population Histograms
Abstract	Empirical observation of galaxy population density in redshift space is inconsistent with expectations based on the canonical cosmological model. The magnitude of this inconsistency implies a significant error in the canonical model's theoretical redshift-distance relationship. A new model has been derived that rests on first principles and which is consistent with observed galaxy population density in redshift space. Additionally, the observed Type Ia supernovae redshift-luminosity curve does not require interpretation as accelerating cosmic expansion. Moreover, the revised redshift–distance relationship of the proposed new model implies that the entire mass of early-type galaxies associated with observed Einstein rings is composed of normal matter; no "dark matter" need be assumed to exist in these systems.
Talk view	

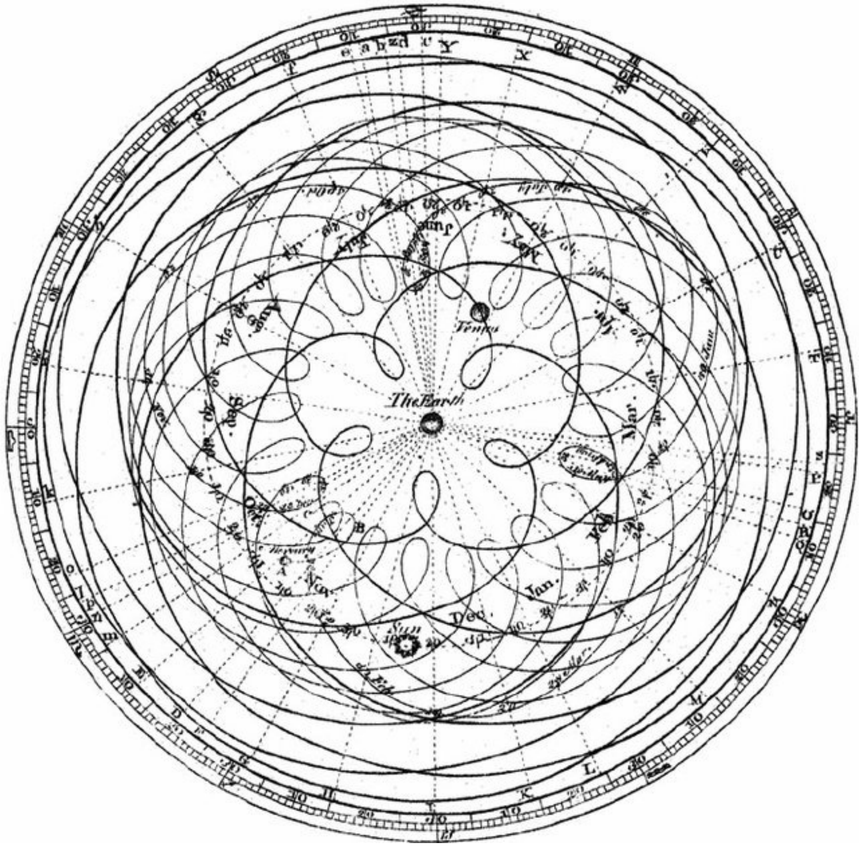
This abstract should be viewable online under L. Cosmological Models **COM2: A**

Geocentrism and Big-Bang cosmology

This is an illustration of the Ptolemaic model of the solar system, which involved tremendous intellectual effort by many people over generations and much complex mathematics. That did not prevent the fact that it is *utter nonsense* due to a fatal false premise.

In light of this report, the Big-Bang theory is similar *utter nonsense*. The Universe is not expanding from a singularity, which is a figment of the imagination that has no correlation to physical reality. The idea that the entire mass-energy of the Universe (some *trillion galaxies*) was, just some billions of years ago, compacted into an infinitely small “Cosmic Egg” is truly *idiotic*; no other term adequately applies to that bizarre, irrational idea, concocted by a religiously-motivated young Catholic priest, likely suffering from severe post-war trauma.

Big-Bang cosmology is *pseudointellectual garbage*; it is high time to abandon that ill-conceived theory. A failure to do so in the face of this new information is an indication of mental and moral disorder.



At least this absurdly complex model could make quite accurate ephemeris predictions, so it was not completely *idiotic*. The same cannot be said for the Big-Bang theory, which has no correlation to empirical reality, and arguably encourages irrational thinking.